Krzysztof Wiśniewski

FINITE ROTATIONS OF SHELLS AND BEAMS EXTENDED EQUATIONS AND NUMERICAL MODELS

9/1997

WARSZAWA 1997

ISSN 0208-5658

Praca wpłynęła do Redakcji dnia 4 listopada 1996r.

Recenzent - Prof.zw.dr hab. inż. Wojciech Pietraszkiewicz

Praca habilitacyjna

Instytut Podstawowych Problemów Techniki PAN
Naklad 100 egz. Ark. wyd. 9,0 Ark. druk. 11,0
Oddano do drukarni we wrześniu 1997r.

ATOS Poligrafia-Reklama, Warszawa, Stawki 14

Krzysztof Wiśniewski
Instytut Podstawowych Problemów Techniki PAN
ul. Świętokrzyska 21, 00-049 Warszawa

FINITE ROTATIONS OF SHELLS AND BEAMS EXTENDED EQUATIONS AND NUMERICAL MODELS

Abstract

The thesis is concerned with theoretical and numerical aspects of modeling of shells and beams undergoing finite (unrestricted) rotations. It is demonstrated that numerical analyses of such shells and beams involve not only a sophisticated algorithmic treatment of rotations and nonlinear equations, but also require a non-trivial task of extending the governing equations.

The formulation is based on the Biot stress and right stretch strain, and the hyperelastic (linear or Mooney-Rivlin) constitutive equations. The theoretical part of the thesis comprises two extensions of the finite rotation equations, which are related to the drilling rotation and the transverse normal stretch.

1. The shell equations with rotations as an independent variable are derived in a variationally consistent manner, within the classical continuum mechanics. The rotation constraint is introduced to ensure that the rotation used in the Reissner hypothesis satisfies the equation of the polar decomposition of the deformation gradient. The drilling rotation of the shell (6th degree of freedom) is naturally included.

2. The beam equations for the Reissner hypothesis, with an additional scalar parameter for the normal stretch, are derived. The conversion formula for the middle-line and the interface variables, valid in the range of finite rotations, is proposed. The conversion formula is introduced consistently with the kinematical hypothesis, and sets up a basis for development of the layer-wise models of finite rotation multi-layer beams.

In its numerical part, the thesis deals with finite element models accounting for finite rotations, and incorporates:

1. the systematization and description of questions related to parametrization and algorithmic treatment of rotations, from the view-point of applications in continuum and structural mechanics. Also the advanced problems, such as increments of a rotation vector in two different tangent planes and symmetry of the tangent operator, when the potential energy depends on rotations, are addressed.

2. the implementation of a nonlinear finite element with drilling rotation, what requires an exact linearization of the basic equations and the use of advanced techniques to control the spurious modes of the element. The method of implementation of the design sensitivity analysis for the problems with the rotational degrees of freedom is described, and the design derivatives are calculated along the path in the whole pre- and post-critical range. These questions are presented on several numerical examples, some exhibiting highly nonlinear equilibrium paths and requiring the arc-length (continuation) method.

3. the construction of multi-layer beam elements based on the concept of layer-wise models, such as the interface variables model and the hierarchical model using Taylor or Chebyshev series expansions. The stress recovery procedure for the multi-layer element is developed and tested. In case of finite rotations, the linearization of the conversion formula and the stabilization of the element are described, implemented and tested. These elements provide either the accuracy of the layer-wise theory, or the effectiveness of the single-layer theory, depending on the problem being solved.

1 Introduction

The finite element analysis of flexible structures undergoing large rotations and displacements has attracted considerable interest in the recent years. In mechanical engineering, interest has emerged, among others, from the competition to obtain accurate and inexpensive manufacturing processes, and to develop a new generation of robots capable of performing high-precision tasks such as micro-spot welding and assembling. In the aerospace field, a part of this attention comes from analysis and design of high-performance aircrafts, helicopter blades and turbo-machinery. Further interest has been brought by establishing challenging goals for space research, aiming at constructing space stations, space-based antennas for improved communication, telescopes, solar arrays and others.

These applications have strongly motivated the development of a more accurate mechanical description, and efficient computational models and methods. These two goals are linked, and, as indicate the references on the subject, the growing computational capabilities often motivate new theoretical developments, leading to a more adequate description.

1.1 Rotations as primary variables

Rotations are commonly used as primary variables in rigid-body dynamics, see e.g. [Rosenberg, 1977] or [Goldstein, 1980], while for deformable bodies they explicitly appear in the theories of polar media, such as of E. and F. Cosserat, see e.g. [Eringen, Kadafar, 1976], and in some shell theories. In classical continuum mechanics, which is of interest of the present work, for a long time rotations were used mostly in the theory of constitutive equations, see e.g. [Truesdell, Noll, 1965]. In the sixties and early seventies several works appeared using rotations to derive some non-classical forms of the compatibility conditions. Rotations became more popular as primary variables when the variational principles involving them were formulated, and the computer implementations turned out to be very efficient. It is likely that the turning point was the paper by [Fraeijs de Veubeke, 1972], which introduces the rotations as independent variables, with the help of the polar decomposition of the deformation gradient, and derives the variational principles for finite elasticity, constituting a basis for the eventual finite element implementations. Later, [Pietraszkiewicz, Badur, 1983] investigated finite rotations in the deformation of a continuum. In this work the rotations are related to displacements, and spatial derivatives of rotations are examined in order to find compatibility conditions. Several variational principles involving the rotation tensor and various stress vectors are discussed by [Atluri, 1984]. Recently, [Blinowski, 1994] published the first part of a work devoted to rotations of deformable three-dimensional bodies.

In three-dimensional bodies, finite rotations appear only at finite strains, but in thin bodies, such as beams and shells, they may occur even in the case of small strains. Although the rotational part of deformation in thin bodies is particularly important, this was not reflected by the first nonlinear theories of shells (and beams), which were formulated in terms of displacements, see e.g. [Wozniak, 1966] and [Naghdi, 1972]. This has gradually changed, and presently dominate the shell (and beam) theories explicitly involving rotations. One of the first works was the one by [Simmonds, Danielson, 1972],

where a nonlinear shell theory was derived in terms of the finite rotation and stress function vectors, and that of [Reissner, 1972] with a theory of a planar beam. In the seventies, the subject of finite rotations of thin bodies was developed and systematized in several works, see e.g. [Pietraszkiewicz, 1977, 1979].

Rotations became popular variables also due to the advantages of the C^0 class of finite elements, based on the Reissner-type shell equations. The Reissner kinematical hypothesis explicitly introduces rotations, but they are not equal to the rotations yielded by the polar decomposition of the deformation gradient. In the papers on numerical models of shells, most often that difference remains unnoticed, see papers cited e.g. in [Zienkiewicz, Taylor,1991] Chapter 1-5, what is justified only when the shear strain in the shell is negligible. The attention is paid to it in some theoretical works. For instance, [Pietraszkiewicz, 1979], expressed the rotation tensor resulting from the polar decomposition theorem in terms of a displacement vector and a vector of the difference between the deformed and undeformed director, which depends on the kinematical hypothesis. Note that in the Reissner hypothesis, the rotation tensor acts upon the director of the undeformed shell, and, therefore, for a standard shell formulation based on the Green strain only the tangent rotation vector can be considered.

The properties of rotation tensors are substantially different than those of displacement vectors, and several additional questions regarding an optimal parametrization and an algorithmic treatment must be solved, see e.g. [Stuelpnagel, 1964], [Argyris, 1982], [Argyris, Poterasu, 1993]. While the rotation field is usually described by a proper orthogonal tensor, in numerical implementations a parametrization in terms of a rotation vector is more convenient. Several rotation vectors can be used, what results in different rules of composition of these vectors, and different linearized forms of equations.

From the algorithmic point of view, the concept of exponential mapping and parallel transport in $SO(3)$ must be used to devise the update procedures for rotations, and to construct an extension of the Newton-Raphson solution scheme for the rotational degrees of freedom. Note that the extension of the Newmark time-stepping procedure, in dynamics, is additionally complicated by the presence of the inertia operator, [Simo, Vu-Quoc, 1986b]. The plane tangent to $SO(3)$, in which increments of the rotation parameters take place and are compounded, is a matter of choice, but it affects symmetry of the tangent operator and effectiveness of numerical implementations. Generally, the parametrization of the increment of the rotations should involve three parameters and be singularity free, while the update of these parameters must be efficient, singularity free and provide a symmetric tangent matrix.

1.2 Extended shell and beam models with finite rotations

The finite element method has achieved remarkable sophistication, but also great complexity, see for instance some fundamental works, such as [Bathe, 1982], [Hughes, 1987], [Kleiber, 1989], and [Zienkiewicz, Taylor, 1989, 1991]. The requirements which new elements should satisfy have become better defined and more demanding. A wide range of applications of shell and beam elements implies that a good element should account for finite rotations and strains, admit the incorporation of various constitutive laws and enable convenient linking with other elements. As indicate the so far published papers, see

References, due to several difficulties, no such versatile element has yet been developed. Some of these difficulties are discussed below.

The constitutive equations for integral stress measures, such as stress and couple resultants are inherently inadequate for some problems, because material properties are local, and not always can be equivalently expressed in an integral form. For such problems the continuum-based approach to beams and shells, which necessitates a numerical through-the-thickness integration, but exploits the standard constitutive equations, seems to be the best, see e.g. [Bates, 1987] or [Buechter, Ramm, 1992], [Parish, 1995]. Nonetheless, the equations obtained by the analytical integration are proven to be the most effective ones for a large class of problems, especially those involving small strains and elastic linear consttutive equations. Also membranes, even subject to finite strains, with 2nd order elastic/non-elastic constitutive laws, can be conveniently treated in this way.

However, a derivation of the constitutive equations for the analytically integrated shells (and beams) is complicated, since the strain energy function depends on strains being polynomials of the thickness coordinate, e.g. of a 2nd order for typical approximations used for shell kinematics. The multiplicity of terms renders that only the terms of low order can be retained, and a special methodology, proposed in [John, 1965,1971] and later successfully developed in [Koiter, 1966] and Pietraszkiewicz, see e.g. [Pietraszkiewicz, 1984, 1989], must be used to construct consistent approximations to the strain energy.

Two of the difficulties related to the kinematics of shell, one related to incorporating the drilling rotations, and the other to the transverse normal strain, are discussed below, and it is shown that they can be overcome extending the equations.

Drilling rotation. The rotation around the vector normal to the shell reference surface is called the drilling rotation. The presence of the drilling rotation as the 6th degree of freedom in shell finite elements is very convenient, because it enables linking with other structural elements which have three rotational degrees of freedom (such as three-dimensional beams), and connecting of shell elements of different spatial orientation (e.g. at corners of a non-differentiable shell).

In case of the Reissner kinematics the drilling rotation does not affect the deformation gradient, because the rotation tensor acts upon the director of the undeformed shell, and for the drilling rotation the axis of rotation coincides with the vector being rotated. In consequence, the shell measures derived from the Green strain do not depend on this rotation, and the sixth equilibrium equation degenerates to $0 = 0$, making the stiffness matrix singular. Note that this singularity is often masked by transformations performed on the stiffness matrix, but usually manifests itself when several elements of zero Gaussian curvature are co-planar at a node. There have been proposed till now in the literature several ways of remedying the difficulties related to the drilling degree of freedom in the 5-parameter shells.

One of them is purely numerical, e.g. we can add a small value to the diagonal, what can be interpreted as adding a fictitious spring. But then, unless the node is connected to other elements which provide a real value of the stiffness for this degree of freedo... the obtained value of the drilling rotation is meaningless.

The other way of introducing the drilling rotation is via the hierarchical shape functions and an auxiliary equation eliminating in-plane shear locking of the element. This leads to the so called Allman-type shape functions for the in-plane displacements, expressed in terms of nodal displacements and the nodal drilling rotations, see e.g. [Taylor, 1988].

This way yields the stiffness matrix which is rank deficient, and the hourglass mode for rotations must be additionally suppressed.

Within the next way a constraint with a drilling rotation defined in terms of other variables, can be imposed on use of the penalty method, see e.g. [Bates, 1987] for a rate form of such a constraint.

The above methods work reasonably well when the drilling degree of freedom is used to facilitate connecting of various elements. But even the last two methods do not suffice in the sensitivity analysis and in design optimization, as erroneous design derivatives are obtained for the standard implementation of the Adjoint System Method, see e.g. [Santos, Wisniewski, Apostol, 1995], and [Wisniewski, Santos, 1996] for the exposition of the links between the solution scheme and the design derivatives involved.

To avoid a non-standard treatment of the drilling degree of freedom the shell equations must be extended in a more rigorous way. For this purpose we derive shell equations from the equations of a three-dimensional elasticity which incorporate the rotation as an independent variable, [Wisniewski, 1996a].

The rotations can be introduced into a classical three-dimensional elasticity on use of the so called rotation constraint, obtained from the polar decomposition equation for the deformation gradient. Such formulations for three-dimensional elasticity are based either on the right Cauchy-Green tensor, e.g. [Hughes, Brezzi, 1989], [Simo, Fox, Hughes, 1992], or on the right stretching tensor, e.g. [Fraeijs de Veubeke, 1972], [Reissner, 1984], [Bufler, 1985]. For isotropic materials both forms are equally convenient; for both the Lagrange multiplier vanishes when the rotation constraint is satisfied, and both are amenable to regularization, which locally convexifies the extended potential energy functional. Note that so introduced rotations are the 3-parameter ones, and several related variational principles can be derived for them, see [Atluri, Cazzani, 1995].

The three-dimensional equations incorporating rotations are subsequently used in the present work to derive the shell equations. Note that for shell theories with independent rotations the equations based on the (right and/or left) stretching tensor dominate, see e.g. [Simmonds, Danielson, 1970, 1972], [Atluri, 1984], [Makowski, Stumpf, 1986], [Badur, Pietraszkiewicz, 1986], [Wriggers, Gruttmann, 1993], [Gruttmann, Stein, Wriggers, 1989], [Gruttmann, Wagner, Wriggers, 1992], [Ibrahimbegovic, 1994], [Ibrahimbegovic, Frey, 1995]. The stretching tensor is also exploited in the present work, in which the earlier papers are extended in the following way:

1) Some of them from the outset are limited to membranes, e.g. [Gruttmann, Taylor, 1992] or [Ibrahimbegovic, Frey, 1995], leaving aside the question whether the methodology applied can be generalized to the case involving bending and shearing. In some, e.g. [Simmonds, Danielson, 1970, 1972] and [Atluri, 1984], the Kirchhoff-type kinematics is applied, what excludes shear strains. In the present paper, we use the Reissner kinematics, which allows to include the effects of bending and shearing, and explicitly involves the rotation tensor providing strain measures of a particularly simple form.

2) In some works on shells the role played by the rotation constraint is not recognized. For instance in [Chroscielewski, Makowski, Stumpf, 1992] this constraint is not present. In some works a notion of a rotation constraint is not introduced explicitly, but some of strain components are enforced to be symmetric, e.g in [Simmonds, Danielson, 1970, 1972] or [Wriggers, Gruttmann, 1993], see the discussion in Section 3.4.3. In the present work the rotation constraint is explicitly introduced in the three- dimensional form, and its shell counterparts are derived. This allows to capture the limitations of the approach

to shells based on the stretching tensor, which cannot be detected when the rotation constraint is directly inserted into the deformation gradient. Note that when the Kirchhoff kinematics and the first approximation to the strain energy is considered, as in [Badur, Pietraszkiewicz, 1986], these effects are negligible.

3) The aforementioned papers on shells tacitly assume that the approach exploiting the right stretch strain is advantageous over the one based on the Green strain. We try to establish the limits within which the above is true, especially considering possibility of modeling large strains and a curved geometry of the shell.

4) For the incompressible materials, the generalized kinematical hypothesis with the scalar extension function are often used, e.g. [Stumpf, Makowski, 1986], [Makowski, Stumpf, 1986] and [Schieck, Pietraszkiewicz, Stumpf, 1992]. We show that the generalized Reissner hypothesis with the scalar extension parameter or the standard Reissner hypothesis also can be used for thin shells if the normal strain is properly recovered from the incompressibility condition, and a suitable form of the constitutive equations is exploited. Such an approach leads to less complicated equations than the approach based on the extension function.

Normal strain. The side-effect of the standard Reissner (or Kirchhoff) hypothesis is that the normal component of the strain is equal to zero. As indicate three-dimensional solutions, the magnitude of this component is not negligible, and it must be accounted for in the strain energy and the constitutive equation. Hence, it is recovered on use of the auxiliary equations, such as: the plane (zero normal) stress condition, e.g. [Naghdi, 1972], [Pietraszkiewicz, 1979b], or the incompressibility condition, [Wisniewski, 1996a].

In some situations, however, the auxiliary conditions are not realistic enough to be used, and/or the normal strain plays an important role in the analysis and must be accurate. For instance, a bending of a multi-layer beam or shell causes that layers press at each other, and the normal stress and strain is large. Accurate modelling of strains is important in prediction of the de-bonding of layers, caused by a concentration of stresses at their interfaces, see e.g. [Basar, Ding, 1994]. Then, it is better to incorporate explicitly the normal strain into the beam (or shell) theory. This can be done by generalization of the kinematical hypothesis, by introducing either a scalar parameter or a scalar extension function, as discussed earlier for the incompressible materials.

In the present work we identify another reason to include explicitly the normal strain into the formulation: for generating the so called layer-wise models of beams or shells, which are used for multi-layer (laminated) composites.

In a general classification presented in [Reddy, 1989] three classes of theories of laminated composites are distinguished: equivalent single-layer theories, layer-wise theories and continuum-based theories. [Baczynski, 1985], discussing the concepts of modeling of multi-layer bodies, additionally divides the equivalent single-layer theories into: theories of effective moduli and theories of a continuum with micro-structure.

The equivalent single-layer theories use continuous displacements and their derivatives in the thickness direction of the laminate, what leads to incorrect, discontinuous shear stresses at layer interfaces, see [Reddy, 1987]. Such theories can only be used to extract global responses of a laminated structure.

Stresses and warping of a layered composite are much better modeled by the layer-wise and the continuum-based theories. In the layer-wise theories first kinematical hypotheses

are used separately within each layer and then layers are aggregated together. For example, [Epstein, Glockner, 1977] and [Epstein, Huttelmaier, 1983] introduced a piecewise linear thickness coordinate and thickness vectors implying equations expressed in terms of displacements and the thickness vector deformations. A piecewise linear displacement distribution has also been used in [Reddy, Barbero, Teply, 1989], where equations in terms of mid-plane variables have been derived. This approach is also called a discrete-continuous approach, e.g. [Baczynski, 1985], and the theory of non-classical continuum with internal constraints of [Wozniak, 1973] is one of the first examples of it.

In the continuum-based theories layers are just aggregated together, without the use of any kinematical hypotheses, see for example [Owen, Li, 1987]. In both of the last approaches the applied hypotheses or the approximation functions lead to discontinuous derivatives of displacements at layer interfaces. This results in discontinuous strains, and much better approximations of shear stresses.

The approach developed in the present work falls into the class of the layer-wise theories, with layers modeled by equations constrained by a kinematical hypothesis. The problem of assembling the layers of elements in order to generate a multi-layer cross-section is solved by imposition of the compatibility conditions on the surfaces separating layers. This leads to the interface variable (IFV) models, defined in terms of the variables associated with the separating surfaces, on which the hierarchical models, expressed in terms of variables characterizing the whole cross-section, can be constructed.

Note that if the compatibility conditions at interfaces are used to assemble the layers of elements, then a conversion formula between the middle-line and the interface variables in needed. For linear kinematics and the Reissner assumption the respective conversion formula is formulated and tested in [Wisniewski, Schrefler, 1993a], and the accuracy of obtained model is very good. Also, the stresses yielded by the enhanced stress recovery procedure, which was proposed in [Wisniewski, Schrefler, 1993b], compare very well with two-dimensional results. However, the extension of the above methodology to the case of finite rotations is not so straightforward. Firstly, due to the conversion formula. For small rotations, the rotation angle is related to the derivative of the tangent displacements with respect to the thickness coordinate, and the conversion formula is readily obtained. In case of finite rotations, the rotation angle cannot be linked with only tangent displacements, and a different method must be devised. We propose [Wisniewski, 1996b] to derive this formula in a way consistent with the kinematical assumptions. This yields a nonlinear formula depending on all component displacements, which subsequently is a subject to exact linearization.

Secondly, we establish that in case of finite rotations, a conversion formula cannot be derived for the standard Reissner hypothesis, as the number of its independent parameters is too small. Therefore, a generalized Reissner hypothesis with a scalar parameter for the transverse extension (thickness changes) is applied. This hypothesis is used in many papers: the classical ones, e.g. [Green, Naghdi, Wenner, 1971], [Naghdi, 1972], which present the theory, and in the recent ones, e.g. [Simo, Rifai, Fox, 1990], [Schieck, Pietraszkiewicz, Stumpf, 1992] [Krätzig, 1993], [Basar, Ding, 1994], [Sansour, 1995], where computational models are also presented. The finite rotation equations of the extensible director beam derived in the present work are based on the right stretch strain, and exploit the concept of the co-rotational frame, what makes them very convenient for numerical implementations. They reduce to the equations presented in [Reissner, 1972] and [Cardona, Geradin, 1988], when inextensibility of the director is assumed.

Finally, in case of finite rotations, the equilibrium paths very often are highly nonlinear, and possess critical (limit and bifurcation) points. what necessitates special numerical tools. To follow the paths, the so called arc-length methods are used, described e.g. in [Riks, 1972], [Ramm, 1981], [Schweizerhof, Wriggers, 1986]. Another class of methods must be used to detect the singular points, and switch the branch of solution at the bifurcation points, see e.g. [Wriggers, Simo, 1990], [Wagner, 1992]. At present, these methods still are in the stage of development which does not admit full automatization of computations, and complicated cases must be analyzed interactively.

1.3 Scope of the work and basic results

The developments of the present work can be considered in two aspects. The first is theoretical, and consists of the derivation of shell equations with drilling rotations and beam equations with extensible director, both accounting for finite rotations. The second aspect is numerical, and incorporates the description of the algorithmic approach to finite rotations, implementation and testing of finite elements accounting for finite rotations, extension of the continuum Adjoint System Method of the design sensitivity analysis for the rotational parameters, and construction of layer-wise models of multi-layer beams.

In Chapter 2 the questions related to the parametrization and algorithmic treatment of rotations are described. Considering a rotation of a vector around a given axis the rotation tensor is introduced. The left and right rules for composition of rotation tensors are defined, and properties of both the superposed rotations are related. Subsequently, several parametrizations of rotation tensor are discussed. In case of the Euler (or quaternion) parameters, the difficulties encountered when the Newton-Raphson method is used, are illustrated. As a remedy, a concept of a rotation vector is introduced and several related parametrizations are presented. Next, the classical description in terms of the Euler angles is introduced, and two-parameter Euler angles for rotations of shell directors are over-viewed. This part is closed by a presentation of composition rules in terms of rotation parameters.

The second part of this chapter presents more advanced topics related to algorithmic treatment of rotations. First, a variation of the rotation tensor is presented, and then increments of a canonical rotation vector in two different tangent planes are considered. Subsequently, the question of symmetry of the tangent operator for the formulation in terms of the canonical rotation vector belonging to the initial tangent plane is addressed. This leads to the conclusion that the canonical rotation vector is not suitable for compounding the rotations, and the quaternion parameters are chosen for this purpose. This chapter demonstrates that combining the canonical rotation vector with the quaternion parameters, and using the co-rotational basis, the rotations and their increments are singularity free and the tangent matrix is symmetric.

Shell equations with independent rotations, including also the drilling rotation, are derived in Chapter 3.

In Section 3.1 the formulation of a three-dimensional elasticity with independent rotations is presented. The Lagrangean balance equations for the 1st Piola-Kirchhoff stress,

are subsequently expressed in terms of the Biot stress and rotations, yielded by the polar decomposition of the deformation gradient. The polar decomposition equation is appended to the basic equations as a rotation constraint, furnishing a mixed formulation in terms of a deformation, a skew part of the Biot stress, and rotations. Then, the balance equations and the rotation constraint are transformed to a weak form, and the virtual work equation and its potential are given. The so called *relaxed* strain measure is introduced, which yields a right stretch strain, when the rotation constraint is fully enforced. This strain measure is symmetric and a hyperelastic constitutive equation for the symmetric *relaxed* Biot stress can be postulated. For an isotropic material, the skew stress vanishes when the rotation constraint is satisfied, and the penalty method can be used to eliminate this skew stress from the formulation. In the case of an anisotropic material the skew stress does not vanish, and either a three-field mixed problem must be solved, or a series of sub-problems is solved on use of a combination of a penalty method and a staggered scheme.

In Section 3.2 the truncated Taylor series of the thickness coordinate are used to introduce the middle surface variables. A linear approximation of the deformation and a constant of rotations is assumed. For the product $\mathbf{Q}^T\mathbf{F}$, the constant and linear, as well as the symmetric and skew parts, are separated, and the shell form of the right stretch strain is given. Subsequently, the virtual work equations for an arbitrary and isotropic material are integrated over the shell thickness. The stress and couple resultants for a shell are introduced, and the shell forms of these equations are derived. The difficulties rendered by the constant approximation of rotations are identified and discussed. A scalar coefficient is introduced to decide, which part of the rotation constraint is actually enforced, in this way ensuring a correct response either for membrane states or for bending-shearing states.

In Section 3.3 the deformation gradient is specified in a local basis. The generalized Reissner hypothesis admitting the extension of the director, and standard Reissner hypothesis are introduced and expressed in a co-rotational basis. The derivatives of the rotated director are expressed in this basis using skew-symmetric tensors. In consequence, the deformation gradient and its variation are functions of the displacements, the extension coefficient, and the axial vectors associated with rotations. It is shown that the drilling rotation does not influence the deformation gradient.

In Section 3.4 the shell counterparts of the *relaxed* right stretch strain tensor and the skew parts of $\mathbf{Q}^T\mathbf{F}$ are determined for both forms of the deformation gradient. The right stretch strain depends on the drilling rotation, but some of the normal components are equal to zero, Subsequently, the simplified methods of symmetrization of the strain measures are over-viewed. Finally, the rotated-forward strain and stress resultants as well as a co-rotational variation of the Green-McInnis-Naghdi type are introduced to facilitate a description in a co-rotational basis. It is shown that the co-rotational variations of strain measures involve skew-symmetric but not orthogonal tensors.

In Section 3.5 the basic (balance and rotation constraint) equations are derived from the virtual work equation for a shell with Reissner kinematics.

In Section 3.6 the strain energy assumed in terms of the *relaxed* right stretching tensor, is expressed in terms of the corresponding shell tensors, and integrated over the shell thickness. Constitutive equations for shell counterparts of the *relaxed* Biot stress are found. Two materials are considered, the 1st order (linear) one, which yields uncoupled constitutive equations, and the 2nd order Mooney-Rivlin incompressible material, for which the coupled constitutive equations are derived.

Some of the normal strain components vanish due to the Reissner hypotheses but can be recovered, and expressed in terms of other strain components. Two auxiliary conditions are exploited in Section 3.7; the plane stress condition for the 1st order material, and the incompressibility condition for 2nd order Mooney-Rivlin material. The constitutive equations including the normal strain effects are specified.

In Section 3.8 several numerical examples, displaying highly nonlinear equilibrium paths with singular points and the corresponding sensitivity charts are presented. The design sensitivities of displacements and rotations, are calculated along the equilibrium paths, in the whole pre- and post-critical range. In particular, the design sensitivity of the drilling rotation for the in-plane bending problem are calculated. Besides, the implementation of the membrane part of a four-node finite element with drilling rotation is described, and also the method of calculating the design sensitivities is presented.

The equations of a finite rotation-extensible director beam, and numerical models of multi-layer beams are developed in Chapter 4.

Section 4.1 presents a theory of a beam with kinematics based on the generalized Reissner hypothesis, with and additional scalar parameter for the transverse extension. The beam strain and change of curvature measures are obtained from the right stretch strain, and the virtual work is given for the Biot type stress and couple resultants. The strain energy for the 1st order isotropic elastic material is assumed in terms of the right stretch strain, and the constitutive equations for the beam stress and couple resultants are derived.

In Section 4.2 the general equations, derived in the preceding section, are simplified on use of the assumptions limiting rotations and extensibility in the thickness direction. Then, a procedure of constructing the interface variable model and the hierarchical model for multi-layer beams is developed. The interface variable model is characterized by a linear approximation of the tangent displacement, and a constant transverse displacement across the thickness of a layer, what conforms with the results of exact three-dimensional analyses presented in [Srinivas, 1973] and [Pagano, Soni, 1983]. The deformation of a layered cross-section is described using the interface variables for each layer and the compatibility conditions at layer interfaces.

The number of the interface variables is proportional to the number of layers, and hence, in the case of many layers, can cause problems with storage and the time of computation. One of the ways of dealing with this problem is to eliminate a part of variables at the layer level, what however requires the computation of $[K_{11}^p]^{-1}$ for each sub-layer, [Owen, Li, 1987], eq.(18). In the present work, the number of variables is reduced by expanding the tangent displacements in Taylor or Chebyshev series and using the coefficients of the truncated series as new unknowns. The number of terms retained in the series is optional, and the model is hierarchical in the thickness direction. Therefore, the accuracy of the layer-wise theory, or the effectiveness of the single-layer theory of arbitrary order can be obtained depending on the problem solved. A finite element based on the presented procedure is developed, and its accuracy and versatility are confirmed on several numerical examples.

The stress recovery procedure discussed in Section 4.3, refers to the multi-layer element of assembled Timoshenko beam elements described in the preceding section, see [Wisniewski, Schrefler, 1993a, 1993b]. In the case of layers made of different materials the distribution of stresses is not as regular as for a beam with a homogeneous cross-section.

Hence, it is better to compute stresses than the stress and couple resultants, which are integrals of stresses over the thickness. Besides, the stresses cannot be calculated directly, as then they strongly depend on properties of the approximation functions, and are unrealistic for a multi-layer cross-section. Therefore, an enhanced stress calculation procedure is proposed, minimizing the square of the difference between the discontinuous and smoothing stresses, for both expressed in terms of nodal values. Numerical calculations show very good accordance of stresses yielded by this procedure with two-dimensional results.

In Section 4.4 two finite element models are developed from the finite rotation/ extensible director theory specified in Section 4.1. The tangent operator for the Newton-Raphson scheme is calculated, and a uniformly under-integrated, isoparametric, two-noded beam finite element is constructed. The tangent matrix of the element with the extensible director possesses one spurious (zero-energy) mode, and a stabilization method is proposed. Next, it is shown that, even in case of finite rotations, four parameters of the beam can be expressed (consistently with the defined kinematics) in terms of the interface variables. The incremental transformation matrix is derived, and the two-noded beam element is converted to a four-noded plane stress quadrilateral. Finally, both elements are tested on several numerical examples, some exhibiting highly nonlinear characteristics, in order to assess their accuracy.

While the detailed conclusions are presented within chapters, in Chapter 5 we present remarks summarizing the author's original contribution.

In Appendix A a hyperelastic constitutive equation for the rotated Biot stress is derived. The forward-rotated Biot stress and the right stretch strain are defined, and the virtual work of the rotated stress is found. It is shown that it involves a co-rotational variation of the Green- McInnis- Naghdi type. For the strain energy assumed in terms of principal invariants of the right stretching tenor, a constitutive equation and a constitutive (4th rank) operator for the Biot stress is derived. Subsequently, they are subjected to the rotate-forward operation, and it is demonstrated how their structure is carried over to the rotated measures, see [Wisniewski, Turska, 1996].

1.4 Notation

A convected orthonormal system of curvilinear coordinates S^α, $\alpha = 1,2$ is used in this chapter. The bases used are denoted as follows. The reference basis: $\{\mathbf{i}_i\}$, i=1,2,3. The local bases for the initial configuration: $\{\mathbf{t}_i\}$- the orthonormal basis at the middle surface, $\{\mathbf{g}^i\}$ and $\{\mathbf{g}_i\}$- the normal bases at an arbitrary surface.

Notation: small bold letters - vectors, capital bold letters - 2nd rank tensors, capital bold letters with a digit 4 above them - 4th rank tensors, dots "$\cdot$" - scalar products of vectors and tensors, colons ":" - contractions of a 4th and a 2nd rank tensor over two last base vectors yielding a 2nd rank tensor, "$\otimes$" - tensorial products. A split of an arbitrary 2nd rank tensor into a symmetric and a skew-symmetric part is written as $\mathbf{T} = \mathrm{sym}\mathbf{T} + \mathrm{skew}\mathbf{T}$, where $\mathrm{sym}\mathbf{T} = \frac{1}{2}[\mathbf{T} + \mathbf{T}^T]$ and $\mathrm{skew}\mathbf{T} = \frac{1}{2}[\mathbf{T} - \mathbf{T}^T]$.

Within a chapter, the equations are referred to with omission of the first part of the equation number, which indicates the chapter.

2 Finite rotations: parametrization and algorithmic treatment

2.1 Rotation of vector around axis

Consider an arbitrary vector $\mathbf{v}$ rotated around the axis $\mathbf{e}$ by an angle ω, see Fig.2.1. The position of the rotated vector $\mathbf{v}'$ can be obtained from the following formula

$$\mathbf{v}' = \mathbf{v} + \Delta\mathbf{v}, \qquad \Delta\mathbf{v} = \overrightarrow{PQ} + \overrightarrow{QP}' \tag{2.1}$$

where

$$\overrightarrow{PQ} = -\mathbf{e}_1\, \rho\, (1 - \cos\omega), \qquad \overrightarrow{QP}' = \mathbf{e}_2\, \rho\, \sin\omega, \qquad \rho = |\mathbf{v}| \sin\alpha$$

Here, α is an angle between $\mathbf{e}$ and $\mathbf{v}$. The orthonormal vectors $\mathbf{e}_1$ and $\mathbf{e}_2$ of the local basis can be defined in terms of $\mathbf{e}$ and $\mathbf{v}$ as follows

$$\mathbf{e}_2 = \frac{\mathbf{e} \times \mathbf{v}}{|\mathbf{e} \times \mathbf{v}|}, \qquad \mathbf{e}_1 = \mathbf{e}_2 \times \mathbf{e} \tag{2.2}$$

After elementary algebraic transformations, we have

$$\mathbf{v}' = \mathbf{v} + \sin\omega\, (\mathbf{e} \times \mathbf{v}) + (1 - \cos\omega)\, [\mathbf{e} \times (\mathbf{e} \times \mathbf{v})] \tag{2.3}$$

Let us introduce a tensor $\mathbf{S} \in so(3)$, where $so(3)$ is a linear space of skew-symmetric tensors, such that $\mathbf{e}$ is its axial vector, i.e. $\mathbf{Se} = \mathbf{0}$. Useful properties of $\mathbf{S}$ are given in Table 2.1. This tensor is isotropic in the plane perpendicular to $\mathbf{e}$, and hence can be expressed by an arbitrary pair of orthonormal vectors belonging to this plane. E.g. $\mathbf{S} \equiv \mathbf{e}_2 \otimes \mathbf{e}_1 - \mathbf{e}_1 \otimes \mathbf{e}_2$, where $\mathbf{e}_1$ and $\mathbf{e}_2$ may, but need not, be identified with vectors of eq.(1). Then, the cross-products from eq.(3) can be expressed as follows

$$\mathbf{e} \times \mathbf{v} = \mathbf{Sv}, \qquad \mathbf{e} \times (\mathbf{e} \times \mathbf{v}) = \mathbf{S}^2\mathbf{v} \tag{2.4}$$

and this equation can be re-written in the following form

$$\mathbf{v}' = \mathbf{R}\, \mathbf{v}, \qquad \mathbf{R} \equiv \mathbf{I} + \sin\omega\mathbf{S} + (1 - \cos\omega)\mathbf{S}^2 \tag{2.5}$$

Here, $\mathbf{R}$ is a rotation tensor, which belongs to the special orthogonal group, $SO(3)$. See properties of $\mathbf{R}$ listed in Table 2.2. The orthogonality condition $\mathbf{R}\mathbf{R}^T = \mathbf{I}$ yields 6 conditions ($\mathbf{R}\mathbf{R}^T$ is symmetric) and only 3 parameters of $\mathbf{R}$ are independent. The condition for the determinant $\det\mathbf{R} = 1$ precludes reflection. See Fig.2.2 for graphical representation of $\Delta\mathbf{v} = (\mathbf{R} - \mathbf{I})\mathbf{v}$, which explains the meaning of particular terms of $\mathbf{R}$.

Note that both introduced tensors share the eigenvector $\mathbf{e}$, as $\mathbf{Se} = 0\mathbf{e}$ and $\mathbf{Re} = 1\mathbf{e}$, which, as we recall, defines the axis of rotation.

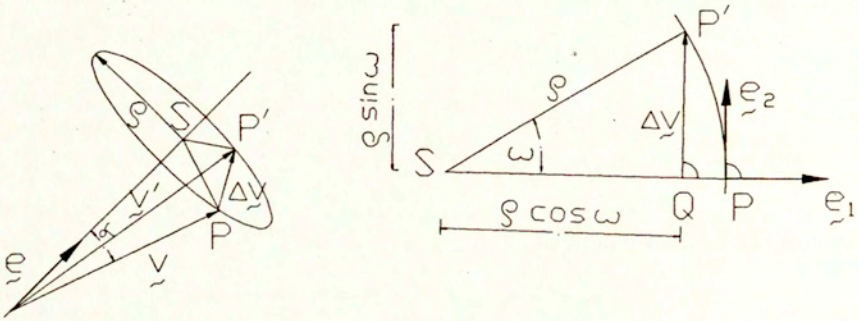

Fig.2.1 Rotation of vector **v** around axis **e**

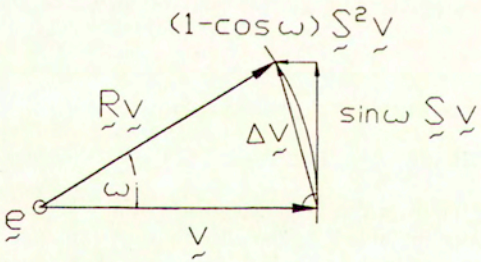

Fig.2.2 Components vectors of $\Delta \mathbf{v} = (\mathbf{R} - \mathbf{I})\mathbf{v}$

Table 2.1. Properties of $\mathbf{S}$

dyadic representation:	$\mathbf{S} = \mathbf{e}_2 \otimes \mathbf{e}_1 - \mathbf{e}_1 \otimes \mathbf{e}_2, \qquad \mathbf{e}_1, \mathbf{e}_2 \perp \mathbf{e}$
skew-symmetricity:	$\mathbf{S}^T = -\mathbf{S}$
powers:	odd $\mathbf{S}^{2n+1} = (-1)^n \mathbf{S}$ i.e. $\mathbf{S}$, $\mathbf{S}^3 = -\mathbf{S}$, $\mathbf{S}^5 = \mathbf{S}$, $\mathbf{S}^7 = -\mathbf{S}, \ldots$ even $\mathbf{S}^{2n+2} = (-1)^{n+2}\mathbf{S}^2$, $n = 0, 1, \ldots$ i.e. $\mathbf{S}^2$, $\mathbf{S}^4 = -\mathbf{S}^2$, $\mathbf{S}^6 = \mathbf{S}^2$, $\mathbf{S}^8 = -\mathbf{S}^2, \ldots$ where $\mathbf{S}^2 = \mathbf{SS} = -[\mathbf{e}_1 \otimes \mathbf{e}_1 + \mathbf{e}_2 \otimes \mathbf{e}_2] = \mathbf{e} \otimes \mathbf{e} - \mathbf{I}$
norms:	$\|\mathbf{S}\|_E = \sqrt{\mathbf{S} \cdot \mathbf{S}} = \sqrt{2}, \quad \|\mathbf{S}\|_2 = 1$
scalar invariants:	$\mathrm{tr}\mathbf{S} = 0, \quad \mathrm{tr}\mathbf{S}^2 = -2, \quad \det \mathbf{S} = 0$
principal invariants:	$I_1(\mathbf{S}) = 0, \quad I_2(\mathbf{S}) = 1, \quad I_3(\mathbf{S}) = 0$
eigenpair in $\mathbb{R} \times \mathbb{R}^3$:	$\{0, \mathbf{e}\}$ i.e. $(\mathbf{S} - 0\mathbf{I})\mathbf{e} = \mathbf{0}$
zero products:	$\mathbf{Se} = \mathbf{0}, \quad \mathbf{S}(\mathbf{e} \otimes \mathbf{e}) = \mathbf{0}, \quad \mathbf{S} \cdot (\mathbf{e} \otimes \mathbf{e}) = 0, \quad \mathbf{S}^2\mathbf{e} = \mathbf{0}$
relation to rotations:	$\mathbf{S} = \frac{1}{\sin\omega}(\mathbf{R} - \mathbf{R}^T), \quad \mathbf{S}^2 = \frac{1}{2(1-\cos\omega)}(\mathbf{R} + \mathbf{R}^T - 2\mathbf{I})$

Table 2.2. Properties of $\mathbf{R}$

dyadic representation:	$\mathbf{R} = \mathbf{I} + \sin\omega\, \mathbf{S} + (1 - \cos\omega)\, \mathbf{S}^2$
exponential representation:	$\mathbf{R} = \exp(\omega\mathbf{S}) = \mathbf{I} + \omega\mathbf{S} + \frac{1}{2!}\omega^2\mathbf{S}^2 + \ldots$
orthogonality:	$\mathbf{R}^T = \mathbf{R}^{-1}$
norms:	$\|\mathbf{R}\|_E = \sqrt{\mathbf{R} \cdot \mathbf{R}} = \sqrt{3}, \quad \|\mathbf{R}\|_2 = 1$
scalar invariants:	$\mathrm{tr}\mathbf{R} = 1 + 2\cos\omega, \quad \mathrm{tr}\mathbf{R}^2 = 1 + 2\cos 2\omega, \quad \det \mathbf{R} = 1$
principal invariants:	$I_1(\mathbf{R}) = \; I_2(\mathbf{R}) = 1 + 2\cos\omega, \quad I_3(\mathbf{R}) = 1$
eigenpair in $\mathbb{R} \times \mathbb{R}^3$:	$\{1, \mathbf{e}\}$ i.e. $(\mathbf{R} - 1\mathbf{I})\mathbf{e} = 0$
products:	$\mathbf{Re} = \mathbf{e}, \quad \mathbf{R}(\mathbf{e} \otimes \mathbf{e}) = \mathbf{e} \otimes \mathbf{e}$
invariance of length:	$\|\mathbf{Rx}\|_2 = \|\mathbf{x}\|_2, \qquad \mathbf{x}$ - vector
invariance of angle:	$\mathbf{x} \cdot \mathbf{y} = (\mathbf{Rx}) \cdot (\mathbf{Ry}), \qquad \mathbf{x}, \mathbf{y}$ - unit vectors

2.2 Left and right composition of rotations

Rotate a vector from position $\mathbf{v}$ to position $\mathbf{v}' = \overset{1}{\mathbf{R}}\,\mathbf{v}$ and then from position $\mathbf{v}'$ to position $\mathbf{v}'' = \overset{2}{\mathbf{R}}\,\mathbf{v}'$. Composing these two component rotations we obtain

$$\mathbf{v}'' = \overset{2}{\mathbf{R}}\,(\overset{1}{\mathbf{R}}\,\mathbf{v}) = (\overset{2}{\mathbf{R}}\overset{1}{\mathbf{R}})\mathbf{v} = \overset{t}{\mathbf{R}}\,\mathbf{v} \tag{2.6}$$

i.e. the rule for composing the rotation tensors, $\overset{t}{\mathbf{R}} \equiv \overset{2}{\mathbf{R}}\overset{1}{\mathbf{R}}$, where $\overset{t}{\mathbf{R}}$ is the total rotation. Unless both component rotation tensors share the same eigenvector, their composition is not commutative, i.e. $\overset{2}{\mathbf{R}}\overset{1}{\mathbf{R}} \neq \overset{1}{\mathbf{R}}\overset{2}{\mathbf{R}}$. However, we can introduce another rotation tensor, denoted in the sequel by $\overset{2}{\mathbf{R}}^{\bullet}$, which, when applied to $\overset{1}{\mathbf{R}}$ from the right, yields the same total rotation, i.e. $\overset{t}{\mathbf{R}} = \overset{1}{\mathbf{R}}\overset{2}{\mathbf{R}}^{\bullet}$. These two composition rules imply the relation

$$\overset{2}{\mathbf{R}}^{\bullet} = \overset{1}{\mathbf{R}}^{T}\,\overset{2}{\mathbf{R}}\,\overset{1}{\mathbf{R}} \tag{2.7}$$

which can be interpreted as a rotate-back operation performed on $\overset{2}{\mathbf{R}}$. From the above the following properties of $\overset{2}{\mathbf{R}}$ and $\overset{2}{\mathbf{R}}^{\bullet}$ can be derived.

1. In a back-rotated orthonormal basis $\mathbf{a}_i^{\bullet} = \overset{1}{\mathbf{R}}^{T}\mathbf{a}_i$ the representation of $\overset{2}{\mathbf{R}}^{\bullet}$ is equal to the representation of $\overset{2}{\mathbf{R}}$ in the basis $\{\mathbf{a}_i\}$. Note that for the back-rotated basis we have $\mathbf{a}_i^{\bullet} \otimes \mathbf{a}_j^{\bullet} = \overset{1}{\mathbf{R}}^{T}\,[\mathbf{a}_i \otimes \mathbf{a}_j]\;\overset{1}{\mathbf{R}}$, what validates this statement. It can be shown also in terms of components

$$\mathbf{a}_i^{\bullet} \cdot (\overset{1}{\mathbf{R}}^{T}\,\overset{2}{\mathbf{R}}\overset{1}{\mathbf{R}}\,\mathbf{a}_j^{\bullet}) = \mathbf{a}_i^{\bullet} \cdot (\overset{1}{\mathbf{R}}^{T}\,\overset{2}{\mathbf{R}}\,\mathbf{a}_j) = (\overset{2}{\mathbf{R}}^{T}\,\overset{1}{\mathbf{R}}\,\mathbf{a}_i^{\bullet}) \cdot \mathbf{a}_j = (\overset{2}{\mathbf{R}}^{T}\mathbf{a}_i) \cdot \mathbf{a}_j = \mathbf{a}_i \cdot (\overset{2}{\mathbf{R}}\,\mathbf{a}_j)$$

In other words, $\overset{2}{\mathbf{R}}^{\bullet}$ can be considered as $\overset{2}{\mathbf{R}}$, parallel transported from the currant to the back-rotated basis.

2. The eigenvalues of $\overset{2}{\mathbf{R}}$ and $\overset{2}{\mathbf{R}}^{\bullet}$ are identical and the eigenvectors are rotated like the basis. This results from the fact that the operation $\overset{1}{\mathbf{R}}^{T}\,\overset{2}{\mathbf{R}}\overset{1}{\mathbf{R}}$ is a similarity transformation. For $\overset{2}{\mathbf{R}}\,\boldsymbol{\lambda} = \mu\boldsymbol{\lambda}$ and $\boldsymbol{\lambda}^{\bullet} = \overset{1}{\mathbf{R}}^{T}\boldsymbol{\lambda}$ we can check that

$$\overset{2}{\mathbf{R}}^{\bullet}\boldsymbol{\lambda}^{\bullet} = (\overset{1}{\mathbf{R}}^{T}\,\overset{2}{\mathbf{R}}\overset{1}{\mathbf{R}})\boldsymbol{\lambda}^{\bullet} = \overset{1}{\mathbf{R}}^{T}\,\overset{2}{\mathbf{R}}\,(\overset{1}{\mathbf{R}}\,\boldsymbol{\lambda}^{\bullet}) = \overset{1}{\mathbf{R}}^{T}(\overset{2}{\mathbf{R}}\,\boldsymbol{\lambda}) = \overset{1}{\mathbf{R}}^{T}(\mu\boldsymbol{\lambda}) = \mu\boldsymbol{\lambda}^{\bullet}$$

and $\{\mu, \boldsymbol{\lambda}^{\bullet}\}$ is the eigenpair indeed.

3. The angles of rotation corresponding to $\overset{2}{\mathbf{R}}$ and $\overset{2}{\mathbf{R}}^{\bullet}$ are equal. Note that $\mathrm{tr}\,\overset{2}{\mathbf{R}}^{\bullet} = \mathrm{tr}(\overset{1}{\mathbf{R}}^{T}\,\overset{2}{\mathbf{R}}\overset{1}{\mathbf{R}}) = \mathrm{tr}(\overset{1}{\mathbf{R}}\overset{1}{\mathbf{R}}^{T}\,\overset{2}{\mathbf{R}}) = \mathrm{tr}\,\overset{2}{\mathbf{R}}$. Hence, the angles of rotation, if calculated from $\mathrm{tr}\,\overset{2}{\mathbf{R}} = 1 + 2\cos\overset{2}{\omega}$ and $\mathrm{tr}\,\overset{2}{\mathbf{R}}^{\bullet} = 1 + 2\cos\overset{2}{\omega}^{\bullet}$, are also equal.

The left and right composition rules are used in continuum mechanics also in conjunction with the polar decomposition of the deformation gradient,

$$\mathbf{F} = \mathbf{V}\,\mathbf{R} = \mathbf{R}\,\mathbf{U} \tag{2.8}$$

where $\mathbf{F}$ is the deformation gradient, and $\mathbf{V}, \mathbf{U}$ are the left and right stretching tensors. The above implies

$$\mathbf{U} = \mathbf{R}^T \mathbf{V}\, \mathbf{R} \tag{2.9}$$

which is a rotate-back operation performed on $\mathbf{V}$. Similarity of the above equation with eq.(7) is apparent, and hence also the properties (1 and 2) established earlier are valid, as they do not depend on the object being rotated.

Consider the deformation of the body characterized by the deformation gradient $\overset{1}{\mathbf{F}}$. Let the rotation $\overset{1}{\mathbf{R}}$ be defined as satisfying the polar decomposition equation, $\overset{1}{\mathbf{F}}=\overset{1}{\mathbf{V}}\overset{1}{\mathbf{R}}=\overset{1}{\mathbf{R}}\overset{1}{\mathbf{U}}$. Associate the basis $\{\mathbf{a}_i^*\}$ with the initial configuration of the body. Then, the basis $\{\mathbf{a}_i\}$, where $\mathbf{a}_i = \overset{1}{\mathbf{R}}\, \mathbf{a}_i^*$, is associated with the deformed configuration of the body. If $\overset{2}{\mathbf{R}}$ is expressed in $\{\mathbf{a}_i\}$ then $\overset{2}{\mathbf{R}^*}$ must be expressed in $\{\mathbf{a}_i^*\}$, to satisfy $\mathbf{a}_i^* \otimes \mathbf{a}_j^* = \overset{1}{\mathbf{R}}{}^T [\mathbf{a}_i \otimes \mathbf{a}_j]\ \overset{1}{\mathbf{R}}$. Additionally, assume that $\overset{1}{\mathbf{R}}$ is expressed in $\{\mathbf{a}_i^*\}$. In the sequel of the thesis we denote the initial basis as $\mathbf{a}_i^* = \mathbf{t}_i$. Summarizing both rules of composition we have

$$\overset{t}{\mathbf{R}} = \overset{2}{\mathbf{R}}(\mathbf{a}_i)\ \overset{1}{\mathbf{R}}(\mathbf{t}_i) = \overset{1}{\mathbf{R}}(\mathbf{t}_i)\ \overset{2}{\mathbf{R}^*}(\mathbf{t}_i) \tag{2.10}$$

When $\overset{1}{\mathbf{R}}$ is given and $\overset{t}{\mathbf{R}}$ is sought then either $\overset{2}{\mathbf{R}}$ or $\overset{2}{\mathbf{R}^*}$ can serve as the unknown, and the choice must match the description, which is used for the problem.

2.3 Parametrization of rotations

Several parametrizations of SO(3) have been compared in [Stuelpnagel, 1964], and it was found that four parameters provide a globally singularity free parametrization. The three-parameter approaches do not have this property, and can be used locally, for increments of rotations.

2.3.1 Euler (quaternion) parameters

The expression for the rotation tensor, which depends on four parameters $\{\omega, \mathbf{e}\}$, must be supplemented by the constraint on the length of $\mathbf{e}$,

$$\begin{cases} \mathbf{R} \equiv \mathbf{I} + \sin\omega \mathbf{S} + (1 - \cos\omega)\mathbf{S}^2 \\ \mathbf{e} \cdot \mathbf{e} = 1 \end{cases} \tag{2.11}$$

to yield three independent parameters. Easier to manipulate than the set $\{\omega, \mathbf{e}\}$ are the so called Euler (quaternion) parameters, see [Altman, 1986] for a broad exposition of questions related to quaternions. The quaternions are defined as

$$q_0 = \cos(\omega/2), \qquad \mathbf{q} = \sin(\omega/2)\mathbf{e} \tag{2.12}$$

Then, the set (11) becomes

$$\begin{cases} \mathbf{R} \equiv \mathbf{I} + 2q_0\tilde{\mathbf{q}} + 2\tilde{\mathbf{q}}\tilde{\mathbf{q}} \\ q_0^2 + \mathbf{q} \cdot \mathbf{q} = 1 \end{cases} \tag{2.13}$$

where the skew-symmetric tensor $\tilde{\mathbf{q}} = \sin(\omega/2)\mathbf{S}$. To obtain the expression with only 3 parameters, we can eliminate e.g. $q_0 = \sqrt{1 - \mathbf{q} \cdot \mathbf{q}}$ from the second equation. Then, the expression for the rotation tensor will depend on the square root, which can cause divergence of the Newton-Raphson method, as in the example given below.

Example. Consider the equation $y = \sqrt{1 - x^2} = 0$, and solve it by the Newton-Raphson method,

$$\begin{cases} y_i' \, \Delta x = -y_i \\ x_{i+1} = x_i + \Delta x \end{cases} \tag{2.14}$$

Here, $y_i = \sqrt{1 - x_i^2}$ and $y_i' = -x_i/\sqrt{1 - x_i^2}$. The argument of the square root function in y_i' is negative when $|x_i| > 1$. This value can be generated in course of iterating, hence the convergence of the process is not sure.

The present example has two other peculiarities. At the root, $x = 1$, the tangent operator $y' \to \infty$. If we solve the first of eq.(14) for Δx and insert it into the second equation then we obtain $x_{i+1} = 1/x_i$, thus eliminating the dependence on the square root. Even then, $|x_i| < 1$ yields $|x_{i+1}| > 1$, i.e. a start from the domain yields a value outside the domain.

2.3.2 Rotation vectors

The difficulties inherent in reducing of the number of parameters of the rotation tensor, can be avoided if the so called rotation vector (or pseudo-vector) is the primary variable. Three independent components of this vector are independent variables, while the axial vector $\mathbf{e}$ and the rotation angle ω are recovered only if necessary.

Several rotation vectors $\boldsymbol{\psi}$ have been proposed in the literature; all of them have the direction of $\mathbf{e}$, but differ in the length of the rotation vector. Some of them are discussed below. Let us denote the rotation vector by $\boldsymbol{\psi}$, and the associated skew-symmetric tensor by a tilde, as $\tilde{\boldsymbol{\psi}}$. In the derivation which follows we frequently use the relation $\tilde{\boldsymbol{\psi}} = \boldsymbol{\psi} \times \mathbf{I}$, where the cross-product of a vector and a tensor is defined as in [deBoer, p.74].

Canonical vector: $\boldsymbol{\psi} = \omega \mathbf{e}$

For $\boldsymbol{\psi} = \omega \mathbf{e}$ we have

$$\tilde{\boldsymbol{\psi}} = \omega \mathbf{S}, \qquad \tilde{\boldsymbol{\psi}}^2 = \omega^2 \mathbf{S}^2, \qquad \tilde{\boldsymbol{\psi}} \cdot \tilde{\boldsymbol{\psi}} = 2\omega^2 \tag{2.15}$$

The rotation tensor in eq.(5) can be represented in terms of the skew-symmetric $\tilde{\boldsymbol{\psi}}$ as follows

$$\mathbf{R} \equiv \mathbf{I} + \frac{\sin\omega}{\omega}\tilde{\boldsymbol{\psi}} + \frac{1 - \cos\omega}{\omega^2}\tilde{\boldsymbol{\psi}}^2, \qquad \omega^2 = \frac{1}{2}\tilde{\boldsymbol{\psi}} \cdot \tilde{\boldsymbol{\psi}} = \boldsymbol{\psi} \cdot \boldsymbol{\psi} = \|\boldsymbol{\psi}\|^2 \tag{2.16}$$

If $\mathbf{R}$ is known then we can recover

$$\tilde{\boldsymbol{\psi}} = \frac{\omega}{2\sin\omega}(\mathbf{R} - \mathbf{R}^T) \tag{2.17}$$

Remark. Note that

$$\lim_{\omega \to 0} \frac{\sin\omega}{\omega} = 1, \qquad \lim_{\omega \to 0} \frac{1 - \cos\omega}{\omega^2} = \frac{1}{2} \tag{2.18}$$

hence the representation (16) is singularity free. However, when the above limits are calculated numerically then the first one converges correctly, while the second does not. In double precision it becomes inaccurate starting from $\omega = 10^{-8}$. Note that the accuracy of calculating the sine and cosine functions in double precision is about 3×10^{-8}. The remedy is to use the identity $1-\cos\omega = 2\sin^2(\omega/2)$, and modify the calculated expression as follows

$$\frac{1-\cos\omega}{\omega^2} = 2\frac{\sin^2(\omega/2)}{\omega^2} = \frac{1}{2}\left[\frac{\sin(\omega/2)}{(\omega/2)}\right]^2 \tag{2.19}$$

what ensures correct convergence.

Semi-tangential vector: $\boldsymbol{\psi} = \tan(\omega/2)\mathbf{e}$

This vector is attributed to Rodrigues, see [Goldstein, 1980]. Denote $\tan(\omega/2) = t$. Then for $\boldsymbol{\psi} = t\mathbf{e}$ we have

$$\tilde{\boldsymbol{\psi}} = t\mathbf{S}, \qquad \tilde{\boldsymbol{\psi}}^2 = t^2\mathbf{S}^2, \qquad \tilde{\boldsymbol{\psi}} \cdot \tilde{\boldsymbol{\psi}} = 2t^2 \tag{2.20}$$

Transform the trigonometric functions in eq.(5) on use of

$$\sin\omega = \frac{2t}{1+t^2}, \qquad \cos\omega = \frac{1-t^2}{1+t^2} \tag{2.21}$$

and insert (20). The rotation tensor can be represented in terms of $\tilde{\boldsymbol{\psi}}$ as

$$\mathbf{R} \equiv \mathbf{I} + \frac{2}{1+t^2}\left(\tilde{\boldsymbol{\psi}} + \tilde{\boldsymbol{\psi}}^2\right) = (\mathbf{I}+\tilde{\boldsymbol{\psi}})(\mathbf{I}-\tilde{\boldsymbol{\psi}})^{-1}, \qquad t^2 = \frac{1}{2}\tilde{\boldsymbol{\psi}}\cdot\tilde{\boldsymbol{\psi}} = \boldsymbol{\psi}\cdot\boldsymbol{\psi} = \|\boldsymbol{\psi}\|^2 \tag{2.22}$$

If $\mathbf{R}$ is known then we can recover

$$\tilde{\boldsymbol{\psi}} = \frac{\mathbf{R}-\mathbf{R}^T}{1+\mathrm{tr}\mathbf{R}} \tag{2.23}$$

Remark. Note that the denominator in eq.(22) $1 + t^2 \neq 0$, and this representation is never singular. For $t \to \infty$ the functions of eq.(21) converge to 0 or -1, respectively, but, to handle numerically large values of t, the 2nd of eq.(21) should be transformed to $\cos\omega = -1 + 2(1+t^2)^{-1}$.

Sine vector: $\boldsymbol{\psi} = \sin\omega\mathbf{e}$

For $\boldsymbol{\psi} = \sin\omega\mathbf{e}$ we have

$$\tilde{\boldsymbol{\psi}} = \sin\omega\mathbf{S}, \qquad \tilde{\boldsymbol{\psi}}^2 = \sin^2\omega\mathbf{S}^2, \qquad \tilde{\boldsymbol{\psi}} \cdot \tilde{\boldsymbol{\psi}} = 2\sin^2\omega \tag{2.24}$$

Transform the trigonometric function in eq.(5) on use of the identity $\cos\omega = \sqrt{1-\sin^2\omega}$. On use of the above the rotation tensor can be represented in terms of the skew-symmetric $\tilde{\boldsymbol{\psi}}$ as follows

$$\mathbf{R} \equiv \mathbf{I} + \tilde{\boldsymbol{\psi}} + \frac{1}{1+\sqrt{1-\sin^2\omega}}\tilde{\boldsymbol{\psi}}^2, \qquad \sin^2\omega = \frac{1}{2}\tilde{\boldsymbol{\psi}}\cdot\tilde{\boldsymbol{\psi}} = \boldsymbol{\psi}\cdot\boldsymbol{\psi} = \|\boldsymbol{\psi}\|^2 \tag{2.25}$$

If $\mathbf{R}$ is known then we can recover

$$\tilde{\boldsymbol{\psi}} = \frac{1}{2}(\mathbf{R}-\mathbf{R}^T) \tag{2.26}$$

Remark. Note that the denominator in eq.(25) can be transformed as follows: $1 + \sqrt{1 - \sin^2\omega} = 1 + \cos\omega = 2\cos^2(\omega/2)$. Thus, $\omega = (2k+1)\pi$, $k = ..., -1, 0, 1, ...$ yields singularity of $\mathbf{R}$.

For all the above parametrizations, if the skew tensor $\tilde{\boldsymbol{\psi}}$ is known then we can compute its axial vector, angle of rotation, and the versor of the axis of rotation,

$$\boldsymbol{\psi} = \frac{1}{2}(\mathbf{I} \times \tilde{\boldsymbol{\psi}}), \qquad \omega = \arccos\frac{1}{2}(\mathrm{tr}\mathbf{R} - 1), \qquad \mathbf{e} = \boldsymbol{\psi}/\|\boldsymbol{\psi}\| \tag{2.27}$$

If values of ω exceed the range of arccos, i.e. $[0, \pi]$, then incremental formulae must be devised to update ω.

Note that in terms of components the relation between the skew-symmetric tensor and its axial vector is quite simple. Skew-symmetricity of $\tilde{\boldsymbol{\psi}}$ (i.e. $\tilde{\boldsymbol{\psi}} = -\tilde{\boldsymbol{\psi}}^T$) implies that its representation in an arbitrary basis must have the following form

$$(\tilde{\boldsymbol{\psi}})_{ij} = \begin{bmatrix} 0 & -a & -b \\ a & 0 & -c \\ b & c & 0 \end{bmatrix} \tag{2.28}$$

Assume the axial vector as $\boldsymbol{\psi} = \{\psi_1, \psi_2, \psi_3\}$. As $\det\tilde{\boldsymbol{\psi}} = 0$ hence the set of equations $\tilde{\boldsymbol{\psi}}\boldsymbol{\psi} = \mathbf{0}$ is undetermined, and one solution must be chosen. On use of $a = \psi_3$ the remaining two equations yield $b = -\psi_2$ and $c = \psi_1$. Then,

$$(\tilde{\boldsymbol{\psi}})_{ij} = \begin{bmatrix} 0 & -\psi_3 & \psi_2 \\ \psi_3 & 0 & -\psi_1 \\ -\psi_2 & \psi_1 & 0 \end{bmatrix}, \qquad (\tilde{\boldsymbol{\psi}}^2)_{ij} = \begin{bmatrix} \psi_1^2 - \psi^2 & \psi_2\psi_1 & \psi_3\psi_1 \\ \psi_1\psi_2 & \psi_2^2 - \psi^2 & \psi_3\psi_2 \\ \psi_1\psi_3 & \psi_2\psi_3 & \psi_3^2 - \psi^2 \end{bmatrix} \tag{2.29}$$

where ψ is the length of $\boldsymbol{\psi}$. Hence, the skew-symmetric tensor can be conveniently expressed in terms of the components of its axial vector.

2.3.3 Euler angles

Let us express the unit vector defining the axis of rotation in the spherical coordinates,

$$\mathbf{e} = \sin\omega_1\cos\omega_2\mathbf{t}_1 + \sin\omega_1\sin\omega_2\mathbf{t}_2 + \cos\omega_1\mathbf{t}_3 \tag{2.30}$$

where ω_1 and ω_2 are the so called Euler angles. Here $\omega_1 \in [0, \pi]$ is the angle measured from $\mathbf{t}_3$, and $\omega_2 \in (-\pi, \pi]$ is the angle between $\mathbf{t}_1$ and the projection of $\mathbf{e}$ on the plane $\{\mathbf{t}_1, \mathbf{t}_2\}$. It can be shown that for this parametrization any rotation is equivalent to the sequence of three elementary rotations,

$$\mathbf{R} = \mathbf{R}_3(\omega, \mathbf{e})\ \mathbf{R}_2(\omega_1, \mathbf{t}_1')\ \mathbf{R}_1(\omega_2, \mathbf{t}_3) \tag{2.31}$$

where $\mathbf{t}_1' = \mathbf{R}_1\mathbf{t}_1$ and $\mathbf{e} = \mathbf{t}_3'' = \mathbf{R}_2\mathbf{t}_3'$.

The elementary rotation is defined as a rotation around a chosen versor of the orthonormal basis. For instance, the elementary rotation around $\mathbf{t}_3$ is defined as follows: $\mathbf{e} = \mathbf{t}_3$, $\mathbf{e}_1 = \mathbf{t}_1$ and $\mathbf{e}_2 = \mathbf{t}_2$. Then, the skew-symmetric tensor and the rotation tensor are

$$\mathbf{S} = \mathbf{t}_2 \otimes \mathbf{t}_1 - \mathbf{t}_1 \otimes \mathbf{t}_2 \tag{2.32}$$

$$\mathbf{R} = \cos\omega_1(\mathbf{t}_1 \otimes \mathbf{t}_1 + \mathbf{t}_2 \otimes \mathbf{t}_2) + \sin\omega_1(\mathbf{t}_2 \otimes \mathbf{t}_1 - \mathbf{t}_1 \otimes \mathbf{t}_2) + \mathbf{t}_3 \otimes \mathbf{t}_3 \tag{2.33}$$

or in components,

$$(\mathbf{S})_{ij} = \begin{bmatrix} 0 & -1 & 0 \\ +1 & 0 & 0 \\ 0 & 0 & 0 \end{bmatrix}, \qquad (\mathbf{R})_{ij} = \begin{bmatrix} \cos\omega_1 & -\sin\omega_1 & 0 \\ +\sin\omega_1 & \cos\omega_1 & 0 \\ 0 & 0 & 1 \end{bmatrix} \tag{2.34}$$

This elementary rotation introduces one unknown parameter, ω_1.

The elementary rotations are not unique for $\omega_2 = (k-1)\pi$. In case of the infinitesimal rotations only two parameters are involved: $\omega_1 + \omega$ and ω_2.

The parametrization based on Euler angles is classical, and used for many problems of mechanics, such different as e.g. rigid body motion, [Hassenpflug, 1993], and crystal orientation, [Dluzewski, 1991]. It is also exploited in the description of rotation of the shell director in case of shell theories with two rotational parameters.

2.3.4 Two-parameter rotation of shell director

In the Reissner-type shell theories based on the Green strain only two rotational parameters can be assumed, as the rotation around the shell director does not influence these equations. Hence, the rotation vector is perpendicular to the director, i.e. $\boldsymbol{\psi} \cdot \mathbf{t}_3 = 0$, and a position of the axis of rotation is characterized by one parameter.

A survey of literature shows that dominate parametrizations based on the Euler angles, with rotations around the tangent basis vectors. For example in [Ramm, 1976] the following formula is used to describe a position of the shell director

$$\mathbf{a}_3 = \mathbf{R}_2(\pi/2 - \omega_2, \mathbf{t}_3')\ \mathbf{R}_1(\omega_1, \mathbf{t}_1)\ \mathbf{t}_2 = \mathbf{R}_1(\omega_1, \mathbf{t}_1)\ \mathbf{R}_2^*(\pi/2 - \omega_2, \mathbf{t}_3)\ \mathbf{t}_2 \tag{2.35}$$

where $\mathbf{t}_3' = \mathbf{R}_1\mathbf{t}_3$, and the angles ω_1 and ω_2 are shown in Fig.2.3. In the basis $\{\mathbf{t}_i\}$ the components are

$$(\mathbf{R}_1)_{ij} = \begin{bmatrix} 1 & 0 & 0 \\ 0 & c_1 & -s_1 \\ 0 & s_1 & c_1 \end{bmatrix}, \qquad (\mathbf{R}_2^*)_{ij} = \begin{bmatrix} c_2 & s_2 & 0 \\ -s_2 & c_2 & 0 \\ 0 & 0 & 1 \end{bmatrix}, \qquad (\mathbf{t}_2)_i = \begin{Bmatrix} 0 \\ 1 \\ 0 \end{Bmatrix} \tag{2.36}$$

where $s_1 = \sin\omega_1$, $c_1 = \cos\omega_1$ and $s_2 = \sin(\pi/2 - \omega_2)$, $c_2 = \cos(\pi/2 - \omega_2)$. On use of the trigonometric identities $\sin(\pi/2 - \omega_2) = \cos\omega_2$ and $\cos(\pi/2 - \omega_2) = \sin\omega_2$, and multiplication we obtain

$$(\mathbf{R}_1\mathbf{R}_2^*)_{ij} = \begin{bmatrix} s_2 & c_2 & 0 \\ -c_1c_2 & c_1s_2 & -s_1 \\ -s_1c_2 & s_1s_2 & c_1 \end{bmatrix}, \qquad (\mathbf{a}_3)_i = \begin{Bmatrix} c_2 \\ c_1s_2 \\ s_1s_2 \end{Bmatrix} \tag{2.37}$$

where $s_2 = \sin\omega_2$ and $c_2 = \cos\omega_2$.

Alternatively, the director can be related to the normal vector $\mathbf{t}_3$, see e.g. in [Wriggers, Gruttmann, 1993],

$$\mathbf{a}_3 = \mathbf{R}_2(\omega_1, \mathbf{t}_1')\ \mathbf{R}_1(\omega_2, \mathbf{t}_2)\ \mathbf{t}_3 = \mathbf{R}_1(\omega_2, \mathbf{t}_2)\ \mathbf{R}_2^*(\omega_1, \mathbf{t}_1)\ \mathbf{t}_3 \tag{2.38}$$

where $\mathbf{t}_1' = \mathbf{R}_1\mathbf{t}_1$. In the basis $\{\mathbf{t}_i\}$ the components are

$$(\mathbf{R}_1)_{ij} = \begin{bmatrix} c_2 & 0 & -s_2 \\ 0 & 1 & 0 \\ s_2 & 0 & c_2 \end{bmatrix}, \qquad (\mathbf{R}_2^*)_{ij} = \begin{bmatrix} 1 & 0 & 0 \\ 0 & c_1 & -s_1 \\ 0 & s_1 & c_1 \end{bmatrix}, \qquad (\mathbf{t}_3)_i = \begin{Bmatrix} 0 \\ 0 \\ 1 \end{Bmatrix} \tag{2.39}$$

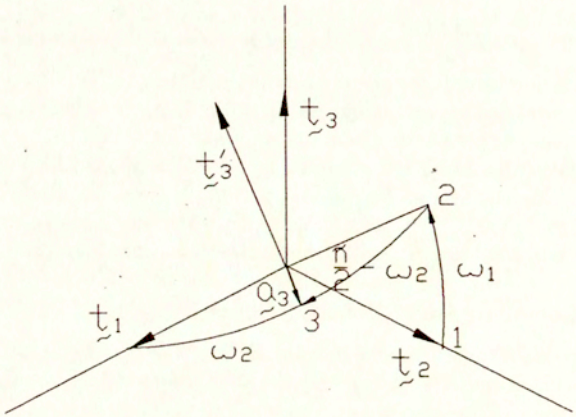

Fig.2.3 Position of shell director, [Ramm, 1986]

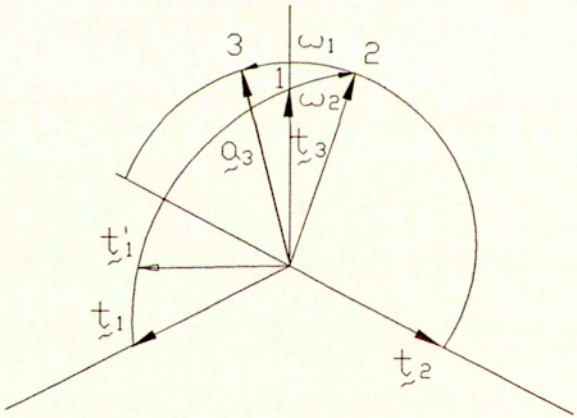

Fig.2.4 Position of shell director, [Wriggers, Gruttmann, 1993]

Here, $s_1 = \sin\omega_1$, $c_1 = \cos\omega_1$ and $s_2 = \sin\omega_2$, $c_2 = \cos\omega_2$, where ω_1 and ω_2 are defined in Fig.2.4. Then,

$$(\mathbf{R}_1\mathbf{R}_2^*)_{ij} = \begin{bmatrix} c_2 & -s_1s_2 & -c_1s_2 \\ 0 & c_1 & -s_1 \\ s_2 & s_1c_2 & c_1c_2 \end{bmatrix}, \qquad (\mathbf{a}_3)_i = \begin{Bmatrix} -c_1s_2 \\ -s_1 \\ c_1c_2 \end{Bmatrix} \tag{2.40}$$

2.4 Composition of rotation parameters

Euler parameters (quaternions)

A very convenient tool for the composition of rotations provide the quaternion parameters $\{q_0, \mathbf{q}\}$. The rotation tensor $\mathbf{R} \equiv \mathbf{I} + 2q_0\tilde{\mathbf{q}} + 2\tilde{\mathbf{q}}\tilde{\mathbf{q}}$ can be expressed in terms of the quaternion parameters as follows

$$\mathbf{R} \equiv (2q_0^2 - 1)\mathbf{I} + 2q_0\mathbf{q} \times \mathbf{I} + 2\mathbf{q} \otimes \mathbf{q} \tag{2.41}$$

where $q_0 = \cos(\omega/2)$ and $\mathbf{q} = \sin(\omega/2)\mathbf{e}$. Consider a tensorial product of two rotation tensors, i.e. $\overset{t}{\mathbf{R}} \equiv \overset{2}{\mathbf{R}}\overset{1}{\mathbf{R}}$, where

$$\overset{1}{\mathbf{R}} \equiv (2q_0^2 - 1)\mathbf{I} + 2q_0\mathbf{q} \times \mathbf{I} + 2\mathbf{q} \otimes \mathbf{q}, \qquad \overset{2}{\mathbf{R}} \equiv (2p_0^2 - 1)\mathbf{I} + 2p_0\mathbf{p} \times \mathbf{I} + 2\mathbf{p} \otimes \mathbf{p} \tag{2.42}$$

Note that $\overset{1}{\mathbf{R}}$ is expressed by the quaternion $\{q_0, \mathbf{q}\}$ and $\overset{2}{\mathbf{R}}$ by the quaternion $\{p_0, \mathbf{p}\}$. The total rotation must have the analogous form

$$\overset{t}{\mathbf{R}} \equiv (2r_0^2 - 1)\mathbf{I} + 2r_0\mathbf{r} \times \mathbf{I} + 2\mathbf{r} \otimes \mathbf{r} \tag{2.43}$$

Define the composition of quaternions as follows

$$\{p_0, \mathbf{p}\} \circ \{q_0, \mathbf{q}\} \equiv \{p_0q_0 - \mathbf{p} \cdot \mathbf{q}, \quad p_0\mathbf{q} + q_0\mathbf{p} + \mathbf{p} \times \mathbf{q}\} \tag{2.44}$$

If the quaternion corresponding to $\overset{t}{\mathbf{R}}$ is given as

$$\{r_0, \mathbf{r}\} = \{p_0, \mathbf{p}\} \circ \{q_0, \mathbf{q}\} \tag{2.45}$$

then $\overset{t}{\mathbf{R}} = \overset{2}{\mathbf{R}}\overset{1}{\mathbf{R}}$ is satisfied for representations (42) and (43), what can be checked by direct calculations. On use of eq.(43) the rotation tensor components are

$$(\overset{t}{\mathbf{R}})_{ij} = 2\begin{bmatrix} r_0^2 + r_1^2 - \frac{1}{2} & r_1r_2 - r_3r_0 & r_1r_3 + r_2r_0 \\ r_1r_2 + r_3r_0 & r_0^2 + r_2^2 - \frac{1}{2} & r_2r_3 - r_1r_0 \\ r_1r_3 - r_2r_0 & r_2r_3 + r_1r_0 & r_0^2 + r_3^2 - \frac{1}{2} \end{bmatrix} \tag{2.46}$$

for $\mathbf{r} = r_1\mathbf{t}_1 + r_2\mathbf{t}_2 + r_3\mathbf{t}_3$.

The angle of rotation and the vector defining the rotation axis can be extracted from the known quaternion as follows

$$\begin{cases} \overset{t}{\omega} = 2\arccos r_0 \\ \mathbf{e} = \mathbf{r}/\sqrt{\mathbf{r}\cdot\mathbf{r}} \end{cases} \qquad \text{or} \qquad \overset{t}{\omega} = 2\arcsin\sqrt{\mathbf{r}\cdot\mathbf{r}} \tag{2.47}$$

The formula with the arccos function should not be used for the values of argument around zero, while this with the arcsin function for the values of argument around one. Note that the arguments of both functions should be smaller than 1. The angle calculated from (47) is determined up to $2n\pi$, $n = ..., 0, -1, 0, ...$

Rotation vectors

A rule of composition in terms of the rotation vectors can be derived from the rule of composition for quaternions. The quaternion parameters in terms of the Euler parameters are defined as follows

$$q_0 = \cos(\omega_1/2), \qquad \mathbf{q} = \sin(\omega_1/2)\,\overset{1}{\mathbf{e}} \tag{2.48}$$

$$p_0 = \cos(\omega_2/2), \qquad \mathbf{p} = \sin(\omega_2/2)\,\overset{2}{\mathbf{e}} \tag{2.49}$$

$$r_0 = \cos(\omega_3/2), \qquad \mathbf{r} = \sin(\omega_3/2)\,\overset{3}{\mathbf{e}} \tag{2.50}$$

If we insert them into the formula (45), defining the product of quaternions, then we obtain

$$r_0 = c_1c_2 - s_1s_2(\overset{1}{\mathbf{e}}\cdot\overset{2}{\mathbf{e}}), \qquad \mathbf{r} = c_2s_1\,\overset{1}{\mathbf{e}} + c_1s_2\,\overset{2}{\mathbf{e}} - s_1s_2(\overset{1}{\mathbf{e}}\times\overset{2}{\mathbf{e}}) \tag{2.51}$$

where $s_i = \sin(\omega_i/2)$ and $c_i = \cos(\omega_i/2)$. On use of the semi-tangential rotation vectors $\overset{i}{\boldsymbol{\psi}} = \tan(\omega_i/2)\,\overset{i}{\mathbf{e}}$ the above equations yield

$$r_0 = c_1c_2\left[1 - t_1t_2(\overset{2}{\mathbf{e}}\cdot\overset{2}{\mathbf{e}})\right] = c_1c_2\left[1 - \overset{1}{\boldsymbol{\psi}}\cdot\overset{2}{\boldsymbol{\psi}}\right] \tag{2.52}$$

$$\mathbf{r} = c_1c_2\left[t_1\,\overset{1}{\mathbf{e}} + t_2\,\overset{2}{\mathbf{e}} - t_1t_2(\overset{1}{\mathbf{e}}\times\overset{2}{\mathbf{e}})\right] = c_1c_2\left[\overset{1}{\boldsymbol{\psi}} + \overset{2}{\boldsymbol{\psi}} - \overset{1}{\boldsymbol{\psi}}\times\overset{2}{\boldsymbol{\psi}}\right] \tag{2.53}$$

where $t_i = \tan(\omega_i/2)$. As $\overset{3}{\boldsymbol{\psi}} = \tan(\omega_3/2)\,\overset{3}{\mathbf{e}} = \mathbf{r}/r_0$ hence we obtain

$$\overset{3}{\boldsymbol{\psi}} = \frac{1}{1 - \overset{1}{\boldsymbol{\psi}}\cdot\overset{2}{\boldsymbol{\psi}}}\left(\overset{1}{\boldsymbol{\psi}} + \overset{2}{\boldsymbol{\psi}} - \overset{1}{\boldsymbol{\psi}}\times\overset{2}{\boldsymbol{\psi}}\right) \tag{2.54}$$

which furnishes the rule of composition of the semi-tangential rotation vectors. The above formula is singular for $\overset{1}{\boldsymbol{\psi}}\cdot\overset{2}{\boldsymbol{\psi}} = 1$, what reduces to $\tan(\omega_1/2)\tan(\omega_2/2) = 1$ for co-axial rotations.

For the other types of the rotation vectors the composition formulas are much more complicated.

Euler angles

The parametrization in terms of Euler angles can be given, as stated earlier, as a sequence of three elementary rotations around versors of an orthonormal basis, hence it inherently utilizes the rule for composition of rotation tensors. Here we only mention that for the right (material) composition of rotations the elementary rotations are performed around the initial (fixed) versors. Then the order of elementary rotations is reversed, and for eq.(31) we obtain

$$\mathbf{R} = \mathbf{R}_1(\omega_2, \mathrm{t}_3)\ \mathbf{R}_2^*(\omega_1, \mathrm{t}_1)\ \mathbf{R}_3^*(\omega, \mathrm{t}_3) \tag{2.55}$$

2.5 Variation of rotation tensor

Consider the left composition of rotations, $\overset{\mathrm{t}}{\mathbf{R}} = \overset{2}{\mathbf{R}}\ \mathbf{R}$, where $\overset{2}{\mathbf{R}} = \exp(\tilde{\theta})$ and the canonical skew-symmetric tensor $\tilde{\theta} \equiv \omega\ \overset{2}{\mathbf{S}}$. A variation of $\mathbf{R}$ is defined as the directional derivatives of $\overset{\mathrm{t}}{\mathbf{R}}$ at $\mathbf{R}$ in direction $\tilde{\theta}$,

$$\delta\mathbf{R} \equiv \frac{\mathrm{d}}{\mathrm{d}\epsilon}[\exp(\epsilon\tilde{\theta})\mathbf{R}]_{\epsilon=0} = \tilde{\theta}\mathbf{R} \tag{2.56}$$

Similarly for the right composition of rotations, $\overset{\mathrm{t}}{\mathbf{R}} = \mathbf{R}\ \overset{2}{\mathbf{R}}{}^*$, where $\overset{2}{\mathbf{R}}{}^* = \exp(\tilde{\Theta})$ and the canonical skew-symmetric tensor $\tilde{\Theta} \equiv \omega\ \overset{2}{\mathbf{S}}{}^*$. A variation of $\mathbf{R}$ is defined as the directional derivatives of $\overset{\mathrm{t}}{\mathbf{R}}$ at $\mathbf{R}$ in direction $\tilde{\Theta}$,

$$\delta\mathbf{R} \equiv \frac{\mathrm{d}}{\mathrm{d}\epsilon}[\mathbf{R}\exp(\epsilon\tilde{\Theta})]_{\epsilon=0} = \mathbf{R}\tilde{\Theta} \tag{2.57}$$

Eq.(56) and (57) provide a formula linking the left and right linearized rotations,

$$\tilde{\Theta} = \mathbf{R}^T\ \tilde{\theta}\ \mathbf{R}, \qquad \Theta = \mathbf{R}^T\theta \tag{2.58}$$

where Θ and θ are the associated axial vectors. Note that very often the skew tensors and their axial vectors are preceded by the symbol of variation, δ, i.e. $\delta\tilde{\Theta}$, $\delta\tilde{\theta}$ and $\delta\Theta$, $\delta\theta$.

The set of all infinitesimal rotations $\tilde{\theta}$ superposed onto a finite rotation $\mathbf{R}$, i.e. $T_R SO(3) = \{\tilde{\theta}\mathbf{R} \mid \text{for } \tilde{\theta} \in so(3)\}$, is referred to as the plane tangent to $SO(3)$ at $\mathbf{R}$. The initial tangent plane is defined as a plane tangent to $SO(3)$ at $\mathbf{I}$, and $T_I SO(3) = so(3)$.

2.6 Increments of rotation vectors

Below a relation between the linearized (infinitesimal) rotations belonging to the tangent spaces at two different rotations, namely $\mathbf{R}_A$ and $\mathbf{R}_B$, is established for the left composition rule. The relation between the rotation is equal to $\mathbf{R}_B = \overset{1}{\mathbf{R}}\ \mathbf{R}_A$, where

Table 2.3. Useful directional derivatives

$\mathrm{D}\mathbf{e}\cdot\mathbf{h} \equiv \frac{\mathrm{d}}{\mathrm{d}\epsilon}[\mathbf{e}+\epsilon\mathbf{h}]_{\epsilon=0} = -\mathbf{S}^2\mathbf{h}$
$\mathrm{D}\|\mathbf{e}\|\cdot\mathbf{h} \equiv \frac{\mathrm{d}}{\mathrm{d}\epsilon}\|\mathbf{e}+\epsilon\mathbf{h}\|_{\epsilon=0} = \mathbf{e}\cdot\mathbf{h}$
$\mathrm{D}\mathbf{R}\cdot\tilde{\boldsymbol{\theta}} \equiv \frac{\mathrm{d}}{\mathrm{d}\epsilon}[\exp(\epsilon\tilde{\boldsymbol{\theta}})\mathbf{R}]_{\epsilon=0} = \tilde{\boldsymbol{\theta}}\mathbf{R}$
$\mathrm{D}\mathbf{R}\cdot\tilde{\boldsymbol{\Theta}} \equiv \frac{\mathrm{d}}{\mathrm{d}\epsilon}[\mathbf{R}\exp(\epsilon\tilde{\boldsymbol{\Theta}})]_{\epsilon=0} = \mathbf{R}\tilde{\boldsymbol{\Theta}}$

$\overset{1}{\mathbf{R}} = \exp(\tilde{\boldsymbol{\psi}})$, see Fig.2.5, which explains the notation. The perturbed rotation $\mathbf{R}_{B\varepsilon}$ can be related to $\mathbf{R}_A$ and $\mathbf{R}_B$ as follows

$$\mathbf{R}_{B\varepsilon} = \exp(\varepsilon\tilde{\boldsymbol{\theta}}_B)\mathbf{R}_B, \qquad \mathbf{R}_{B\varepsilon} = \exp(\tilde{\boldsymbol{\psi}}_\varepsilon)\mathbf{R}_A \tag{2.59}$$

where $\tilde{\boldsymbol{\psi}}_\varepsilon = \tilde{\boldsymbol{\psi}} + \varepsilon\tilde{\boldsymbol{\theta}}_A$, or in terms of the axial vectors $\boldsymbol{\psi}_\varepsilon = \boldsymbol{\psi} + \varepsilon\boldsymbol{\theta}_A$, as $\tilde{\boldsymbol{\psi}}_\varepsilon = \boldsymbol{\psi}_\varepsilon \times \mathbf{I}$. Note that

$$\tilde{\boldsymbol{\psi}}\mathbf{R}_A \in T_{R_A}SO(3), \qquad \tilde{\boldsymbol{\psi}}_\varepsilon\mathbf{R}_A \in T_{R_A}SO(3), \qquad \tilde{\boldsymbol{\theta}}_B\mathbf{R}_B \in T_{R_B}SO(3) \tag{2.60}$$

i.e. the increments $\tilde{\boldsymbol{\theta}}_A$ and $\tilde{\boldsymbol{\theta}}_B$ belong to different tangent spaces. Equating both expressions for $\mathbf{R}_{B\varepsilon}$ we obtain

$$\exp(\varepsilon\tilde{\boldsymbol{\theta}}_B)\mathbf{R}_B = \exp(\tilde{\boldsymbol{\psi}}_\varepsilon)\mathbf{R}_A \tag{2.61}$$

which reduces to

$$\exp(\varepsilon\tilde{\boldsymbol{\theta}}_B) = \exp(\tilde{\boldsymbol{\psi}}_\varepsilon)\exp(-\tilde{\boldsymbol{\psi}}) \tag{2.62}$$

Note that $\exp(\tilde{\boldsymbol{\psi}}_\varepsilon)\exp(-\tilde{\boldsymbol{\psi}}) \neq \exp(\tilde{\boldsymbol{\psi}}_\varepsilon - \tilde{\boldsymbol{\psi}})$. This equation can be re-written in terms of the rotation vectors and then linearized with respect to $\boldsymbol{\theta}_A$ and $\boldsymbol{\theta}_B$. Define the semi-tangential rotation vectors as follows

$$\overline{\boldsymbol{\psi}} \equiv \tan(\|\boldsymbol{\psi}\|/2)\frac{\boldsymbol{\psi}}{\|\boldsymbol{\psi}\|}, \qquad \overline{\boldsymbol{\psi}_\varepsilon} \equiv \tan(\|\boldsymbol{\psi}_\varepsilon\|/2)\frac{\boldsymbol{\psi}_\varepsilon}{\|\boldsymbol{\psi}_\varepsilon\|} \tag{2.63}$$

$$\overline{\varepsilon\boldsymbol{\theta}_B} \equiv \tan(\|\varepsilon\boldsymbol{\theta}_B\|/2)\frac{\varepsilon\boldsymbol{\theta}_B}{\|\varepsilon\boldsymbol{\theta}_B\|} \tag{2.64}$$

where the new vectors are marked by a horizontal line. On use of the rule of composition for these vectors (54) we obtain the following equation corresponding to eq.(62)

$$\overline{\varepsilon\boldsymbol{\theta}_B} = \frac{1}{1+\overline{\boldsymbol{\psi}_\varepsilon}\cdot\overline{\boldsymbol{\psi}}}\left[-\overline{\boldsymbol{\psi}} + \overline{\boldsymbol{\psi}_\varepsilon} + \overline{\boldsymbol{\psi}} \times \overline{\boldsymbol{\psi}_\varepsilon}\right] \tag{2.65}$$

This equation is nonlinear w.r.t. $\boldsymbol{\theta}_A$ and $\boldsymbol{\theta}_B$, and is linearized in the sequel. Taking a derivative of this equation with respect to ε at $\varepsilon = 0$ we obtain for the left-hand-side the expression

$$\left.\frac{d}{d\varepsilon}\right|_{\epsilon=0} (\text{l-h-s}) = \boldsymbol{\theta}_B/2 \tag{2.66}$$

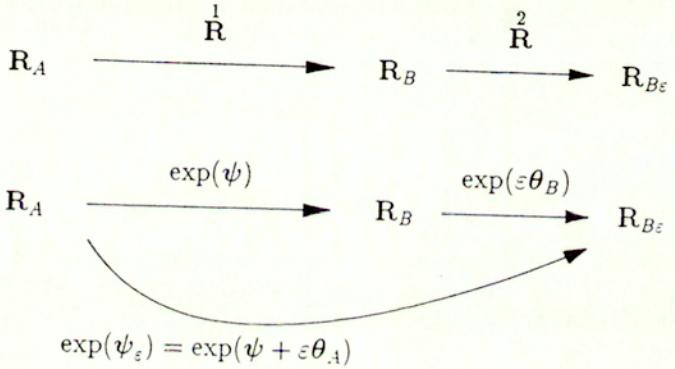

Fig.2.5 Scheme of increments of rotations

and for the right-hand-side expression

$$\left.\frac{d}{d\varepsilon}\right|_{\varepsilon=0} (\text{r-h-s}) = \frac{1}{1+\|\overline{\boldsymbol{\psi}}\|^2}\left(\mathbf{I}+\overline{\boldsymbol{\psi}}\times\mathbf{I}\right) D\overline{\boldsymbol{\psi}}\cdot\boldsymbol{\theta}_A \tag{2.67}$$

where

$$D\overline{\boldsymbol{\psi}}\cdot\boldsymbol{\theta}_A = \boldsymbol{\theta}_A\left[\frac{\tan(\omega/2)}{\omega}(\mathbf{I}-\mathbf{e}\otimes\mathbf{e})+\frac{1}{2\cos^2(\omega/2)}\mathbf{e}\otimes\mathbf{e}\right] \tag{2.68}$$

where $\omega = \|\boldsymbol{\psi}\|$ and $\mathbf{e} \equiv \boldsymbol{\psi}/\|\boldsymbol{\psi}\|$. Finally, after algebraic transformations, we obtain a linearized form of eq.(62)

$$\boldsymbol{\theta}_B = \boldsymbol{\theta}_A \mathbf{T}(\boldsymbol{\psi}) \tag{2.69}$$

where

$$\mathbf{T}(\boldsymbol{\psi}) = \frac{\sin\omega}{\omega}\mathbf{I}+\left[1-\frac{\sin\omega}{\omega}\right]\mathbf{e}\otimes\mathbf{e}-\frac{1}{2}\left[\frac{\sin(\omega/2)}{(\omega/2)}\right]^2\tilde{\boldsymbol{\psi}} \tag{2.70}$$

For $\boldsymbol{\psi}\to 0$ we find that $\mathbf{T}(\boldsymbol{\psi})\to\mathbf{I}$. Alternatively, $\boldsymbol{\theta}_B = \mathbf{T}^T\boldsymbol{\theta}_A$, and in $\mathbf{T}^T$ the term with $\tilde{\boldsymbol{\psi}}$ will have the opposite sign than in $\mathbf{T}$. Note that so defined $\mathbf{T}$ is equal to $\mathbf{T}^{-1}$ from [Simo, Vu-Quoc, 1986], where the covariant implicit time-stepping algorithm is written in the material setting. The representation of $\mathbf{T}$ in the eigen-basis $\{\mathbf{e}_1, \mathbf{e}_2, \mathbf{e}\}$ is as follows

$$(\mathbf{T})_{ij} = \begin{bmatrix} a & -b & 0 \\ +b & a & 0 \\ 0 & 0 & 1 \end{bmatrix} \tag{2.71}$$

where $a = \sin\omega/\omega$ and $b = -(1-\cos\omega)/\omega$.

Remark. To verify the obtained form of $\mathbf{T}$, the value of $\boldsymbol{\theta}_B$ can be calculated numerically in two ways: on use of the formula (69) and exploiting the vectorial equation (65). For $\boldsymbol{\psi} = \{0,0,1\}$ and $\boldsymbol{\theta}_A$ with one entry taken as 10^{-8} while the other as zeros, both calculated $\boldsymbol{\theta}_B$ are in perfect agreement.

For the right rule of composition of rotations the transformation operator is derived in [Cardona, Geradin, 1988].

2.7 Symmetry of tangent operator

Consider a conservative system, e.g. a body of the hyper-elastic material and the deformation independent loads, for which a potential energy exists and depends on displacements and rotations. The question of symmetry of the tangent operator (stiffness matrix) for the Newton-Raphson method, yielded by the second directional derivative of the potential energy, is addressed. To fully consider the symmetry of the tangent operator, the displacements and rotations should be accounted for together, and the bi-invariant metric should be used, as e.g. in [Simo, 1992], also the more recent work of [Makowski, Stumpf, 1995]. However, for simplicity, in the sequel displacements are disregarded, and only the dependence of π on the rotations is considered. Denote the potential energy of the whole body as $\Pi = \int_V \pi dV$, where π is the potential energy density.

Assume that the reference rotation $\mathbf{R}_A = \mathbf{I}$ so that

$$\mathbf{R}_B = \exp(\tilde{\psi})\mathbf{R}_A = \mathbf{R}_A \exp(\tilde{\psi})^* = \exp(\tilde{\psi}) \tag{2.72}$$

for both composition rules. The same notation as in the preceding section is used here. The canonical rotation vector belonging to the initial tangent plane, i.e. $\tilde{\psi} \in T_I SO(3)$, is taken as the unknown. For the canonical parametrization of rotations we have

$$\mathbf{R}_B = \exp(\tilde{\psi}) = \mathbf{I} + \frac{\sin\omega}{\omega}\tilde{\psi} + \frac{1}{2}\left(\frac{\sin\omega/2}{\omega/2}\right)^2 \tilde{\psi}^2, \qquad \omega = \|\psi\| \tag{2.73}$$

In the sequel, we denote $\mathbf{R}_B = \mathbf{R}$, $\boldsymbol{\theta}_A = \boldsymbol{\theta}$, and $\Theta_A = \Theta$.

Recall from the preceding section that the perturbed rotation vector is $\boldsymbol{\psi}_\varepsilon = \boldsymbol{\psi} + \varepsilon\boldsymbol{\theta}$ and $\tilde{\boldsymbol{\psi}}_\varepsilon = \tilde{\boldsymbol{\psi}} + \varepsilon\tilde{\boldsymbol{\theta}} \in T_I SO(3)$. In the sequel we distinguish two differentials, which are defined as follows

$$\delta a = \frac{d}{d\varepsilon} a(\boldsymbol{\psi} + \varepsilon\boldsymbol{\theta}^-)\Big|_{\varepsilon=0}, \qquad \chi a = \frac{d}{d\varepsilon} a(\boldsymbol{\psi} + \varepsilon\boldsymbol{\theta}^+)\Big|_{\varepsilon=0} \tag{2.74}$$

The first and the second differential of the potential energy density are

$$\delta\pi = \frac{\partial\pi}{\partial\mathbf{R}} \cdot \delta\mathbf{R}, \qquad \chi(\delta\pi) = \chi\left(\frac{\partial\pi}{\partial\mathbf{R}}\right) \cdot \delta\mathbf{R} + \frac{\partial\pi}{\partial\mathbf{R}} \cdot \chi(\delta\mathbf{R}) \tag{2.75}$$

For the first component of the second differential we have

$$\chi\left(\frac{\partial\pi}{\partial\mathbf{R}}\right) \cdot \delta\mathbf{R} = \left(\left[\frac{\partial^2\pi}{\partial\mathbf{R}\partial\mathbf{R}}\right]\chi\mathbf{R}\right) \cdot \delta\mathbf{R} = \left(\left[\frac{\partial^2\pi}{\partial\mathbf{R}\partial\mathbf{R}}\right]^T \delta\mathbf{R}\right) \cdot \chi\mathbf{R} \tag{2.76}$$

The last form is obtained on use of the identity (K8) from [DeBoer, 1982], p.62, and the term in brackets is a 4th rank tensor. On use of $\delta\mathbf{R} = \tilde{\boldsymbol{\theta}}_B^- \mathbf{R}(\boldsymbol{\psi})$ and $\boldsymbol{\theta}_B^- = \boldsymbol{\theta}^- \mathbf{T}(\boldsymbol{\psi})$ as well as $\chi\mathbf{R} = \tilde{\boldsymbol{\theta}}_B^+ \mathbf{R}(\boldsymbol{\psi})$ and $\boldsymbol{\theta}_B^+ = \boldsymbol{\theta}^+ \mathbf{T}(\boldsymbol{\psi})$ we have

$$\delta\mathbf{R} = [\boldsymbol{\theta}^- \mathbf{T}] \times \mathbf{R}, \qquad \chi\mathbf{R} = [\boldsymbol{\theta}^+ \mathbf{T}] \times \mathbf{R} \tag{2.77}$$

where the left rule of composition is adopted. Above, $\mathbf{T} = \mathbf{T}(\boldsymbol{\psi})$ is the transformation operator for the rotation vectors, eq.(70). The cross-product of a vector and 2nd rank tensor is used in the standard way, see e.g. [deBoer, 1982]. From eq.(76) we can see that symmetry of the term in brackets implies symmetry of the whole component w.r.t. $\boldsymbol{\theta}^-$ and $\boldsymbol{\theta}^+$.

Note that at equilibrium, when $\partial\pi/\partial\mathbf{R} = \mathbf{0}$, the second component of $\chi(\delta\pi)$ vanishes. However, away from equilibrium its contribution is non trivial. The second differential of $\mathbf{R}$ in eq.(75) can be expressed as follows

$$\chi(\delta\mathbf{R}) = \frac{d}{d\varepsilon}\left\{[\boldsymbol{\theta}^- \mathbf{T}(\boldsymbol{\psi} + \varepsilon\boldsymbol{\theta}^+)] \times \mathbf{R}(\boldsymbol{\psi} + \varepsilon\boldsymbol{\theta}^+)\right\}\Big|_{\varepsilon=0} \tag{2.78}$$

A derivative with respect to the scalar ε of a cross-product of a vector and a tensor is $(\mathbf{a} \times \mathbf{A})' = \mathbf{a}' \times \mathbf{A} + \mathbf{a} \times \mathbf{A}'$, and hence we can write

$$\chi(\delta\mathbf{R}) = [\boldsymbol{\theta}^- \chi\mathbf{T}] \times \mathbf{R} + [\boldsymbol{\theta}^- \mathbf{T}] \times \chi\mathbf{R} \tag{2.79}$$

The differential $\chi\mathbf{R}$ is given in eq.(77), and hence the second component becomes

$$[\theta^-\mathbf{T}] \times \chi\mathbf{R} = [\theta^-\mathbf{T}] \times \Big\{[\theta^+\mathbf{T}] \times \mathbf{R}\Big\} = \Big\{[\theta^-\mathbf{T}] \otimes [\theta^+\mathbf{T}] - ([\theta^-\mathbf{T}] \cdot [\theta^+\mathbf{T}])\mathbf{I}\Big\}\,\mathbf{R} \quad (2.80)$$

where the identity $\mathbf{a} \times \{\mathbf{b} \times \mathbf{C}\} = \{\mathbf{a} \otimes \mathbf{b} - (\mathbf{a} \cdot \mathbf{b})\mathbf{I}\}\,\mathbf{C}$ is used. Furthermore,

$$[\theta^-\mathbf{T}] \otimes [\theta^+\mathbf{T}] = \mathbf{T}^T(\theta^- \otimes \theta^+)\mathbf{T} \quad (2.81)$$

We can see that the dot product in eq.(80) is symmetric with respect to θ^- and θ^+ but the tensorial product is not. The differential of $\mathbf{T}$ in the first component of eq.(79) is as follows

$$\begin{aligned} \chi\mathbf{T} = D\mathbf{T} \cdot \theta^+ \;&=\; a_1\,(\mathbf{I} \otimes \mathbf{e})\theta^+ \;+\; a_2\,(\theta^+ \otimes \mathbf{e} + \mathbf{e} \otimes \theta^+) \\ &+\; a_3\,(\mathbf{e} \otimes \mathbf{e} \otimes \mathbf{e})\theta^+ \;+\; a_4\,(\tilde{\psi} \otimes \mathbf{e})\theta^+ \;+\; a_5\,(\theta^+ \times \mathbf{I}) \end{aligned} \quad (2.82)$$

where $\mathbf{e} = \psi/\|\psi\|$, and the coefficients are

$$a_1 = \frac{\cos\omega}{\omega} - \frac{\sin\omega}{\omega^2}, \qquad a_2 = \frac{1}{\omega} - \frac{\sin\omega}{\omega^2}, \qquad a_3 = 3\frac{\sin\omega}{\omega^2} - \frac{\cos\omega}{\omega} - \frac{2}{\omega}$$

$$a_4 = \frac{1}{\omega}\left(\frac{\sin\omega/2}{\omega/2}\right)^2 - \frac{\sin\omega}{\omega^2}, \qquad a_5 = -\frac{1}{2}\left(\frac{\sin\omega/2}{\omega/2}\right)^2$$

For $\psi \to \mathbf{0}$ we find that $\chi\mathbf{T} \to -\frac{1}{2}(\theta^+ \times \mathbf{I})$.

Remark. The derivation of the above formula is cumbersome, but its correctness can be verified easier. E.g. assume $(\psi)_i = \{0, 0, 1\}$ and $(\theta^+)_i = \{0, 0, \tau\}$, where τ is a small value chosen in the way established for the finite difference operators, [Dennis, Schnabel, 1983]. Then, calculate $D\mathbf{T} \cdot \theta^+$ in two ways: first using eq.(82) and then an approximate formula $D\mathbf{T} \cdot \theta^+ \approx \mathbf{T}(\psi + \theta^+) - \mathbf{T}(\psi)$.

For the derived $\chi\mathbf{T}$ the product in the first component of eq.(79) is as follows

$$\begin{aligned} [\theta^-\,\chi\mathbf{T}] \;&=\; a_1\,\theta^-(\mathbf{I} \otimes \mathbf{e})\theta^+ \;+\; a_2\,\theta^-\left(\theta^+ \otimes \mathbf{e} + \mathbf{e} \otimes \theta^+\right) \\ &+\; a_3\,\theta^-(\mathbf{e} \otimes \mathbf{e} \otimes \mathbf{e})\theta^+ \;+\; a_4\,\theta^-\left(\tilde{\psi} \otimes \mathbf{e}\right)\theta^+ \;+\; a_5\,\theta^-(\theta^+ \times \mathbf{I}) \end{aligned} \quad (2.83)$$

and, on multiplications,

$$\begin{aligned} [\theta^-\,\chi\mathbf{T}] \;&=\; a_1\,\theta^-(\mathbf{e} \cdot \theta^+) \;+\; a_2\,\left((\theta^- \cdot \theta^+)\mathbf{e} + (\theta^- \cdot \mathbf{e})\theta^+\right) \\ &+\; a_3\,(\theta^- \cdot \mathbf{e})(\mathbf{e} \cdot \theta^+)\mathbf{e} \;+\; a_4\,\theta^-(\mathbf{e} \cdot \theta^+)\tilde{\psi} \;+\; a_5\,\theta^+ \times \theta^- \end{aligned} \quad (2.84)$$

It is evident that only the first of the components pre-multiplied by a_2 and the component multiplied by a_3 are symmetric with respect to θ^- and θ^+. The fifth term is a vectorial product and also is not symmetric. An analogous result has been previously established e.g. by [Simo, Vu-Quoc, 1986] for spatial deformation of elastic rods, and by [Makowski, Stumpf, 1990] for shells undergoing a finite strain deformation.

Evaluate the 2nd differential at $\psi = \mathbf{0}$, for which $\mathbf{R} = \mathbf{I}$ and $\mathbf{T} = \mathbf{I}$. Then, we have

$$\delta\mathbf{R} = \theta^- \times \mathbf{I}, \qquad \chi\mathbf{R} = \theta^+ \times \mathbf{I}, \qquad \chi\mathbf{T} = -\frac{1}{2}\,(\theta^+ \times \mathbf{I}) \quad (2.85)$$

$$[\theta^- \chi \mathbf{T}] \times \mathbf{R} = \frac{1}{2}(\theta^+ \times \theta^-) \times \mathbf{I}, \qquad [\theta^- \mathbf{T}] \times \chi\mathbf{R} = \theta^- \times (\theta^+ \times \mathbf{I}) \tag{2.86}$$

$$\chi(\delta\mathbf{R}) = \frac{1}{2}\left[\theta^+ \times (\theta^- \times \mathbf{I}) + \theta^- \times (\theta^+ \times \mathbf{I})\right] \tag{2.87}$$

i.e. the second component of (75) becomes symmetric w.r.t. θ^- and θ^+.

Summarizing, for the left composition of rotations the transformation operator must be used to transform increments of the canonical rotation vectors to the initial tangent plane where they are compounded. Due to the presence of the transformation operator and the rotation tensor, the second differential of the potential energy is non-symmetric away from equilibrium, while at equilibrium, when $\partial\pi/\partial\mathbf{R} = \mathbf{0}$, it is symmetric.

Symmetry of the second differential is preserved at $\psi = 0$. To take advantage of this fact the tangent plane must be continuously updated, what renders that a directional derivative of a vector (such as the equilibrium equations) is identical to its covariant derivative. The continuous update of the tangent plane requires the update of the rotation $\mathbf{R}_B \leftarrow \exp(\tilde{\psi})\mathbf{R}_B$ and the co-rotational basis $\mathbf{a}_k \leftarrow \exp(\tilde{\psi})\mathbf{a}_k$ after each iteration in the Newton-Raphson scheme, see the so called Eulerian description of [Cardona, Geradin, 1988], and the procedure of [Buechter, Ramm, 1992].

Example. Rotation around the known axis

Consider a rotation of a unit vector $\mathbf{a}$ onto another vector $\mathbf{b}$, both belonging to the plane spanned by $\mathbf{t}_1$ and $\mathbf{t}_2$, around the axis of rotation $\mathbf{e} \equiv \mathbf{t}_3$, The governing equation can be written as follows

$$\mathbf{g} = \mathbf{R}\mathbf{a} - \mathbf{b} = \mathbf{0}, \qquad \mathbf{R} = \mathbf{R}(\omega, \mathbf{t}_3) \tag{2.88}$$

where $\mathbf{g}$ is a residual. This equation constitutes a set of two nonlinear equations for one unknown, ω. Note that due to periodicity of the sine and cosine functions each of the equations has multiple solutions; of our interest are only those which satisfy both equations. The solution is $\omega = \arccos(\mathbf{a}\cdot\mathbf{b}) + 2k\pi$, but we want to obtain it on use of the Newton-Raphson method combined with the penalty method. In terms of components we have

$$\mathbf{a} = a_1\mathbf{t}_1 + a_2\mathbf{t}_2, \qquad \mathbf{b} = b_1\mathbf{t}_1 + b_2\mathbf{t}_2 \tag{2.89}$$

$$\mathbf{S} = \mathbf{t}_2 \otimes \mathbf{t}_1 - \mathbf{t}_1 \otimes \mathbf{t}_2, \qquad \mathbf{S}^2 = -\mathbf{I}, \qquad \mathbf{R} = \cos\omega\mathbf{I} + \sin\omega\mathbf{S} \tag{2.90}$$

The Newton-Raphson scheme can be written as

$$D\mathbf{g}\cdot\Delta\omega = -\mathbf{g}, \qquad \omega = \bar{\omega} + \Delta\omega \tag{2.91}$$

where the differential of $\mathbf{g}$ is $D\mathbf{g}\cdot\Delta\omega = (D\mathbf{R}\cdot\Delta\omega)\mathbf{a}$. For

$$D\mathbf{R}\cdot\Delta\omega = \frac{d\mathbf{R}}{d\omega}\Delta\omega, \qquad \frac{d\mathbf{R}}{d\omega} = -\sin\omega\mathbf{I} + \cos\omega\mathbf{S} \tag{2.92}$$

we have

$$D\mathbf{g}\cdot\Delta\omega = (-\sin\omega\mathbf{I} + \cos\omega\mathbf{S})\mathbf{a}\Delta\omega = \mathbf{S}\mathbf{R}\mathbf{a}\Delta\omega \tag{2.93}$$

where the identity $\mathbf{S}^2 = -\mathbf{I}$ and the definition of $\mathbf{R}$ are used to obtain the last form. Note that $\mathbf{SR}$ defines the tangent plane at $\mathbf{R}$, and $\mathbf{SRa} = \mathbf{S}\bar{\mathbf{a}}$, where $\bar{\mathbf{a}} = \mathbf{R}\mathbf{a}$ is the updated (co-rotational) $\mathbf{a}$.

We use the penalty method with $\alpha = 10^{-10}$, and a strategy of choosing the order in which the equations are solved based on a comparison of residuals. To establish the convergence of this method the vector $\mathbf{a}$ is taken at 360 uniformly spaced initial locations, differing from $\mathbf{b}$ by the angle $0^\circ - 360^\circ$. For $\mathbf{b} = \{0, 1\}$ and the tolerance $\tau = 10^{-10}$, the convergence is attained on average in about 2.45 iteration per one starting point, with the maximum of 7 iterations. This fast convergence confirms that the method has been properly implemented. The same strategy but with the penalty number $\alpha = 0$ yields divergence for several starting points.

This example demonstrates that the advantage of updating the tangent plane also lies in separating the terms associated with the update of the rotated vector $\mathbf{a}$.

N.B. the covariant derivative can be obtained by symmetrization of the tangent operator yielded by the directional derivative, as shown in [Simo, 1992], what explains the correct rate of convergence of the Newton-Raphson method with the symmetrized tangent operator observed e.g. in [Crisfield, 1990].

In numerical applications, e.g. in a finite element code, it is convenient to continuously update the rotations and the co-rotational basis, on use of two sets of parameters for rotations:

1. the canonical rotation vector for increments of the rotation in the Newton-Raphson equations, as they involve only three parameters,

2. the quaternion parameters for updates, as they are easy to calculate from the rotation vector and can be conveniently updated,

In this way we can avoid complicated formulas for composition of canonical vectors. Comparing with the rotation tensor, only 4 parameters are stored instead of 9 and only operations on vectors are performed. The update procedure combining the canonical rotation vector $\boldsymbol{\theta} = \omega \mathbf{e}$ and the quaternion is given in Table 2.4.

Table 2.4. Update procedure. Known $(q_0, \mathbf{q})^i$ and $\Delta\boldsymbol{\theta}$

1. Find angle and axis of rotation for given increment $\Delta\boldsymbol{\theta}$
$$\Delta\omega = \|\Delta\boldsymbol{\theta}\| = \sqrt{\Delta\boldsymbol{\theta} \cdot \Delta\boldsymbol{\theta}}, \qquad \Delta\mathbf{e} = \Delta\boldsymbol{\theta}/\|\Delta\boldsymbol{\theta}\|$$

2. Find quaternion
$$\Delta q_0 = \cos(\Delta\omega/2), \qquad \Delta\mathbf{q} = \sin(\Delta\omega/2)\Delta\mathbf{e}$$

3. Update quaternion
$$(q_0)^{i+1} = \Delta q_0 (q_0)^i - \Delta\mathbf{q} \cdot (\mathbf{q})^i$$
$$(\mathbf{q})^{i+1} = \Delta q_0 (\mathbf{q})^i + (q_0)^i \Delta\mathbf{q} + \Delta\mathbf{q} \times (\mathbf{q})^i$$

4. Update vector $\mathbf{a}^{i+1} = \mathbf{R}\mathbf{a}^i \qquad (\mathbf{a}^0 = \mathbf{R}\mathbf{t})$
$$\mathbf{a}^{i+1} = (2\Delta q_0^2 - 1)\mathbf{a}^i + 2\Delta q_0 \Delta\mathbf{q} \times \mathbf{a}^i + 2(\Delta\mathbf{q} \cdot \mathbf{a}^i)\Delta\mathbf{q}$$

2.8 Conclusions

Summarizing, the rotation tensors, which are orthogonal non-commutative transformations, require a substantially different treatment than displacements. The contents of the present section addresses the following issues related to rotations.

1. It has been established that a successful numerical treatment of rotations sets several requirements. The parametrization of increments of rotations should be singularity free and involve three parameters, while the global parametrization of rotations, should also be non-singular, what requires more than three parameters, [Stuelpnagel, 1964], and the compounding formulas should have a convenient (vectorial) form. Several different parametrizations of rotations are presented, and those suitable for numerical implementations are identified. The canonical rotation vector is a convenient choice to parametrize the increments of rotations, however it is found that it involves the transformation operator from one tangent plane to another when used for compounding of the increments. Conversely the quaternion parameters, which are excellent only for compounding of the increments of rotations. It is shown that these two parametrizations can be conveniently matched together.

2. Symmetry of the tangent operator for problems depending explicitly on rotations should be preserved in course of the Newton-Raphson solution process, also for the configurations away from equilibrium. It is shown for a parametrization in terms of the canonical rotation vector, that this symmetry is disturbed by the presence of the rotation tensor and the transformation operator mentioned earlier. These effects can be neutralized when the tangent plane, in which the increments of rotations are compounded, is continuously updated. This can be achieved on use of the co-rotational basis, updated after each Newton-Raphson iteration.

3 Shell equations with independent rotations

3.1 Three-dimensional elasticity with independent rotations

In this section a three-dimensional elasticity is extended to include rotations as an independent variable via a polar decomposition of the deformation gradient. The presentation is similar to that of [Simo, Fox, Hughes, 1992], but with a constitutive equation for the Biot stress and the right stretch strain.

3.1.1 Formulation in terms of deformation

Consider a formulation in terms of deformation $\boldsymbol{\chi} : B \mapsto B_\chi$, where B is the reference and B_χ is the current (deformed) configuration of the body. The local balance equations and the boundary conditions are as follows:

1. linear momentum balance equation:

$$\mathrm{Div}\mathbf{P} + \rho_{\mathrm{R}}\mathbf{b} = \mathbf{0}, \qquad \mathrm{Div}\mathbf{P} \equiv (\mathrm{Grad}\mathbf{P})\,\mathbf{I} \tag{3.1}$$

   where $\mathbf{P}$ is the 1st Piola-Kirchhoff stress tensor (non-symmetric), ρ_R is the mass density for the reference (initial) configuration, and $\mathbf{b}$ is the body force.

2. rotational momentum balance equation:

$$\mathbf{F} \times \mathbf{P} = \mathbf{0} \qquad \text{or} \qquad \mathrm{skew}(\mathbf{P}\mathbf{F}^{\mathbf{T}}) = \mathbf{0} \tag{3.2}$$

   where $\mathbf{F} = \mathrm{Grad}\boldsymbol{\chi}$ and $\det\mathbf{F} > 0$. The first one is a vectorial equation, while the second one is a tensorial equation, and their equivalence results from the known relation between the skew tensor and its axial vector, $\frac{1}{2}(\mathbf{F}\times\mathbf{P})\times\mathbf{I} = \frac{1}{2}(\mathbf{F}\mathbf{P}^T - \mathbf{P}\mathbf{F}^T)$.

3. boundary conditions:

$$\boldsymbol{\chi} = \bar{\boldsymbol{\chi}} \quad \text{on} \quad \partial\mathrm{B}_\chi \qquad \text{and} \qquad \mathbf{P}\mathbf{n} = \hat{\mathbf{p}} \quad \text{on} \quad \partial\mathrm{B}_\sigma \tag{3.3}$$

   where $\mathbf{n}$ is the outward normal vector and $\hat{\mathbf{p}}$ is the external load (surface traction).

Let us introduce a stress tensor defined as $\mathbf{T}^B \equiv \mathbf{R}^T\mathbf{P}$, where $\mathbf{R} \in SO(3)$ is the rotation tensor obtained from the polar decomposition of the deformation gradient. The symmetric part of this stress tensor, i.e. $\mathbf{T}^B_s \equiv \mathrm{sym}\mathbf{T}^B = \mathrm{sym}(\mathbf{R}^T\mathbf{P})$, is called the Biot stress. The balance equations can be re-written as

$$\left.\begin{aligned} \mathrm{Div}\{\mathbf{R}(\mathbf{T}^{\mathrm{B}}_{\mathrm{s}} + \mathbf{T}^{\mathrm{B}}_{\mathrm{a}})\} + \rho_{\mathrm{R}}\mathbf{b} = \mathbf{0} \\ \mathrm{skew}(\mathbf{R}(\mathbf{T}^B_s + \mathbf{T}^B_a)\mathbf{F}^T) = \mathbf{0} \end{aligned}\right\} \tag{3.4}$$

where $\mathbf{T}_a^B \equiv \text{skew}\mathbf{T}^B = \text{skew}(\mathbf{R}^T\mathbf{P})$. For the symmetric Biot stress we can postulate the constitutive equation assuming existence of the strain energy function, $\mathcal{W}(\mathbf{U})$, where $\mathbf{U} \equiv (\mathbf{F}^T\mathbf{F})^{\frac{1}{2}}$ is the right stretch tensor, which automatically satisfies the frame indifference requirement, [Ogden, 1984]. Then, the constitutive equation takes the form

$$\mathbf{T}_s^B = \partial_U \mathcal{W}(\mathbf{U}) \tag{3.5}$$

where $\partial_U \mathcal{W}(\mathbf{U}) = \partial \mathcal{W}(\mathbf{U})/\partial \mathbf{U}$.

3.1.2 Formulation with independent rotations

To incorporate rotations the relation implied by the polar decomposition of the deformation gradient is relaxed. Let us introduce an auxiliary tensor $\mathbf{Q} \in SO(3)$, which is equal to the rotation $\mathbf{R}$, yielded by the polar decomposition of the deformation gradient, when the constraint

$$\mathbf{Q}^T\mathbf{F} - \mathbf{U} = \mathbf{0} \qquad \text{or} \qquad \text{skew}(\mathbf{Q}^T\mathbf{F}) = \mathbf{0} \tag{3.6}$$

is satisfied. It can be checked that the above two forms of the constraint are fully equivalent. Then, using $\mathbf{Q}$ instead of $\mathbf{R}$, and $\mathbf{Q}^T\mathbf{F}$ instead of $\mathbf{U}$ in the basic equations (4), and appending the constraint on rotations we obtain

$$\left.\begin{aligned} \text{Div}\left\{\mathbf{Q}(\partial_U \mathcal{W} + \mathbf{T}_a^B)\right\} + \rho_R \mathbf{b} = 0 \\ \text{skew}\left(\mathbf{Q}(\partial_U \mathcal{W} + \mathbf{T}_a^B)\mathbf{F}^T\right) = 0 \\ \text{skew}(\mathbf{Q}^T\mathbf{F}) = 0 \end{aligned}\right\} \tag{3.7}$$

where $\partial_U \mathcal{W} = \partial \mathcal{W}(\text{sym}(\mathbf{Q}^T\mathbf{F}))/\partial \text{sym}(\mathbf{Q}^T\mathbf{F})$. The above equations are expressed in terms of $\{\boldsymbol{\chi}, \mathbf{Q}, \mathbf{T}_a^B\}$, and we can see that also $\mathbf{Q}$ and $\mathbf{T}_a^B$ are the independent variables. These equations embody 9 scalar equations for 9 unknowns.

To show that the skew tensor $\mathbf{T}_a^B$ vanishes for an isotropic material let us examine the rotational balance equation. For $\mathbf{Q}^T\mathbf{F} = \mathbf{U}$ from the rotational balance equation we obtain

$$\mathbf{T}_a^B\mathbf{U} + \mathbf{U}\mathbf{T}_a^B = \mathbf{T}_s^B\mathbf{U} - \mathbf{U}\mathbf{T}_s^B \tag{3.8}$$

As for an isotropic material $\mathbf{T}_s^B$ and $\mathbf{U}$ are coaxial and hence commutative, the right-hand side expression is equal to zero, and provides

$$\mathbf{T}_a^B\mathbf{U} + \mathbf{U}\mathbf{T}_a^B = \mathbf{0} \tag{3.9}$$

Note that $\mathbf{U}$ is symmetric and positive definite, and $\mathbf{T}_a^B$ is skew-symmetric, hence the assumptions of Lemma 3.1 in [Simo, Fox, Hughes, 1992] are satisfied. On this lemma the above equation is satisfied only when $\mathbf{T}_a^B = \mathbf{0}$, what completes the proof. We note in passing that when the constraint equation is not satisfied or the material is anisotropic, the right-hand side of (8) does not vanish what renders that $\mathbf{T}_a^B \neq \mathbf{0}$.

3.1.3 Weak form of basic equations

In this section we derive the weak form of the balance equations and the constraint equation for three-dimensional elasticity with independent rotations. For the equilibrium equation we calculate

$$\int_B \left[\mathrm{Div}(\mathbf{Q}\mathbf{T}^B) + \rho_R \mathbf{b}\right] \cdot \delta\boldsymbol{\chi}\, dV = 0 \tag{3.10}$$

where $\delta\boldsymbol{\chi}$ is the kinematically admissible variation of deformation. On use of the formula for the divergence of a product of a tensor and a vector, [DeBoer, 1982, p.143, eq.(5.5.19)], the Gauss' theorem, and the identity $(\mathbf{Q}\mathbf{T}^B)\cdot\delta\mathbf{F} = \mathbf{T}^B \cdot (\mathbf{Q}^T\delta\mathbf{F})$, we obtain

$$\int_B \left[\mathbf{T}^B \cdot (\mathbf{Q}^T\delta\mathbf{F}) \; - \; \rho_R \mathbf{b}\cdot\delta\boldsymbol{\chi}\right] dV - \delta\mathcal{A} = 0, \qquad \delta\mathcal{A} = \int_{\partial B} \hat{\mathbf{p}}\cdot\delta\boldsymbol{\chi}\, dA \tag{3.11}$$

where $\delta\mathbf{F} = \delta\mathrm{Grad}\boldsymbol{\chi}$. The integration is performed over the initial configuration, i.e. over the volume dV and the surface traction boundary area dA.

To obtain a weak form of the rotational balance equation we re-write it in the form $\mathrm{skew}[\mathbf{T}^B(\mathbf{Q}^T\mathbf{F})^T] = \mathbf{0}$, and calculate an integral of its scalar product with a skew-symmetric (right) tensor $\delta\tilde{\boldsymbol{\Theta}}$,

$$\int_B \mathrm{skew}[\mathbf{T}^B(\mathbf{Q}^T\mathbf{F})^T] \cdot \delta\tilde{\boldsymbol{\Theta}}\; dV = 0 \tag{3.12}$$

On use of $\mathbf{T}^B(\mathbf{Q}^T\mathbf{F})^T\cdot\delta\tilde{\boldsymbol{\Theta}} = \mathbf{T}^B\cdot(\delta\tilde{\boldsymbol{\Theta}}\mathbf{Q}^T\mathbf{F})$, and $\delta\mathbf{Q} \equiv \mathbf{Q}\delta\tilde{\boldsymbol{\Theta}}$, the weak form of the rotational balance equation becomes

$$\int_B \mathbf{T}^B \cdot (\delta\mathbf{Q}^T\mathbf{F})\, dV = 0 \tag{3.13}$$

To determine a weak form of the constraint on rotations we calculate an integral of a scalar product of this equation with a skew- symmetric tensor $\delta\mathbf{T}_a^B$,

$$\int_B \mathrm{skew}(\mathbf{Q}^T\mathbf{F}) \cdot \delta\mathbf{T}_a^B\; dV = 0 \tag{3.14}$$

A reason for using here a variation of $\mathbf{T}_a^B$ will become obvious in the sequel.

Adding the scalar equations (11), (13) and (14), and noting that $\delta(\mathbf{Q}^T\mathbf{F}) = \delta\mathbf{Q}^T\mathbf{F} + \mathbf{Q}^T\delta\mathbf{F}$, we can write

$$\int_B \left[\mathbf{T}^B\cdot\delta(\mathbf{Q}^T\mathbf{F}) + \delta\mathbf{T}_a^B\cdot\mathrm{skew}(\mathbf{Q}^T\mathbf{F})\right] dV - \int_B \rho_R\mathbf{b}\cdot\delta\boldsymbol{\chi}\, dV - \delta\mathcal{A} = 0 \tag{3.15}$$

which is a virtual work equation comprising the equilibrium equation, the angular balance equation and the constraint equation. A split into a sum of products of symmetric and skew parts yields

$$\mathbf{T}^B\cdot\delta(\mathbf{Q}^T\mathbf{F}) = \mathbf{T}_s^B\cdot\mathrm{sym}\;\delta(\mathbf{Q}^T\mathbf{F}) + \mathbf{T}_a^B\cdot\mathrm{skew}\;\delta(\mathbf{Q}^T\mathbf{F}) \tag{3.16}$$

where the operations of taking a symmetric (or skew) part and taking a variation commute, i.e. $\mathrm{sym}\;\delta(\;) = \delta\;\mathrm{sym}(\;)$ and $\mathrm{skew}\;\delta(\;) = \delta\;\mathrm{skew}(\;)$.

For the symmetric stress tensor we can assume that $\mathbf{T}_s^B = \partial\mathcal{W}(\mathrm{sym}(\mathbf{Q}^T\mathbf{F}))/\partial\mathrm{sym}(\mathbf{Q}^T\mathbf{F}) = \partial_U\mathcal{W}$, for which the 1st integral of the virtual eq.(15) can be written as follows

$$\partial_U\mathcal{W}\cdot\mathrm{sym}\;\delta(\mathbf{Q}^T\mathbf{F}) + \mathbf{T}_a^B\cdot\mathrm{skew}\;\delta(\mathbf{Q}^T\mathbf{F}) + \delta\mathbf{T}_a^B\cdot\mathrm{skew}(\mathbf{Q}^T\mathbf{F}) \tag{3.17}$$

This equation is a variation of the potential

$$\Pi(\boldsymbol{\chi}, \mathbf{Q}, \mathbf{T}_a^B) = \int_B \left[\mathcal{W}(\mathrm{sym}(\mathbf{Q}^T\mathbf{F})) + \mathbf{T}_a^B \cdot \mathrm{skew}(\mathbf{Q}^T\mathbf{F})\right] \, dV + \Pi_{ext}(\boldsymbol{\chi}) \tag{3.18}$$

Note that $\mathbf{T}_a^B$ plays the role of the Lagrange multiplier on use of which the rotation constraint is imposed. Conversely, we can state that the first differential of Π yields the Euler-Lagrange equations in the form (7), and the traction boundary condition $\mathbf{Q}\mathbf{T}^B\mathbf{n} = \hat{\mathbf{p}}$ on $\partial \mathrm{B}_\sigma$. Therefore, Π of eq.(18) is a correct potential of the governing equations, and the use of $\delta\mathbf{T}_a^B$ as the Lagrange multiplier for the rotation constraint in eq.(14) is correct indeed.

If we assume that the external loads are conservative then their potential can be specified. This potential has a particularly simple form for the deformation independent external loads,

$$\Pi_{ext}(\boldsymbol{\chi}) = -\int_B \rho_R \mathrm{b} \cdot \boldsymbol{\chi} \, dV - \int_{\partial \mathrm{B}_\sigma} \hat{\mathrm{p}} \cdot \boldsymbol{\chi} \, dA \tag{3.19}$$

3.1.4 Strain measure

The strain measure can be deduced as the work conjugate to $\mathbf{T}_s^B$. On the basis of the scalar product $\mathbf{T}_s^B \cdot \mathrm{sym}\, \delta(\mathbf{Q}^T\mathbf{F})$, we can define the so called *relaxed* right stretch strain,

$$\mathbf{H} = \mathrm{sym}(\mathbf{Q}^T\mathbf{F}) - \mathbf{I} \tag{3.20}$$

This tensor yields the right stretch strain, $\mathbf{H} = \mathbf{U} - \mathbf{I}$, when the rotation constraint is satisfied. Then, also the product of skew tensors $\mathbf{T}_a^B \cdot \mathrm{skew}\, \delta(\mathbf{Q}^T\mathbf{F})$ in (15) vanishes, similarly as shown for the stress power in [Ogden, 1984].

3.1.5 Algorithmic approaches

Eq.(15) can be solved directly, e.g. by the finite element method with the order of approximation for particular fields conforming with the stability condition for mixed formulations, the so called LBB condition, see e.g. [Zienkiewicz, Taylor, 1989]. The mixed formulation is used e.g. in [Atluri, 1984], [Iura, Atluri, 1989, 1992], [Cazzani, Atluri, 1993], and [Seki, Atluri, 1994].

In case of an isotropic material, we can devise a method eliminating $\mathbf{T}_a^B$ from the formulation, and solve a two-field mixed problem. Note that $\mathbf{T}_a^B = 0$ when $\mathbf{Q}^T\mathbf{F} = \mathbf{U}$, and this condition can be imposed on the rotation constraint equation using a penalty method as follows

$$\mathrm{skew}(\mathbf{Q}^T\mathbf{F}) - \frac{1}{\gamma}\mathbf{T}_a^B = 0, \qquad \gamma \in (0, \infty) \tag{3.21}$$

where γ is the penalty number. Then, calculating $\mathbf{T}_a^B$ from the above equation and inserting it into the balance equations (7) and the potential energy (18) we obtain

$$\mathrm{Div}\left\{\mathbf{Q}(\partial_U \mathcal{W} + \gamma \mathrm{skew}(\mathbf{Q}^T\mathbf{F}))\right\} + \rho_R \mathrm{b} = 0 \tag{3.22}$$

$$\text{skew}\left[\mathbf{Q}(\partial_U \mathcal{W} + \gamma \text{skew}(\mathbf{Q}^T\mathbf{F}))\mathbf{F}^T\right] = \mathbf{0} \tag{3.23}$$

$$\tilde{\Pi}(\boldsymbol{\chi}, \mathbf{Q}) = \int_B \left[\mathcal{W}(\text{sym}(\mathbf{Q}^T\mathbf{F})) + \gamma \text{skew}(\mathbf{Q}^T\mathbf{F}) \cdot \text{skew}(\mathbf{Q}^T\mathbf{F})\right] dV + \Pi_{ext}(\boldsymbol{\chi}) \tag{3.24}$$

what furnishes a formulation in terms of $\{\boldsymbol{\chi}, \mathbf{Q}\}$. Note that $\text{skew}(\mathbf{Q}^T\mathbf{F}) \cdot \text{skew}(\mathbf{Q}^T\mathbf{F}) = 1/\gamma^2 \|\mathbf{T}_a^B\|^2$, and this term locally convexifies the potential energy functional Π for $\mathbf{T}_a^B$. In consequence, instead of eq.(15), the virtual work equation is as follows

$$\int_B \left[\mathbf{T}_s^B \cdot \delta\text{sym}(\mathbf{Q}^T\mathbf{F}) + \gamma \text{skew}(\mathbf{Q}^T\mathbf{F}) \cdot \delta\text{skew}(\mathbf{Q}^T\mathbf{F})\right] dV - \int_B \rho_R \mathbf{b} \cdot \delta\boldsymbol{\chi}\, dV - \delta\mathcal{A} = 0 \tag{3.25}$$

We note in passing that there exists also an alternative method of treating $\mathbf{T}_a^B$, which is a combination of the penalty method and a staggered solution scheme. The staggered schemes are often used for problems involving different types of variables. This method does not exploit the condition $\mathbf{T}_a^B = \mathbf{0}$, so it can be also used for anisotropic materials. For instance, for the problem at hand, the following equations can be considered:

$$\left.\begin{aligned} \int_B \left[(\mathbf{Q}\mathbf{T}^B) \cdot \delta\mathbf{F} - \rho_R \mathbf{b} \cdot \delta\boldsymbol{\chi}\right] dV - \delta\mathcal{A} = 0 \\ \int_B \left[\mathbf{T}^B \cdot (\delta\mathbf{Q}^T\mathbf{F}) + \gamma\delta\mathbf{T}_a^B \cdot \text{skew}(\delta\mathbf{Q}^T\mathbf{F})\right] dV = 0 \end{aligned}\right\} \tag{3.26}$$

where $\mathbf{T}^B = \partial_U \mathcal{W} + \mathbf{T}_a^B$. The first equation is the equilibrium equation (11), while the second one is the rotational balance eq.(13) with the rotational constraint (14) imposed on use of the penalty method. Then, a two-step staggered scheme can be applied:
1) For the known $\boldsymbol{\chi}_{i-1}$ and $\mathbf{Q}_{i-1}$ find a new $(\mathbf{T}_a^B)_i$ from the 1st equation, which is a set of 3 equations for 3 unknowns.
2) For the known $(\mathbf{T}_a^B)_i$ find a new $\boldsymbol{\chi}_i$ and $\mathbf{Q}_i$ from the 2nd equation, which is a set of 6 equations for 6 unknowns. In this way $\mathbf{T}_a^B$ is not the unknown in the second step, in which only $\boldsymbol{\chi}$ and $\mathbf{Q}$ are retained.

Several staggered schemes can be constructed, and their numerical properties are, in general, different. The conceptual work of inventing such schemes is not difficult, but a rigorous analysis of their convergence properties can be complicated, see e.g. [Wisniewski, Turska, Simoni, Schrefler, 1991] and [Turska, Wisniewski, Schrefler, 1994].

3.2 Two-dimensional approximation of basic equations

In this section the three-dimensional basic equations presented in the previous section, are approximated by a truncated Taylor series and integrated over the shell thickness in order to derive their two-dimensional counterparts. The stress and couple resultants, which are the integral stress measures for a shell, are introduced. We consider a thin shell, the initial geometry of which satisfies the condition $h\mathbf{B} \ll \mathbf{I}_0$, where h is the thickness, and $\mathbf{B}$ is the curvature tensor of the mid-surface of the shell. As shown in Section 3.3, this condition renders that the shifter $\mathbf{Z} \approx \mathbf{I}_0$ and $\mu = \det \mathbf{Z} \approx 1$. Note that for thin shells this condition is weaker than the condition $\mathbf{B} \approx \mathbf{0}$, which characterizes the so called shallow shells.

3.2.1 Basic approximations and shell strain measures

We shall assume a linear distribution of the deformation across the thickness,

$$\boldsymbol{\chi}(\zeta) = \boldsymbol{\chi}_0 + \zeta(\boldsymbol{\chi}_{,\zeta})_0 + O(\zeta^2) \tag{3.27}$$

where $\zeta \in [-h/2, +h/2]$ is a coordinate in the direction normal to the middle surface of the shell. For the assumed geometry of the shell eq.(27) implies a linear approximation of the deformation gradient across the thickness. Let us combine a linear approximation of the deformation gradient with a constant approximation of rotations,

$$\mathbf{F}(\zeta) = \mathbf{F}_0 + \zeta\ (\mathbf{F}_{,\zeta})_0 + O(\zeta^2), \qquad \mathbf{Q}(\zeta) = \mathbf{Q}_0 + O(\zeta) \tag{3.28}$$

where $\mathbf{Q}, \mathbf{Q}_0 \in SO(3)$. Hence, for the product $\mathbf{Q}^T\mathbf{F}$, which appears in the basic equations, we obtain

$$\mathbf{Q}^T\mathbf{F} = \mathbf{Q}_0^T\mathbf{F}_0 + \zeta\mathbf{Q}_0^T(\mathbf{F}_{,\zeta})_0 + O(\zeta) \tag{3.29}$$

The symmetric part of the product becomes

$$\operatorname{sym}(\mathbf{Q}^T\mathbf{F}) = \operatorname{sym}(\mathbf{Q}^T\mathbf{F})_0 + \zeta\ \operatorname{sym}(\mathbf{Q}^T\mathbf{F}_{,\zeta})_0 + O(\zeta) \tag{3.30}$$

where

$$\operatorname{sym}(\mathbf{Q}^T\mathbf{F})_0 = \frac{1}{2}\left[\mathbf{Q}_0^T\mathbf{F}_0 + \mathbf{F}_0^T\mathbf{Q}_0\right], \qquad \operatorname{sym}(\mathbf{Q}^T\mathbf{F}_{,\zeta})_0 = \frac{1}{2}\left[\mathbf{Q}_0^T(\mathbf{F}_{,\zeta})_0 + (\mathbf{F}_{,\zeta})_0^T\mathbf{Q}_0\right]$$

The skew-symmetric part of the product is defined analogously

$$\operatorname{skew}(\mathbf{Q}^T\mathbf{F}) = \operatorname{skew}(\mathbf{Q}^T\mathbf{F})_0 + \zeta\ \operatorname{skew}(\mathbf{Q}^T\mathbf{F}_{,\zeta})_0 + O(\zeta) \tag{3.31}$$

where

$$\operatorname{skew}(\mathbf{Q}^T\mathbf{F})_0 = \frac{1}{2}\left[\mathbf{Q}_0^T\mathbf{F}_0 - \mathbf{F}_0^T\mathbf{Q}_0\right], \qquad \operatorname{skew}(\mathbf{Q}^T\mathbf{F}_{,\zeta})_0 = \frac{1}{2}\left[\mathbf{Q}_0^T(\mathbf{F}_{,\zeta})_0 + (\mathbf{F}_{,\zeta})_0^T\mathbf{Q}_0\right]$$

Besides, for the assumed geometry we have the expansion of the identity tensor, $\mathbf{I}(\zeta) = \mathbf{I}_0 + \zeta(\mathbf{I}_{,\zeta})_0 + O(\zeta^2)$, see Section 3.4 for details. Therefore, the relaxed right stretch strain tensor defined by eq.(20) can be written as

$$\mathbf{H}(\zeta) = \mathbf{H}_0 + \zeta\ (\mathbf{H}_{,\zeta})_0 + O(\zeta) \tag{3.32}$$

where

$$\mathbf{H}_0 \equiv \operatorname{sym}(\mathbf{Q}^T\mathbf{F})_0 - \mathbf{I}_0, \qquad (\mathbf{H}_{,\zeta})_0 \equiv \operatorname{sym}(\mathbf{Q}^T\mathbf{F}_{,\zeta})_0 - (\mathbf{I}_{,\zeta})_0$$

In a traditional notation, the shell strain $\mathbf{H}_0$ is denoted as $\boldsymbol{\varepsilon}$, and the shell change of curvature measure $(\mathbf{H}_{,\zeta})_0$ is denoted as $\boldsymbol{\kappa}$.

3.2.2 Virtual work equation for shells

A virtual work of stress for a shell, $\delta\Sigma$, is defined as an integral over the shell thickness,

$$\delta\Sigma \equiv \int_{-\frac{h}{2}}^{+\frac{h}{2}} \mathbf{T}^B \cdot \delta(\mathbf{Q}^T\mathbf{F})\ \mu\ d\zeta \tag{3.33}$$

For the assumed geometry of the shell we have $\mathbf{T}^B = \mathbf{t}_\alpha^B \otimes \mathbf{t}^\alpha$, where $\mathbf{t}_\alpha^B$ is a stress vector corresponding with the cross-section normal to $\mathbf{t}_\alpha$. Here $\mathbf{t}_\alpha$ is a tangent vector of the orthonormal triad associated with the middle surface, see Section 3.3. Let us define the stress and couple resultant vectors as follows

$$\mathbf{n}_\alpha^B \equiv \int_{-\frac{h}{2}}^{+\frac{h}{2}} \mathbf{t}_\alpha^B(\zeta)\ \mu\ d\zeta, \qquad \mathbf{m}_\alpha^B \equiv \int_{-\frac{h}{2}}^{+\frac{h}{2}} \zeta\ \mathbf{t}_\alpha^B(\zeta)\ \mu\ d\zeta \tag{3.34}$$

We note in passing that in Section 3.5 the above definition of the couple resultant vector is related to the alternative definition involving a vector product, i.e. $\mathbf{m}_\alpha^B \equiv \int_{-\frac{h}{2}}^{+\frac{h}{2}} \zeta \mathbf{t}_3 \times \mathbf{t}_\alpha^B(\zeta)\ \mu\ d\zeta$. The stress and couple resultant tensors can be introduced as satisfying the relations $\mathbf{N}^B = \mathbf{n}_\alpha^B \otimes \mathbf{t}^\alpha$ and $\mathbf{M}^B = \mathbf{m}_\alpha^B \otimes \mathbf{t}^\alpha$, what provides

$$\mathbf{N}^B \equiv \int_{-\frac{h}{2}}^{+\frac{h}{2}} \mathbf{T}^B(\zeta)\ \mu\ d\zeta, \qquad \mathbf{M}^B \equiv \int_{-\frac{h}{2}}^{+\frac{h}{2}} \zeta\ \mathbf{T}^B(\zeta)\ \mu\ d\zeta \tag{3.35}$$

On use of the linear Taylor approximation of the product $\mathbf{Q}^T\mathbf{F}$ around the middle surface, eq.(29), and the above definitions of shell resultant tensors we obtain

$$\delta\Sigma = \mathbf{N}^B \cdot \delta(\mathbf{Q}^T\mathbf{F})_0 + \mathbf{M}^B \cdot \delta(\mathbf{Q}^T\mathbf{F}_{,\zeta})_0 \tag{3.36}$$

which can be split into a sum of products of the symmetric and skew parts

$$\begin{aligned} \delta\Sigma \ &= \ \mathbf{N}_s^B \cdot \delta\mathrm{sym}(\mathbf{Q}^T\mathbf{F})_0 + \mathbf{M}_s^B \cdot \delta\mathrm{sym}(\mathbf{Q}^T\mathbf{F}_{,\zeta})_0 \\ &+ \ \mathbf{N}_a^B \cdot \delta\mathrm{skew}(\mathbf{Q}^T\mathbf{F})_0 + \mathbf{M}_a^B \cdot \delta\mathrm{skew}(\mathbf{Q}^T\mathbf{F}_{,\zeta})_0 \end{aligned} \tag{3.37}$$

where the symmetric and skew parts of $(\mathbf{Q}^T\mathbf{F})_0$ and $(\mathbf{Q}^T\mathbf{F}_{,\zeta})_0$ are defined by eq.(30) and (31).

The constitutive equations for the resultants $\mathbf{N}_s^B$ and $\mathbf{M}_s^B$ can be obtained as follows. First, the strain energy $\mathcal{W}(\mathrm{sym}(\mathbf{Q}^T\mathbf{F}))$ is expanded w.r.t. ζ on use of eq.(30), and integrated over the thickness, what provides the two-dimensional shell strain energy $\Sigma = \Sigma(\mathrm{sym}(\mathbf{Q}^T\mathbf{F})_0, \mathrm{sym}(\mathbf{Q}^T\mathbf{F}_{,\zeta})_0)$. Then, the symmetric parts of the stress and couple resultants are defined as

$$\mathbf{N}_s^B = \frac{\partial\Sigma}{\partial\mathrm{sym}(\mathbf{Q}^T\mathbf{F})_0}, \qquad \mathbf{M}_s^B = \frac{\partial\Sigma}{\partial\mathrm{sym}(\mathbf{Q}^T\mathbf{F}_{,\zeta})_0} \tag{3.38}$$

In this way the resultants are derived for the linear material and the Mooney-Rivlin material in Section 3.6.

Remark 1. For the introduced approximations and the right stretch strain $\mathbf{H}$, as the strain measure, in case of the linear material, the integrand of $\mathcal{W}$ is a 2nd order polynomial

of ζ. For comparison, the same approximation of $\mathbf{F}$ yields the Green strain of 2nd order, and the integrand of $\mathcal{W}$ is a 4th order polynomial of ζ. For the incompressible Mooney-Rivlin material the respective polynomials are two orders higher.

Remark 2. Assume that for the rotations we use the approximation $\mathbf{Q} = \mathbf{Q}_0 + \zeta\,(\mathbf{Q}_{,\zeta})_0 + O(\zeta^2)$, where $\mathbf{Q}, \mathbf{Q}_0, (\mathbf{Q}_{,\zeta})_0 \in SO(3)$ and $(\mathbf{Q}_{,\zeta})_0$ is an additional rotation variable. Then, the integrand of $\mathcal{W}$ for the right stretch strain is of the 4th order, similarly as for the Green strain.

The virtual work of the rotation constraint, given by the term $\delta\mathbf{T}_a^B \cdot \mathrm{skew}(\mathbf{Q}^T\mathbf{F})$ in eq.(15), has the following counterpart for a shell,

$$\int_{-\frac{h}{2}}^{+\frac{h}{2}} \delta\mathbf{T}_a^B \cdot \mathrm{skew}(\mathbf{Q}^T\mathbf{F})\ \mu\ d\zeta = \delta\mathbf{N}_a^B \cdot \mathrm{skew}(\mathbf{Q}^T\mathbf{F})_0 + \delta\mathbf{M}_a^B \cdot \mathrm{skew}(\mathbf{Q}^T\mathbf{F}_{,\zeta})_0 \tag{3.39}$$

where the shell stress and couple resultants are defined in eq.(34).

The virtual work of the body force is defined as $\int_B \rho_R \mathbf{b} \cdot \delta\boldsymbol{\chi}\ dV$. On use of eq.(27) and integration over the thickness, with $\mu \approx 1$, we obtain

$$\int_{-\frac{h}{2}}^{+\frac{h}{2}} \rho_R \mathbf{b} \cdot \delta\boldsymbol{\chi}\ \mu\ d\zeta = \rho_R h\ \mathbf{b} \cdot \delta\boldsymbol{\chi}_0 \tag{3.40}$$

The virtual work of external forces acting on the upper and lower surface bounding the shell is defined as

$$\delta\mathcal{A} = \hat{\mathbf{p}}_3^+ \cdot \delta\boldsymbol{\chi}^+ + \hat{\mathbf{p}}_3^- \cdot \delta\boldsymbol{\chi}^- \tag{3.41}$$

where $\hat{\mathbf{p}}_3$ denotes the external force corresponding to the vector normal to the middle surface. The subscript "+" indicates the upper surface at $\zeta = +h/2$, and "-" indicates the lower surface at $\zeta = -h/2$. Specifying $\delta\boldsymbol{\chi}(\zeta) = \delta\boldsymbol{\chi}_0 + \zeta\delta(\boldsymbol{\chi}_{,\zeta})_0 + O(\zeta^2)$ for the appropriate ζ we obtain

$$\delta\mathcal{A} = \hat{\mathbf{q}} \cdot \delta\boldsymbol{\chi}_0 + \hat{\mathbf{m}} \cdot \delta(\boldsymbol{\chi}_{,\zeta})_0 \tag{3.42}$$

where $\hat{\mathbf{q}} \equiv \hat{\mathbf{p}}_3^+ + \hat{\mathbf{p}}_3^-$ and $\hat{\mathbf{m}} \equiv \frac{h}{2}(\hat{\mathbf{p}}_3^+ - \hat{\mathbf{p}}_3^-)$.

Finally, combining eq.(36), (39) (40) and (42), the virtual work equation for a shell becomes

$$\begin{aligned}
\delta\Pi_{2d} \;=\; & \int_S \Big[\mathbf{N}_s^B \cdot \delta\mathrm{sym}(\mathbf{Q}^T\mathbf{F})_0 + \mathbf{M}_s^B \cdot \delta\mathrm{sym}(\mathbf{Q}^T\mathbf{F}_{,\zeta})_0 \\
& + \mathbf{N}_a^B \cdot \delta\mathrm{skew}(\mathbf{Q}^T\mathbf{F})_0 + \mathbf{M}_a^B \cdot \delta\mathrm{skew}(\mathbf{Q}^T\mathbf{F}_{,\zeta})_0 \\
& + \delta\mathbf{N}_a^B \cdot \mathrm{skew}(\mathbf{Q}^T\mathbf{F})_0 + \delta\mathbf{M}_a^B \cdot \mathrm{skew}(\mathbf{Q}^T\mathbf{F}_{,\zeta})_0 \\
& - \rho_R h\ \mathbf{b} \cdot \delta\boldsymbol{\chi}_0 - \hat{\mathbf{q}} \cdot \delta\boldsymbol{\chi}_0 - \hat{\mathbf{m}} \cdot \delta(\boldsymbol{\chi}_{,\zeta})_0\Big]\ dS
\end{aligned} \tag{3.43}$$

where S denotes the middle surface of the shell, with an apparent similarity to eq.(15) for a three-dimensional body.

3.2.3 Virtual work equation for isotropic shells

On use of the linear approximation given by eq.(31) the constraint equation (21) becomes

$$\text{skew}(\mathbf{Q}^T\mathbf{F})_0 + \zeta\text{skew}(\mathbf{Q}^T\mathbf{F}_{,\zeta})_0 - \frac{1}{\gamma}\mathbf{T}_a^B = 0 \tag{3.44}$$

Integrating this equation, and its product with ζ, over the shell thickness we obtain

$$\int_{-\frac{h}{2}}^{+\frac{h}{2}} (...)\, d\zeta = h\text{skew}(\mathbf{Q}^T\mathbf{F})_0 - \frac{1}{\gamma}\mathbf{N}_a^B = 0 \tag{3.45}$$

$$\int_{-\frac{h}{2}}^{+\frac{h}{2}} \zeta\,(...)\, d\zeta = \frac{h^3}{12}\text{skew}(\mathbf{Q}^T\mathbf{F}_{,\zeta})_0 - \frac{1}{\gamma}\mathbf{M}_a^B = 0 \tag{3.46}$$

for the stress and couple resultants $\mathbf{N}^B$ and $\mathbf{M}^B$ defined in eq.(34). Hence, for a shell we have two constraint equations, instead of one equation (21) for a three-dimensional body.

Recall that for a three-dimensional body the skew-symmetric $\mathbf{T}_a^B$ can be eliminated on use of the penalty method. Similarly for shells, the constraint equations (45) and (46) can be used to get rid of the skew-symmetric resultant tensors from the virtual work (43). Finally, the virtual work equation for a shell of an isotropic material, comprising the contribution of stress and couple resultants, the rotation constraint and the external loads, becomes

$$\begin{aligned}\delta\Pi_{2d} \;=\; & \int_S \Big[\mathbf{N}_s^B \cdot \delta\text{sym}(\mathbf{Q}^T\mathbf{F})_0 + \mathbf{M}_s^B \cdot \delta\text{sym}(\mathbf{Q}^T\mathbf{F}_{,\zeta})_0 \\ & + \gamma\, h\text{skew}(\mathbf{Q}^T\mathbf{F})_0 \cdot \delta\text{skew}(\mathbf{Q}^T\mathbf{F})_0 + \gamma\,\frac{h^3}{12}\text{skew}(\mathbf{Q}^T\mathbf{F}_{,\zeta})_0 \cdot \delta\text{skew}(\mathbf{Q}^T\mathbf{F}_{,\zeta})_0 \\ & - \rho_R h\, \mathbf{b}\cdot\delta\boldsymbol{\chi}_0 - \hat{\mathbf{q}}\cdot\delta\boldsymbol{\chi}_0 - \hat{\mathbf{m}}\cdot\delta(\boldsymbol{\chi}_{,\zeta})_0\Big]\, dS\end{aligned} \tag{3.47}$$

with an apparent similarity to eq.(25) for a three-dimensional body.

Note that the idea of using the constraint on rotations is transferred from the three-dimensional theory, where the rotation tensor $\mathbf{Q}$ symmetrizes $\mathbf{Q}^T\mathbf{F}$. In case of shells with the constant representation of $\mathbf{Q}$, one rotation tensor $\mathbf{Q}_0$ should symmetrize $\mathbf{Q}_0^T\mathbf{F}_0$ and $\mathbf{Q}_0^T(\mathbf{F}_{,\zeta})_0$, what is not feasible when $\mathbf{F}_0$ and $(\mathbf{F}_{,\zeta})_0$ are not co-axial.

When one type of the strains dominates over the other then it is justified to enforce the corresponding part of the constraint. In numerical implementations this can be achieved on use of an auxiliary factor α, introduced in the following way

$$\alpha\,\gamma h\ \text{skew}(\mathbf{Q}^T\mathbf{F})_0 \cdot \delta\text{skew}(\mathbf{Q}^T\mathbf{F})_0 \;+\; (1-\alpha)\,\gamma\frac{h^3}{12}\ \text{skew}(\mathbf{Q}^T\mathbf{F}_{,\zeta})_0 \cdot \delta\text{skew}(\mathbf{Q}^T\mathbf{F}_{,\zeta})_0 \tag{3.48}$$

When the previous iteration indicates that the membrane strains are much larger than the bending-shearing strains then $\alpha = 1$ is used. When the bending- shearing strains are larger than the membrane ones then $\alpha = 0$ is used. In this way, a pure membrane state (even for finite strains) or pure bending- shearing state can be correctly modeled. In a similar way the factor α can be introduced into eq.(43).

Remark 3. Note that a linear approximation of rotations, as specified in *Remark 2*, provides the additional variable $(\mathbf{Q}_{,\zeta})_0$. Two fields $\mathbf{Q}_0$ and $(\mathbf{Q}_{,\zeta})_0$ can yield both terms of $\mathbf{Q}^T\mathbf{F}$ symmetric, when the rotation constraint is enforced.

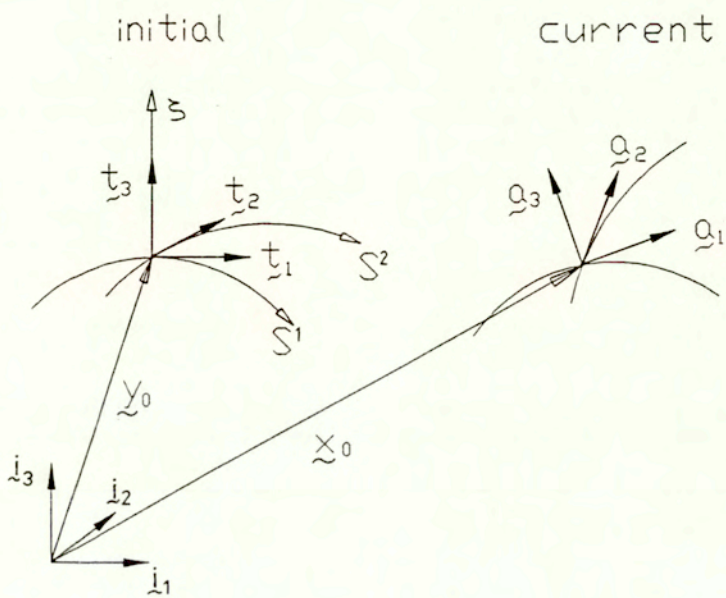

Fig.3.1 Local bases on the middle surface of shell

3.3 Deformation gradient

In this section the deformation gradient and its variation is derived for the standard and generalized Reissner hypothesis.

Assume that S^α $(\alpha = 1,2)$ are the arc-length orthogonal coordinates on the mid-surface and ζ is the coordinate in the direction normal to the surface, $-\frac{h}{2} \leq \zeta \leq +\frac{h}{2}$, where h denotes the thickness of the shell. The triad $\{\mathbf{i}_i\}$ $(i = 1,2,3)$ denotes an orthonormal (Cartesian) global basis.

For the initial (undeformed) configuration the local basis is defined as $\mathbf{g}_\alpha = \partial \mathbf{y}/\partial S^\alpha$ and $\mathbf{t}_3 = \partial \mathbf{y}/\partial \zeta$, where $\mathbf{y}$ is the position vector. At the middle surface $\mathbf{g}_\alpha|_{\zeta=0} \equiv \mathbf{t}_\alpha$. Hence, $\{\mathbf{t}_i\}$ is a tangent orthonormal basis associated with the middle surface of the shell in the initial configuration, see Fig.3.1.

For the chosen coordinate system the position vector in an initial configuration can

be decomposed as follows

$$\mathbf{y}(\zeta) = \mathbf{y}_0 + \zeta \left.\frac{\partial \mathbf{y}}{\partial \zeta}\right|_{\zeta=0} = \mathbf{y}_0 + \zeta \mathbf{t}_3 \tag{3.49}$$

where $\mathbf{y}_0$ is a position of the middle surface point. This equation can be used to introduce a relation between $\mathbf{g}_\alpha$ and the mid-surface vectors $\mathbf{t}_\alpha$. Differentiating this equation with respect to S^α we obtain

$$\mathbf{g}_\alpha = \mathbf{t}_\alpha + \zeta \mathbf{t}_{3,\alpha} = (\mathbf{I}_0 - \zeta \mathbf{B})\, \mathbf{t}_\alpha = \mathbf{Z}\, \mathbf{t}_\alpha \tag{3.50}$$

where $\mathbf{B} \equiv -\mathbf{t}_{3,\alpha} \otimes \mathbf{t}^\alpha$ is the curvature tensor, and $\mathbf{I}_0 \mathbf{t}_\alpha \otimes \mathbf{t}^\alpha$ is the metric tensor of the middle surface. The shifter tensor is defined as $\mathbf{Z} \equiv \mathbf{I}_0 - \zeta \mathbf{B}$, and its inverse is as follows

$$\mathbf{Z}^{-1} = \mu^{-1} \left[\mathbf{I}_0 - \zeta (\det \mathbf{B}) \mathbf{B}^{-1}\right] = \mu^{-1} \left[\mathbf{I}_0 - \zeta (2H\mathbf{I} - \mathbf{B})\right] \tag{3.51}$$

where $(\det \mathbf{B})\mathbf{B}^{-1} = 2H\mathbf{I}_0 - \mathbf{B}$ is obtained on use of the Cayley-Hamilton formula. Besides, $\mu = \det \mathbf{Z} = 1 - 2\zeta H + \zeta^2 K$, where $H = \frac{1}{2}\mathrm{tr}\mathbf{B}$ is the mean curvature, and $K = \det \mathbf{B}$ is the Gaussian curvature. Note that μ^{-1} is an infinite series of ζ.

For the current position vector the Taylor expansion around $\zeta = 0$ yields

$$\mathbf{x}(\zeta) = \mathbf{x}_0 + \zeta \left.\frac{\partial \mathbf{x}}{\partial \zeta}\right|_{\zeta=0} + O(\zeta^2) \approx \mathbf{x}_0 + \zeta \mathbf{d} \tag{3.52}$$

where $\mathbf{x}_0$ is a position of the middle surface in the current configuration, and the vector $\mathbf{d} \equiv \partial \mathbf{x}/\partial \zeta|_{\zeta=0}$ is a deformed director. The above form of the position vector involves $\mathbf{x}_0$ and $\mathbf{x}_{,\zeta}|_{\zeta=0}$. Within the so called continuum-based (or degenerated) approach to shells, an approximation function is used in the thickness direction to determine both of them. In a classical approach to shells, which is also used below, this dependence is eliminated on use of the kinematical hypothesis. Let us introduce the extension coefficient $\lambda = \|\mathbf{d}\|$. Then, we can write $\mathbf{d} = \lambda \mathbf{a}_3$, where $\mathbf{a}_3 = \mathbf{d}/\|\mathbf{d}\|$. Alternatively, the current position vector is written as follows

$$\mathbf{x}(\zeta) = \mathbf{x}_0 + \zeta \lambda \mathbf{a}_3 \tag{3.53}$$

which can be considered as the generalized form of the Reissner hypothesis, including a parameter for the uniform extension of the director. If we assume $\lambda = 1$, i.e. the inextensibility of the director $\mathbf{d}$, then the current position vector has a form characteristic for the standard Reissner hypothesis,

$$\mathbf{x}(\zeta) = \mathbf{x}_0 + \zeta \mathbf{a}_3 \tag{3.54}$$

Note that $\mathbf{a}_3$ is a unit vector, and it can be obtained from the unit vector $\mathbf{t}_3$ on use of the rotation tensor $\mathbf{Q}_0 \in SO(3)$, i.e. $\mathbf{a}_3 = \mathbf{Q}_0 \mathbf{t}_3$. Within the present formulation this arbitrary $\mathbf{Q}_0$ is forced to converge to $\mathbf{R}$, which satisfies the polar decomposition theorem. For the future use, we introduce the rotated vectors $\mathbf{a}_i = \mathbf{Q}_0 \mathbf{t}_i$ (i=1,2,3), which form the co-rotational basis $\{\mathbf{a}_i\}$. This basis is orthonormal, but not tangent to the deformed middle surface, unless the transverse shear deformation is equal to zero. Note that though we shall exploit the co-rotational basis, by no means our formulation

can be called the co-rotational theory, with rotations confined to the frame, see the recent survey of shell elements and co-rotational theories by [Stolarski, Belytschko, Lee, 1995].

Note that the initial and the current configuration of the shell are characterized by pairs of vectors, $\{\mathbf{y}_0, \mathbf{t}_3\}$ and $\{\mathbf{x}_0, \mathbf{a}_3\}$, with an apparent similarity to a (one-director) Cosserat surface. The difference is that here the rotations are introduced via the polar decomposition of the deformation gradient, while in the Cosserat theory the rotations are not linked kinematically with displacements.

The deformation function $\boldsymbol{\chi}: \mathbf{x} = \boldsymbol{\chi}(\mathbf{y})$ maps the reference configuration of the shell onto the current (deformed) one. For the convected coordinate system $\{S^\alpha, \zeta\}$ we have $\mathbf{x} = \boldsymbol{\chi}(S^\alpha(\mathbf{y}), \zeta(\mathbf{y}))$, and the deformation gradient can be written as follows

$$\mathbf{F}(\zeta) \equiv \frac{\partial \boldsymbol{\chi}}{\partial \mathbf{y}} = \frac{\partial \boldsymbol{\chi}}{\partial S^\alpha} \otimes \frac{\partial S^\alpha}{\partial \mathbf{y}} + \frac{\partial \boldsymbol{\chi}}{\partial \zeta} \otimes \frac{\partial \zeta}{\partial \mathbf{y}} \tag{3.55}$$

Note that $\partial S^\alpha / \partial \mathbf{y} = \mathbf{g}^\alpha$ and $\partial \zeta / \partial \mathbf{y} = \mathbf{t}^3 = \mathbf{t}_3$. As the co-vectors $\mathbf{g}^\alpha$ belong to the plane spanned by $\mathbf{g}_\alpha$ hence the same shifter $\mathbf{Z}$ can be used to relate them to the middle-surface vectors. Then,

$$\mathbf{x}_{,\alpha} \otimes \mathbf{g}^\alpha = (\mathbf{x}_{,\alpha} \otimes \mathbf{t}^\alpha)\, \mathbf{Z}^{-1} \tag{3.56}$$

To simplify the derivation we shall assume that $\mathbf{Z} \approx \mathbf{Z}^{-1} \approx \mathbf{I}$ what provides $\mu = \mu^{-1} = 1$ and $\mathbf{g}^\alpha = \mathbf{t}^\alpha = \mathbf{t}_\alpha$. This form of the shifter and its inverse can be obtained if the undeformed shell is shallow, i.e. when $\mathbf{B} \approx \mathbf{0}$. As already pointed out in the literature, e.g. in [DeBoer, Walther, 1986], to obtain the same approximation it suffices to assume that $h\mathbf{B} \ll \mathbf{I}_0$, which to a lesser degree restricts the curvature when the shell is thin. In consequence, the deformation gradient has the following simple form

$$\mathbf{F}(\zeta) = \mathbf{x}_{,\alpha} \otimes \mathbf{t}_\alpha + \mathbf{x}_{,\zeta} \otimes \mathbf{t}_3 \tag{3.57}$$

For the generalized Reissner hypothesis, eq.(53), $\mathbf{x}_{,\alpha} = \mathbf{x}_{0,\alpha} + \zeta(\lambda \mathbf{a}_3)_{,\alpha}$, and separating the terms multiplied by ζ we obtain

$$\mathbf{F}(\zeta) = \mathbf{F}_0 + \zeta(\mathbf{F}_{,\zeta})_0 \tag{3.58}$$

where

$$\mathbf{F}_0 \equiv \mathbf{x}_{0,\alpha} \otimes \mathbf{t}_\alpha + (\lambda \mathbf{a}_3) \otimes \mathbf{t}_3, \qquad (\mathbf{F}_{,\zeta})_0 \equiv (\lambda \mathbf{a}_3)_{,\alpha} \otimes \mathbf{t}_\alpha \tag{3.59}$$

The variation of the deformation gradient $\mathbf{F}$ can be expressed as

$$\delta \mathbf{F}(\zeta) = \delta \mathbf{F}_0 + \zeta \delta(\mathbf{F}_{,\zeta})_0 \tag{3.60}$$

where

$$\delta \mathbf{F}_0 \equiv \delta \mathbf{x}_{0,\alpha} \otimes \mathbf{t}_\alpha + \delta(\lambda \mathbf{a}_3) \otimes \mathbf{t}_3, \qquad \delta(\mathbf{F}_{,\zeta})_0 \equiv \delta(\lambda \mathbf{a}_3)_{,\alpha} \otimes \mathbf{t}_\alpha \tag{3.61}$$

For a derivative of the forward-rotated director $\mathbf{a}_3$ the following formula involving skew-symmetric tensors can be obtained,

$$\mathbf{a}_{3,\alpha} = (\mathbf{Q}_0 \mathbf{t}_3)_{,\alpha} = \mathbf{Q}_{0,\alpha} \mathbf{t}_3 + \mathbf{Q}_0 \mathbf{t}_{3,\alpha} = \bar{\boldsymbol{\Omega}}_\alpha \mathbf{a}_3 = \bar{\boldsymbol{\omega}}_\alpha \times \mathbf{a}_3 \tag{3.62}$$

where the skew-symmetric tensors and their axial vectors are as follows

$$\bar{\Omega}_\alpha = \Omega_\alpha + \mathbf{Q}_0\Omega^0_\alpha\mathbf{Q}_0^T\,, \quad \bar{\omega}_\alpha = \omega_\alpha + \mathbf{Q}_0\omega^0_\alpha$$
$$\Omega_\alpha = \mathbf{Q}_{0,\alpha}\mathbf{Q}_0^T\,, \qquad \Omega_\alpha\mathbf{a}_3 = \omega_\alpha \times \mathbf{a}_3 \tag{3.63}$$
$$\Omega^0_\alpha = \mathbf{Q}^0_{0,\alpha}(\mathbf{Q}^0_0)^T\,, \qquad \Omega^0_\alpha\mathbf{a}_3 = \omega^0_\alpha \times \mathbf{a}_3$$

Here, $\mathbf{Q}^0_0$ is a rotation tensor describing a position of $\mathbf{t}_3$, i.e. $\mathbf{t}_3 = \mathbf{Q}^0_0\mathbf{i}_3$. For a shallow shell $\mathbf{Q}^0_{0,\alpha} \approx 0$ and $\bar{\Omega}_\alpha \approx \Omega_\alpha$. Note that we could have used here the 2nd Christoffel symbol, and write $\mathbf{t}_{3,\alpha} = \Gamma^k_{3\alpha}\mathbf{t}_k$.

For the standard Reissner hypothesis the deformation gradient consists of the following components

$$\mathbf{F}_0 \equiv \mathbf{x}_{0,\alpha} \otimes \mathbf{t}_\alpha + \mathbf{a}_3 \otimes \mathbf{t}_3, \qquad (\mathbf{F}_{,\zeta})_0 \equiv \mathbf{a}_{3,\alpha} \otimes \mathbf{t}_\alpha = [\bar{\omega}_\alpha \times \mathbf{a}_3] \otimes \mathbf{t}_\alpha \tag{3.64}$$

The variation of the deformation gradient $\mathbf{F}$, eq.(60), has the following components

$$\delta\mathbf{F}_0 = \delta\mathbf{x}_{0,\alpha} \otimes \mathbf{t}_\alpha + \delta\mathbf{a}_3 \otimes \mathbf{t}_3, \qquad \zeta\delta(\mathbf{F}_{,\zeta})_0 \equiv \delta[\bar{\omega}_\alpha \times \zeta\mathbf{a}_3] \tag{3.65}$$

where

$$\delta[\bar{\omega}_\alpha \times \zeta\mathbf{a}_3] = \delta\mathbf{x}_{0,\alpha} + \delta\bar{\omega}_\alpha \times \zeta\mathbf{a}_3 + \bar{\omega}_\alpha \times \zeta\delta\mathbf{a}_3 \tag{3.66}$$

$$\delta\bar{\omega}_\alpha = \delta\boldsymbol{\theta}_{,\alpha} + \delta\boldsymbol{\theta} \times \bar{\omega}_\alpha, \qquad \delta\mathbf{a}_3 = \delta\mathbf{Q}_0\mathbf{t}_3 = \delta\tilde{\boldsymbol{\theta}}\mathbf{a}_3 = \delta\boldsymbol{\theta} \times \mathbf{a}_3 \tag{3.67}$$

In the above $\delta\tilde{\boldsymbol{\theta}} = \delta\boldsymbol{\theta} \times \mathbf{I}$ is a left skew-symmetric tensor and $\delta\boldsymbol{\theta}$ is its axial vector. $\delta\mathbf{F}(\zeta)$ is expressed by a variation of displacements, $\delta\mathbf{x}_0 = \delta\mathbf{u}_0$, and by the axial vector, $\delta\boldsymbol{\theta}$, corresponding with a rotation of the mid-surface.

Consider a deformation of the shell characterized by the drilling rotation ω around the normal vector $\mathbf{t}_3$. Then, $\mathbf{t}_3$ is an eigenvector of $\mathbf{Q}_0$ associated with the eigenvalue $+1$. Note that in (59) and (64) the rotation tensor operates only on the normal vector. Hence, $\mathbf{a}_3 = \mathbf{Q}_0\mathbf{t}_3 = \mathbf{t}_3$, and the components of the deformation gradient are as follows

$$\mathbf{F}_0 \equiv \mathbf{x}_{0,\alpha} \otimes \mathbf{t}_\alpha + \mathbf{t}_3 \otimes \mathbf{t}_3, \qquad (\mathbf{F}_{,\zeta})_0 \equiv \mathbf{t}_{3,\alpha} \otimes \mathbf{t}_\alpha \tag{3.68}$$

They do not depend explicitly on the rotation angle, ω, i.e. are insensitive to the drilling rotation. The same is true for the tensors which depend only on the deformation gradient, such as the right Cauchy-Green tensor, $\mathbf{C} = \mathbf{F}^T\mathbf{F}$ and the Green strain, $\mathbf{E} = \frac{1}{2}(\mathbf{C} - \mathbf{I})$. Therefore, for the formulation based on the Green strain measure only two-parameter rotations can be considered, such as e.g. presented in Section 2.3.4.

A different property has the right stretch strain, which is defined as the product of the deformation gradient and the rotation. It naturally admits a three parameter representation of rotations since the rotation tensor operates also on the tangent vectors.

3.4 Shell strains and skew tensors

In this section we specify in the local bases the relaxed right stretch strains and the skew-symmetric parts of $\mathbf{Q}^T\mathbf{F}$, using both forms of the deformation gradient derived earlier.

For the generalized Reissner hypothesis, and representations (59) of $\mathbf{F}_0$ and $(\mathbf{F}_{,\zeta})_0$, the components of the product $\mathbf{Q}^T\mathbf{F}$ become

$$\begin{cases} \mathbf{Q}_0^T\mathbf{F}_0 = (\mathbf{Q}_0^T\mathbf{x}_{0,\alpha}) \otimes \mathbf{t}_\alpha + \lambda \mathbf{t}_3 \otimes \mathbf{t}_3 \\ \mathbf{Q}_0^T(\mathbf{F}_{,\zeta})_0 = \mathbf{Q}_0^T(\lambda \mathbf{a}_3)_{,\alpha} \otimes \mathbf{t}_\alpha \end{cases} \tag{3.69}$$

For the standard Reissner hypothesis we can use the representation (64), what yields

$$\begin{cases} \mathbf{Q}_0^T\mathbf{F}_0 = (\mathbf{Q}_0^T\mathbf{x}_{0,\alpha}) \otimes \mathbf{t}_\alpha + \mathbf{t}_3 \otimes \mathbf{t}_3 \\ \mathbf{Q}_0^T(\mathbf{F}_{,\zeta})_0 = \left(\mathbf{Q}_0^T\mathbf{Q}_{0,\alpha} + \Omega_\alpha^0\right)\mathbf{t}_3 \otimes \mathbf{t}_\alpha = \left[(\mathbf{Q}_0^T\bar{\omega}_\alpha) \times \mathbf{t}_3\right] \otimes \mathbf{t}_\alpha \end{cases} \tag{3.70}$$

The Taylor approximation of the identity tensor can be written as follows

$$\mathbf{I}(\zeta) \equiv \frac{\partial \mathbf{y}}{\partial \mathbf{y}} = \frac{\partial \mathbf{y}}{\partial S^\alpha} \otimes \frac{\partial S^\alpha}{\partial \mathbf{y}} + \frac{\partial \mathbf{y}}{\partial \zeta} \otimes \frac{\partial \zeta}{\partial \mathbf{y}} \tag{3.71}$$

On use of $\partial S^\alpha/\partial \mathbf{y} = \mathbf{g}^\alpha$, $\partial \zeta/\partial \mathbf{y} = \mathbf{t}^3 = \mathbf{t}_3$, we obtain $\mathbf{y}_{,\alpha} \otimes \mathbf{g}^\alpha = \left(\mathbf{y}_{,\alpha} \otimes \mathbf{t}^\alpha\right)\mathbf{Z}^{-1}$. For the assumed geometry of shells, the shifter tensor $\mathbf{Z} \approx \mathbf{Z}^{-1} \approx \mathbf{I}$ what provides $\mu = \mu^{-1} = 1$ and $\mathbf{g}^\alpha = \mathbf{t}^\alpha = \mathbf{t}_\alpha$. Then, on use of $\mathbf{y}_{,\zeta} = \mathbf{t}_3$ and $\mathbf{y}_{0,\alpha} = \mathbf{t}_\alpha$ in $\mathbf{y}_{,\alpha} = \mathbf{y}_{0,\alpha} + \zeta \mathbf{t}_{3,\alpha}$, the identity tensor can be written as follows

$$\mathbf{I}(\zeta) = \mathbf{I}_0 + \zeta\, (\mathbf{I}_{,\zeta})_0 \tag{3.72}$$

where $\mathbf{I}_0 \equiv \mathbf{t}_i \otimes \mathbf{t}_i$ is the metric tensor, and $(\mathbf{I}_{,\zeta})_0 \equiv \mathbf{t}_{3,\alpha} \otimes \mathbf{t}^\alpha = -\mathbf{B}$, is the curvature tensor, both for to the middle surface of the initial configuration of the shell. Note that for the assumed geometry of the shell the second component of the above equation is negligible in comparison to the first one.

3.4.1 Relaxed right stretch strain for shell

The relaxed right stretch strain for a shell is defined in eq.(32) as $\mathbf{H}(\zeta) = \boldsymbol{\varepsilon} + \zeta\boldsymbol{\kappa}$. Exploiting the symmetry of $\mathbf{I}_0$ and $(\mathbf{I}_{,\zeta})_0$, and using eq.(69) we obtain for the generalized Reissner hypothesis

$$\begin{cases} \boldsymbol{\varepsilon} = \mathrm{sym}\left[(\mathbf{Q}_0^T\mathbf{x}_{0,\alpha} - \mathbf{t}_\alpha) \otimes \mathbf{t}_\alpha\right] + \mathrm{sym}\left[(\lambda - 1)\mathbf{t}_3 \otimes \mathbf{t}_3\right] \\ \boldsymbol{\kappa} = \mathrm{sym}\left[(\mathbf{Q}_0^T(\lambda \mathbf{a}_3)_{,\alpha} - \mathbf{t}_{3,\alpha}) \otimes \mathbf{t}_\alpha\right] \end{cases} \tag{3.73}$$

Components of these measures in the basis $\{\mathbf{t}_i\}$ are as follows

$$\begin{gathered} \varepsilon_{11} = \mathbf{x}_{0,1} \cdot \mathbf{a}_1 - 1, \qquad \varepsilon_{22} = \mathbf{x}_{0,2} \cdot \mathbf{a}_2 - 1, \qquad \varepsilon_{33} = \lambda - 1 \\ \varepsilon_{12} = \varepsilon_{21} = \frac{1}{2}\left(\mathbf{x}_{0,1} \cdot \mathbf{a}_2 + \mathbf{x}_{0,2} \cdot \mathbf{a}_1\right), \qquad \varepsilon_{\alpha 3} = \varepsilon_{3\alpha} = \frac{1}{2}\mathbf{x}_{0,\alpha} \cdot \mathbf{a}_3 \\ \kappa_{11} = (\lambda \mathbf{a}_3)_{,1} \cdot \mathbf{a}_1 - \mathbf{t}_{3,1} \cdot \mathbf{t}_1, \qquad \kappa_{22} = (\lambda \mathbf{a}_3)_{,2} \cdot \mathbf{a}_2 - \mathbf{t}_{3,2} \cdot \mathbf{t}_2, \qquad \kappa_{33} = 0 \end{gathered} \tag{3.74}$$

$$\kappa_{12} = \kappa_{21} = \frac{1}{2}\left[(\lambda \mathbf{a}_3)_{,1} \cdot \mathbf{a}_2 + (\lambda \mathbf{a}_3)_{,2} \cdot \mathbf{a}_1\right], \qquad \kappa_{\alpha 3} = \kappa_{3\alpha} = \frac{1}{2}\left[(\lambda \mathbf{a}_3)_{,\alpha} \cdot \mathbf{a}_3 - \mathbf{t}_{3,\alpha} \cdot \mathbf{t}_3\right]$$

For the standard Reissner hypothesis and eq.(70), we obtain in place of (74) the following measures

$$\begin{cases} \boldsymbol{\varepsilon} = \mathrm{sym}\left[(\mathbf{Q}_0^T \mathbf{x}_{0,\alpha} - \mathbf{t}_\alpha) \otimes \mathbf{t}_\alpha\right] \\ \boldsymbol{\kappa} = \mathrm{sym}\left[(\mathbf{Q}_0^T \mathbf{Q}_{0,\alpha})\mathbf{t}_3 \otimes \mathbf{t}_\alpha\right] \end{cases} \tag{3.75}$$

Components of these measures in the basis $\{\mathbf{t}_i\}$ are as follows

$$\begin{gathered} \varepsilon_{11} = \mathbf{x}_{0,1} \cdot \mathbf{a}_1 - 1, \qquad \varepsilon_{22} = \mathbf{x}_{0,2} \cdot \mathbf{a}_2 - 1, \qquad \varepsilon_{33} = 0 \\ \varepsilon_{12} = \varepsilon_{21} = \frac{1}{2}\left(\mathbf{x}_{0,1} \cdot \mathbf{a}_2 + \mathbf{x}_{0,2} \cdot \mathbf{a}_1\right), \qquad \varepsilon_{\alpha 3} = \varepsilon_{3\alpha} = \frac{1}{2}\mathbf{x}_{0,\alpha} \cdot \mathbf{a}_3 \\ \kappa_{11} = (\mathbf{Q}_{0,1}\mathbf{t}_3) \cdot \mathbf{a}_1, \qquad \kappa_{22} = (\mathbf{Q}_{0,2}\mathbf{t}_3) \cdot \mathbf{a}_2, \qquad \kappa_{33} = 0 \\ \kappa_{12} = \kappa_{21} = \frac{1}{2}\left[(\mathbf{Q}_{0,1}\mathbf{t}_3) \cdot \mathbf{a}_2 + (\mathbf{Q}_{0,2}\mathbf{t}_3) \cdot \mathbf{a}_1\right], \qquad \kappa_{\alpha 3} = \kappa_{3\alpha} = \frac{1}{2}(\mathbf{Q}_{0,\alpha}\mathbf{t}_3) \cdot \mathbf{a}_3 \end{gathered} \tag{3.76}$$

On comparison of (74) and (76), we can see that inextensibility hypothesis affected all components but $\varepsilon_{\alpha\beta}$ and κ_{33}. Hence, the measures for the standard Reissner kinematics may be used for the finite strain deformation, when only the membrane components $\varepsilon_{\alpha\beta}$ are finite. Note that the normal component of the curvature tensor, i.e. κ_{33}, is equal to zero for both hypotheses. The inextensibility of the director for the standard Reissner hypothesis gives a side-effect that the normal strain component $\varepsilon_{33} = 0$, what is non-realistic for most cases of deformation; more accurate values of the normal strain can be recovered as shown in Section 3.7.

On use of (74) and (76) we can show that the shell strain measures derived from the right stretch strain include effects of the drilling rotation, in this way admitting three-parameter rotations. Consider a deformation of the shell characterized by the drilling rotation ω around the normal vector $\mathbf{t}_3$. Then, $\mathbf{t}_3$ is an eigenvector of $\mathbf{Q}_0$ associated with the eigenvalue $+1$. Hence, $\mathbf{a}_3 = \mathbf{Q}_0\mathbf{t}_3 = \mathbf{t}_3$, i.e. the normal vector remains unaltered by the drilling rotation. But for the tangent vectors we have $\mathbf{a}_\alpha = \mathbf{Q}_0\mathbf{t}_\alpha$, i.e. $\mathbf{t}_\alpha$ are rotated around $\mathbf{t}_3$ by an angle ω. Because, $\varepsilon_{\alpha\beta}$ and $\kappa_{\alpha\beta}$ depend on $\mathbf{a}_\alpha$, hence they include effects of the drilling rotation.

For a shallow shell we have $\mathbf{t}_{3,\alpha} \approx \mathbf{0}$, and in consequence $\mathbf{Q}_{0,\alpha}\mathbf{t}_3 \approx (\mathbf{Q}_0\mathbf{t}_3)_{,\alpha} \approx \mathbf{t}_{3,\alpha} \approx \mathbf{0}$, Hence, $\kappa_{\alpha\beta} = 0$ and only the membrane components are affected by the drilling rotation.

3.4.2 Skew parts of $\mathbf{Q}^T\mathbf{F}$ for shell

For the generalized Reissner kinematics, the skew tensors appearing in eq.(43) and (47), on use of the approximations specified by eq.(69), can be expressed as follows

$$\begin{cases} \mathbf{C} \equiv \mathrm{skew}(\mathbf{Q}^T\mathbf{F})_0 = \mathrm{skew}\left[(\mathbf{Q}_0^T\mathbf{x}_{0,\alpha}) \otimes \mathbf{t}_\alpha + \lambda \mathbf{t}_3 \otimes \mathbf{t}_3\right] \\ \mathbf{D} \equiv \mathrm{skew}(\mathbf{Q}^T\mathbf{F}_{,\zeta})_0 = \mathrm{skew}\left[\mathbf{Q}_0^T(\lambda \mathbf{a}_3)_{,\alpha} \otimes \mathbf{t}_\alpha\right] \end{cases} \tag{3.77}$$

Hence, their nonzero components in the basis $\{\mathbf{t}_i\}$ are as follows

$$C_{12} = -C_{21} = \tfrac{1}{2}(\mathbf{x}_{0,2}\cdot\mathbf{a}_1 - \mathbf{x}_{0,1}\cdot\mathbf{a}_2), \qquad C_{\alpha 3} = -C_{3\alpha} = -\tfrac{1}{2}\mathbf{x}_{0,\alpha}\cdot\mathbf{a}_3$$

$$D_{12} = -D_{21} = \tfrac{1}{2}[(\lambda\mathbf{a}_3)_{,2}\cdot\mathbf{a}_1 - (\lambda\mathbf{a}_3)_{,1}\cdot\mathbf{a}_2], \qquad D_{\alpha 3} = -D_{3\alpha} = -\tfrac{1}{2}(\lambda\mathbf{a}_3)_{,\alpha}\cdot\mathbf{a}_3 \tag{3.78}$$

For the standard Reissner kinematics the approximations specified by eq.(70) yield the skew tensors of the following form

$$\begin{cases} \mathbf{C} \equiv \mathrm{skew}(\mathbf{Q}^T\mathbf{F})_0 = \mathrm{skew}\left[(\mathbf{Q}_0^T\mathbf{x}_{0,\alpha})\otimes\mathbf{t}_\alpha + \mathbf{t}_3\otimes\mathbf{t}_3\right] \\ \mathbf{D} \equiv \mathrm{skew}(\mathbf{Q}^T\mathbf{F}_{,\zeta})_0 = \mathrm{skew}\left[(\mathbf{Q}_0^T\mathbf{a}_{3,\alpha})\otimes\mathbf{t}_\alpha\right] \end{cases} \tag{3.79}$$

Their nonzero components in the basis $\{\mathbf{t}_i\}$ are as follows

$$C_{12} = -C_{21} = \tfrac{1}{2}(\mathbf{x}_{0,2}\cdot\mathbf{a}_1 - \mathbf{x}_{0,1}\cdot\mathbf{a}_2), \qquad C_{\alpha 3} = -C_{3\alpha} = -\tfrac{1}{2}\mathbf{x}_{0,\alpha}\cdot\mathbf{a}_3$$

$$D_{12} = -D_{21} = \tfrac{1}{2}(\mathbf{a}_{3,2}\cdot\mathbf{a}_1 - \mathbf{a}_{3,1}\cdot\mathbf{a}_2), \qquad D_{\alpha 3} = -D_{3\alpha} = -\tfrac{1}{2}\mathbf{a}_{3,\alpha}\cdot\mathbf{a}_3 \tag{3.80}$$

For a shallow shell D_{12} and $D_{\alpha 3}$ reduce to

$$D_{12} = \frac{1}{2}[(\mathbf{Q}_{0,2}\mathbf{t}_3)\cdot\mathbf{a}_1 - (\mathbf{Q}_{0,1}\mathbf{t}_3)\cdot\mathbf{a}_2)], \qquad D_{\alpha 3} = D_{3\alpha} = -\frac{1}{2}(\mathbf{Q}_{0,\alpha}\mathbf{t}_3)\cdot\mathbf{a}_3$$

For the drilling rotation ω around the normal vector $\mathbf{t}_3$ and the shallow shell $D_{12} = D_{\alpha 3} = 0$.

3.4.3 Symmetry of strain measures - discussion of other approaches

Symmetry of strain measures is important because it allows to uniquely invert the constitutive equation, and to introduce the complementary energy principle. For the so called generalized displacement gradient, which can be identified as equal to $\mathbf{Q}^T\mathbf{F}$, the question of symmetry is considered by [Reissner, 1984] and [Bufler, 1985]. In [Reissner, 1984], the rotation is chosen so that $\mathbf{Q}^T\mathbf{F}$ is symmetric, and a symmetric part of the 1st Piola-Kirchhoff $\mathbf{P}$ is used. Hence, the inverse constitutive equation becomes $(\mathbf{Q}^T\mathbf{F}) = \partial V(\mathrm{sym}\mathbf{P})/\partial(\mathrm{sym}\mathbf{P})$, where V is the complementary energy. In the present work, the strain measures are always symmetric because in the definition of the *relaxed* right stretch strain the symmetric part of $\mathbf{Q}^T\mathbf{F}$ is exploited.

Below we discuss for comparison the methods published in the literature, which attempt to obtain symmetric strain measures for shells by a suitable choice of the rotation tensor. [Wriggers, Gruttmann, 1993] and [Gruttmann, Wagner, Wriggers, 1992], developed two simplified methods, which consist of symmetrizing only the membrane components of the strain tensor. The first of the papers adopts the method proposed by [Reissner, 1984]. The elementary rotations are $\mathbf{Q} = \mathbf{Q}_2\mathbf{Q}_1\mathbf{\Lambda}$, where $\mathbf{Q}_1$ and $\mathbf{Q}_2$ are rotations around the tangent vectors, and $\mathbf{\Lambda}$ is a rotation around the normal vector of the local basis. First, a set of vectors, which are back-rotated by $\mathbf{Q}_2\mathbf{Q}_1$, is introduced, i.e. $\tilde{\mathbf{e}}_\alpha \equiv \mathbf{Q}_1^T\mathbf{Q}_2^T\mathbf{x}_{0,\alpha}$ and $\tilde{\mathbf{n}}_\alpha \equiv \mathbf{Q}_1^T\mathbf{Q}_2^T\mathbf{n}_\alpha^*$, where $\mathbf{x}_{0,\alpha}$ corresponds with $\mathbf{F}$, and $\mathbf{n}_\alpha^*$ with the 1st Piola-Kirchhoff stress $\mathbf{P}$. Hence,

$$\mathbf{e}_\alpha = \mathbf{\Lambda}^T(\mathbf{Q}_1^T\mathbf{Q}_2^T\mathbf{x}_{0,\alpha}) = \mathbf{\Lambda}^T\tilde{\mathbf{e}}_\alpha, \qquad \mathbf{n}_\alpha = \mathbf{\Lambda}^T(\mathbf{Q}_1^T\mathbf{Q}_2^T\mathbf{n}_\alpha^*) = \mathbf{\Lambda}^T\tilde{\mathbf{n}}_\alpha \tag{3.81}$$

and the respective tensors are $\mathbf{e} \equiv \mathbf{\Lambda}^T \check{\mathbf{e}}_\alpha \otimes \mathbf{t}_\alpha = \mathbf{\Lambda}^T \check{\mathbf{e}}$ and $\mathbf{N} \equiv \mathbf{\Lambda}^T \check{\mathbf{n}}_\alpha \otimes \mathbf{t}_\alpha = \mathbf{\Lambda}^T \check{\mathbf{N}}$. Subsequently, $\mathbf{\Lambda}$ is defined as the rotation involved in the polar decomposition of $\check{\mathbf{e}}$,

$$\check{\mathbf{e}}_s = \mathbf{\Lambda}^T \check{\mathbf{e}} \tag{3.82}$$

where $\check{\mathbf{e}}_s = (\check{\mathbf{e}}^T \check{\mathbf{e}})^{\frac{1}{2}}$. The angle of rotation λ of $\mathbf{\Lambda}(\lambda, \mathbf{t}_3)$ is determined from the symmetry condition for $\check{\mathbf{e}}$, and is treated as an intermediate variable depending on $\check{\mathbf{e}}$. The shell strain measure is introduced as $\boldsymbol{\varepsilon} = (\mathbf{\Lambda}^T \check{\mathbf{e}}_\alpha - \mathbf{t}_\alpha) \otimes \mathbf{t}_\alpha$. For the change of curvature terms and the couple resultants the following procedure is used. First, they are back-rotated by $\mathbf{\Lambda}$, $\bar{\boldsymbol{\kappa}}_\alpha = \mathbf{\Lambda}^T \check{\boldsymbol{\kappa}}_\alpha$ and $\bar{\mathbf{m}}_\alpha = \mathbf{\Lambda}^T \check{\mathbf{m}}_\alpha$. In general, this operation yields non-symmetric $\bar{\boldsymbol{\kappa}} = \bar{\boldsymbol{\kappa}}_\alpha \otimes \mathbf{t}_\alpha$ and $\bar{\mathbf{M}} = \bar{\mathbf{m}}_\alpha \otimes \mathbf{t}_\alpha$, and hence only a product of their symmetric parts is taken. The integrand of the virtual work is approximated as follows

$$\mathbf{N} \cdot \delta \mathbf{e} + \mathbf{M} \cdot \delta \boldsymbol{\kappa} \approx (\mathbf{\Lambda}^T \check{\mathbf{N}}) \cdot \delta(\mathbf{\Lambda}^T \check{\mathbf{e}}) + \mathrm{sym}\bar{\mathbf{M}} \cdot \mathrm{sym}\delta\bar{\boldsymbol{\kappa}} \tag{3.83}$$

Note that $\mathbf{\Lambda}^T \check{\mathbf{e}}$ symmetrizes only the in-plane components 12 and 21, so the method is exact only for membranes as the rotation constraint implies full symmetry of $\mathbf{Q}^T \mathbf{F}$. The bending-shearing terms are treated differently than the membrane ones, and we can expect difficulties even in the absence of the membrane strains.

In the above approach, the drilling rotation angle λ is an intermediate variable depending on $\check{\mathbf{e}}$, and cannot be used as a degree of freedom. Hence, in [Gruttmann, Wagner, Wriggers, 1992], the above method is extended in order to include explicitly the drilling rotation. A three-field formulation, in terms of displacements $\mathbf{u}$, a scalar N, and a scalar ω for the unknown drilling rotation, is developed. The potential energy functional is amended by the terms $N(\Theta - \omega) - N^2/(2\gamma)$, where Θ is the drilling rotation yielded by the polar decomposition theorem, and γ is the penalty number.

From the point of view of our development the interpretation of the Lagrange multiplier N as associated with the skew part of the membrane forces does not seem to be correct. As indicates our formulation the skew part of the membrane forces must be multiplied by the skew part of $(\mathbf{Q}^T \mathbf{F})_0$. For N so defined it would not be $(\Theta - \omega)$, but $\frac{1}{2}(\mathbf{x}_{0,2} \cdot \mathbf{a}_1 - \mathbf{x}_{0,1} \cdot \mathbf{a}_2)$, on use of $C_{12} = -C_{21}$ of eq.(80). Besides, in this formulation the virtual work equations cf.(16) and (20) are written for the measures which are not symmetric so the tangent operator also will lack the symmetry. That lead the authors to developing of the third approach based on the Green strain, cf.(33).

The method developed in the present work from the outset assumes a three-parameter rotation tensor $\mathbf{Q}$, uses the symmetric *relaxed* right strain measures, and treats in the same way the membrane terms and the bending terms. The penalty method is used to impose the rotation constraint, and a simple logic to decide, which part of the constraint is enforced, what allows to model correctly pure bending-shearing strains.

3.4.4 Rotated shell measures - comparison with [Chroscielewski, Makowski, Stumpf, 1992]

In this section the forward rotated shell strain and stress measures are introduced and a corresponding form of the virtual work principle is provided.

Consider the symmetric parts $\mathbf{N}_s^B$ and $\mathbf{M}_s^B$ of the stress and couple resultants defined by eq.(35), and strain measures $\boldsymbol{\varepsilon}$ and $\boldsymbol{\kappa}$ given by eq.(75). Define the forward rotated stress resultants as

$$\mathbf{N}_s^* \equiv \mathbf{Q}_0\, \mathbf{N}_s^B\, \mathbf{Q}_0^T = \mathrm{sym}[(\mathbf{Q}_0\mathbf{n}_\alpha^B) \otimes (\mathbf{Q}_0\mathbf{t}_\alpha)] = \mathrm{sym}\,[\mathbf{n}_\alpha^* \otimes \mathbf{a}_\alpha] \tag{3.84}$$

where $\mathbf{n}_\alpha^* = \mathbf{Q}_0\mathbf{n}_\alpha^B$. The forward rotated shell counterparts of the relaxed right stretch strain $\mathbf{H} = \mathrm{sym}(\mathbf{Q}_0^T\mathbf{F}) - \mathbf{I}$ are defined as

$$\boldsymbol{\varepsilon}^* \equiv \mathbf{Q}_0\, \boldsymbol{\varepsilon}\, \mathbf{Q}_0^T = \mathrm{sym}\,[(\mathbf{Q}_0\boldsymbol{\varepsilon}_\alpha) \otimes (\mathbf{Q}_0\mathbf{t}_\alpha)] = \mathrm{sym}\,[\boldsymbol{\varepsilon}_\alpha^* \otimes \mathbf{a}_\alpha] \tag{3.85}$$

where $\boldsymbol{\varepsilon}_\alpha^* \equiv \mathbf{Q}_0\, \boldsymbol{\varepsilon}_\alpha$. For the variation $\delta\boldsymbol{\varepsilon} = \mathrm{sym}[\delta\boldsymbol{\varepsilon}_\alpha \otimes \mathbf{t}_\alpha]$ the co-rotational variation of the rotated strain is defined as

$$\overset{\circ}{\delta}\boldsymbol{\varepsilon}^* \equiv \mathbf{Q}_0\, \delta\boldsymbol{\varepsilon}\, \mathbf{Q}_0^T = \mathbf{Q}_0\, \delta(\mathbf{Q}_0^T\boldsymbol{\varepsilon}^*\mathbf{Q}_0)\, \mathbf{Q}_0^T \tag{3.86}$$

and has a form of the Green-McInnis-Naghdi objective rate. The above definition yields

$$\overset{\circ}{\delta}\boldsymbol{\varepsilon}^* = \mathrm{sym}\,[(\mathbf{Q}_0\delta\boldsymbol{\varepsilon}_\alpha) \otimes (\mathbf{Q}_0\mathbf{t}_\alpha)] = \mathrm{sym}[\,\overset{\circ}{\delta}\boldsymbol{\varepsilon}_\alpha^* \otimes \mathbf{a}_\alpha] \tag{3.87}$$

where $\overset{\circ}{\delta}\boldsymbol{\varepsilon}_\alpha^* \equiv \mathbf{Q}_0\, \delta\boldsymbol{\varepsilon}_\alpha$. The couple resultants $\mathbf{M}_s^*$, the bending strain $\boldsymbol{\kappa}^*$ and the variation $\overset{\circ}{\delta}\boldsymbol{\kappa}^*$ can be introduced in a similar way. On use of elementary identities

$$\mathbf{N}_s^B \cdot \delta\boldsymbol{\varepsilon} = \mathrm{tr}(\mathbf{N}_s^{\mathrm{B}}\, \delta\boldsymbol{\varepsilon}^{\mathrm{T}}) = \mathrm{tr}(\mathbf{Q}_0\mathbf{N}_s^{\mathrm{B}}\mathbf{Q}_0^{\mathrm{T}}\, \mathbf{Q}_0\delta\boldsymbol{\varepsilon}^{\mathrm{T}}\mathbf{Q}_0^{\mathrm{T}}) = \mathbf{N}_s^* \cdot \overset{\circ}{\delta}\boldsymbol{\varepsilon}^* \tag{3.88}$$

Hence, for the rotated strain and change of curvature measures, the virtual work of the shell can be expressed as follows

$$\delta\Sigma = \mathbf{N}_s^* \cdot \overset{\circ}{\delta}\boldsymbol{\varepsilon}^* + \mathbf{M}_s^* \cdot \overset{\circ}{\delta}\boldsymbol{\kappa}^* \tag{3.89}$$

For the standard Reissner kinematics the rotated counterparts of the *relaxed* right stretch strain are as follows

$$\boldsymbol{\varepsilon}^* = \mathrm{sym}\,[\boldsymbol{\varepsilon}_\alpha^* \otimes \mathbf{a}_\alpha], \qquad \boldsymbol{\varepsilon}_\alpha^* = \mathbf{Q}_0\boldsymbol{\varepsilon}_\alpha = \mathbf{Q}_0(\mathbf{Q}_0^T\mathbf{x}_{0,\alpha} - \mathbf{t}_\alpha) = \mathbf{x}_{0,\alpha} - \mathbf{a}_\alpha \tag{3.90}$$

$$\boldsymbol{\kappa}^* = \mathrm{sym}\,[\boldsymbol{\kappa}_\alpha^* \otimes \mathbf{a}_\alpha], \qquad \boldsymbol{\kappa}_\alpha^* = \mathbf{Q}_0\boldsymbol{\kappa}_\alpha = \mathbf{Q}_0(\mathbf{Q}_0^T\bar{\boldsymbol{\omega}}_\alpha - \mathbf{t}_{3,\alpha}) = \bar{\boldsymbol{\omega}}_\alpha - \mathbf{Q}_0\mathbf{t}_{3,\alpha} \tag{3.91}$$

For a shallow initial geometry $\boldsymbol{\kappa}_\alpha^* = \boldsymbol{\omega}_\alpha$ as $\bar{\boldsymbol{\omega}}_\alpha \approx \boldsymbol{\omega}_\alpha$ and $\mathbf{t}_{3,\alpha} \approx \mathbf{0}$. Then, only $\boldsymbol{\varepsilon}_\alpha^*$ depends on the co-rotational $\mathbf{a}_\alpha$.

The above form of the measures is suitable for comparison with the measures of [Chroscielewski, Makowski, Stumpf, 1992], where the shell equations are derived directly from the three-dimensional integral balance laws, as in the approach of [Simmonds, 1984].

Note that in [Chroscielewski, Makowski, Stumpf, 1992] not $\boldsymbol{\varepsilon}^*$ and $\boldsymbol{\kappa}^*$ but the vectors $\boldsymbol{\varepsilon}_\alpha^*$ and $\boldsymbol{\kappa}_\alpha^*$ are used as shell strain measures. The characteristic feature of these vectors is that their co-rotational variations are conjugate to the stress and couple resultants for the 1st Piola-Kirchhoff stress. Hence, they are the shell counterparts of the deformation gradient, as the 1st Piola-Kirchhoff stress and a variation of the deformation gradient are a conjugate pair.

The next difference between the present and cited work concerns rotations. The rotation constraint is not used in the aforementioned paper hence we cannot expect that the

rotations yielded by their formulation, namely $\mathbf{Q}_0$, will satisfy the equation of the polar decomposition of the deformation gradient. The difference between the rotation tensor introduced in the kinematical hypothesis and that yielded by the polar decomposition of the deformation gradient is known in the literature, see for instance [Pietraszkiewicz, 1979a, Chapter 4], but typically passes unnoticed in the works on numerical models of shells, see papers cited e.g. in [Zienkiewicz, Taylor,1991] Chapter 1-5. For the two-parameter rotations this difference can be neglected if the transverse shear strain in the shell is infinitesimal. However, the membrane shear strain in the shell can be significant and then the difference between both the drilling rotations can be important.

Example. Strain vectors $\boldsymbol{\varepsilon}_\alpha$ and $\boldsymbol{\varepsilon}^*_\alpha$ for a planar deformation

Let us specify strain $\boldsymbol{\varepsilon}_1$ in the basis $\{\mathbf{t}_i\}$ for a deformation in the plane $\{\mathbf{t}_1, \mathbf{t}_3\}$. A displacement vector is decomposed as $\mathbf{u} = u\mathbf{t}_1 + w\mathbf{t}_3$. The derivative of the initial position vector is $\mathbf{y}_{0,1} = \mathbf{t}_1$ for the arc-length coordinate S_1. For $\mathbf{x}_0 = \mathbf{y}_0 + \mathbf{u}$ we get the derivative of the current position

$$\mathbf{x}_{0,1} = (1 + u_{,1})\mathbf{t}_1 + w_{,1}\mathbf{t}_3$$

The rotation tensor can be expressed as

$$\mathbf{Q}_0 = \cos\beta\,[\mathbf{t}_1 \otimes \mathbf{t}_1 + \mathbf{t}_3 \otimes \mathbf{t}_3] - \sin\beta\,[\mathbf{t}_1 \otimes \mathbf{t}_3 - \mathbf{t}_3 \otimes \mathbf{t}_1] + \mathbf{t}_2 \otimes \mathbf{t}_2$$

where β is an angle of rotation. The strain vector is expressed as

$$\boldsymbol{\varepsilon}_1 = [(1 + u_{,1})\cos\beta + w_{,1}\sin\beta - 1]\;\mathbf{t}_1 + [-(1 + u_{,1})\sin\beta + w_{,1}\cos\beta]\;\mathbf{t}_3 \qquad (3.92)$$

Subsequently, for the same deformation, the strain $\boldsymbol{\varepsilon}^*_1$ is specified in the basis $\{\mathbf{a}_i\}$. A displacement vector is decomposed as $\mathbf{u} = u\mathbf{a}_1 + w\mathbf{a}_3$. The derivative of the initial position vector is $\mathbf{y}_{0,1} = \mathbf{t}_1 = \mathbf{Q}_0\mathbf{a}_1 = \cos\beta\mathbf{a}_1 - \sin\beta\mathbf{a}_3$, where the rotation tensor

$$\mathbf{Q}_0 = \cos\beta\,[\mathbf{a}_1 \otimes \mathbf{a}_1 + \mathbf{a}_3 \otimes \mathbf{a}_3] - \sin\beta\,[\mathbf{a}_1 \otimes \mathbf{a}_3 - \mathbf{a}_3 \otimes \mathbf{a}_1] + \mathbf{a}_2 \otimes \mathbf{a}_2$$

and β is an angle of rotation. For $\mathbf{x}_0 = \mathbf{y}_0 + \mathbf{u}$ we get a derivative of the current position

$$\mathbf{x}_{0,1} = (\cos\beta + u_{,1})\mathbf{a}_1 + (\sin\beta + w_{,1})\mathbf{a}_3$$

The strain vector is expressed as

$$\boldsymbol{\varepsilon}^*_1 = (\cos\beta - 1 + u_{,1})\mathbf{a}_1 + (-\sin\beta + w_{,1})\mathbf{a}_3 \qquad (3.93)$$

Comparing eq.(92) and (93) we note that $\boldsymbol{\varepsilon}^*_1$ has a simpler form than $\boldsymbol{\varepsilon}_1$. See Fig.3.2 for a geometrical interpretation of both vectors.

From the definition of the co-rotational variation of a strain tensor (87) we obtain a co-rotational variation of the strain vector

$$\overset{\circ}{\delta}\boldsymbol{\varepsilon}^*_\alpha \equiv \mathbf{Q}_0\delta\boldsymbol{\varepsilon}_\alpha = \mathbf{Q}_0\left[\delta(\mathbf{Q}_0^T\boldsymbol{\varepsilon}^*_\alpha)\right] \qquad (3.94)$$

where a relation to $\boldsymbol{\varepsilon}_\alpha$ can be identified for particular operations as follows:

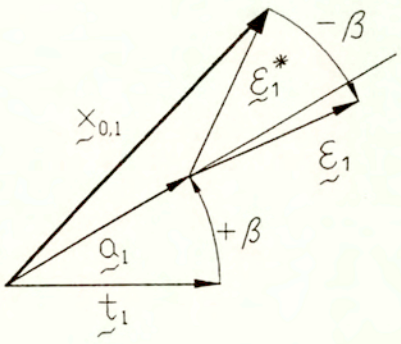

Fig.3.2 Geometrical interpretation of strain measures $\boldsymbol{\varepsilon}_1$ and $\boldsymbol{\varepsilon}_1^*$

1. rotate-back $\boldsymbol{\varepsilon}_\alpha^*$, i.e. $\mathbf{Q}_0^T\boldsymbol{\varepsilon}_\alpha^* = \mathbf{Q}_0^T\mathbf{x}_{0,\alpha} - \mathbf{t}_\alpha \qquad (= \boldsymbol{\varepsilon}_\alpha)$.

2. take variation, i.e. $\delta(\mathbf{Q}_0^T\boldsymbol{\varepsilon}_\alpha^*) = \delta\mathbf{Q}_0^T\mathbf{x}_{0,\alpha} + \mathbf{Q}_0^T\delta\mathbf{x}_{0,\alpha} \qquad (= \delta\boldsymbol{\varepsilon}_\alpha)$,

3. rotate-forward, i.e. $\mathbf{Q}_0\left[\delta(\mathbf{Q}_0^T\boldsymbol{\varepsilon}_\alpha^*)\right] = (\mathbf{x}_{0,\alpha}\times\delta\boldsymbol{\theta}) + \delta\mathbf{u}_{0,\alpha} \qquad (= \mathbf{Q}_0\delta\boldsymbol{\varepsilon}_\alpha)$.

Similarly, for the change of curvature tensor we obtain $\overset{\circ}{\delta}\boldsymbol{\kappa}_\alpha^* = (\bar{\boldsymbol{\omega}}_\alpha\times\delta\boldsymbol{\theta}) + \delta\bar{\boldsymbol{\omega}}_\alpha$. Note that both variations do not depend on the rotation tensor, but only on the (left) axial vector $\delta\boldsymbol{\theta}$.

3.5 Basic equations for shells with Reissner kinematics

In this section the virtual work equation for shells is specified for the standard Reissner kinematics, and the basic equations are derived.

Consider the virtual work of the shell stress and couple resultants, eq.(43). On use of the approximations (70) for the standard Reissner hypothesis, and the representations $\mathbf{N}^B = \mathbf{n}_\alpha^B\otimes\mathbf{t}_\alpha$ and $\mathbf{M}^B = \mathbf{m}_\alpha^B\otimes\mathbf{t}_\alpha$ (α=1,2) we have

$$\mathbf{N}^B\cdot\delta(\mathbf{Q}^T\mathbf{F})_0 = \mathbf{n}_\alpha^B\cdot\delta(\mathbf{Q}_0^T\mathbf{x}_{0,\alpha}) \tag{3.95}$$

$$\mathbf{M}^B\cdot\delta(\mathbf{Q}^T\mathbf{F}_{,\zeta})_0) = \mathbf{m}_\alpha^B\cdot\delta[(\mathbf{Q}_0^T\bar{\boldsymbol{\omega}}_\alpha)\times\mathbf{t}_3] \tag{3.96}$$

where the stress and couple resultant vectors for the Biot stress are defined as follows

$$\mathbf{n}_\alpha^B \equiv \int_{-\frac{h}{2}}^{+\frac{h}{2}}\mathbf{t}_\alpha^B(\zeta)\,\mu\,d\zeta, \qquad \mathbf{m}_\alpha^B \equiv \int_{-\frac{h}{2}}^{+\frac{h}{2}}\zeta\,\mathbf{t}_\alpha^B(\zeta)\,\mu\,d\zeta \tag{3.97}$$

On use of the identity $\mathbf{a}\cdot(\mathbf{b}\times\mathbf{c})=\mathbf{b}\cdot(\mathbf{c}\times\mathbf{a})$, eq.(96) can be expressed as

$$\mathbf{m}^B_\alpha\cdot[\delta(\mathbf{Q}_0^T\bar{\boldsymbol{\omega}}_\alpha)\times\mathbf{t}_3]=[\mathbf{t}_3\times\mathbf{m}^B_\alpha]\cdot\delta(\mathbf{Q}_0^T\bar{\boldsymbol{\omega}}_\alpha) \tag{3.98}$$

The term $\mathbf{t}_3\times\mathbf{m}^B_\alpha=\int_{-\frac{h}{2}}^{+\frac{h}{2}}\zeta\mathbf{t}_3\times\mathbf{t}^B_\alpha(\zeta)\,\mu\,d\zeta$ is an alternative definition of the shell couple resultant.

The virtual work of external forces acting on the upper and lower surface bounding the shell is defined by eq.(41). Assume the orientation of both bounding surfaces as given approximately by the vector $\mathbf{a}_3=\mathbf{Q}_0\mathbf{t}_3$. Hence, $\hat{\mathbf{p}}_3$ denotes the external force corresponding to $\mathbf{a}_3$. For the standard Reissner kinematics we have $\delta\boldsymbol{\chi}(\zeta)=\delta\mathbf{x}(\zeta)=\delta\mathbf{x}_0+\delta\boldsymbol{\theta}\times\zeta\mathbf{a}_3$. Using this expression with the appropriate values of ζ, in eq.(42) we obtain

$$\delta\mathcal{A}=\hat{\mathbf{q}}\cdot\delta\mathbf{x}_0+\hat{\mathbf{m}}\cdot\delta\boldsymbol{\theta} \tag{3.99}$$

where $\hat{\mathbf{q}}\equiv\hat{\mathbf{p}}_3^+ + \hat{\mathbf{p}}_3^-$ and $\hat{\mathbf{m}}\equiv(\frac{h}{2}\mathbf{a}_3)\times(\hat{\mathbf{p}}_3^+-\hat{\mathbf{p}}_3^-)$.

The virtual work of the rotation constraints, eq.(39), for the standard Reissner kinematics can be given as follows

$$\delta\mathbf{N}^B_\alpha\cdot\mathrm{skew}(\mathbf{Q}^T\mathbf{F})_0 \;=\; \mathrm{skew}[\delta\mathbf{n}^B_\alpha\otimes\mathbf{t}_\alpha]\cdot\mathrm{skew}[(\mathbf{Q}_0^T\mathbf{x}_{0,\beta})\otimes\mathbf{t}_\beta)] \tag{3.100}$$

$$\delta\mathbf{M}^B_\alpha\cdot\mathrm{skew}(\mathbf{Q}^T\mathbf{F}_{,\zeta})_0 \;=\; \mathrm{skew}[\delta\mathbf{m}^B_\alpha\otimes\mathbf{t}_\alpha]\cdot\mathrm{skew}[(\mathbf{Q}_0^T\bar{\boldsymbol{\omega}}_\beta)\otimes\mathbf{t}_\beta)] \tag{3.101}$$

Taking into account eq.(95) to (96), and (98) to (101) the virtual work equation for a shell, eq.(43), can be written as

$$\begin{aligned}\delta\Pi_{2d} \;=\; &\int_S \mathbf{n}^B_\alpha\cdot\delta(\mathbf{Q}_0^T\mathbf{x}_{0,\alpha})+[\mathbf{t}_3\times\mathbf{m}^B_\alpha]\cdot\delta(\mathbf{Q}_0^T\bar{\boldsymbol{\omega}}_\alpha)\\ &+\;\delta\mathbf{N}^B_\alpha\cdot\mathrm{skew}[(\mathbf{Q}_0^T\mathbf{x}_{0,\alpha})\otimes\mathbf{t}_\alpha)]+\delta\mathbf{M}^B_\alpha\cdot\mathrm{skew}[(\mathbf{Q}_0^T\bar{\boldsymbol{\omega}}_\alpha)\otimes\mathbf{t}_\alpha)]\\ &-\;h\rho_R\mathbf{b}\cdot\delta\mathbf{x}_0-\hat{\mathbf{q}}\cdot\delta\mathbf{x}_0-\hat{\mathbf{m}}\cdot\delta\boldsymbol{\theta}\;\;dS=0\end{aligned} \tag{3.102}$$

where S denotes the middle surface of the shell.

On use of the forward-rotated stress and couple resultants, see eq.(85), the virtual work of stress and couple resultants can be written in the co-rotational basis $\{\mathbf{a}_i\}$ as

$$\mathbf{n}^*_\alpha\cdot[\delta\mathbf{x}_{0,\alpha}+\boldsymbol{\theta}\times\mathbf{x}_{0,\alpha}]+[\mathbf{a}_3\times\mathbf{m}^*_\alpha]\cdot\delta\boldsymbol{\theta}_{,\alpha} \tag{3.103}$$

where the identity $\delta\bar{\boldsymbol{\omega}}_\alpha+\boldsymbol{\theta}\times\bar{\boldsymbol{\omega}}_\alpha=\delta\boldsymbol{\theta}_{,\alpha}$ was exploited. This identity is valid only for the Reissner kinematics, and it can be verified by calculating a vector product of both sides of the identity with the co-rotational vector $\mathbf{a}_i$, and applying the Lagrange identity for the triple cross-product of vectors. On use of the divergence theorem and the Gauss' theorem in eq.(102) we obtain

$$\begin{aligned}&\int_S-[\mathbf{n}^*_{\alpha,\alpha}+\hat{\mathbf{q}}+h\rho_R\mathbf{b}]\cdot\delta\mathbf{x}_0-[(\mathbf{a}_3\times\mathbf{m}^*_\alpha)_{,\alpha}+\mathbf{x}_{0,\alpha}\times\mathbf{n}^*_\alpha+\hat{\mathbf{m}}]\cdot\delta\boldsymbol{\theta}\;dS\\ &+\int_S\mathrm{skew}[(\mathbf{Q}_0^T\mathbf{x}_{0,\alpha})\otimes\mathbf{t}_\alpha)]\cdot\delta\mathbf{N}^B_\alpha+\mathrm{skew}[(\mathbf{Q}_0^T\bar{\boldsymbol{\omega}}_\alpha)\otimes\mathbf{t}_\alpha)]\cdot\delta\mathbf{M}^B_\alpha\;dS\\ &+\int_{\partial S}[(\mathbf{n}^*_\alpha\otimes\mathbf{a}_\alpha)\boldsymbol{\nu}]\cdot\delta\mathbf{x}_0+[\mathbf{t}_3\times(\mathbf{m}^*_\alpha\otimes\mathbf{a}_\alpha)\boldsymbol{\nu}]\cdot\delta\boldsymbol{\theta}\;d\partial S=0\end{aligned} \tag{3.104}$$

where ∂S identifies the curve bounding the mid-surface, and $\boldsymbol{\nu}$ is a vector tangent to the mid-surface and normal to this curve. This scalar equation provides

$$\mathbf{n}^*_{\alpha,\alpha} + h\rho_R \mathbf{b} + \hat{\mathbf{q}} = \mathbf{0} \qquad \text{in S}$$

$$(\mathbf{a}_3 \times \mathbf{m}^*_\alpha)_{,\alpha} + \mathbf{x}_{0,\alpha} \times \mathbf{n}^*_\alpha + \hat{\mathbf{m}} = \mathbf{0} \qquad \text{in S}$$

$$\text{skev}[(\mathbf{Q}_0^T \mathbf{x}_{0,\alpha}) \otimes \mathbf{t}_\alpha)] = \mathbf{0}, \qquad \text{skew}[(\mathbf{Q}_0^T \bar{\boldsymbol{\omega}}_\alpha) \otimes \mathbf{t}_\alpha)] = \mathbf{0} \qquad \text{in S}$$

$$(\mathbf{n}^*_\alpha \otimes \mathbf{a}_\alpha)\boldsymbol{\nu} = \mathbf{0}, \qquad \mathbf{t}_3 \times (\mathbf{m}^*_\alpha \otimes \mathbf{a}_\alpha)\boldsymbol{\nu} = \mathbf{0} \qquad \text{on } \partial S \quad (3.105)$$

which are the linear and angular balance equations, the rotation constraints, and the natural boundary conditions for a shell with the standard Reissner kinematics.

For an sotropic material, the virtual work equation (47) can be written for the standard Reissner kinematics as follows

$$\begin{aligned} \delta\Pi_{2d} &= \int_S \mathbf{N}^B_s \cdot \delta\text{sym}[(\mathbf{Q}_0^T \mathbf{x}_{0,\alpha}) \otimes \mathbf{t}_\alpha)] + \mathbf{M}^B_s \cdot \delta\text{sym}[(\mathbf{Q}_0^T \bar{\boldsymbol{\omega}}_\alpha) \otimes \mathbf{t}_\alpha)] \\ &+ \gamma h \ \text{skew}(\mathbf{Q}_0^T \mathbf{x}_{0,\alpha} \otimes \mathbf{t}_\alpha) \cdot \delta\text{skew}(\mathbf{Q}_0^T \mathbf{x}_{0,\alpha} \otimes \mathbf{t}_\alpha) \\ &+ \gamma \frac{h^3}{12} \ \text{skew}\left[(\mathbf{Q}_0^T \bar{\boldsymbol{\omega}}_\alpha \times \mathbf{t}_3) \otimes \mathbf{t}_\alpha\right] \cdot \delta\text{skew}\left[(\mathbf{Q}_0^T \bar{\boldsymbol{\omega}}_\alpha \times \mathbf{t}_3) \otimes \mathbf{t}_\alpha\right] \\ &- h\rho_R \mathbf{b} \cdot \delta\mathbf{x}_0 - \hat{\mathbf{q}} \cdot \delta\mathbf{x}_0 - \hat{\mathbf{m}} \cdot \delta\boldsymbol{\theta} \ \ dS = 0 \end{aligned} \quad (3.106)$$

Proceeding in a standard manner we can derive the set of balance equations, and the boundary conditions, corresponding to eq.(105) for a three-dimensional body.

3.6 Constitutive equation for Biot shell resultants

In this section the 1st and 2nd order constitutive equations are derived for the shell counterparts of the Biot stress and right stretching tensor. The structure of constitutive equations and the elasticity tensors is the same for the rotated measures, on the arguments presented for three-dimensional elasticity in [Wisniewski,Turska, 1996] and Appendix A. In this section we assume that the right stretching tensor is a linear polynomial of the thickness coordinate, but we do not specify a form of the shell strain tensors. In particular, these tensors cannot be identified with the strains obtained for any of the Reissner hypotheses, unless the normal strains are recovered, see Section 3.7. Note that the shell strains must be specified in advance if consistent approximations to the strain energy are sought on use of the methodology proposed by John and successfully developed by Koiter and Pietraszkiewicz, see e.g. [Pietraszkiewicz, 1984, 1989].

3.6.1 Linear material

Consider a standard form of the strain energy function for the 1st order isotropic elastic material expressed in terms of the right stretch strain $\mathbf{H}$,

$$\mathcal{W}(\mathbf{H}) = \frac{1}{2}\lambda\ (\mathrm{tr}\mathbf{H})^2 + \mathrm{G}\ \mathrm{tr}\mathbf{H}^2 \tag{3.107}$$

where λ and G are Lamé constants. This form of the strain energy function can be used only for small strains, what, however, does not exclude finite rotations of a shell. The above function is defined per unit volume of the initial configuration. The symmetric part of the Biot stress tensor can be given as follows

$$\mathbf{T}_s^B \equiv \frac{\partial \mathcal{W}(\mathbf{H})}{\partial \mathbf{H}} = \lambda\ (\mathrm{tr}\mathbf{H})\mathbf{I} + 2\mathrm{G}\ \mathbf{H} \tag{3.108}$$

where the identities $\partial(\mathrm{tr}\mathbf{H})/\partial\mathbf{H} = \mathbf{I}$ and $\partial(\mathrm{tr}\mathbf{H})^2/\partial\mathbf{H} = 2\mathbf{H}$ were used.

Next we derive a constitutive equation for the strain expressed as a linear polynomial of the thickness coordinate ζ, i.e. as $\mathbf{H} = \boldsymbol{\varepsilon} + \zeta\boldsymbol{\kappa}$, where $\boldsymbol{\varepsilon}$ and $\boldsymbol{\kappa}$ are the 2nd order symmetric tensors. Note that these components cannot be identified with those of eq.(73) or (75), unless the normal components are recovered as discussed in Section 3.7. Then,

$$\mathrm{tr}\mathbf{H} = \mathrm{tr}\boldsymbol{\varepsilon} + \zeta\mathrm{tr}\boldsymbol{\kappa}, \qquad (\mathrm{tr}\mathbf{H})^2 = (\mathrm{tr}\boldsymbol{\varepsilon})^2 + 2\zeta(\mathrm{tr}\boldsymbol{\varepsilon})(\mathrm{tr}\boldsymbol{\kappa}) + \zeta^2(\mathrm{tr}\boldsymbol{\kappa})^2 \tag{3.109}$$

$$\mathbf{H}^2 = \boldsymbol{\varepsilon}^2 + \zeta(\boldsymbol{\varepsilon}\boldsymbol{\kappa} + \boldsymbol{\kappa}\boldsymbol{\varepsilon}) + \zeta^2\boldsymbol{\kappa}^2, \qquad \mathrm{tr}\mathbf{H}^2 = \mathrm{tr}\boldsymbol{\varepsilon}^2 + 2\zeta\mathrm{tr}(\boldsymbol{\varepsilon}\boldsymbol{\kappa}) + \zeta^2\mathrm{tr}\boldsymbol{\kappa}^2 \tag{3.110}$$

Substituting the above into the strain energy (107) and integrating over the thickness we obtain

$$\Sigma = \int_{-\frac{h}{2}}^{+\frac{h}{2}} \mathcal{W}(\mathbf{H})\ \mu d\zeta = h\ \mathcal{W}(\boldsymbol{\varepsilon}) + \frac{h^3}{12}\ \mathcal{W}(\boldsymbol{\kappa}) \tag{3.111}$$

Note that the coupling products $(\mathrm{tr}\boldsymbol{\varepsilon})(\mathrm{tr}\boldsymbol{\kappa})$ and $\mathrm{tr}(\boldsymbol{\varepsilon}\boldsymbol{\kappa})$ dropped out because the integral of the terms depending linearly on ζ yields zero. In the above Σ denotes a two-dimensional strain energy per unit area of the middle surface in the initial configuration. A kinematically admissible variation of the shell strain energy is as follows

$$\delta\Sigma = \frac{\partial\Sigma}{\partial\boldsymbol{\varepsilon}} \cdot \delta\boldsymbol{\varepsilon} + \frac{\partial\Sigma}{\partial\boldsymbol{\kappa}} \cdot \delta\boldsymbol{\kappa} \tag{3.112}$$

The stress and couple resultants can be defined as

$$\mathbf{N}_s^B \equiv \frac{\partial\Sigma}{\partial\boldsymbol{\varepsilon}} = h\ \frac{d\mathcal{W}(\boldsymbol{\varepsilon})}{d\boldsymbol{\varepsilon}}, \qquad \mathbf{M}_s^B \equiv \frac{\partial\Sigma}{\partial\boldsymbol{\kappa}} = \frac{h^3}{12}\ \frac{d\mathcal{W}(\boldsymbol{\kappa})}{d\boldsymbol{\kappa}} \tag{3.113}$$

and then the variation of the shell strain energy can be concisely written as

$$\delta\Sigma = \mathbf{N}_s^B \cdot \delta\boldsymbol{\varepsilon} + \mathbf{M}_s^B \cdot \delta\boldsymbol{\kappa} \tag{3.114}$$

For

$$\frac{d\mathcal{W}(\boldsymbol{\varepsilon})}{d\boldsymbol{\varepsilon}} = \lambda\ (\mathrm{tr}\boldsymbol{\varepsilon})\mathbf{I} + 2\mathrm{G}\ \boldsymbol{\varepsilon}, \qquad \frac{\mathrm{d}\mathcal{W}(\boldsymbol{\kappa})}{\mathrm{d}\boldsymbol{\kappa}} = \lambda\ (\mathrm{tr}\boldsymbol{\kappa})\mathbf{I} + 2\mathrm{G}\ \boldsymbol{\kappa} \tag{3.115}$$

the constitutive equations for the stress and couple resultants are expressed as follows

$$\mathbf{N}_s^B = h\ [\lambda\ (\mathrm{tr}\varepsilon)\mathbf{I} + 2\mathrm{G}\ \boldsymbol{\varepsilon}], \qquad \mathbf{M}_s^B = \frac{h^3}{12}\ [\lambda\ (\mathrm{tr}\boldsymbol{\kappa})\mathbf{I} + 2\mathrm{G}\ \boldsymbol{\kappa}] \tag{3.116}$$

To obtain these resultants we could have also directly used the definitions (35) with the constitutive equation for $\mathbf{T}_s^B$ specified by eq.(108).

In reality the distribution of the shear stresses over the thickness is nonlinear. Therefore, additionally, the constitutive equations for the components $N_{\alpha 3}^B$ and $M_{\alpha 3}^B$ are typically corrected on use of the factor $\frac{5}{6}$.

3.6.2 Mooney-Rivlin material

Consider the class of incompressible (rubber-like) materials defined by $\det \mathbf{F} = 1$. As $\mathbf{F} = \mathbf{QU}$ and $\det \mathbf{Q} = 1$ the incompressibility condition implies $\det \mathbf{U} = 1$, where $\det \mathbf{U}$ is the third invariant of $\mathbf{U}$. In consequence, for the incompressible material the strain energy depends on the two first principal invariants of $\mathbf{U}$, i.e. $\tilde{\mathcal{W}} = \tilde{\mathcal{W}}(I_1(\mathbf{U}), I_2(\mathbf{U}))$, where the principal invariants of $\mathbf{U}$ are

$$I_1(\mathbf{U}) = \mathrm{tr}\mathbf{U}, \qquad \mathrm{I}_2(\mathbf{U}) = \frac{1}{2}\left[(\mathrm{tr}\mathbf{U})^2 - \mathrm{tr}\mathbf{U}^2\right] \tag{3.117}$$

The constitutive equation for the Biot stress tensor is defined as

$$\mathbf{T}_s^B \equiv \frac{\partial \mathcal{W}(\mathbf{U})}{\partial \mathbf{U}} + p\mathbf{I} = \frac{\partial \tilde{\mathcal{W}}(I_1(\mathbf{U}), I_2(\mathbf{U}))}{\partial \mathbf{U}} + p\mathbf{I} \tag{3.118}$$

On the chain rule of differentiation we obtain

$$\frac{\partial \tilde{\mathcal{W}}}{\partial \mathbf{U}} = \frac{\partial \tilde{\mathcal{W}}}{\partial I_1}\frac{\partial I_1}{\partial \mathbf{U}} + \frac{\partial \tilde{\mathcal{W}}}{\partial I_2}\frac{\partial I_2}{\partial \mathbf{U}} \tag{3.119}$$

where $\partial I_1/\partial \mathbf{U} = \mathbf{I}$ and $\partial I_2/\partial \mathbf{U} = I_1\ \mathbf{I} - \mathbf{U}$. Thus, the constitutive equation can be rewritten as a linear polynomial of $\mathbf{U}$, i.e. $\mathbf{T}_s^B = \beta_0\mathbf{I} + \beta_1\mathbf{U}$, where β_0 and β_1 are scalar coefficients depending on the invariants.

Consider the second order hyper-elastic Mooney-Rivlin material defined by the following strain energy function, see e.g. [Green, Adkins, 1970],

$$\tilde{\mathcal{W}}(I_\alpha(\mathbf{C})) = c_1[I_1(\mathbf{C}) - 3] + c_2[I_2(\mathbf{C}) - 3], \qquad \alpha = 1, 2 \tag{3.120}$$

where $\mathbf{C} = \mathbf{U}^2$, and c_1 and c_2 are material constants. The first part, pre-multiplied by c_1, defines the so-called neo-Hookean material, depending only on the 1st invariant of $\mathbf{C}$. The invariants of $\mathbf{C}$ can be written as functions of the invariants of $\mathbf{U}$,

$$I_1(\mathbf{C}) = I_1^2(\mathbf{U}) - 2I_2(\mathbf{U}), \qquad I_2(\mathbf{C}) = I_2^2(\mathbf{U}) - 2I_1(\mathbf{U})I_3(\mathbf{U}) \tag{3.121}$$

where the second one further reduces for $I_3(\mathbf{U}) = 1$ to $I_2(\mathbf{C}) = I_2^2(\mathbf{U}) - 2I_1(\mathbf{U})$. Thus, the Mooney-Rivlin strain energy in terms of the invariants of $\mathbf{U}$ is as follows

$$\tilde{\mathcal{W}}(I_\alpha(\mathbf{U})) = c_1[I_1^2(\mathbf{U}) - 2I_2(\mathbf{U}) - 3] + c_2[I_2^2(\mathbf{U}) - 2I_1(\mathbf{U}) - 3] \tag{3.122}$$

Assume that the right stretching tensor is given as a linear polynomial of the thickness coordinate of the shell, i.e. $\mathbf{U} = \mathbf{e} + \zeta\mathbf{k}$, where $\mathbf{e}$ and $\mathbf{k}$ are the 2nd order symmetric tensors. Similarly, as in case of the tensors $\boldsymbol{\varepsilon}$ and $\boldsymbol{\kappa}$ for the linear material, we do not specify $\mathbf{e}$ and $\mathbf{k}$. In particular, the tensors (69) and (70) cannot be used in this context unless the normal components are recovered as specified in Section 3.7. For the given expansion the invariants of $\mathbf{U}$ can be expressed as follows

$$I_1(\mathbf{U}) = I_1(\mathbf{e}) + \zeta I_1(\mathbf{k}), \qquad I_2(\mathbf{U}) = I_2(\mathbf{e}) + \zeta A + \zeta^2 I_2(\mathbf{k}) \tag{3.123}$$

$$I_3(\mathbf{U}) = \frac{1}{6}\left[I_3(\mathbf{e}) + \zeta B(\mathbf{e},\mathbf{k}) + \zeta^2 B(\mathbf{k},\mathbf{e}) + \zeta^3 I_3(\mathbf{k})\right] \tag{3.124}$$

where the two auxiliary scalars are

$$A \equiv I_1(\mathbf{e})I_1(\mathbf{k}) - \mathrm{tr}(\mathbf{ek}) \tag{3.125}$$

$$B(\mathbf{a},\mathbf{b}) \equiv 6\left[I_2(\mathbf{a})I_1(\mathbf{b}) + \mathrm{tr}(\mathbf{a}^2\mathbf{b}) - \mathrm{I}_1(\mathbf{a})\mathrm{tr}(\mathbf{ab})\right] \tag{3.126}$$

for the 2nd rank tensors $\mathbf{a}$ and $\mathbf{b}$. Note the presence of the coupling terms in A and $B(\mathbf{a},\mathbf{b})$, which render that the 2nd and 3rd invariant of $\mathbf{U}$ are not expressible in terms of the invariants of $\mathbf{e}$ and $\mathbf{k}$. For the squares of invariants of $\mathbf{U}$, which are also present in eq.(122), we have

$$I_1^2(\mathbf{U}) = I_1^2(\mathbf{e}) + 2\zeta I_1(\mathbf{e})I_1(\mathbf{k}) + \zeta^2 I_1^2(\mathbf{k}) \tag{3.127}$$

$$I_2^2(\mathbf{U}) = I_2^2(\mathbf{e}) + \zeta^2 A^2 + \zeta^4 I_2^2(\mathbf{k}) + 2\zeta I_2(\mathbf{e})A + 2\zeta^2 I_2(\mathbf{e})I_2(\mathbf{k}) + 2\zeta^3 I_2(\mathbf{k})A \tag{3.128}$$

where

$$A^2 = I_1^2(\mathbf{e})I_1^2(\mathbf{k}) - 2I_1(\mathbf{e})I_1(\mathbf{k})\mathrm{tr}(\mathbf{ek}) + [\mathrm{tr}(\mathbf{ek})]^2 \tag{3.129}$$

Note that for the assumed approximations of $\mathbf{U}$ the strain energy is a 2nd order polynomial of ζ for the neo-Hookean material, and of the 4th order in case of the Mooney-Rivlin material.

Let us define the shell strain energy density, per unit area of the middle surface in the initial configuration, as the integral of the strain energy over the thickness, i.e.

$$\tilde{\Sigma}(I_\alpha(\mathbf{U})) \equiv \int_{-\frac{h}{2}}^{+\frac{h}{2}} \tilde{\mathcal{W}}(I_\alpha(\mathbf{U}))\, \mu d\zeta \tag{3.130}$$

The integration over the thickness renders that the terms of $\tilde{\mathcal{W}}(I_\alpha(\mathbf{U}))$ multiplied by even powers of ζ are equal to zero, and the shell energy splits as follows

$$\tilde{\Sigma} = c_1\, \tilde{\Sigma}_1 \; + \; c_2\, \tilde{\Sigma}_2 \tag{3.131}$$

where

$$\tilde{\Sigma}_1 = h\left[I_1^2(\mathbf{e}) - 2I_2(\mathbf{e}) - 3\right] + \frac{h^3}{12}\left[I_1^2(\mathbf{k}) - 2I_2(\mathbf{k})\right] \tag{3.132}$$

$$\tilde{\Sigma}_2 = h\left[I_2^2(\mathbf{e}) - 2I_1(\mathbf{e}) - 3\right] + \frac{h^3}{12}\left[A^2 + I_2(\mathbf{e})I_2(\mathbf{k})\right] + \frac{h^5}{80} I_2^2(\mathbf{k}) \tag{3.133}$$

In the component $\tilde{\Sigma}_1$ for the neo-Hookean material, the terms depending on $\mathbf{e}$ and $\mathbf{k}$ are separated, what leads to uncoupled constitutive equations. The second component, $\tilde{\Sigma}_2$,

contains the coupling terms such as $I_1(\mathbf{e})I_1(\mathbf{k})$, $I_2(\mathbf{e})I_2(\mathbf{k})$, $\mathrm{tr}(\mathbf{ek})$, and some products and powers of them.

For symmetric $\mathbf{e}$, $\delta\mathbf{e}$, $\mathbf{k}$ and $\delta\mathbf{k}$ a variation of the shell strain energy may be written as

$$\delta\tilde{\Sigma}(\mathbf{e},\mathbf{k}) = \mathbf{N}_s^B \cdot \delta\mathbf{e} + \mathbf{M}_s^B \cdot \delta\mathbf{k} \tag{3.134}$$

where the stress and couple resultants are defined as follows

$$\mathbf{N}_s^B \equiv \frac{d\tilde{\Sigma}}{d\mathbf{e}}, \qquad \mathbf{M}_s^B \equiv \frac{d\tilde{\Sigma}}{d\mathbf{k}} \tag{3.135}$$

To facilitate further differentiation we calculate in advance the following derivatives

$$\frac{\partial \mathrm{tr}(\mathbf{ek})}{\partial \mathbf{e}} = \mathbf{k}, \qquad \frac{\partial [\mathrm{tr}(\mathbf{ek})]^2}{\partial \mathbf{e}} = 2\mathrm{tr}(\mathbf{ek})\ \mathbf{k}, \qquad \frac{\partial \mathrm{A}^2}{\partial \mathbf{e}} = 2\mathrm{A}\ \mathbf{D}(\mathbf{k}) \tag{3.136}$$

$$\frac{\partial \mathrm{tr}(\mathbf{ek})}{\partial \mathbf{k}} = \mathbf{e}, \qquad \frac{\partial [\mathrm{tr}(\mathbf{ek})]^2}{\partial \mathbf{k}} = 2\mathrm{tr}(\mathbf{ek})\ \mathbf{e}, \qquad \frac{\partial \mathrm{A}^2}{\partial \mathbf{k}} = 2\mathrm{A}\ \mathbf{D}(\mathbf{e}) \tag{3.137}$$

where the auxiliary tensor is defined as follows

$$\mathbf{D}(\mathbf{A}) \equiv I_2(\mathbf{A})_{,\mathbf{A}} = I_1(\mathbf{A})\mathbf{I} - \mathbf{A} \tag{3.138}$$

The derivatives of the shell strain energy are

$$\frac{\partial \tilde{\Sigma}_1}{\partial \mathbf{e}} = 2h\mathbf{e}, \qquad \frac{1}{2}\frac{\partial \tilde{\Sigma}_2}{\partial \mathbf{e}} = h\left(I_2(\mathbf{e})\mathbf{D}(\mathbf{e}) - \mathbf{I}\right) + \frac{h^3}{12}\boldsymbol{\pi}(\mathbf{k},\mathbf{e}) \tag{3.139}$$

$$\frac{\partial \tilde{\Sigma}_1}{\partial \mathbf{k}} = 2\frac{h^3}{12}\mathbf{k}, \qquad \frac{1}{2}\frac{\partial \tilde{\Sigma}_2}{\partial \mathbf{k}} = \frac{h^3}{12}\boldsymbol{\pi}(\mathbf{e},\mathbf{k}) + \frac{h^5}{80}I_2(\mathbf{k})\mathbf{D}(\mathbf{k}) \tag{3.140}$$

where the term, which couples the contribution of $\mathbf{e}$ and $\mathbf{k}$ is defined as follows

$$\boldsymbol{\pi}(\mathbf{a},\mathbf{b}) = A\ \mathbf{D}(\mathbf{b}) + \frac{1}{2}I_2(\mathbf{b})\ \mathbf{D}(\mathbf{a}) \tag{3.141}$$

On the above equations the following coupled constitutive equations for the shell are obtained

$$\mathbf{N}_s^B = c_1\left[2h\mathbf{e}\right] + c_2 2\left[h\left(I_2(\mathbf{e})\mathbf{D}(\mathbf{e}) - \mathbf{I}\right) + \frac{h^3}{12}\boldsymbol{\pi}(\mathbf{k},\mathbf{e})\right] \tag{3.142}$$

$$\mathbf{M}_s^B = c_1\left[2\frac{h^3}{12}\mathbf{k}\right] + c_2 2\left[\frac{h^3}{12}\boldsymbol{\pi}(\mathbf{e},\mathbf{k}) + \frac{h^5}{80}I_2(\mathbf{k})\mathbf{D}(\mathbf{k})\right] \tag{3.143}$$

Note that these constitutive equations for the hyper-elastic incompressible material have a relatively simple form and have been obtained without constructing approximations to the strain energy.

3.7 Constitutive equations accounting for normal strain of shell

Deriving in the preceding section the constitutive equations for a shell we assumed that the shell right stretch strain or right stretching tensors are symmetric and of the 2nd order, but their form has not been specified. If we try to use the strains obtained for the Reissner hypotheses then we have the problem of the normal components which are equal to zero; $\varepsilon_{33} = \kappa_{33} = 0$ for the standard hypothesis, and $\kappa_{33} = 0$ for the generalized hypothesis. These values are inadequate, and lead to erroneous solutions, so in the present section the normal strains are recovered on use of auxiliary equations, implied by the plane stress condition or the incompressibility condition. The recovered normal components can be directly inserted into a standard form of the shell constitutive equations derived in Section 3.6. Then, we can specify a modified version of the constitutive equations, as typically done in the shell literature. This operation puts some order into the formulas, but is purely formal and does not increase the accuracy of the constitutive equations.

A very simple scheme of treating the normal component has been reported for a degenerate shell model in [Hughes, Liu, 1981]. The nonlinear governing equations are solved iteratively, and this component is evaluated via an auxiliary equation for the last solution. The value of normal strain lags one iteration behind, but it is acceptable as long as the iterations converge.

3.7.1 Linear material

As indicate three-dimensional solutions for the linear material, the normal strain in a shell is not negligible. Components of the Green strain can be evaluated for shells as follows, see e.g. [Pietraszkiewicz, 1977], p.112,

$$\varepsilon_{\alpha\beta} \sim h\kappa_{(\alpha\beta)} = O(\eta), \qquad \varepsilon_{3\beta} \sim h\kappa_{3\beta} = O(\eta\theta), \qquad \varepsilon_{33} = O(\nu\eta). \tag{3.144}$$

where η is a maximum eigenvalue of the Green strain, and ν is the Poisson ratio. The small parameter θ is defined in [Pietraszkiewicz, 1977], p.111, eq.(6.3.4). Obviously, ε_{33} is not small comparing to the other components, and its contribution to the strain energy is not negligible.

The linear material is applicable to small strain problems, for which the plane stress condition is physically meaningful for shells, and classically used as the auxiliary condition, see e.g. [Naghdi, 1972], [Pietraszkiewicz, 1977, 1979]. From the condition of the zero normal stress, $T^B_{s33} = \lambda\, U_{ii} + 2\mu\, U_{33} = 0$, $i = 1, 2, 3$, we calculate the normal component

$$U_{33} = -\frac{\lambda}{\lambda + 2\mu}(U_{11} + U_{22}) \tag{3.145}$$

Subsequently, we assume that the right stretching tensor can be expanded as $\mathbf{U}^* = \boldsymbol{\varepsilon}^* + \zeta\boldsymbol{\kappa}^*$, where in $\boldsymbol{\varepsilon}^*$ and $\boldsymbol{\kappa}^*$ the normal components 33 are not present. On use of the expanded U_{11} and U_{22} we obtain $U_{33} = (U_{33})_0 + \zeta\ (U_{33})_1$, where

$$(U_{33})_0 = -\frac{\lambda}{\lambda + 2\mu}(\varepsilon_{11} + \varepsilon_{22}), \qquad (U_{33})_1 = -\frac{\lambda}{\lambda + 2\mu}(\kappa_{11} + \kappa_{22}) \tag{3.146}$$

In order to keep the notation consistent we can denote $(U_{33})_0 \equiv \varepsilon_{33}$ and $(U_{33})_1 \equiv \kappa_{33}$. Inserting the expressions for the normal components into the standard constitutive equation, eq.(116), we obtain the modified constitutive equations. For example, for the stress resultant we have

$$\mathbf{N}_s^{B*} = h\, C\, [\nu\ (\mathrm{tr}\boldsymbol{\varepsilon}^*)\mathbf{I} + 2(1-\nu)\boldsymbol{\varepsilon}^*] \tag{3.147}$$

where in $\mathbf{N}_s^{B*}$ the normal component 33 is not present, and $C = E/(1-\nu^2)$. Note that this equation incorporates (145), and hence it accounts for the thickness changes, although it does not explicitly contain ε_{33}.

A variation of the normal strain is $\delta\varepsilon_{33} = -\frac{\lambda}{\lambda+2\mu}(\delta\varepsilon_{11} + \delta\varepsilon_{22})$, and inserting this expression into the first component of the variation of strain energy, eq.(114), we obtain

$$N^B_{s\alpha i}\ \delta\varepsilon_{\alpha i} + N^B_{s33}\ \delta\varepsilon_{33} = \left(N^B_{s\alpha i} - N^B_{s33}\frac{\lambda}{\lambda+2\mu}\delta_{\alpha i}\right)\ \delta\varepsilon_{\alpha i} \tag{3.148}$$

or $\mathbf{N}_s^B \cdot \delta\boldsymbol{\varepsilon} = \mathbf{N}_s^{B*} \cdot \delta\boldsymbol{\varepsilon}^*$. It can be checked that the same results are obtained if the expression for ε_{33} is inserted directly into the strain energy. Then, from $\mathcal{W}(\boldsymbol{\varepsilon})$ we obtain $\mathcal{W}^* \equiv \mathcal{W}(\boldsymbol{\varepsilon}^*)$, and the stress resultant is defined as $\mathbf{N}_s^{B*} \equiv h\ d\mathcal{W}^*/d\boldsymbol{\varepsilon}^*$.

3.7.2 Incompressible material

Consider the class of incompressible materials, which undergo an isochoric (or volume-preserving) deformation. Two methods of incorporating the incompressibility condition into the formulation can be used. Firstly, the potential (18) can be extended on use of the Lagrange multiplier method, $\Pi'(\boldsymbol{\chi}, \mathbf{Q}, \mathbf{T}_a^B, p) = \Pi(\boldsymbol{\chi}, \mathbf{Q}, \mathbf{T}_a^B) + p\ (\det \mathrm{Grad}\boldsymbol{\chi} - 1)$, where the mean pressure p is a Lagrange multiplier. Note that unless p is included as a variable the calculated stress is determined up to the mean pressure, see [Truesdell, Noll, 1965], p.70-72. This method is generally applicable, and frequently used for three-dimensional bodies, see e.g. several algorithmically motivated variants of it given in [Simo, Taylor, 1991] and in the literature cited therein. Secondly, the incompressibility condition can be appended to the variational equations, and then, e.g. for shells, it can be treated as an auxiliary equation to alleviate the problem with the normal strain components.

The incompressibility condition implies a nonlinear relation between the normal strain and the other strain components. Hence, even a linear distribution of the other components yields a nonlinear distribution of the normal strain over the thickness. To capture this effect the kinematical hypothesis are generalized, e.g. in [Stumpf, Makowski, 1986] and [Schieck, Pietraszkiewicz, Stumpf, 1992] the generalized Kirchhoff hypothesis is used, while in [Makowski, Stumpf, 1986] the generalized Reissner hypothesis is exploited. In these papers a scalar extension function over the thickness is introduced and determined from the incompressibility condition.

For instance, in [Stumpf, Makowski, 1986] the current position vector is assumed as $\mathbf{x}(\zeta) = \mathbf{x}_0 + \lambda(\zeta)\bar{\mathbf{n}}$, where $\bar{\mathbf{n}}$ is a unit vector normal to the deformed middle surface, $\lambda(\zeta)$ is an extension function. This form of the position vector furnishes a generalization of the Kirchhoff hypothesis, with an interesting feature that a non-zero transverse shear strain is obtained for surfaces other then the mid-surface, see eq.(2.13). This approach has a disadvantage that the transverse shear strain assumes a zero value at the middle surface.

Note that for linear materials, the transverse shear strain has a parabolic distribution with a maximum at the middle surface and with zero values at the external surfaces. Hence we can expect that for the incompressible material this distribution is not so different. This effect is not present in [Makowski, Stumpf, 1986], see expression for $\bar{g}_{\alpha 3}$ in eq.(3.14). In the latter paper the current position vector is assumed as $\mathbf{x}(\zeta) = \mathbf{x}_0 + \lambda(\zeta)\,\mathbf{a}_3$. Since $\mathbf{a}_3$ is a unit vector it can be obtained from the unit vector normal to the undeformed configuration $\mathbf{t}_3$ on use of a rotation tensor, as we do in Section 1.3, but the discussed paper does not introduce this tensor as a variable. In both cited works, a general form of $\lambda(\zeta)$ is obtained as a solution of the cubic equation resulting from the incompressibility condition, see eq.(3.7) in [Stumpf, Makowski, 1986].

Example

In [Stumpf, Makowski, 1986] the example of an inversion of a spherical cap is considered in detail. The deformed configuration of this shell also has a spherical shape, and an explicit form of $\lambda(\zeta)$ can be obtained, cf. eq.(6.4). The normal strain has the following form

$$\varepsilon_{33}(\hat{\xi}) \equiv \frac{\partial \lambda}{\partial \xi} = \frac{(1 + \frac{h}{R}\hat{\xi})^2}{\left[1 + \lambda^3 - (1 + \frac{h}{R}\hat{\xi})^3\right]^{2/3}} \tag{3.149}$$

where $\hat{\xi} = -(\zeta + h/2)/h$, $\hat{\xi} \in [-1, 0]$, and λ is a stretch of the reference surface. Although, the above ε_{33} is a complicated function of $\hat{\xi}$ it assumes a simpler form for two limit cases identified below:

1. Thin and/or flat shells. For $h/R \to 0$ we have $\varepsilon_{33}(\hat{\xi}) \to \frac{1}{\lambda^3}$. Hence, the dependence on $\hat{\xi}$ vanishes, and a constant approximation of the normal strain in the thickness direction is correct. This kind of approximation has been used in [Gruttmann, Taylor, 1992] for shells of $h/R = 0.01$, and good accuracy is preserved.

2. Large stretches. For $\lambda \to \infty$ we have $\varepsilon_{33}(\hat{\xi}) = O(\frac{1}{\lambda^3}) \to 0$, i.e. the normal strain vanishes. In reality, the inflated structures made of rubber-like materials undergo stretches up to $\lambda = 10$. If the shell is thin then ε_{33} becomes of secondary importance, and its dependence on $\hat{\xi}$ can be safely neglected.

In consequence, for both the above cases a constant approximation of the normal strain is sufficient. The dependence of ε_{33} on $\hat{\xi}$ certainly cannot be neglected for the shell analyzed in [Stumpf, Makowski, 1986], which is thick and/or strongly curved with $h/R = 0.2$ and undergoes 20% stretches of the middle surface. Note that bodies of such a geometry are traditionally considered as remaining beyond the area of application of shell equations, and are analyzed using three-dimensional equations and finite elements. We have verified the approximations which are given for eq.(149), and we found that for the expansion around $\hat{\xi} = 0$, which is used in the cited paper, the series does not converge properly. It seems that the radius of convergence of the series is smaller than the range of $\hat{\xi}$. Hence, we expanded $\varepsilon_{33}(\hat{\xi})$ around the middle surface, $\hat{\xi} = -0.5$, and a correct convergence was obtained. Then, we found that a 1% error at the external surface $\hat{\xi} = -1$ is obtained on use of the 4th, 3rd and 2nd order Taylor series for $\lambda = 0.8, 1.0, 1.2$, respectively. For higher order approximations this error diminishes rapidly.

Finally, we calculated the relative error of a linear expansion of $\varepsilon_{33}(\hat{\xi})$ around $\hat{\xi} = -0.5$, for various values of λ and h/R, see Table 3.1. Assuming as acceptable the 1% error at the external surface, $\hat{\xi} = -1$, we can see that the linear expansion is sufficient for a wide range of both parameters. In particular, for thin shells of $h/R \leq 0.05$, a linear approximation of the normal strain is justified for arbitrary stretches.

Table 3.1. Percentage error at $\hat{\xi} = -1$ for the linear expansion of $\varepsilon_{33}(\hat{\xi})$ at $\hat{\xi} = -0.5$

λ	h/R				
	0.2	0.1	0.05	0.01	0.001
0.5	14.95	4.98	1.53	0.070	0.00080
1.0	8.57	2.42	0.67	0.030	0.00030
1.5	3.54	0.83	0.20	0.008	0.00008
2.0	2.37	0.51	0.12	0.005	0.00005
5.0	1.61	0.32	0.07	0.003	0.00003
10.0	1.57	0.31	0.07	0.003	0.00003

In the sequel two forms of exploiting the incompressibility condition are presented. The first one is suitable for membranes: it is stated in principal axes and assumes that strains are constant over the thicknes. The second form is quite general and can be applied to arbitrary shells. If a linear expansion of $\varepsilon_{33}(\hat{\xi})$ is retained then the shell geometry and the stretches must remain within a range, which we may expect to be similar to that found for the inversion of the spherical cap.

Membrane shells

For a three-dimensional body, in order to specify the principal directions of $\mathbf{U}$, we have to find a rotation $\mathbf{Q} \in SO(3)$ such that $\mathbf{Q}\mathbf{U}\mathbf{Q}^T = \hat{\mathbf{U}}$, where $\hat{\mathbf{U}}$ has a diagonal representation $\hat{\mathbf{U}} = \mathrm{diag}\{\lambda_1, \lambda_2, \lambda_3\}$. The eigenvalues λ_i are called the principal stretches. For isotropic materials the Biot stress $\hat{\mathbf{T}}_s^B$ is coaxial with $\hat{\mathbf{U}}$ and hence also $\mathbf{Q}\mathbf{T}_s^B\mathbf{Q}^T = \hat{\mathbf{T}}_s^B$ holds, where $\hat{\mathbf{T}}_s^B$ has a diagonal representation, $\hat{\mathbf{T}}_s^B = \mathrm{diag}\{t_1, t_2, t_3\}$, and t_i are the principal values of the Biot stress.

For a constitutive equation given in terms of principal values of the stress and strain tensors the virtual work must also be given in the principal values. Then, two additional constraint equations must be appended to the virtual work equation

$$\begin{cases} \delta\mathcal{W}(\mathbf{U}) - \delta A = 0 \\ \mathbf{C}_1 = \mathbf{Q}\mathbf{U}\mathbf{Q}^T - \hat{\mathbf{U}} = \mathbf{0} \\ \mathbf{C}_2 = \mathbf{Q}\mathbf{T}_s^B\mathbf{Q}^T - \hat{\mathbf{T}}_s^B = \mathbf{0} \end{cases} \tag{3.150}$$

In the above we assumed isotropy of the material by taking the same $\mathbf{Q}$ in $\mathbf{C}_1$ and $\mathbf{C}_2$. Subsequently, $\mathbf{U}$ and $\mathbf{T}_s^B$ may be calculated from the constraint equations and inserted into the virtual work principle. Then, the integrand of the virtual work of stresses becomes as follows

$$\delta\mathcal{W}(\mathbf{U}) = \mathbf{T}_s^B \cdot \delta\mathbf{U} = \left(\mathbf{Q}^T\hat{\mathbf{T}}_s^B\mathbf{Q}\right) \cdot \delta\left(\mathbf{Q}^T\hat{\mathbf{U}}\mathbf{Q}\right) \tag{3.151}$$

The variation of the strain can be transformed to $\delta\left(\mathbf{Q}^T\hat{\mathbf{U}}\mathbf{Q}\right) = \mathbf{Q}^T\,(\overset{\circ}{\delta}\hat{\mathbf{U}})\,\mathbf{Q}$, where the co-rotational variation is defined as $\overset{\circ}{\delta}\hat{\mathbf{U}} = \delta\hat{\mathbf{U}} + \left(\hat{\mathbf{U}}\,\delta\bar{\boldsymbol{\theta}} - \delta\bar{\boldsymbol{\theta}}\,\hat{\mathbf{U}}\right)$ and $\delta\bar{\boldsymbol{\theta}} = \delta\mathbf{Q}\mathbf{Q}^T$ is a left skew-symmetric tensor. Then, the virtual work of stress can be transformed further

$$\delta\mathcal{W}(\mathbf{U}) = \left(\mathbf{Q}^T\hat{\mathbf{T}}_s^B\mathbf{Q}\right)\cdot\left(\mathbf{Q}^T\,(\overset{\circ}{\delta}\hat{\mathbf{U}})\,\mathbf{Q}\right) = \hat{\mathbf{T}}_s^B\cdot\overset{\circ}{\delta}\hat{\mathbf{U}} = t_i\,\delta\lambda_i \tag{3.152}$$

Assume that the strain energy is given as a function of the principal invariants of $\mathbf{U}$, which in the principal axes are expressed in terms of the eigenvalues λ_i of $\mathbf{U}$,

$$\tilde{\mathcal{W}}(I_i(\mathbf{U})) = \hat{\mathcal{W}}(I_i(\hat{\mathbf{U}})), \qquad i = 1,2,3 \tag{3.153}$$

where the principal invariants of $\hat{\mathbf{U}}$ are as follows

$$I_1(\hat{\mathbf{U}}) = \lambda_1+\lambda_2+\lambda_3, \qquad I_2(\hat{\mathbf{U}}) = \lambda_1\lambda_2+\lambda_2\lambda_3+\lambda_3\lambda_1, \qquad I_3(\hat{\mathbf{U}}) = \lambda_1\lambda_2\lambda_3 \tag{3.154}$$

The constitutive equation for the principal values of the Biot stress is calculated as

$$t_i \equiv \frac{\partial\hat{\mathcal{W}}(I_j(\hat{\mathbf{U}}))}{\partial\lambda_i} = \frac{\partial\hat{\mathcal{W}}}{\partial I_j}\frac{\partial I_j}{\partial\lambda_i}, \qquad i,j = 1,2,3 \tag{3.155}$$

For the incompressible materials, from the condition $I_3(\hat{\mathbf{U}}) = 1$ we calculate $\lambda_3 = (\lambda_1\lambda_2)^{-1}$, which is a nonlinear function of λ_1 and λ_2. Hence, $\delta\lambda_3 = (\partial\lambda_3/\partial\lambda_\alpha)\,\delta\lambda_\alpha$, and the virtual work equation becomes

$$\delta\hat{\mathcal{W}}(I_\alpha(\mathbf{U})) = t_\alpha\,\delta\lambda_\alpha + t_3\,\delta\lambda_3 = (t_\alpha + t_3\lambda_{3,\alpha})\,\delta\lambda_\alpha \tag{3.156}$$

In an alternative approach the auxiliary relation $\lambda_3 = (\lambda_1\lambda_2)^{-1}$ can be directly used in the strain energy. Inserting λ_3 into the two first invariants we obtain

$$I_1^*(\hat{\mathbf{U}}) = \lambda_1+\lambda_2+(\lambda_1\lambda_2)^{-1}, \qquad I_2^*(\hat{\mathbf{U}}) = \lambda_1\lambda_2+(\lambda_1)^{-1}+(\lambda_2)^{-1} \tag{3.157}$$

The strain energy becomes a function of λ_1 and λ_2, i.e. $\tilde{\mathcal{W}}(I_\alpha^*(\mathbf{U})) = \hat{\mathcal{W}}(I_\alpha^*(\hat{\mathbf{U}}))$, $\alpha = 1,2$, and the constitutive equation is calculated as,

$$t_\alpha^* \equiv \frac{\partial\hat{\mathcal{W}}(I_\beta^*(\hat{\mathbf{U}}))}{\partial\lambda_\alpha} = \frac{\partial\hat{\mathcal{W}}}{\partial I_\beta^*}\frac{\partial I_\beta^*}{\partial\lambda_\alpha}, \qquad \alpha,\beta = 1,2 \tag{3.158}$$

and the virtual work equation becomes $\delta\hat{\mathcal{W}}(I_\alpha^*(\mathbf{U})) = t_\alpha^*\cdot\delta\lambda_\alpha$. It can be checked that $t_\alpha^* = t_\alpha + t_3\lambda_{3,\alpha}$, what proves equivalence of both approaches.

Note that the description in principal axes can be used for the membrane shells, for which stretches are constant over the thickness. Then, λ_3 can be assumed as the stretch causing the thickness changes, and $\mathbf{Q}$ of eq.(146) is a one-parameter rotation around the director of the shell, see e.g. [Gruttmann, Taylor, 1992].

Arbitrary shells

Let us write the incompressibility condition in terms of the right stretching tensor,

$$\det\mathbf{U} = U_{31}\,D_{31} - U_{32}\,D_{32} + U_{33}\,D_{33} = 1 \tag{3.159}$$

where the minors are defined as follows

$$D_{31} = U_{12}U_{23} - U_{13}U_{22}, \qquad D_{32} = U_{11}U_{23} - U_{13}U_{12}, \qquad D_{33} = U_{11}U_{22} - U_{12}^2 \quad (3.160)$$

The normal component U_{33} appears in this equation only once, and can be readily calculated as

$$U_{33} = \frac{1}{D_{33}}(1 \; - \; U_{31}\, D_{31} \; + \; U_{32}\, D_{32}) \quad (3.161)$$

Subsequently, we assume that the right stretching tensor can be expanded as $\mathbf{U}^* = \mathbf{e}^* + \zeta \mathbf{k}^*$. Note that this expansion is performed for all the components except the normal one, 33, what is indicated by the asterisks. On use of this expansion U_{33} becomes a rational function of ζ, with a polynomial of 3rd order in the nominator, and of 2nd order in the denominator. Hence, unless the denominators are equal to zero, $U_{33}(\zeta)$ is infinitly times differentiable, and we can perform the Taylor series expansion of it around the middle surface, retaining as many terms as necessary,

$$U_{33}(\zeta) = (U_{33})_0 + (U_{33,\zeta})_0\, \zeta + \frac{1}{2}(U_{33,\zeta\zeta})_0\, \zeta^2 + O(\zeta^3) \quad (3.162)$$

In order to keep the notation consistent, the first two terms of the expansion can be denoted as $(U_{33})_0 \equiv e_{33}$ and $(U_{33,\zeta})_0 \equiv k_{33}$.

If we use a linear expansion of the normal strain $\varepsilon_{33}(\hat{\xi}) = e_{33} + \zeta k_{33} + O(\zeta^2)$, then, in general, the class of the geometry and the deformation considered must be narrowed. A rigorous analysis of such question is complicated, see [Schieck, Pietraszkiewicz, Stumpf, 1992], but some insight provides the earlier analyzed example of the spherical shell, which indicates that the linear expansion is justified for arbitrary stretches when the shell is thin, $h/R \leq 0.05$.

For the standard Reissner kinematics, the above calculated e_{33} and k_{33} can be directly used in the Mooney-Rivlin constitutive equations (142) and (143). The other strain components can be used in a form (74). For the generalized Reissner kinematics, the obtained e_{33} can be used to eliminate λ from (76), as $\varepsilon_{33} = \lambda - 1$. The obtained form of k_{33} is used directly in (143).

Below, as an example, the case of a negligible transverse shear strain, $U_{\alpha 3} \approx 0$ is considered. For this case the normal strain is as follows

$$U_{33} = 1/(U_{11}U_{22} - U_{12}^2) \quad (3.163)$$

and after the expansion of $U_{\alpha\beta}$ we obtain

$$U_{33}(\zeta) = \frac{1}{\det \mathbf{e}^* + A(\mathbf{e}^*, \mathbf{k}^*)\, \zeta + \det \mathbf{k}^*\, \zeta^2} \quad (3.164)$$

where the denominator is a polynomial of 2nd order, and $A(\mathbf{e}^*, \mathbf{k}^*) = (\mathrm{tr}\mathbf{e}^*)(\mathrm{tr}\mathbf{k}^*) - \mathrm{tr}(\mathbf{e}^*\mathbf{k}^*)$. In terms of components we have

$$\det \mathbf{e}^* = e_{11}e_{22} - e_{12}^2, \quad A(\mathbf{e}^*, \mathbf{k}^*) = e_{11}k_{22} - 2e_{12}k_{12} + e_{22}k_{11}, \quad \det \mathbf{k}^* = k_{11}k_{22} - k_{12}^2 \quad (3.165)$$

Hence, for the Taylor expansion of U_{33} we have

$$e_{33} = \frac{1}{\det \mathbf{e}^*}, \qquad k_{33} = \frac{-A(\mathbf{e}^*, \mathbf{k}^*)}{(\det \mathbf{e}^*)^2}, \qquad (U_{33,\zeta\zeta})_0 = \frac{2A(\mathbf{e}^*, \mathbf{k}^*)^2}{(\det \mathbf{e}^*)^3} - \frac{2 \det \mathbf{k}^*}{(\det \mathbf{e}^*)^2} \quad (3.166)$$

Note that k_{33} and $(U_{33,\zeta\zeta})_0$ depend on the invariants of $\mathbf{e}^*$, $\mathbf{k}^*$ and $(\mathbf{e}^*\mathbf{k}^*)$.

In general, all the terms of the expansion (162) contain couplings of $\mathbf{e}^*$ and $\mathbf{k}^*$, similarily as the constitutive equations for the Mooney-Rivlin material derived in Section 3.6.2. Due to these couplings the virtual work of stress, eq.(134), is further complicated. Let us split the virtual work of stress into $\delta\bar{\Sigma} = \delta\bar{\Sigma}_{\mathbf{e}} + \delta\bar{\Sigma}_{\mathbf{k}}$. As all the terms of U_{33} depend on $e_{\alpha i}$ and $k_{\alpha i}$ hence

$$\delta\bar{\Sigma}_{\mathbf{e}} = \mathbf{N}_s^B \cdot \delta\mathbf{e} = N_{s\alpha i}^B\, \delta e_{\alpha i} + N_{s33}^B\, \delta e_{33}(e_{\alpha i}, k_{\alpha i}) \tag{3.167}$$

The variation of the normal components yields $\delta e_{33} = \frac{\partial e_{33}}{\partial e_{\alpha i}}\, \delta e_{\alpha i} + \frac{\partial e_{33}}{\partial k_{\alpha i}}\, \delta k_{\alpha i}$, and the virtual work becomes

$$\delta\bar{\Sigma}_{\mathbf{e}} = \left(N_{s\alpha i}^B + N_{s33}^B \frac{\partial e_{33}}{\partial e_{\alpha i}} \right) \delta e_{\alpha i} \; + \; N_{s33}^B \frac{\partial e_{33}}{\partial k_{\alpha i}}\, \delta k_{\alpha i} \tag{3.168}$$

3.8 Numerical examples

In this section, first, the implementation of the membrane part of a four-node finite element with drilling rotation is described, and then the way in which the design sensitivities are calculated for shells is presented. Subsequently, several numerical examples, displaying highly nonlinear equilibrium paths with singular points, are computed using the isoparametric 4-node elements, and the arc-length control (Riks) method. The design sensitivities of displacements and rotations are calculated along the equilibrium paths in the whole pre- and post-critical range, and are presented on the sensitivity charts. It is demonstrated that there exists a correspondence between the singularity points (minimum, maximum and inflection points) on the equilibrium paths and the asymptotes on the sensitivity charts. The accuracy of the sensitivities is assessed by comparison with the finite difference results. In particular, the example testing the formulation with the drilling rotation and calculating the design sensitivity of the drilling rotation is presented.

Implementation of a four-node finite element with drilling rotation

Below we describe the implementation of the membrane part of the 4-node shell element. Consider the plane stress problem in the plane tangent to the shell, with two in-plane displacement components and one rotation angle associated with the drilling rotation vector. The position vector $\mathbf{y}_0$ for the undeformed middle surface of is approximated as follows

$$\mathbf{y}_0(\xi,\eta) = \sum_{I=1}^{4} N_I(\xi,\eta)\; \mathbf{y}_{0I} \tag{3.169}$$

where $N_I(\xi,\eta) = \frac{1}{4}(1+\xi\xi)(1+\eta_I\eta)$, $I = 1,2,3,4$ are the standard bi-linear shape functions, $\xi,\eta \in [-1,+1]$. In the vectorial form the shape functions can be written as

$$4\mathbf{N}_I(\xi,\eta) = \mathbf{s} + \boldsymbol{\xi}\xi + \boldsymbol{\eta}\eta + \mathbf{h}\xi\eta \tag{3.170}$$

where $\mathbf{s} = \{1,1,1,1\}$, $\boldsymbol{\xi} = \{-1,1,1,-1\}$, $\boldsymbol{\eta} = \{-1,-1,1,1\}$, $\mathbf{h} = \{1,-1,1,-1\}$. The derivatives with respect to S^α are found from the derivatives with respect to ξ and

η in the standard manner, see e.g. [Zienkiewicz, Taylor, 1989]. The same bilinear shape functions are used for displacements and the drilling rotation,

$$\mathbf{u}_0(\xi,\eta) = \sum_{I=1}^{4} N_I(\xi,\eta)\ \mathbf{u}_{0I}, \qquad \omega(\xi,\eta) = \sum_{I=1}^{4} N_I(\xi,\eta)\ \omega_I \tag{3.171}$$

This element suffers a severe locking if it is fully integrated, and to alleviate this problem a uniformly reduced (one-point) integration rule is used. The one-point integration leads to the most efficient elements, see e.g. [Belytschko, Ong, Liu, Kennedy, 1984], [Liu, Ong, Uras, 1985], [Zhu, Cescotto, 1995], [Zhu, Zacharia, 1996], and a survey in [Chroscielewski, 1996], but the control of their parasitic modes can be quite complicated.

The tangent matrix of our under-integrated element possesses 8 zero eigenvalues, of which 5 are spurious. The non-zero modes are as follows: 3 displacement modes (one dilatational and two shearing) and 1 rotational mode, i.e. the rigid element motion in terms of rotations, i.e. the mode $\mathbf{s}$. Interestingly, the $\mathbf{s}$-mode is directly related to the rotation constraint; if this constraint is neglected then one additional spurious mode appears. Note that this mode has been reported as spurious for the element of [Jetteur, Frey, 1986].

The zero-energy modes can be identified as follows. For rotations: the bending modes $\boldsymbol{\xi}$ and $\boldsymbol{\eta}$, and the hourglass mode $\mathbf{h}$. For displacements: two hourglass modes $\mathbf{h}$ for each of the displacement components. To include the the zero-energy modes and prevent hourglassing the stabilization matrix has been developed, in which the position vector is expanded into the Taylor series at the center of the element. We have expanded the position vector in both (undeformed and deformed) configurations with respect to the coordinates parameterizing the middle surface as follows. First, we expand

$$\mathbf{y}(\xi,\eta) = \mathbf{y}_0 + \xi\ \mathbf{t}_2, \qquad \mathbf{x}(\xi,\eta) = \mathbf{x}_0 + \xi\lambda_2\ \mathbf{a}_2 \tag{3.172}$$

where $\xi = S^2 - S_0^2$, $\mathbf{t}_2 = \partial\mathbf{y}/\partial S^2$, and $\mathbf{a}_2 = \mathbf{R}\mathbf{t}_2$. Here, λ_2 is the extension coefficient in the $\mathbf{a}_2$ direction, which later is eliminated. This allows to write the components of the expanded strain tensor as

$$U_{11} = \varepsilon_{11} + \xi\kappa_{11}, \qquad U_{12} = \varepsilon_{12} + \xi\kappa_{12} \tag{3.173}$$

where

$$\varepsilon_{11} = \mathbf{x}_{0,1}\cdot\mathbf{a}_1 - 1, \qquad 2\varepsilon_{12} = \mathbf{x}_{0,1}\cdot\mathbf{a}_2, \qquad \kappa_{11} \approx -\omega_{,1}, \qquad 2\kappa_{12} = \lambda_{2,1} = \varepsilon_{22,1}$$

Additionally, $U_{22} = \varepsilon_{22} = \lambda_2 - 1$ is used to eliminate λ_2 from κ_{12}. Similarly for the other direction, the position vectors is expanded as follows

$$\mathbf{y}(\xi,\eta) = \mathbf{y}_0 + \eta\ \mathbf{t}_1, \qquad \mathbf{x}(\xi,\eta) = \mathbf{x}_0 + \eta\lambda_1\ \mathbf{a}_1 \tag{3.174}$$

where $\eta = S^1 - S_0^1$, $\mathbf{t}_1 = \partial\mathbf{y}/\partial S^1$, and $\mathbf{a}_1 = \mathbf{R}\mathbf{t}_1$. Here, λ_1 is the extension coefficient into the $\mathbf{a}_1$ direction, which later is eliminated. This allows to write the components of the expanded strain tensor as

$$U_{22} = \varepsilon_{22} + \eta\kappa_{22}, \qquad U_{21} = \varepsilon_{21} + \eta\kappa_{21} \tag{3.175}$$

where

$$\varepsilon_{22} = \mathbf{x}_{0,2}\cdot\mathbf{a}_2 - 1, \qquad 2\varepsilon_{21} = \mathbf{x}_{0,2}\cdot\mathbf{a}_1, \qquad \kappa_{22} \approx -\omega_{,2}, \qquad 2\kappa_{21} = \lambda_{1,2} = \varepsilon_{11,2}$$

Additionally, $U_{11} = \varepsilon_{11} = \lambda_1 - 1$ is used to eliminate λ_1 from κ_{21}.

For the one-point integration at $\xi = \eta = 0$ only the ε-terms remain, and form the tangent matrix. The κ-terms can be exploited to construct the stabilization matrix. For this purpose the strain energy with $U_{\alpha\beta}$ given by eq.(173) and (175) is integrated exactly. Then, κ_{11} and κ_{22} provide the bending modes ξ and η for rotations, while κ_{12} and κ_{21} provide the $\mathbf{h}$ modes for displacement components. The hourglass mode $\mathbf{h}$ for rotations is introduced by adding the term $(\mathbf{h} \cdot \delta\omega)(\mathbf{h} \cdot \omega)$ to the virtual work equation, where ω is a vector of nodal rotations for the quadrilateral. Enforcement of this term via the penalty method is equivalent to adding of $\mathbf{h} \otimes \mathbf{h}$ to the tangent matrix. N.B. it has been checked that this mode is non-communicable (incompatible), and disappears for a patch of even two elements.

The developed method of stabilization resembles the approach used for beams in Section 4.1, and is also similar to the method of [Liu, Ong, Uras, 1985], where the tangent matrix $\mathbf{B}$ of the strain-displacement relation is expanded into the Taylor series. We note in passing that all the above stabilization terms are a part of the virtual work, and they contribute not only to the tangent matrix but also to the residual vector. Finally, the developed element has 3 zero eigenvalues, corresponding with two rigid translations and one rigid rotation, as required.

This element differs from the currently existing elements with the drilling rotation. The element with the same membrane part of [Ibrahimbegovic, Frey, 1984], uses a 2x2 Gaussian quadrature, and is based on the incompatible modes of [Wilson, Taylor, Doherty, Ghaboussi, 1973], and [Bathe, Dvorkin, 1985]-type shear strain interpolation. The element for the formulation based on the Green strain of [Gruttmann, Wagner, 1992] also uses a 2x2 Gaussian quadrature, and exploits the Allman-type interpolation of displacements. The co-rotational element of [Zhu, Zacharia, 1996] uses a on-point Gaussian quadrature, the Allman-type shape functions, and is based on the rate form of kinematics and the constitutive equation.

Finally, we note that the formulation based on the right stretch strain introduces a strong coupling between rotations and displacements, and, differently than for the formulation based on the Green strain, the use of Allman-type shape functions is not necessary. In consequence, more zero-energy modes have to be stabilized for the reduced integration. Although the developed element performs well in several tests it is likely that applying the Enhanced Assumed Strain (EAS) method a further improvement could be achieved.

Implementation of the design sensitivity analysis for shells

The subject of the design sensitivity analysis (DSA) is calculation of derivatives of the state variables with respect to the design variables. These derivatives, or the so called sensitivities, are subsequently used to modify (re-design) the structure in order to achieve a required performance, see e.g. [Haug, Choi, Komkov, 1986]. The methodology of calculating the design derivatives has already been established for a wide class of materially and kinematically nonlinear problems, see e.g. [Choi, Santos, 1987], [Kleiber, 1990], [Park, Choi, 1990], [Mroz, Haftka, 1993], [Kleiber, Hien, Postek, 1994], [Santos, Wisniewski, Apostol, 1995], [Kleiber, Hien, 1997].

When new values of the design parameters are sought as a solution of an optimization problem then the question of derivatives becomes further complicated. The optimization for nonlinear mechanical problems must be performed in the space of $\{\mathbf{b}, \mathbf{z}, \mu\}$, where $\mathbf{b}$

is the design variable vector, $\mathbf{z}$ is the state variable vector, μ is the load multiplier. Such optimization problems are typically solved on use of the staggered (bordering) solution schemes, which proved to be useful in many contexts, e.g. [Turska, Wisniewski, Schrefler, 1993], in order to separate $\mathbf{b}$ from $\mathbf{z}$ and to perform the optimization in terms of $\mathbf{b}$, only.

Equilibrium paths for nonlinear equilibrium equations may possess extremum and bifurcation points. Essential for designing is the question of the stability of the solution, and it is usually formulated as a requirement that the minimum should be located either on a stable branch, e.g. [Ringertz, 1992], or, at most, at the first critical point, e.g. [Kamat, 1987], [Kamat, Khot, Venkayya, 1984], [Khot, Kamat, 1985], [Arora, Wu, 1987], [Wu, Arora, 1987]. The latter requirement can be formulated as the critical point constraint, and is of interest also in [Wisniewski, Santos, 1995] and [Wisniewski, Turska, Kleiber, 1997]. These works show that the design derivatives depend on the solution scheme which is applied. It is essential, because complexity of nonlinear equilibrium paths renders that specialized algorithms and solution strategies must be used to solve particular optimization problems. Accordingly, new solution schemes and new types of the design derivatives need to be devised to solve new optimization problems.

In this section we consider the design derivatives of displacements and rotations, which in case of the optimization with the critical point constraint, are used by the scheme optimizing at the maximum point.

First, we describe the continuum adjoint method of the design sensitivity analysis for an elastic shell. On use of the notation proposed in [Haug, Choi, Komkov, 1986], the virtual work equation for a shell can be written as

$$a_b(\mathbf{z}, \delta\mathbf{z}) - l_b(\delta\mathbf{z}) = 0 \tag{3.176}$$

where the virtual work of internal and external forces are as follows

$$a_b(\mathbf{z}, \delta\mathbf{z}) = \int_S \left[\mathbf{n}_\alpha \cdot \delta\boldsymbol{\varepsilon}_\alpha + \mathbf{m}_\alpha \cdot \delta\boldsymbol{\kappa}_\alpha\right] \, dS, \qquad l_b(\delta\mathbf{z}) = \int_S \left[\hat{\mathbf{q}} \cdot \delta\mathbf{u}_0 + \hat{\mathbf{m}} \cdot \delta\boldsymbol{\theta}\right] \, dS \tag{3.177}$$

Here, $\mathbf{n}_\alpha$ and $\mathbf{m}_\alpha$ are the stress and couple resultant vectors, while $\boldsymbol{\varepsilon}_\alpha$ and $\boldsymbol{\kappa}_\alpha$ are the shell strain and bending vectors. The state variable is defined as $\mathbf{z} \equiv \{\mathbf{u}_0, \boldsymbol{\psi}\}$, where $\mathbf{u}_0$ is the displacement vector, and $\boldsymbol{\psi}$ denotes parameters of rotations. The scalar b denotes a single design variable. Note that if the form of the virtual work given by eq.(102) is used then also the rotation constraint contributes to the above equation.

Within the continuum approach of the DSA, first, the differential of eq.(176) is calculated with respect to the design variable b , and next the obtained formula is discretized. The design differential of eq.(176) is as follows

$$a_b(\mathbf{z}', \delta\mathbf{z}) + a'_{\delta b}(\mathbf{z}, \delta\mathbf{z}) - l'_{\delta b}(\delta\mathbf{z}) = 0 \tag{3.178}$$

where the prime ($'$) denotes a differential of a function of b in the direction δb. Below, the components of the above equation are specified. First, let us calculate the design derivative of $\mathbf{n}_\alpha \cdot \delta\boldsymbol{\varepsilon}_\alpha$,

$$\frac{d}{db}(\mathbf{n}_\alpha \cdot \delta\boldsymbol{\varepsilon}_\alpha) = \left(\frac{d\mathbf{B}_\varepsilon}{db}\delta\mathbf{z}\right) \cdot \mathbf{n}_\alpha + \delta\boldsymbol{\varepsilon}_\alpha \cdot \left(\frac{d\mathbf{C}_\varepsilon}{db}\boldsymbol{\varepsilon}_\alpha\right) + \delta\boldsymbol{\varepsilon}_\alpha \cdot \left(\mathbf{C}_\varepsilon \frac{d\boldsymbol{\varepsilon}_\alpha}{db}\right) \tag{3.179}$$

where $\mathbf{B}_\varepsilon$ is the tangent operator for the kinematical relation, i.e. $\delta\boldsymbol{\varepsilon}_\alpha = \mathbf{B}_\varepsilon \delta \mathbf{z}$, and $\mathbf{C}_\varepsilon$ is the constitutive operator defined as $\mathbf{n}_\alpha = \mathbf{C}_\varepsilon \boldsymbol{\varepsilon}_\alpha$. In further transformations the following identities are exploited: $(\mathbf{Ta}) \cdot \mathbf{b} = \mathbf{a} \cdot (\mathbf{T}^T \mathbf{b})$, and $\mathbf{Ta} = \mathbf{a}\mathbf{T}^T$. The particular terms of eq.(179) can be transformed as follows:

$$\left(\frac{d\mathbf{B}_\varepsilon}{db}\delta\mathbf{z}\right) \cdot \mathbf{n}_\alpha = \delta\mathbf{z} \cdot \left[\left(\frac{d\mathbf{B}_\varepsilon}{db}\right)^T \mathbf{n}_\alpha\right] = \delta\mathbf{z} \cdot \left[\mathbf{n}_\alpha \frac{d\mathbf{B}_\varepsilon}{db}\right] = \delta\mathbf{z} \cdot \left[\mathbf{n}_\alpha \left(\frac{d\mathbf{B}_\varepsilon}{dz}\right) \frac{dz}{db}\right] \tag{3.180}$$

$$\delta\boldsymbol{\varepsilon}_\alpha \cdot \left(\frac{d\mathbf{C}_\varepsilon}{db}\boldsymbol{\varepsilon}_\alpha\right) = \delta\mathbf{z} \cdot \left[\mathbf{B}_\varepsilon^T \frac{d\mathbf{C}_\varepsilon}{db}\, \boldsymbol{\varepsilon}_\alpha\right] \tag{3.181}$$

$$\delta\boldsymbol{\varepsilon}_\alpha \cdot \left(\mathbf{C}_\varepsilon \frac{d\boldsymbol{\varepsilon}_\alpha}{db}\right) = \delta\mathbf{z} \cdot \left[\mathbf{B}_\varepsilon^T\, \mathbf{C}_\varepsilon\, \mathbf{B}_\varepsilon \frac{dz}{db}\right] \tag{3.182}$$

In a similar way the design derivative of $\mathbf{m}_\alpha \cdot \delta\boldsymbol{\kappa}_\alpha$ can be calculated. On the above equations the components of the design differential, eq.(178), are as follows:

$$\begin{aligned} a_b(\mathbf{z}', \delta\mathbf{z}) \;&=\; \int_S \delta\mathbf{z} \cdot \Big[\mathbf{B}_\varepsilon^T\, \mathbf{C}_\varepsilon\, \mathbf{B}_\varepsilon + \mathbf{B}_\kappa^T\, \mathbf{C}_\kappa\, \mathbf{B}_\kappa \\ &+\; \mathbf{n}_\alpha \left(\frac{d\mathbf{B}_\varepsilon}{dz}\right) + \mathbf{m}_\alpha \left(\frac{d\mathbf{B}_\kappa}{dz}\right)\Big] \frac{dz}{db}\, \delta b\, dS \end{aligned} \tag{3.183}$$

$$a'_{\delta b}(\mathbf{z}, \delta\mathbf{z}) = \int_S \delta\mathbf{z} \cdot \left[\mathbf{B}_\varepsilon^T \frac{d\mathbf{C}_\varepsilon}{db}\, \boldsymbol{\varepsilon}_\alpha + \mathbf{B}_\kappa^T \frac{d\mathbf{C}_\kappa}{db}\, \boldsymbol{\kappa}_\alpha\right] \delta b\, dS \tag{3.184}$$

In the second step of the continuum approach the design differential is discretized as in the finite element method. Then, we obtain

$$a_b(\mathbf{z}', \delta\mathbf{z}) \overset{(\mathrm{d})}{=} \delta\mathbf{z}^T\, \mathbf{K}\, \frac{d\mathbf{z}}{db}\, \delta b, \qquad a'_{\delta b}(\mathbf{z}, \delta\mathbf{z}) - l'_{\delta b}(\delta\mathbf{z}) \overset{(\mathrm{d})}{=} \delta\mathbf{z}^T \frac{\partial \mathbf{r}}{\partial b}\, \delta b \tag{3.185}$$

where $\overset{(\mathrm{d})}{=}$ indicates the discretization process, $\mathbf{r}$ denotes the residual of the equilibrium equation, and $\mathbf{K} = \mathbf{K}_0 + \mathbf{K}_u + \mathbf{K}_\sigma$ is a full tangent matrix. The discretized eq.(178) can be written as

$$\delta\mathbf{z}^T \left(\mathbf{K}\, \frac{d\mathbf{z}}{db} + \frac{\partial \mathbf{r}}{\partial b}\right) \delta b = 0 \tag{3.186}$$

from which the design derivative of the state variable is calculated as follows

$$\frac{d\mathbf{z}}{db} = \mathbf{K}^{-1}\, \frac{\partial \mathbf{r}}{\partial b} \tag{3.187}$$

This derivative can be used to calculate the design differential of a performance Ψ, accounting for the dependence $\mathbf{z} = \mathbf{z}(b)$. which is used to modify the structure.

$$\frac{d\Psi}{db}\delta b \overset{(\mathrm{d})}{=} \left[\frac{\partial \Psi}{\partial b} + \left(\frac{\partial \Psi}{\partial \mathbf{z}}\right)^T \frac{d\mathbf{z}}{db}\right] \delta b = \left[\frac{\partial \Psi}{\partial b} - \left(\frac{\partial \Psi}{\partial \mathbf{z}}\right)^T \mathbf{K}^{-1}\, \frac{\partial \mathbf{r}}{\partial b}\right] \delta b \tag{3.188}$$

Within the Adjoint System Method (ASM) the design derivative of the performance, $d\Psi/db$, is evaluated in two steps:

Step 1. $\boldsymbol{\lambda}^T = \mathbf{K}^{-1}\ (\partial\Psi/\partial\mathbf{z})$,
Step 2. $d\Psi/db = \partial\Psi/\partial b - \boldsymbol{\lambda}\ (\partial\mathbf{r}/\partial b)$.
Traditionally, $\partial\Psi/\partial\mathbf{z}$ is called the adjoint load while $\boldsymbol{\lambda}$ is the adjoint solution.

Below, we explain the scheme of implementation of the ASM, which is very convenient for the numerical implementation of the method. This implementation was used e.g. in [Santos, Choi, 1988], and for problems with rotational degrees of freedom in [Santos, Wisniewski, Apostol, 1995].

Consider the case of the performance $\Psi \equiv (\mathbf{z})_i$, which does not depend explicitly on the design parameter, i.e. $\partial\Psi/\partial b = 0$. Then, $\partial\Psi/\partial\mathbf{z} = \{0, ...1, ...0\}$, where the digit one appears on the i-th position. We assume that the external loads are independent of the design parameter, i.e. $l'_{\delta b}(\delta z) = 0$. Note that for $\boldsymbol{\lambda}$ replacing $\delta\mathbf{z}$ we have $a'_{\delta b}(\mathbf{z}, \boldsymbol{\lambda}) \overset{(d)}{=} \boldsymbol{\lambda}(\partial\mathbf{r}/\partial b)\ \delta b$, which can be used to evaluate the expression of Step 2. Then,

$$a'_{\delta b}(\mathbf{z}, \boldsymbol{\lambda}) = \boldsymbol{\lambda} \cdot \left[\mathbf{B}_\varepsilon^T \frac{d\mathbf{C}_\varepsilon}{db}\ \boldsymbol{\varepsilon}_\alpha + \mathbf{B}_\kappa^T \frac{d\mathbf{C}_\kappa}{db}\ \boldsymbol{\kappa}_\alpha\right] \delta b \tag{3.189}$$

where the terms in brackets are evaluated for the given $\mathbf{z}$. Transforming this expression on use of the identities given earlier we obtain

$$a'_{\delta b}(\mathbf{z}, \boldsymbol{\lambda}) = \left[(\mathbf{B}_\varepsilon\boldsymbol{\lambda}) \cdot \left(\frac{d\mathbf{C}_\varepsilon}{db}\ \boldsymbol{\varepsilon}_\alpha\right) + (\mathbf{B}_\kappa\boldsymbol{\lambda}) \cdot \left(\frac{d\mathbf{C}_\kappa}{db}\ \boldsymbol{\kappa}_\alpha\right)\right] \delta b \tag{3.190}$$

Denoting $\Delta(\boldsymbol{\varepsilon}_\alpha)_L = \mathbf{B}_\varepsilon\boldsymbol{\lambda}$ and $\Delta(\boldsymbol{\kappa}_\alpha)_L = \mathbf{B}_\kappa\boldsymbol{\lambda}$, we can write

$$a'_{\delta b}(\mathbf{z}, \boldsymbol{\lambda}) = \left[\Delta(\boldsymbol{\varepsilon}_\alpha)_L \cdot \left(\frac{d\mathbf{C}_\varepsilon}{db}\ \boldsymbol{\varepsilon}_\alpha\right) + \Delta(\boldsymbol{\kappa}_\alpha)_L \cdot \left(\frac{d\mathbf{C}_\kappa}{db}\ \boldsymbol{\kappa}_\alpha\right)\right] \delta b \tag{3.191}$$

The above expression has been used to incorporate the finite rotation equations into the design sensitivity analysis. It has perhaps the most convenient form for the numerical implementation of the method, because the sensitivities can be computed on use of strains, without resorting to displacements and/or rotations.

As an example, consider a tendon stretched by an axial force, of the initial length L, the cross-section area A, and Young modulus E. One end of the tendon is fixed, and at the other a force P is applied. The Green strain is $\epsilon = \frac{1}{2}[\left(\frac{L+u}{L}\right)^2 - 1]$, where u is the axial displacement at force P. Introducing $z = u/L$ we obtain: $\epsilon = z + \frac{1}{2}z^2$, and $\delta\epsilon = \delta u\ \frac{1}{L}(1+z)$. The virtual work equation can be written as

$$(\delta\epsilon\ EA\ \epsilon)\ \ L - \delta u\ P = 0 \tag{3.192}$$

and, after eliminating $\delta\epsilon$, the equilibrium equation is as follows

$$r = (1+z)\ EA\ (z + \frac{1}{2}z^2) - P = 0 \tag{3.193}$$

This nonlinear equation can be solved by the Newton-Raphson scheme,

$$z^{i+1} = z^i - K^{-1}\ r, \qquad K = EA\ (1 + 3z + 1.5z^2) \tag{3.194}$$

Assume that z is a performance, i.e. $\Psi = z$ and then, $d\Psi/dz = 1$. Take, for instance, $A = bh$, where b is the width and h is the hight of the cross-section. The design derivative of residual with respect to the width b is equal to $r_{,b} = (1+z)\ Eh\ (z + \frac{1}{2}z^2)$.

Within the ASM, first, the adjoint displacement is calculated for the adjoint unit load, i.e. $\lambda = K^{-1}\ 1$. Then, the design sensitivity of performance is as follows

$$d\Psi/db = -\lambda\ r_{,b} = -\lambda(1+z)\ Eh\ (z + \frac{1}{2}z^2) \tag{3.195}$$

As λ denotes the displacement increment Δz due to a unit load, thus note that $\Delta z(1+z)$ is a linear part of the Green strain increment, $\Delta\epsilon = \epsilon_k - \epsilon_{k-1} = \Delta z(1+z) + \frac{1}{2}(\Delta z)^2$. Hence, instead of eq.(195) we can write

$$d\Psi/db = -\Delta\epsilon_L\ Eh\ \epsilon \tag{3.196}$$

where $\Delta\epsilon_L$ is due to the unit load. In this way, the sensitivities can be computed in terms of strains, without resorting to displacements.

Example 1. In-plane bending of a cantilever by a force

This example demonstrates the capability of the element developed by the author to undergo large drilling rotations.

The data is as follows: length $L = 1.0$ in, width $b = 0.1$ in, thickness $h = 0.1$ in, Young modulus $E = 3 \cdot 10^7$ lb/in^2, Poisson ratio $\nu = 0.3$. One end of the cantilever is fixed while at the other a vertical force is applied, see Fig.3.3. The model consists of 40 quadrilateral finite elements.

The initial mesh and the deformed meshes are shown in Fig.3.3. The drilling rotation (denoted by b) and the in-plane displacements (u and v) for up to. $P_{max} = 1000$ lb are shown in Fig.3.4. The obtained curve for the tip deflection v coincides with the one presented in [Gruttmann, Wagner, Wriggers, 1992], Fig.3.

The sensitivity of the drilling rotation with respect to the thickness of the cantilever (a size in the direction perpendicular to the plane of the cantilever) calculated along the solution path is shown in Fig.3.5. The curve for the sensitivity of the drilling rotation has not been presented in the literature, yet. Therefore, for comparison, the solutions obtained by the finite rotation/transverse shear beam element are also given. Both solutions are very close, what confirms that the present implementation is correct.

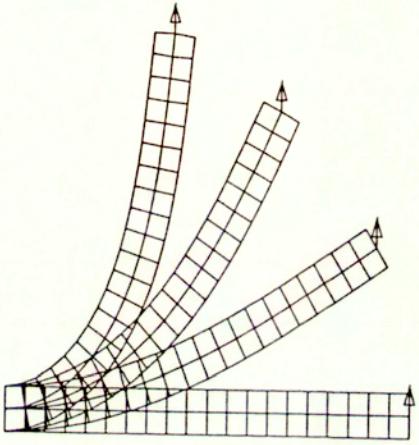

Fig.3.3 In-plane bending. Initial and deformed mesh

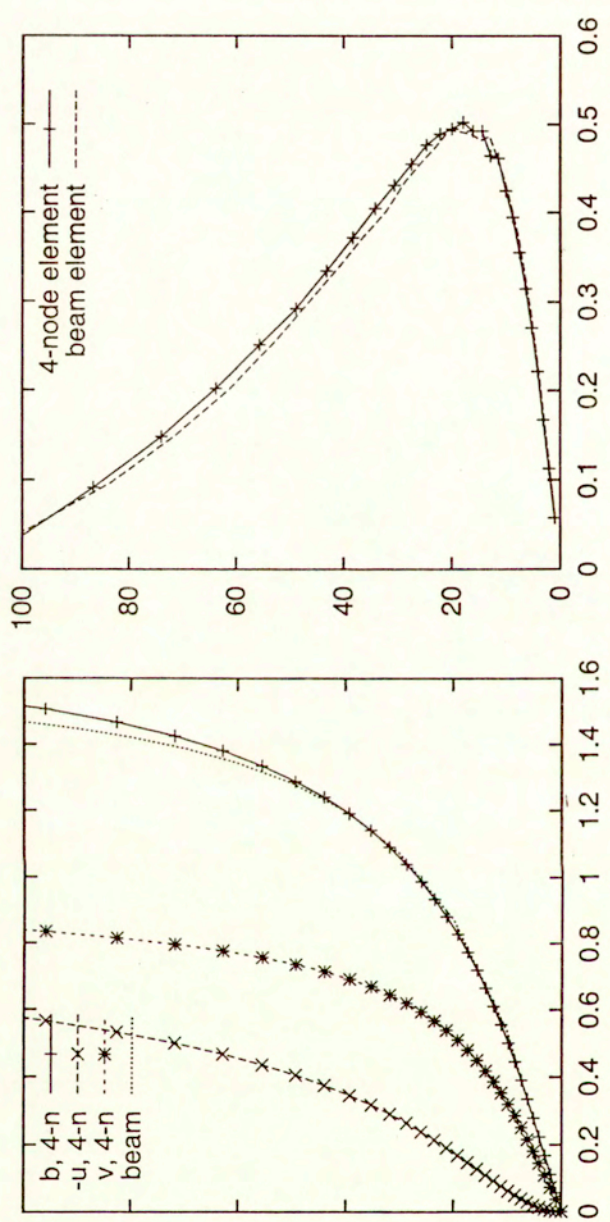

Fig.3.4 In-plane bending.
Drilling rotation and in-plane displacements

Fig.3.5 In-plane bending.
Sensitivity of drilling rotation w.r.t. the thickness

Example 2. Cylindrical roof under a point load

A shallow cylindrical roof under a point load is shown in Fig.3.6. The data is as follows: radius $R = 2.54m$, length $L = 0.254m$, thickness $t = 6.35mm$, Young modulus $E = 3.103Gpa$, Poisson ratio $\nu = 0.3$. The curved edge is free and the straight one is clamped. A vertical point load is applied at the middle of the shell, and $P_{max} = 800N$. A quarter of the shell, with additional boundary conditions enforcing symmetry of the deformation, is analyzed.

A model of 36 four-node shell finite elements, based on the Green strain, isoparametric, under-integrated and with the γ-stabilization, This example is widely used to test a non-linear performance of finite elements, and the load-central deflection curves are given in several works, e.g. [Gruttmann, Wagner, Wriggers, 1992], Fig.5, [Chroscielewski, Makowski, Stumpf, 1992], Fig.1. The sensitivities are the original contribution of the author and co-workers, [Santos, Wisniewski, Apostol, 1995]. The shell thickness is the design parameter, for which the sensitivities are calculated.

The nonlinear equilibrium paths and the corresponding sensitivity charts are presented as follows:

-for the horizontal Z displacement at the middle of the free edge in Fig.3.7a and b,
-for the horizontal Y rotation at the middle of the free edge in Fig.3.8a and b,
-for the vertical X displacement under the force in Fig.3.9a and b,
-for the horizontal Y displacement at the middle of the shell quarter in Fig.3.10a and b,
-for the horizontal Z displacement at the middle of the shell quarter in Fig.3.11a and b,
-for the horizontal Y rotation at the middle of the shell quarter in Fig.3.12a and b.

Note that there are 2 asymptotic lines on the sensitivity charts, which correspond with the maximum point A and the minimum point B on the equilibrium paths. Points A, A', B, B' and C on the sensitivity charts correspond with points A, B and C on the equilibrium paths, and appear in the following order: zero - A - A' - B - B' - C.

Besides, comparative calculations are made for three meshes, i.e. of 6×6, 12×12 and 18×18 elements, and results for $P = 800N$ are shown in Table 3.2. The ratios displayed in the table allow to compare the sensitivities yielded by the continuum adjoint system method (ASM) and the central finite difference method (FDM). hods. Note that the ASM is analytical and therefore, if correctly implemented in the numerical code, it is more accurate than the FDM.

Analyzing results presented in Table 3.2 it can be noticed that for the rotation component X at the middle of the quarter of the shell the sensitivity is inaccurate, and does not improve for finer meshes. Note that this component is almost normal to the middle surface, and we can suspect that the inaccuracy has its source in the way in which the drilling rotation is introduced. This element is based on the Green strain measures, the rotation constraint, $C_{12} = \frac{1}{2}(\mathbf{x}_{0,2} \cdot \mathbf{a}_1 - \mathbf{x}_{0,1} \cdot \mathbf{a}_2) = 0$ of eq.(80), is introduced via the penalty method, and the standard bi-linear shape functions are used. Hence, the coupling between displacements and rotations is provided only by the rotation constraint which is imposed in an approximate way. We can expect that e.g. the use of the Allman-type approximations could remove the above effect.

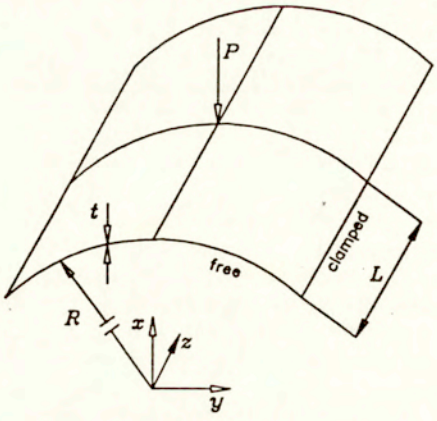

Fig.3.6 Cylindrical roof under a point load. Geometry and load.

Table 3.2. Nonlinear shallow cylindrical shell under point load. Load P = 800 N. Four node shell element. Design parameter: shell thickness t.

Node	Perf. type	Perf. value	ASM Sensitivities	Ratio of sensitivities (ASM/FD) × 100%		
		18 × 18	18 × 18	6 × 6	12 × 12	24 × 24
1	Dis. X	-2.63498e-02	1.73633e-01	99.126	99.586	101.870
1	Dis. Z	2.04509e-05	-1.31841e-02	99.581	99.814	101.151
1	Rot. Y	1.32639e-02	1.39863e+00	45.900	140.214	99.361
2	Dis. X	-3.04506e-02	1.30746e+00	99.923	99.978	98.945
3	Dis. X	-2.01136e-02	2.80921e-01	99.546	99.633	99.459
3	Dis. Y	-5.80394e-05	-3.42847e-03	98.955	99.548	100.413
3	Dis. Z	2.73632e-05	-1.15916e-02	99.913	99.889	99.712
3	Rot. X	1.27003e-04	7.67764e-02	-267.013	-730.965	-705.919
3	Rot. Y	-9.10115e-03	1.74873e+00	130.584	102.866	97.648
3	Rot. Z	-1.08404e-01	1.45057e+00	77.014	96.295	99.058

Node 1 - at the curved edge (middle of the free edge), Node 2 - under the force, Node 3 - at the middle of the quarter.

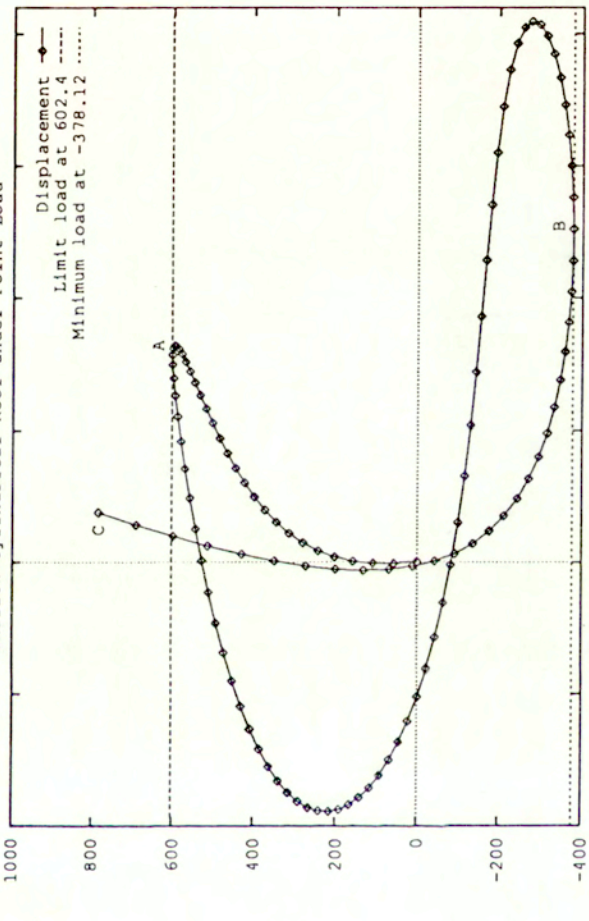

Fig.3.7a Cylindrical roof under a point load. Z-displacement at the middle of free edge.

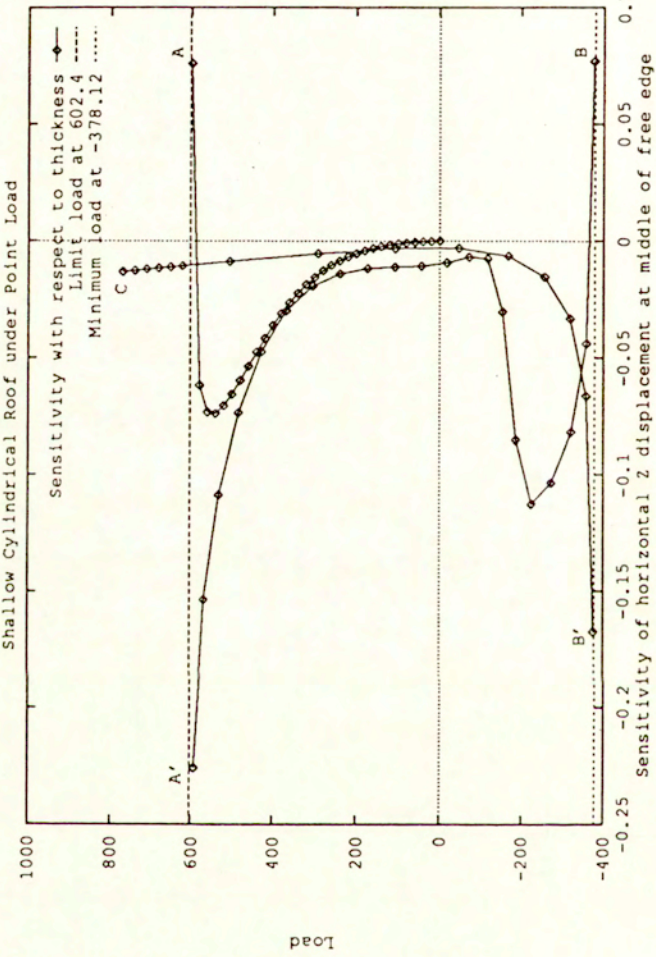

Fig.3.7b Cylindrical roof under a point load.
Sensitivity to thickness of Z-displacement at the middle of free edge.

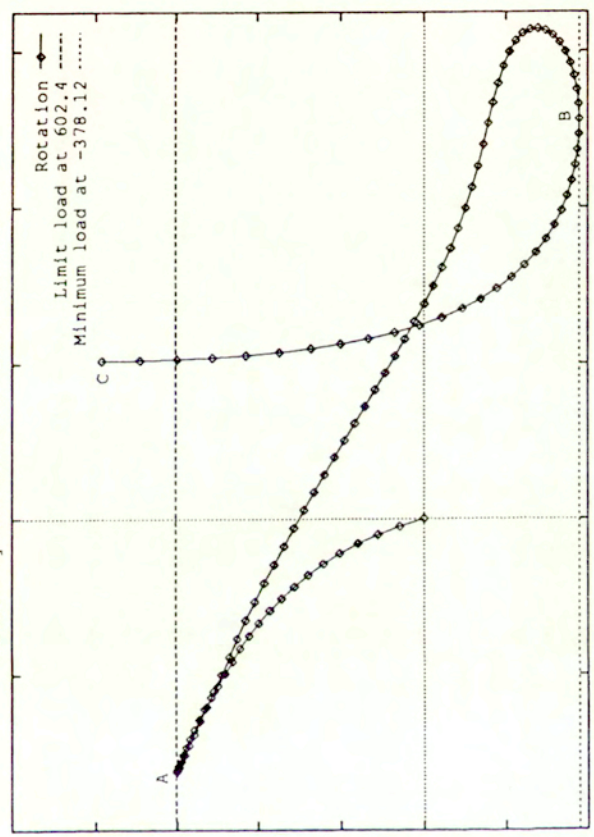

Fig.3.8a Cylindrical roof under a point load. Y-rotation at the middle of free edge.

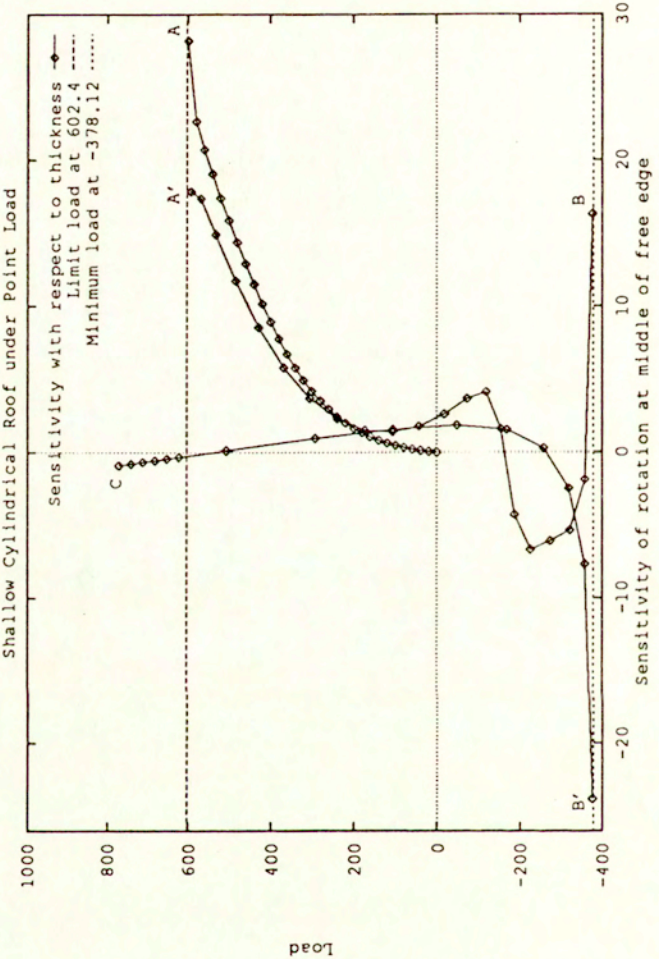

Fig.3.8b Cylindrical roof under a point load.
Sensitivity to thickness of Y-rotation at the middle of free edge

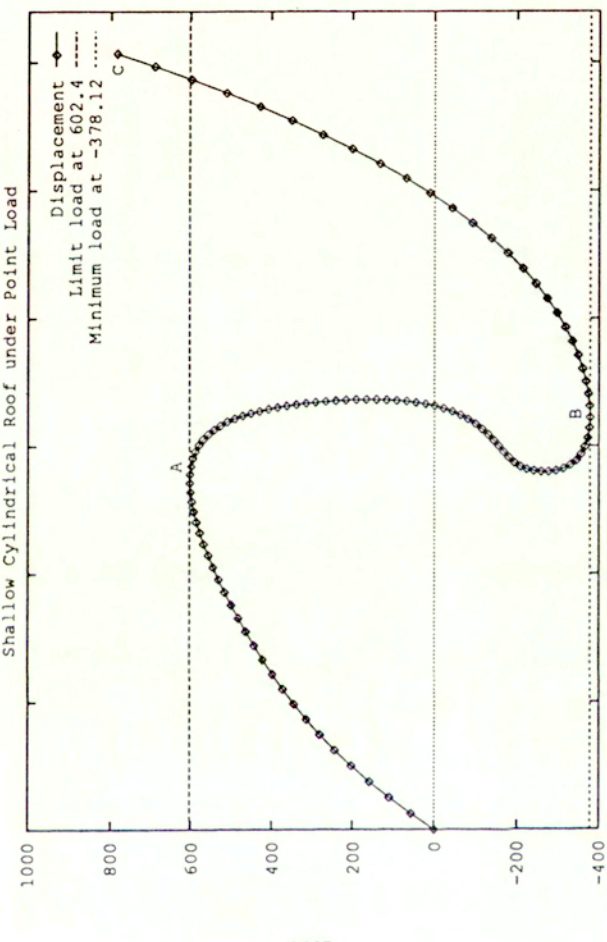

Fig.3.9a Cylindrical roof under a point load. X-displacement under the force.

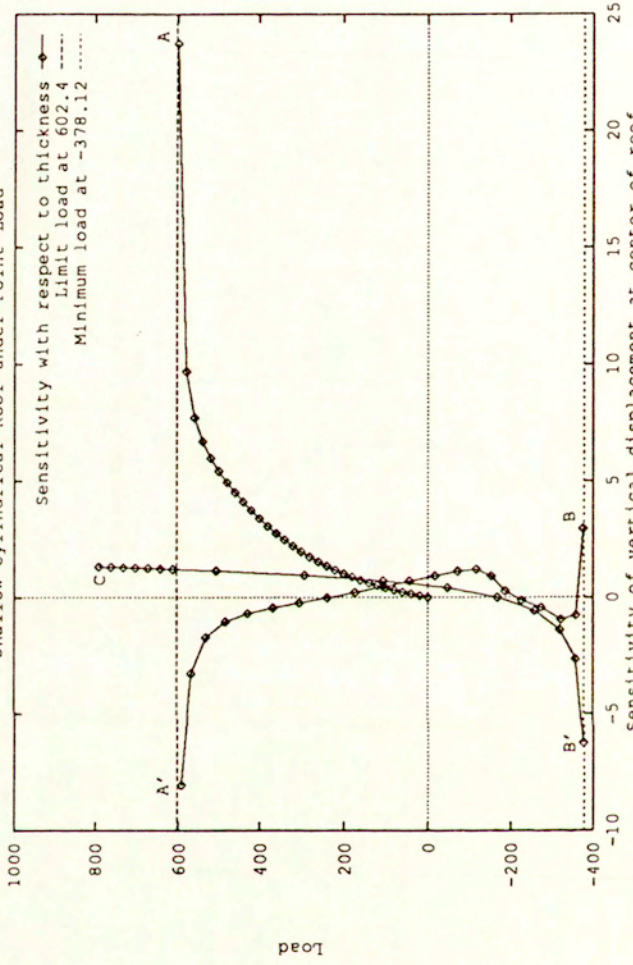

Fig.3.9b Cylindrical roof under a point load.
Sensitivity to thickness of X-displacement under the force.

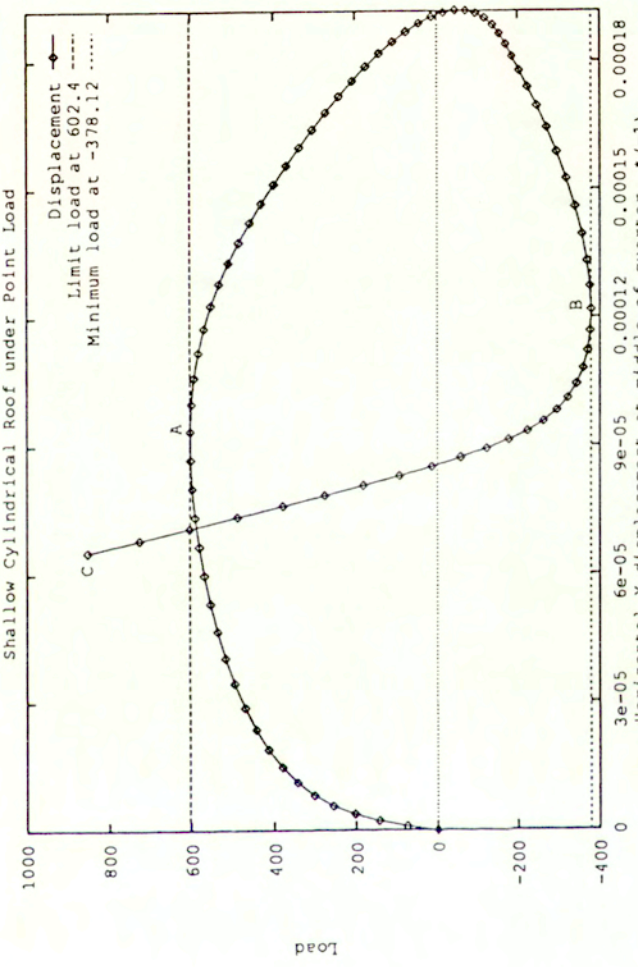

Fig.3.10a Cylindrical roof under a point load.
Y-displacement at the middle of the shell quarter.

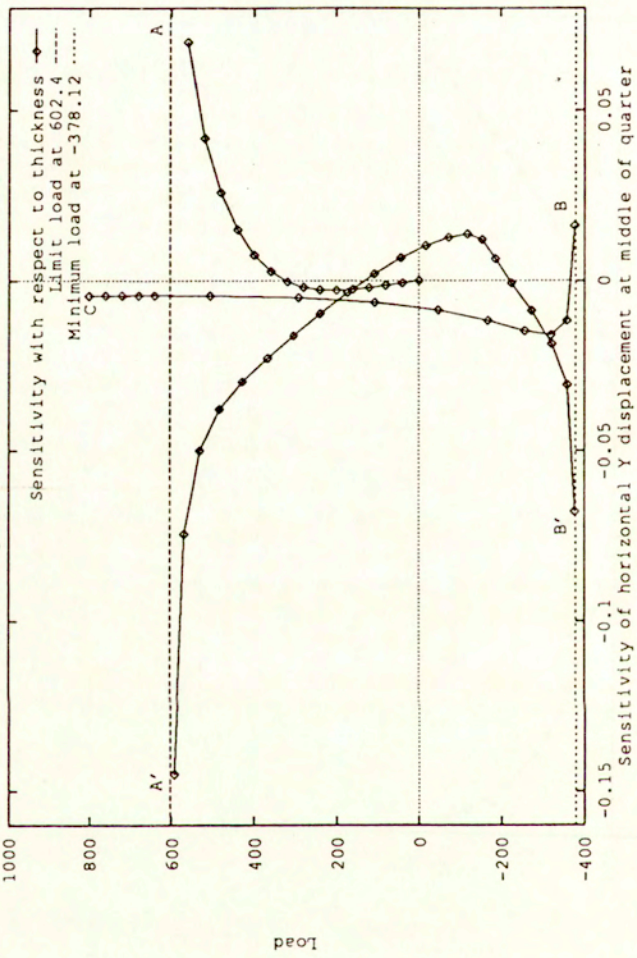

Fig.3.10b Cylindrical roof under a point load.
Sensitivity to thickness of Y-displacement at middle of shell quarter.

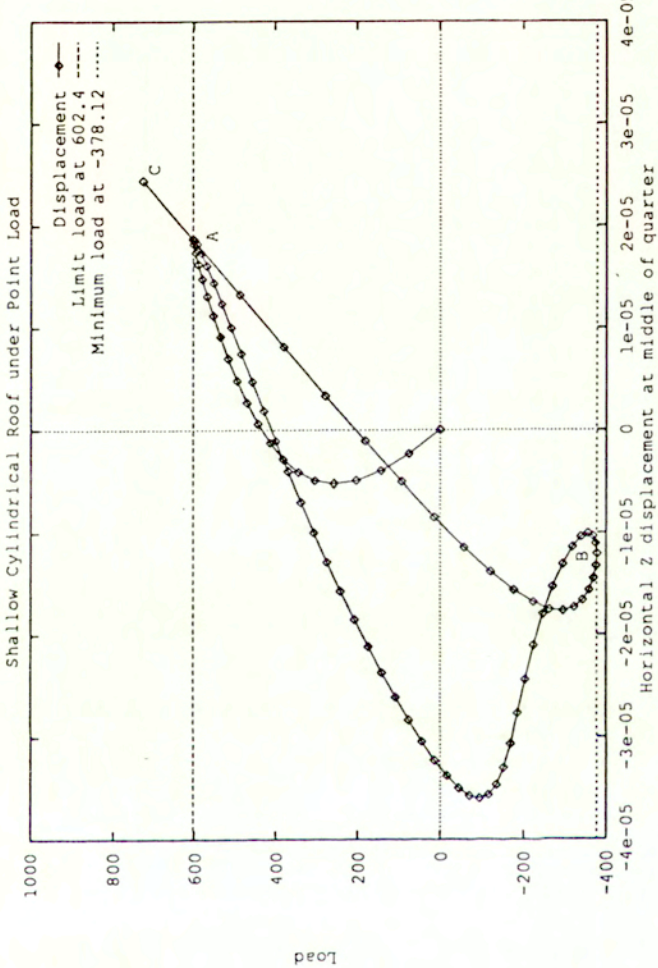

Fig.3.11a Cylindrical roof under a point load. Z-displacement at middle of shell quarter.

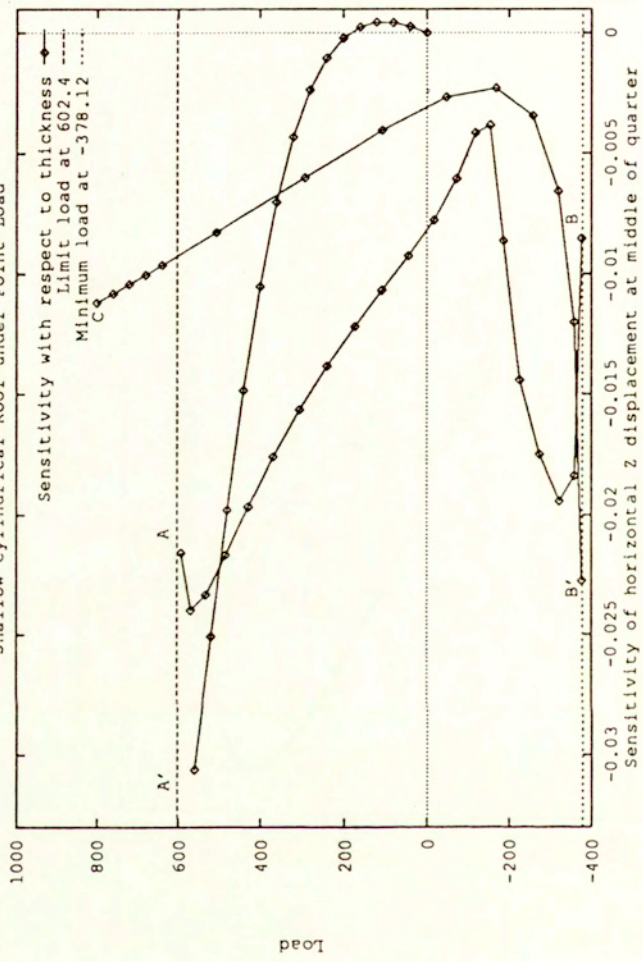

Fig.3.11b Cylindrical roof under a point load.
Sensitivity to thickness of Z-displacement at the middle of shell quarter.

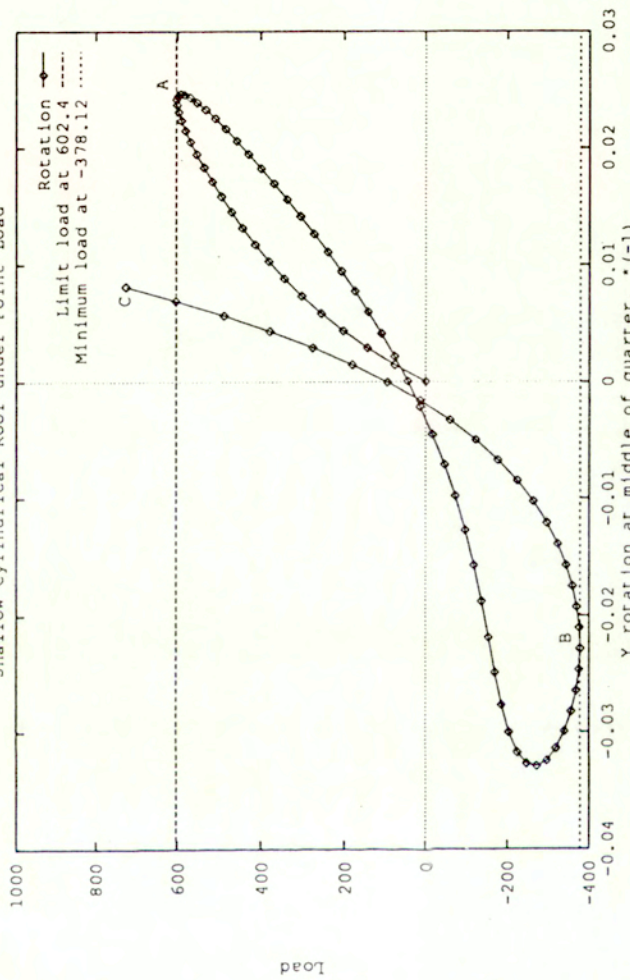

Fig.3.12a Cylindrical roof under a point load. Y-rotation at the middle of shell quarter.

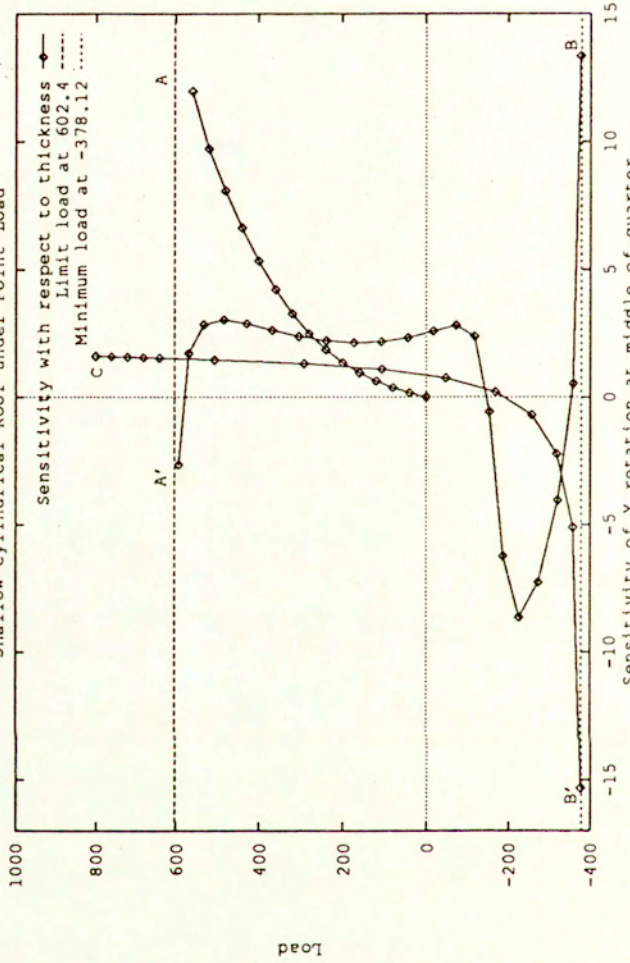

Fig.3.12b Cylindrical roof under a point load.
Sensitivity to thickness of Y-rotation at the middle of shell quarter.

Example 3. Thin-walled C-profile under a point load

The geometry of the C-profile and the load are shown in Fig.3.13. The data is as follows; thickness $h = 0.1$in, length $L = 36$ in, hight of flange $b = 6$ in, width of lower and upper shelf $a = 2$ in, Young modulus $E = 10^7$ lb/in^2, Poisson ratio $\nu = 0.333$. One end of the profile is clamped, at the other the vertical force is applied. 120 four-node shell elements are used. The load $P_{max} = 520$, and the critical load is about 509.6.

The curves for the static analysis correspond with those presented e.g. in [Chroscielewski, Makowski, Stumpf, 1992], Fig.5 and 6, and [Ibrahimbegovic, Frey, 1994], Fig.15. The sensitivities are the original contribution of the author and co-workers, [Santos, Wisniewski, Apostol, 1995]. The shell thickness is the design parameter, for which the sensitivities are calculated.

The nonlinear equilibrium paths and the corresponding sensitivity charts are presented as follows:

- for the Z-displacement at the applied load in Fig.3.14a and b,
- for the X-rotation at the applied load in Fig.3.15a and b.

The rotation of the free end of the beam is finite. Notice that there are 3 asymptotic lines on the sensitivity chart, which correspond with the inflection point A, the maximum point B, and the minimum point C on the equilibrium paths. The points on the sensitivity chart appear in the following order: A - A' - B - B' - C - C' - D.
The sensitivities and sensitivity ratios for the chosen load levels are presented in Table 3.3.

Table 3.3. Thin-walled C-profile. Sensitivities and sensitivity ratios

Perf.	$P = 407.68$		$P = 458.64$		$P = 509.60$		$P = 520.00$	
	ASM	Ratio	ASM	Ratio	ASM	Ratio	ASM	Ratio
Dis.X	4.75e0	99.250	1.59e2	138.590	9.07e2	157.865	1.10e3	104.355
Dis.Y	8.50e1	99.213	1.22e3	138.852	2.11e3	161.869	2.45e2	100.318
Dis.Z	6.30e1	99.235	8.22e2	138.339	2.38e3	156.877	1.83e3	103.465
Rot.X	-2.45e1	99.248	-2.31e2	137.315	-3.02e2	156.398	-1.21e2	109.206
Rot.Y	-2.06e0	109.865	-2.17e1	243.357	-5.44e1	662.227	-4.92e1	-1504.695
Rot.Z	5.19e0	97.720	6.91e1	136.845	1.27e2	135.098	7.98e1	74.851

Ratio = (ASM/FD) $\times$ 100%

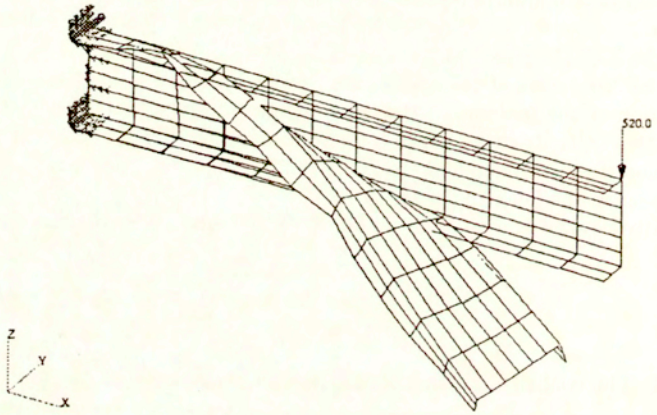

Fig.3.13 Thin-walled C-profile under a point load. Geometry and load.

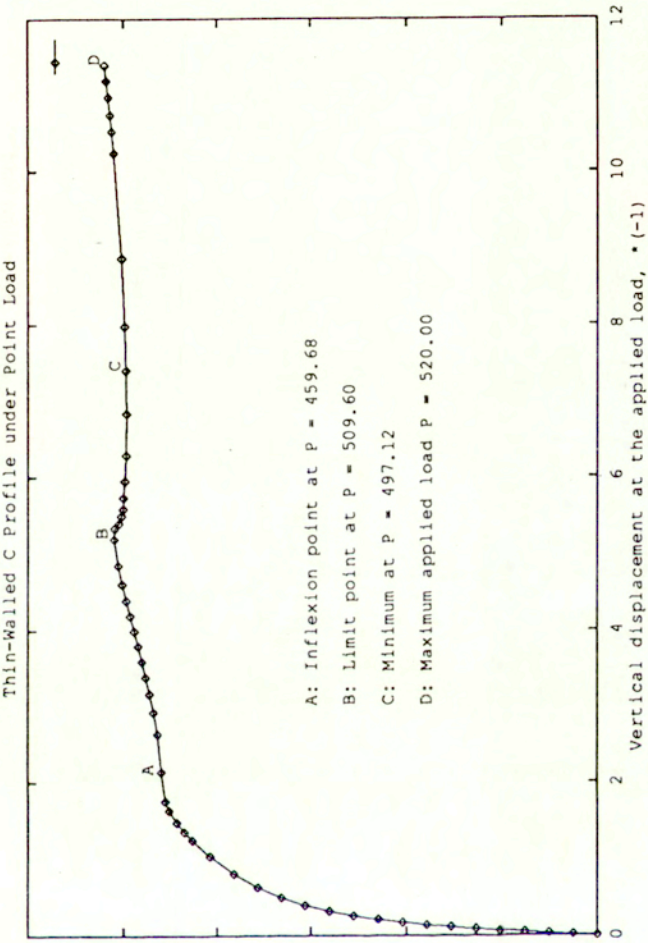

Fig.3.14a Thin-walled C-profile under a point load. Z-displacement at the applied load.

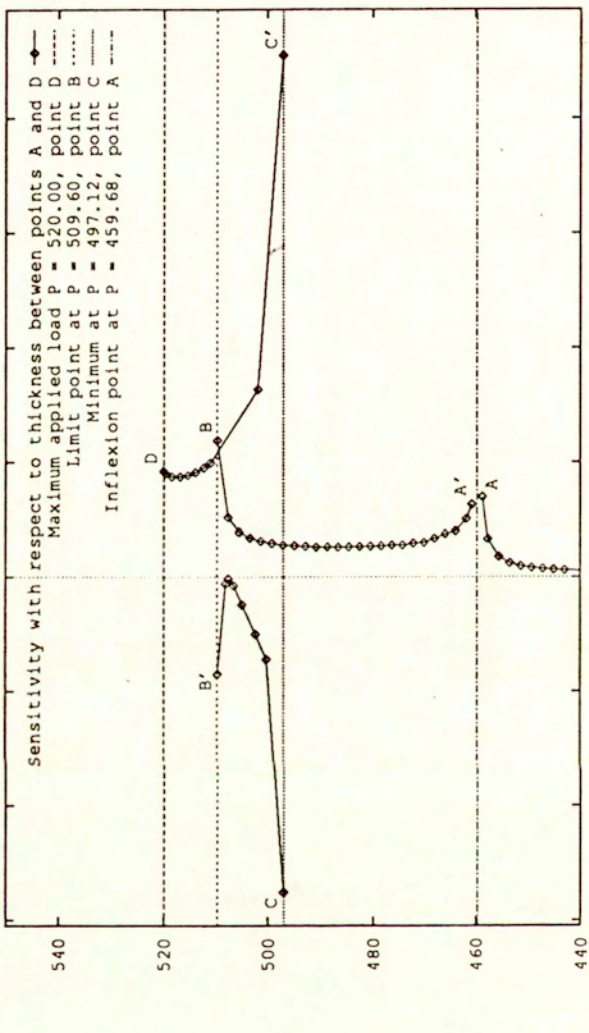

Fig.3.14b Thin-walled C-profile under a point load.
Sensitivity to thickness of Z-displacement at the applied load.

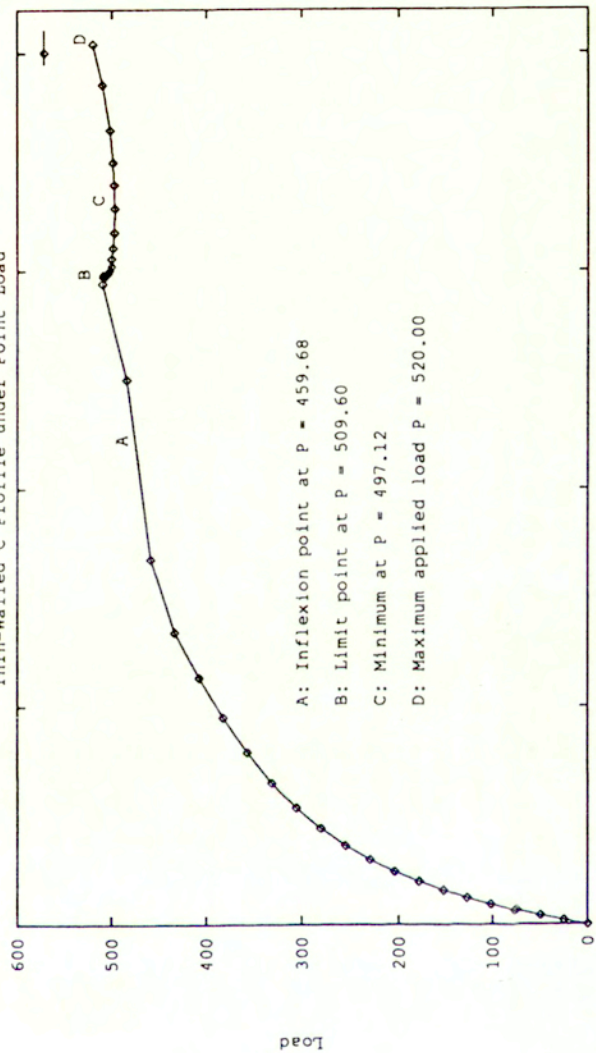

Fig.3.15a Thin-walled C-profile under a point load. X-rotation at the point load.

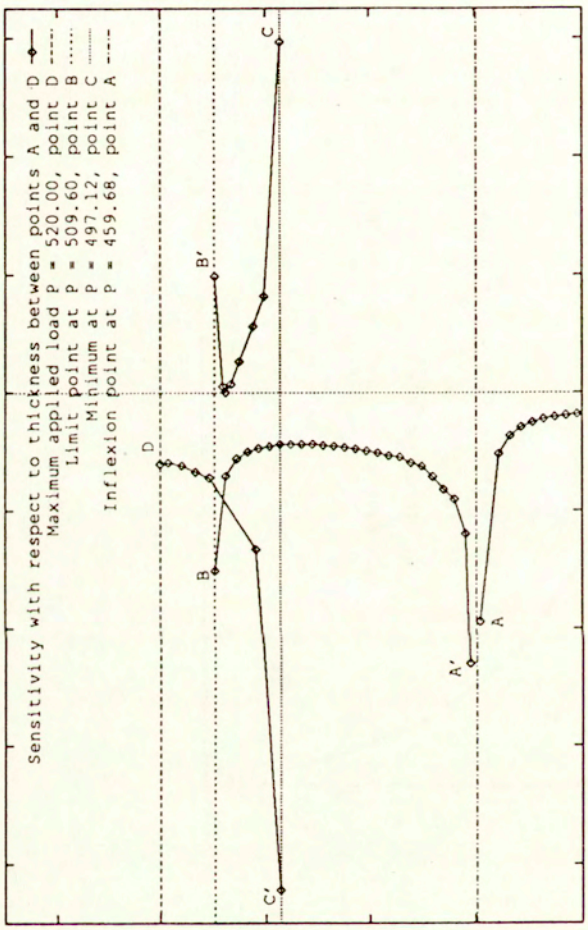

Fig.3.15b Thin-walled C-profile under a point load.
Sensitivity to thickness of X-rotation at the point load.

Example 4. Fuel tank

The tank consists of the following parts, see Fig.3.16,
-a cylinder of radius $R = 1515mm$, hight $H_1 = 1921mm$, thickness $h_1 = 10mm$,
-a skirt of hight $H_2 = 228mm$, thickness $h_2 = 12mm$, and
-a dome of hight $H_3 = 849m$, thickness $h_3 = 7mm$.
The material properties are as follows: the Young modulus $E = 2.1\ 10^5 Nmm^2$, the Poisson ratio $\nu = 0.3$. The external load consists of the inner pressure and three point loads. The inner pressure in the tank is equal to $p = 5.7MPa$, and its value remains constant. The point loads are gradually increased, with the reference value of the central force $P_1 = 3300kN$ and the side forces $P_2 = P_3 = 1900kN$.

The tank is modeled by 1512 shell elements, 1476 four-node quadrilaterals and 36 triangles. The model consists of 1621 nodes with 6 dofs per node. At the lower edge of the cylinder all dofs are constrained. A nonlinear static analysis is performed, and the obtained Von Misses stress for the load multiplier equal to 0.75 are shown in Fig.3.16.

The thickness of particular parts of the tank is the design parameter. A comparison is made between the sensitivities calculated by the ASM and the FDM, see Table 3.4, for the load multiplier equal to 0.75.

Table 3.4. Fuel tank. Sensitivity ratios: ASM FD $\times$ 100%

Node	Performance	Design parameter		
		h_1	h_2	h_3
1	Vertical displ.	99.252	101.805	102.564
	Radial displ.	87.065	102.062	104.356
	Rotation	114.385	101.669	103.976
2	Vertical displ.	101.702	100.870	101.172
	Radial displ.	101.831	101.323	102.123
	Rotation	101.584	100.247	101.532

Node 1: at middle of hight of cylinder, Node 2: at top of skirt

The nonlinear equilibrium paths and the corresponding sensitivity charts for displacements and rotations are presented as follows:
-the vertical displacement at Node 1 and its sensitivity to the cylinder thickness in Fig.3.17a and b,
-the radial displacement at Node 1 and its sensitivity to the cylinder, skirt and dome thicknesses in Fig.3.18a and b,
-the horizontal rotation at Node 2 and its sensitivity to the skirt thickness in Fig.3.19a and b.
Node 1 is located at the middle of the hight of the cylinder, while Node 2 at the top of the skirt, both in the plane of symmetry. Note that there are 2 asymptotic lines on the sensitivity charts, which correspond with the maximum point A and the minimum point B on the equilibrium paths. Points A, A', B, B' on the sensitivity charts are closest to the asymptotes.

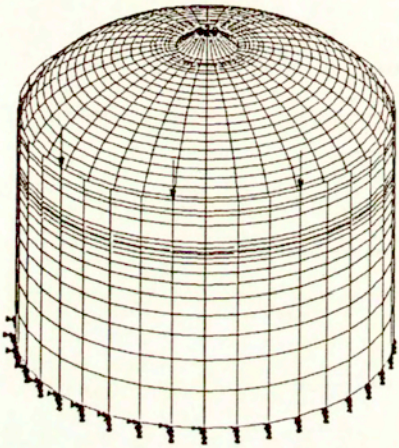

Fig.3.16 Fuel tank. Geometry and load.

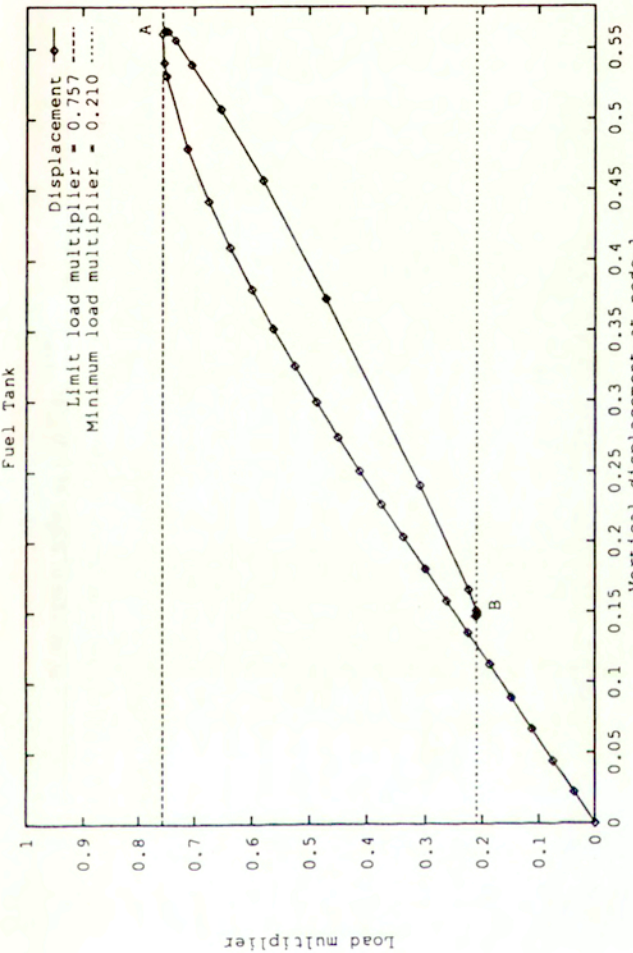

Fig.3.17a Fuel tank. Vertical displacement at middle of hight of cylinder.

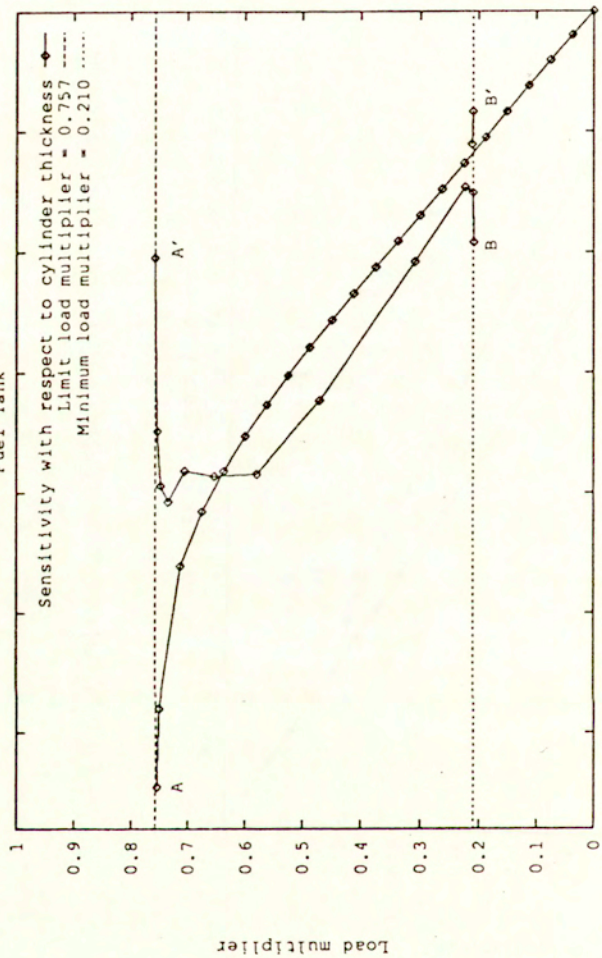

Fig.3.17b Fuel tank. Sensitivity to cylinder thickness of vertical displacement at middle of hight of cylinder.

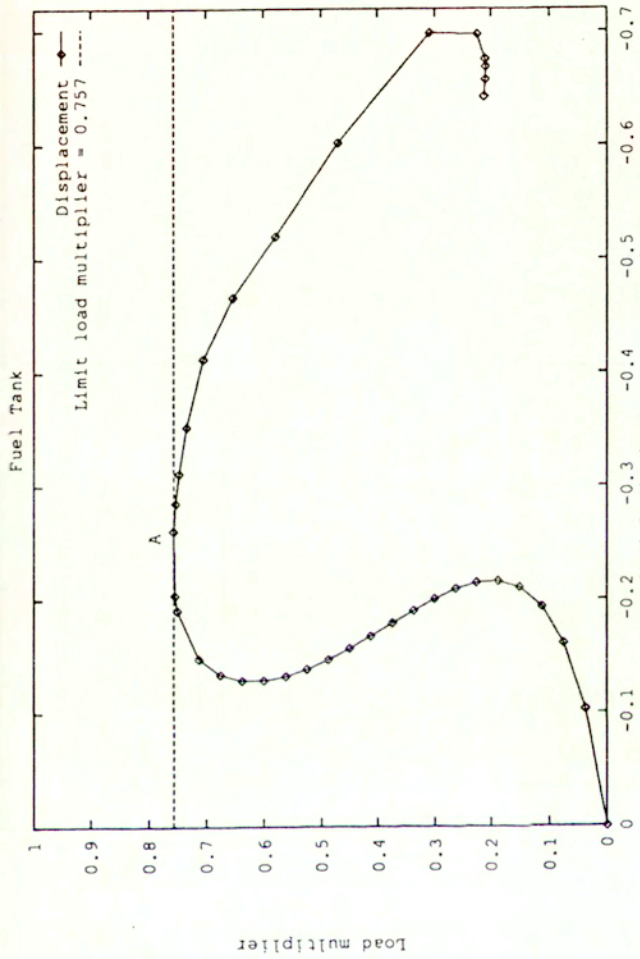

Fig.3.18a Fuel tank. Radial displacement at middle of hight of cylinder.

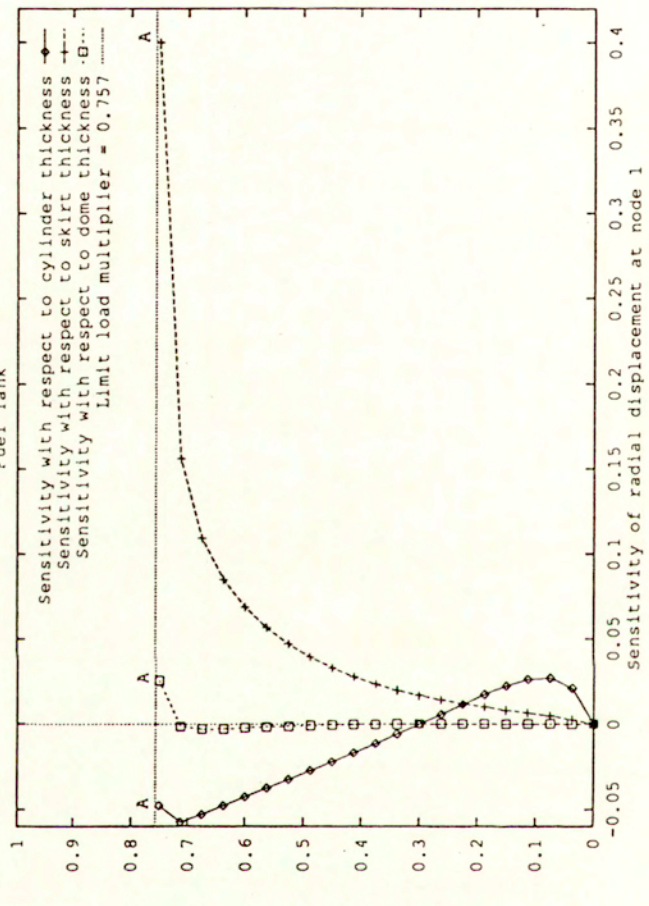

Fig.3.18b Fuel tank. Sensitivity to the cylinder, skirt and dome thickness of radial displacement at the middle of hight of cylinder.

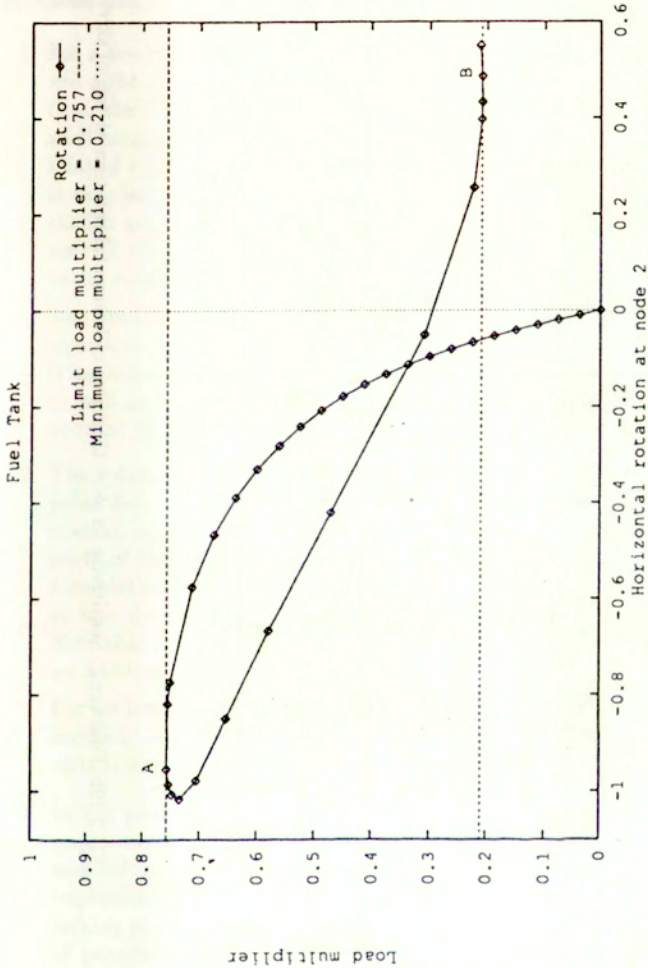

Fig.3.19a Fuel tank. Horizontal rotation at the top of skirt.

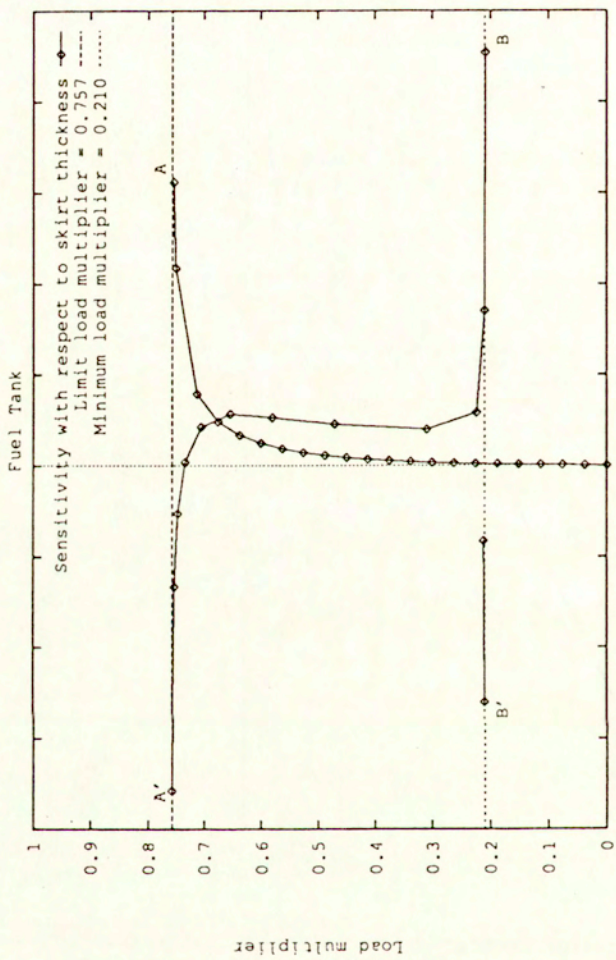

Fig.3.19b Fuel tank. Sensitivity to skirt thickness of horizontal rotation at top of skirt.

3.9 Conclusions

Summarizing, we can say that the derived variant of shell equations consistently incorporates rotations as the independent variable, and the drilling rotation is naturally included. The obtained strain measures have a relatively simple form due to the use of the Reissner hypothesis and the right stretch strain explicitly involves the rotation tensor.

1. For a linear approximation of the deformation and constant of rotations, the relaxed right stretch strain is a polynomial of the thickness coordinate two ranks lower than the Green strain. In consequence, specification of shell strain measures and shell constitutive equations is more convenient within the present formulation. The relaxed right stretch strain is always symmetric, and when the rotation constraint is satisfied it yields the true measure. For the Reissner kinematics, the membrane strains are exact, and therefore can be even finite, while the transverse shear and normal strain are approximate. The drilling rotation is strongly linked with membrane strain components.

   The linear approximation of the right stretch strain allows to derive the constitutive equations for the shell without approximating the strain energy and without specifying kinematics. The shell constitutive equations are found for a linear material, as well as for a second order Mooney-Rivlin incompressible material, and they also account for the normal transverse strain.

2. The rotation constraint in the three-dimensional theory ensures satisfaction of the polar decomposition theorem. For shells, this constraint is the subject of approximation, what causes difficulties, as then one rotation tensor must symmetrize both parts of the deformation gradient, what can be a contradictory task. The present formulation allows to enforce the part of the constraint for the dominant strain state, so also the bending-shearing states can be correctly modeled when they dominate. Note that a linear approximation of rotations would remedy the problem, but then an additional rotation variable would have to be accommodated.

   For an isotropic material the rotation constraint is enforced on use of the penalty method, but this should not corrupt rotations, because they appear also in the virtual work of stress and couple resultants.

3. In the presentation of numerical examples two questions have been exposed: the implementation of the membrane part of the element with the drilling rotation, and calculation of the design derivatives for rotational degrees of freedom. The implementation of the element with the drilling rotation requires eliminating of the locking phenomena and, in case of the reduced integration, an advanced stabilization of parasitic (zero-energy) modes. It has been shown that the design sensitivity analysis for the finite rotation shell equations can be conveniently implemented using the continuum Adjoint System Method. As indicate tests of our element with the drilling rotation, the developed formulation based on the relaxed right stretch strain provides a strong coupling between displacements and the drilling rotation, and if the locking is removed then correct sensitivities of the drilling rotation are obtained.

4 Extensible director beam equations and models of multi-layer beams

4.1 Theory of a finite rotation/extensible director beam

The beam equations including finite rotations have been proposed by a number of authors, and here we only mention some of them. One of the most often cited classical papers is by [Reissner, 1972], which developed the equations for the inextensible director beam using the right-stretch strain. In the most recent papers, typically, the equations are supplemented by the finite element models and the algorithmic questions related to finite rotations are addressed. The equations based on the Reissner hypothesis and the right-stretch strain were subsequently extended to include dynamical effects in [Simo, Vu-Quoc, 1986 a,b] and [Cardona, Geradin, 1988]. Besides, [Dvorkin, Onate, Oliver, 1988] exploited the Reissner hypothesis within a formulation based on the Green strain. [Crisfield, 1990] developed a co-rotational formulation, with non-linearity introduced via the rotation of the frame, and obtained equations which are similar to those for the Kirchhoff hypothesis.

The equations obtained in the aforementioned papers are unsuitable for use in the multi-layer finite rotation models, because they assume inextensibility of the director. Therefore, in [Wisniewski, 1996b], an additional scalar parameter for transverse extension (or the thickness changes) is introduced, and the beam equations for the so generalized Reissner hypothesis are derived. The generalized Reissner hypothesis has already been used in the literature, and a short list of the related papers, mostly for shells, is given in Section 1.4. In the approach developed in [Wisniewski, 1996b] and presented below the beam strain and change of curvature measures are obtained from the right stretch strain, and the virtual work is given for back-rotated (Biot-type) stress and couple resultants. The strain energy for the 1st order isotropic elastic material is assumed in terms of the right stretch strain, and constitutive equations for the beam stress and couple resultants are derived.

4.1.1 Kinematics of a beam with an extensible director

Consider the deformation of a beam as a one-to-one mapping, $\chi : B \to B_\chi$, where B is the beam reference, and B_χ the beam current configuration. The generalized Reissner hypothesis, admitting extension of the director of the beam, can be defined as such $\chi : \mathbf{y}(S,\zeta) \to \mathbf{x}(S,\zeta)$, where

$$\mathbf{y}(S,\zeta) = \mathbf{y}_0(S) + \zeta \mathbf{t}_3(S), \qquad \mathbf{x}(S,\zeta) = \mathbf{x}_0(S) + \zeta \mathbf{d}(S) \tag{4.1}$$

for $\mathbf{y} \in B$, $\mathbf{x} \in B_\chi$. The vector $\mathbf{t}_3$ is a director in the undeformed configuration, see Fig.4.1. The director in the deformed configuration is defined as

$$\mathbf{d}(S) = \lambda(S)\ \mathbf{a}_3(S), \qquad \mathbf{a}_3(S) = \mathbf{R}(S)\ \mathbf{t}_3(S) \tag{4.2}$$

and depends on the extension coefficient $\lambda = \|\mathbf{d}\|$. In the above, S is the arc-length coordinate of the middle line in the initial configuration, and the thickness coordinate

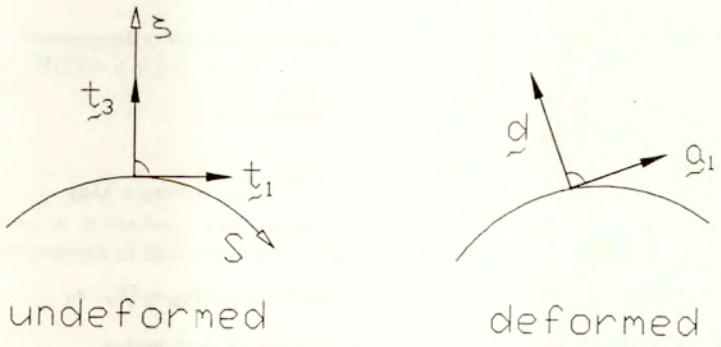

Fig.4.1 Local bases of beam. Vector $\mathbf{a}_1$ is not tangent to deformed middle line.

$\frac{h}{2} \leq \zeta \leq +\frac{h}{2}$. In the sequel the dependence on S is not indicated. For the displacement defined as $\mathbf{u} = \mathbf{x} - \mathbf{y}$, the above hypothesis yields

$$\mathbf{u}(\zeta) = \mathbf{u}_0 + \zeta\,[\lambda \mathbf{a}_3 - \mathbf{t}_3] = \mathbf{u}_0 + \zeta\,[\lambda \mathbf{R} - \mathbf{I}]\,\mathbf{t}_3 \tag{4.3}$$

where $\mathbf{u}_0 = \mathbf{x}_0 - \mathbf{y}_0$. Note that $\mathbf{u} = \mathbf{u}(\mathbf{u}_0, \lambda, \mathbf{R})$, and is a linear function of ζ. Let us assume that the geometry of a beam satisfies the condition $h/R \ll 1$, where h is the thickness, and R is the radius of curvature of the beam. For the assumed geometry and the generalized Reissner kinematics the deformation gradient is as follows

$$\mathbf{F}(\zeta) = \frac{\partial \mathbf{x}}{\partial \mathbf{y}} = \mathbf{x}_{,S} \otimes \mathbf{t}_1 + \mathbf{x}_{,\zeta} \otimes \mathbf{t}_3 \tag{4.4}$$

where

$$\mathbf{x}_{,S} = \mathbf{x}_{0,S} + \zeta(\lambda_{,S}\mathbf{a}_3 + \lambda \mathbf{a}_{3,S}), \qquad \mathbf{x}_{,\zeta} = \lambda \mathbf{a}_3$$

Note that $\mathbf{a}_3 = \mathbf{R}\mathbf{t}_3 = \mathbf{R}\mathbf{R}_0\mathbf{i}_3$, where $\mathbf{R}_0$ is the rotation tensor describing the position of $\mathbf{t}_3$. Then, the derivative $\mathbf{a}_{3,S}$ can be expressed in terms of a skew-symmetric tensor (and its axial vector) as given below

$$\mathbf{a}_{3,S} = \bar{\boldsymbol{\Omega}}\mathbf{a}_3 = \bar{\boldsymbol{\omega}} \times \mathbf{a}_3 \tag{4.5}$$

where

$$\begin{aligned} &\bar{\boldsymbol{\Omega}} = \boldsymbol{\Omega} + \mathbf{R}\boldsymbol{\Omega}_0\mathbf{R}^T\,, && \bar{\boldsymbol{\omega}} = \boldsymbol{\omega} + \mathbf{R}\boldsymbol{\omega}_0 \\ &\boldsymbol{\Omega} = \mathbf{R}_{,S}\mathbf{R}^T\,, && \boldsymbol{\Omega}\mathbf{a}_3 = \boldsymbol{\omega} \times \mathbf{a}_3 \\ &\boldsymbol{\Omega}_0 = \mathbf{R}_{0,S}\mathbf{R}_0^T\,, && \boldsymbol{\Omega}_0\mathbf{a}_3 = \boldsymbol{\omega}_0 \times \mathbf{a}_3 \end{aligned} \tag{4.6}$$

On use of the axial vector $\bar{\boldsymbol{\omega}}$ we obtain

$$\mathbf{F}(\zeta) = [\mathbf{x}_{0,S} + \lambda(\bar{\boldsymbol{\omega}} \times \zeta\mathbf{a}_3) + \lambda_{,S}\zeta\mathbf{a}_3] \otimes \mathbf{t}_1 + \lambda \mathbf{a}_3 \otimes \mathbf{t}_3 \tag{4.7}$$

The variation of the deformation gradient is as follows

$$\delta\mathbf{F}(\zeta) = \delta\mathbf{x}_{,S} \otimes \mathbf{t}_1 + \delta\mathbf{x}_{,\zeta} \otimes \mathbf{t}_3 \tag{4.8}$$

where

$$\delta\mathbf{x}_{,S} = \delta\mathbf{x}_{0,S} + \delta\left\{\lambda(\bar{\boldsymbol{\omega}} \times \zeta\mathbf{a}_3)\right\} + \delta(\lambda_{,S}\zeta\mathbf{a}_3), \qquad \delta\mathbf{x}_{,\zeta} = \delta\lambda\mathbf{a}_3 + \lambda\delta\mathbf{a}_3$$

Additionally, we may exploit

$$\delta\bar{\boldsymbol{\omega}} = \delta\boldsymbol{\theta}_{,S} + \delta\boldsymbol{\theta} \times \bar{\boldsymbol{\omega}}, \qquad \delta\mathbf{a}_3 = \delta\mathbf{R}\mathbf{t}_3 = \delta\mathbf{R}\mathbf{R}^T\mathbf{a}_3 = \delta\tilde{\boldsymbol{\theta}}\mathbf{a}_3 = \delta\boldsymbol{\theta} \times \mathbf{a}_3$$

where $\delta\tilde{\boldsymbol{\theta}}$ is a left skew-symmetric tensor, and $\delta\boldsymbol{\theta}$ denotes its axial vector.

Finally, we address the question of composition and parametrization of the extension coefficient λ. As an example we consider the stretching of the middle line of a straight beam in the direction $\mathbf{t}_1$, only. Then, $\mathbf{a}_3 = \mathbf{t}_3$, and the gradient of deformation and its increment are as follows

$$\bar{\mathbf{F}} = \bar{\mathbf{x}}_{0,S} \otimes \mathbf{t}_1 + \bar{\lambda}\mathbf{t}_3 \otimes \mathbf{t}_3, \qquad \Delta\mathbf{F} = \Delta\mathbf{x}_{0,S} \otimes \mathbf{t}_1 + \Delta\lambda\mathbf{t}_3 \otimes \mathbf{t}_3 \tag{4.9}$$

where the bar indicates the known values. A multiplicative composition of the deformation gradients yields

$$\mathbf{F} = \Delta\mathbf{F}\bar{\mathbf{F}} = (\Delta\mathbf{x}_{0,S} \otimes \bar{\mathbf{x}}_{0,S})\mathbf{t}_1 \otimes \mathbf{t}_1 + \Delta\lambda\bar{\lambda}\mathbf{t}_3 \otimes \mathbf{t}_3 \tag{4.10}$$

and we may establish

$$\mathbf{x}_{0,S} = (\Delta\mathbf{x}_{0,S} \otimes \bar{\mathbf{x}}_{0,S})\mathbf{t}_1, \qquad \lambda = \Delta\lambda\bar{\lambda} \tag{4.11}$$

where the extension coefficient composes multiplicatively. To obtain a description with an additive composition, which is standard in numerical implementations, the so called exponential parametrization, $\lambda = \exp(\mu)$, is introduced, see also e.g. [Green, Naghdi, Wenner, 1971], [Simo, Rifai, Fox, 1990]. Then, for $\bar{\lambda} = \exp(\bar{\mu})$ and $\Delta\lambda = \exp(\Delta\mu)$ we obtain

$$\lambda = \Delta\lambda\bar{\lambda} = \exp(\Delta\mu)\exp(\bar{\mu}) = \exp(\Delta\mu + \bar{\mu}) \tag{4.12}$$

as desired.

4.1.2 Strain measures

Define the right stretch strain tensor as $\mathbf{H} \equiv \mathrm{sym}(\mathbf{R}^T\mathbf{F}) - \mathbf{I}$, where $\mathbf{R}$ satisfies the rotation constraint, obtained from the polar decomposition of the deformation gradient. For the expanded form of the gradient of deformation, eq.(4), on use of the relations introduced in the previous section we have

$$\mathbf{R}^T\mathbf{F} = \left[(\mathbf{R}^T\mathbf{x}_{0,S}) \otimes \mathbf{t}_1 + \lambda\mathbf{t}_3 \otimes \mathbf{t}_3\right] + \zeta\left[\lambda\mathbf{R}^T\mathbf{a}_{3,S} + \lambda_{,S}\mathbf{t}_3\right] \otimes \mathbf{t}_1 \tag{4.13}$$

Furthermore, the identity tensor can be expressed as $\mathbf{I} = \mathbf{t}_1 \otimes \mathbf{t}_1 + \mathbf{t}_3 \otimes \mathbf{t}_3 + \zeta\mathbf{t}_{3,S} \otimes \mathbf{t}_1$, see Section 3.4.

Subsequently, we separate the constant and linear terms in the right stretch strain, i.e. $\mathbf{H}(\zeta) = \boldsymbol{\varepsilon} + \zeta\boldsymbol{\kappa}$, where

$$\begin{cases} \boldsymbol{\varepsilon} = \mathrm{sym}(\mathbf{R}^T\mathbf{x}_{0,S} - \mathbf{t}_1) \otimes \mathbf{t}_1 + (\lambda - 1)\mathbf{t}_3 \otimes \mathbf{t}_3 \\ \boldsymbol{\kappa} = \mathrm{sym}\left[\mathbf{R}^T(\lambda\mathbf{a}_3)_{,S} - \mathbf{t}_{3,S}\right] \otimes \mathbf{t}_1 \end{cases} \tag{4.14}$$

Here, $\boldsymbol{\varepsilon}$ is the beam strain measure, and $\boldsymbol{\kappa}$ is the beam change of curvature measure. Components of these measures in the basis $\{\mathbf{t}_i\}$ are as follows

$$\varepsilon_{11} = \mathbf{x}_{0,S} \cdot \mathbf{a}_1 - 1, \qquad 2\varepsilon_{13} = \mathbf{x}_{0,S} \cdot \mathbf{a}_3, \qquad \varepsilon_{33} = \lambda - 1 \tag{4.15}$$

$$\kappa_{11} = [\lambda\boldsymbol{\omega} + (\lambda - 1)\boldsymbol{\omega}_0] \cdot \mathbf{t}_2, \qquad 2\kappa_{13} = \lambda_{,S}, \qquad \kappa_{33} = 0 \tag{4.16}$$

where the axial vectors $\boldsymbol{\omega}$ and $\boldsymbol{\omega}_0$ are defined in eq.(6). Note that the assumption that the extension coefficient λ is constant over the thickness results in the normal component $\kappa_{33} = 0$. This component can be recovered on use of the auxiliary equation as described in Section 4.1.5. For a straight inextensible director beam, when $\boldsymbol{\omega}_0 = 0$ and $\lambda = 1$, these measures are

$$\varepsilon_{11} = \mathbf{x}_{0,S} \cdot \mathbf{a}_1 - 1, \qquad 2\varepsilon_{13} = \mathbf{x}_{0,S} \cdot \mathbf{a}_3, \qquad \kappa_{11} = \boldsymbol{\omega} \cdot \mathbf{t}_2 \tag{4.17}$$

while $\varepsilon_{33}, \kappa_{13}, \kappa_{33}$ are equal to zero. It can be shown that these simplified measures are equivalent to those given in [Reissner, 1972]. To facilitate the derivation of the virtual work equation in the subsequent section we define strain vectors,

$$\boldsymbol{\varepsilon}_1 \equiv \mathbf{R}^T\mathbf{x}_{0,S} - \mathbf{t}_1, \qquad \boldsymbol{\varepsilon}_3 \equiv (\lambda - 1)\mathbf{t}_3, \qquad \boldsymbol{\kappa}_1 \equiv \lambda_{,S}\mathbf{t}_3 + \bar{\boldsymbol{\kappa}}_1 \times \mathbf{t}_3 - \mathbf{t}_{3,S} \tag{4.18}$$

where $\bar{\boldsymbol{\kappa}}_1 \equiv \lambda\mathbf{R}^T\bar{\boldsymbol{\omega}}$, for which eq.(14) can be written as

$$\boldsymbol{\varepsilon} = \boldsymbol{\varepsilon}_1 \otimes \mathbf{t}_1 + \boldsymbol{\varepsilon}_3 \otimes \mathbf{t}_3, \qquad \boldsymbol{\kappa} = \boldsymbol{\kappa}_1 \otimes \mathbf{t}_1 \tag{4.19}$$

Note that $2\varepsilon_{13} = \boldsymbol{\varepsilon}_1 \cdot \mathbf{t}_3$ but not $\boldsymbol{\varepsilon}_3 \cdot \mathbf{t}_1$.

For a rotation around $\mathbf{t}_2$ and a straight beam we have $\bar{\boldsymbol{\Omega}} = \boldsymbol{\Omega} = \mathbf{R}_{,S}\mathbf{R}^T = \beta_{,S}(\mathbf{t}_3 \otimes \mathbf{t}_1 - \mathbf{t}_1 \otimes \mathbf{t}_3)$ and $\mathbf{R}^T\bar{\boldsymbol{\omega}} = -\beta_{,S}\mathbf{t}_2$, where β is the rotation angle. In consequence, $\bar{\boldsymbol{\kappa}}_1 \times \mathbf{t}_3 = -\lambda\beta_{,S}\mathbf{t}_1$ yielding $\boldsymbol{\kappa}_1 = \lambda_{,S}\mathbf{t}_3 - \lambda\beta_{,S}\mathbf{t}_1 - \mathbf{t}_{3,S}$.

Variations of strain vectors (18) are as follows

$$\delta\boldsymbol{\varepsilon}_1 \equiv \delta\left(\mathbf{R}^T\mathbf{x}_{0,S}\right), \qquad \delta\boldsymbol{\varepsilon}_3 \equiv \delta\lambda\mathbf{t}_3, \qquad \delta\boldsymbol{\kappa}_1 \equiv \delta\lambda_{,S}\mathbf{t}_3 + \delta\bar{\boldsymbol{\kappa}}_1 \times \mathbf{t}_3 \tag{4.20}$$

where $\delta\bar{\boldsymbol{\kappa}}_1 = \delta(\lambda\mathbf{R}^T\bar{\boldsymbol{\omega}})$.

4.1.3 Virtual work of stresses

The virtual work of the 1st Piola-Kirchhoff stress can be written as $\delta\mathcal{W} = \int_B \mathbf{P} \cdot \delta\mathbf{F}\, dV$. Consider the integrand of the virtual work and transform it taking into account the kinematics defined in the previous section. Then, for the assumed geometry of the beam, we have $\mathbf{P} = \mathbf{p}_j \otimes \mathbf{t}_j$, and $\mathbf{F} = \mathbf{x}_j \otimes \mathbf{t}_j$, ($j = 1$ or 3), what yields

$$\mathbf{P} \cdot \delta\mathbf{F} = \mathbf{p}_1 \cdot \delta\mathbf{x}_{,S} + \mathbf{p}_3 \cdot \delta\mathbf{x}_{,\zeta} \tag{4.21}$$

The last component can be transformed with the help of eq.(8) as follows

$$\mathbf{p}_3 \cdot \delta\mathbf{x}_{,\zeta} = \delta\lambda(\mathbf{p}_3 \cdot \mathbf{a}_3) + \lambda(\mathbf{p}_3 \cdot \delta\mathbf{a}_3) \tag{4.22}$$

Furthermore,

$$\begin{aligned} \mathbf{p}_3 \cdot \delta\mathbf{a}_3 \; &= \mathbf{p}_3 \cdot (\delta\boldsymbol{\theta} \times \mathbf{a}_3) \overset{(A)}{=} \delta\boldsymbol{\theta} \cdot (\mathbf{a}_3 \times \mathbf{p}_3) \\ &\overset{(B)}{=} \delta\boldsymbol{\theta} \cdot (\tfrac{1}{\lambda}\mathbf{x}_{,\zeta} \times \mathbf{p}_3) \overset{(C)}{=} -\delta\boldsymbol{\theta} \cdot (\tfrac{1}{\lambda}\mathbf{x}_{,S} \times \mathbf{p}_1) \overset{(A)}{=} -\tfrac{1}{\lambda}\mathbf{p}_1 \cdot (\delta\boldsymbol{\theta} \times \mathbf{x}_{,S}) \end{aligned} \tag{4.23}$$

The identities used above are defined as follows: (A) $\mathbf{a} \cdot (\mathbf{b} \times \mathbf{c}) = \mathbf{b} \cdot (\mathbf{c} \times \mathbf{a})$, (B) $\mathbf{a}_3 = \frac{1}{\lambda}\mathbf{x}_{,\zeta}$, and (C) $\mathbf{x}_{,\zeta} \times \mathbf{p}_3 = -\mathbf{x}_{,S} \times \mathbf{p}_1$, which is yielded by the angular momentum balance, $\mathbf{F} \times \mathbf{P} = \mathbf{0}$. Making use of the above three formulas we write

$$\mathbf{P} \cdot \delta\mathbf{F} = \mathbf{p}_1 \cdot [\delta\mathbf{x}_{,S} - \delta\boldsymbol{\theta} \times \mathbf{x}_{,S}] + \mathbf{p}_3 \cdot (\delta\lambda\mathbf{a}_3) \tag{4.24}$$

Note that the component in brackets has a structure of the so called co-rotational variation, resulting from the rotate-back, take a variation and rotate-forward operations,

$$\overset{\circ}{\delta}\,\mathbf{v} \equiv \delta\mathbf{v} - \delta\boldsymbol{\theta} \times \mathbf{v} = \mathbf{R}\,\delta(\mathbf{R}^T\mathbf{v}) \tag{4.25}$$

for an arbitrary vector $\mathbf{v}$. Application of formula (4) for $\mathbf{x}_{,S}$ to the expression in the brackets yields

$$\delta\mathbf{x}_{,S} - \delta\boldsymbol{\theta} \times \mathbf{x}_{,S} = \mathbf{a} + \mathbf{b} + \mathbf{c} \tag{4.26}$$

where the auxiliary vectors are defined as follows

$$\mathbf{a} = \delta\mathbf{x}_{0,S} - \delta\boldsymbol{\theta} \times \mathbf{x}_{0,S}, \qquad \mathbf{b} = \delta\{\lambda(\bar{\boldsymbol{\omega}} \times \zeta\mathbf{a}_3)\} - \delta\boldsymbol{\theta} \times \lambda(\bar{\boldsymbol{\omega}} \times \zeta\mathbf{a}_3)$$

$$\mathbf{c} = \delta(\lambda_{,S}\zeta\mathbf{a}_3) - \delta\boldsymbol{\theta} \times (\lambda_{,S}\zeta\mathbf{a}_3)$$

and the co-rotational variations are easily identified. For $\mathbf{b}$ and $\mathbf{c}$ we obtain

$$\mathbf{p}_1 \cdot \mathbf{b} = \{\delta\lambda\bar{\boldsymbol{\omega}} + \lambda[\delta\bar{\boldsymbol{\omega}} - \delta\boldsymbol{\theta} \times \bar{\boldsymbol{\omega}}]\} \cdot (\mathbf{a}_3 \times \zeta\mathbf{p}_1), \qquad \mathbf{p}_1 \cdot \mathbf{c} = \zeta\delta\lambda_{,S}(\mathbf{p}_1 \cdot \mathbf{a}_3) \tag{4.27}$$

To evaluate the virtual work of stresses for the beam, $\delta\mathcal{W}_b \equiv \int_{-\frac{h}{2}}^{+\frac{h}{2}} \mathbf{P} \cdot \delta\mathbf{F}\, d\zeta$, we define the beam stress and couple resultant vectors as the integrals over the cross-section of the beam,

$$\mathbf{n}_1 \equiv \int_{-\frac{h}{2}}^{+\frac{h}{2}} \mathbf{p}_1(\zeta)d\zeta, \qquad \mathbf{n}_3 \equiv \int_{-\frac{h}{2}}^{+\frac{h}{2}} \mathbf{p}_3(\zeta)d\zeta, \qquad \mathbf{m}_1 \equiv \int_{-\frac{h}{2}}^{+\frac{h}{2}} \zeta\mathbf{p}_1(\zeta)d\zeta \tag{4.28}$$

Then, we calculate

$$\int_{-\frac{h}{2}}^{+\frac{h}{2}} \mathbf{p}_1 \cdot \mathbf{a}\, d\zeta = \mathbf{n}_1 \cdot [\delta\mathbf{x}_{0,S} - \delta\boldsymbol{\theta} \times \mathbf{x}_{0,S}] \tag{4.29}$$

$$\int_{-\frac{h}{2}}^{+\frac{h}{2}} \mathbf{p}_1 \cdot \mathbf{b}\, d\zeta = (\mathbf{a}_3 \times \mathbf{m}_1) \cdot \{\delta\lambda\bar{\boldsymbol{\omega}} + \lambda[\delta\bar{\boldsymbol{\omega}} - \delta\boldsymbol{\theta} \times \bar{\boldsymbol{\omega}}]\} \tag{4.30}$$

$$\int_{-\frac{h}{2}}^{+\frac{h}{2}} \mathbf{p}_1 \cdot \mathbf{c}\, d\zeta = 0 \tag{4.31}$$

For the term of (24) with $\mathbf{p}_3$ we obtain

$$\int_{-\frac{h}{2}}^{+\frac{h}{2}} \mathbf{p}_3 \cdot (\delta\lambda \mathbf{a}_3)\, d\zeta = \mathbf{n}_3 \cdot \mathbf{a}_3\, \delta\lambda \tag{4.32}$$

The above terms yield the beam virtual work of stress and couple resultants which has the following form

$$\delta\mathcal{W}_b = \mathbf{n}_1 \cdot \{\mathbf{R}\delta(\mathbf{R}^T\mathbf{x}_{0,S})\} + \mathbf{n}_3 \cdot \{\mathbf{R}\delta\lambda\mathbf{t}_3\} + (\mathbf{a}_3 \times \mathbf{m}_1) \cdot \left\{\mathbf{R}\delta(\lambda\mathbf{R}^T\bar{\boldsymbol{\omega}})\right\} \tag{4.33}$$

Note that for a back-rotated stress, $\mathbf{T}^B \equiv \mathbf{R}^T\mathbf{P}$, we have, in terms of the stress vectors, $\mathbf{t}_j^B = \mathbf{R}^T\mathbf{p}_j$. Let us define the stress and couple resultant vectors corresponding to the back-rotated stress as follows

$$\mathbf{n}_1^B \equiv \int_{-\frac{h}{2}}^{+\frac{h}{2}} \mathbf{t}_1^B(\zeta)\, d\zeta, \qquad \mathbf{n}_3^B \equiv \int_{-\frac{h}{2}}^{+\frac{h}{2}} \mathbf{t}_3^B(\zeta)\, d\zeta, \qquad \mathbf{m}_1^B \equiv \int_{-\frac{h}{2}}^{+\frac{h}{2}} \zeta\, \mathbf{t}_1^B(\zeta)\, d\zeta \tag{4.34}$$

Then, comparing with definitions (28), we have $\mathbf{n}_1^B = \mathbf{R}^T\mathbf{n}_1$, $\mathbf{n}_3^B = \mathbf{R}^T\mathbf{n}_3$ and $\mathbf{m}_1^B = \mathbf{R}^T\mathbf{m}_1$. On use of these relations in eq.(33) we obtain

$$\delta\mathcal{W}_b = \mathbf{n}_1^B \cdot \delta(\mathbf{R}^T\mathbf{x}_{0,S}) + \mathbf{n}_3^B \cdot \delta(\lambda\mathbf{t}_3) + \mathbf{m}_1^B \cdot [\delta(\lambda\mathbf{R}^T\bar{\boldsymbol{\omega}}) \times \mathbf{t}_3] \tag{4.35}$$

This equation can be re-written as

$$\delta\mathcal{W}_b = \mathbf{n}_1^B \cdot \delta\boldsymbol{\varepsilon}_1 + \mathbf{n}_3^B \cdot \delta\boldsymbol{\varepsilon}_3 + \mathbf{m}_1^B \cdot [\delta\bar{\boldsymbol{\kappa}}_1 \times \mathbf{t}_3] \tag{4.36}$$

where $\boldsymbol{\varepsilon}_1$, $\boldsymbol{\varepsilon}_3$ and $\bar{\boldsymbol{\kappa}}_1$ are strain and change of curvature vectors, the variations of which are defined in the preceding section by eq.(20). Recall the definition of $\delta\boldsymbol{\kappa}$, and note that only the part $\delta\bar{\boldsymbol{\kappa}}_1 \times \mathbf{t}_3$ is retained, while $\delta\lambda_{,S}\mathbf{t}_3$ vanishes due to integration over the thickness. As $\lambda_{,S} = 2\kappa_{13}$, see eq.(16), hence we conclude that this strain component does not contribute to the virtual work of stress.

4.1.4 Virtual work of external forces

Let us define the virtual work of external forces acting on the upper and a lower surface (or a line) bounding the beam as follows

$$\delta\mathcal{A}_b = \hat{\mathbf{p}}_3^+ \cdot \delta\mathbf{x}^+ + \hat{\mathbf{p}}_3^- \cdot \delta\mathbf{x}^- \tag{4.37}$$

We assume that the orientation of both bounding surfaces is defined by $\mathbf{a}_3$, and the vector $\hat{\mathbf{p}}_3$ denotes the external force. The superscript "+" indicates values for the upper surface (line) at $\zeta = +\frac{h}{2}$, and "−" indicates values for the lower surface (line) at $\zeta = -\frac{h}{2}$. For the kinematics with the extensible director we have $\mathbf{x} = \mathbf{x}_0 + \zeta\lambda\mathbf{a}_3$, and its variation is as follows

$$\delta\mathbf{x} = \delta\mathbf{x}_0 + \delta\lambda(\zeta\mathbf{a}_3) + \lambda(\delta\boldsymbol{\theta} \times \zeta\mathbf{a}_3) \tag{4.38}$$

On use of the above expression with appropriate values of ζ in eq.(37) we obtain

$$\delta\mathcal{A}_b = \hat{\mathbf{p}} \cdot \delta\mathbf{x}_0 + \hat{q}\,\delta\lambda + \hat{\mathbf{m}} \cdot \delta\boldsymbol{\theta} \tag{4.39}$$

where the external forces and moments for the beam are defined as follows

$$\hat{\mathbf{p}} \equiv \hat{\mathbf{p}}_3^+ + \hat{\mathbf{p}}_3^-, \qquad \hat{q} \equiv \frac{h}{2}\mathbf{a}_3 \cdot (\hat{\mathbf{p}}_3^+ - \hat{\mathbf{p}}_3^-), \qquad \hat{\mathbf{m}} \equiv \frac{h}{2}\lambda\, \mathbf{a}_3 \times (\hat{\mathbf{p}}_3^+ - \hat{\mathbf{p}}_3^-) \quad (4.40)$$

Note the presence of the term $\hat{q}\ \delta\lambda$, which is characteristic for the theory with an extensible director, where $\hat{q}$ depends on the component of $(\hat{\mathbf{p}}_3^+ - \hat{\mathbf{p}}_3^-)$ in the direction $\mathbf{a}_3$.

The virtual work of the body force is defined as $\int_{-\frac{h}{2}}^{+\frac{h}{2}} \rho_R \mathbf{b} \cdot \delta\mathbf{x}\, d\zeta$. On use of $\delta\mathbf{x}(\zeta) = \delta\mathbf{x}_0 + \zeta\delta\mathbf{d}$, and integration over the thickness we obtain

$$\delta\mathcal{A}_{bf} = \int_{-\frac{h}{2}}^{+\frac{h}{2}} \rho_R \mathbf{b} \cdot \delta\mathbf{x}\, d\zeta = \rho_R h\ \mathbf{b} \cdot \delta\mathbf{x}_0 \quad (4.41)$$

4.1.5 Constitutive equations for beam stress and couple resultants

Consider the standard form of the strain energy function for the 1st order isotropic elastic material expressed in terms of the right stretch strain $\mathbf{H}$,

$$\mathcal{W}(\mathbf{H}) = \frac{1}{2} l\ (\mathrm{tr}\mathbf{H})^2 + \mathrm{G}\ \mathrm{tr}\mathbf{H}^2 \quad (4.42)$$

where l and G are Lamé constants. Note that traditionally, in place of l, the symbol λ is used, which here is associated with the extension coefficient. The strain energy function is given per unit volume of the initial configuration.

Below, we derive a constitutive equation for the strain assumed as a linear polynomial of the thickness coordinate ζ, i.e. as $\mathbf{H} = \boldsymbol{\varepsilon} + \zeta\boldsymbol{\kappa}$, where $\boldsymbol{\varepsilon}$ and $\boldsymbol{\kappa}$ are symmetric tensors. Note that all the components of the strains (14) can be used here, except κ_{33}, which is equal to zero, and must be recovered.

Integration of the strain energy over the thickness yields, after some rearrangements,

$$\Sigma = \int_{-\frac{h}{2}}^{+\frac{h}{2}} \mathcal{W}(\mathbf{H})\ m d\zeta = h\ \mathcal{W}(\boldsymbol{\varepsilon}) + \frac{h^3}{12}\ \mathcal{W}(\boldsymbol{\kappa}) \quad (4.43)$$

where $m \approx 1$ is a determinant of the translation (shifter) tensor. A kinematically admissible variation of the beam strain energy is: $\delta\Sigma = h\ \delta\mathcal{W}(\boldsymbol{\varepsilon}) + \frac{h^3}{12}\ \delta\mathcal{W}(\boldsymbol{\kappa})$, and can be concisely written as $\delta\Sigma = \mathbf{n}^B \cdot \delta\boldsymbol{\varepsilon} + \mathbf{m}^B \cdot \delta\boldsymbol{\kappa}$, for the back-rotated stress and couple resultants of the beam defined as follows

$$\mathbf{n}^B \equiv h\ \frac{d\mathcal{W}(\boldsymbol{\varepsilon})}{d\boldsymbol{\varepsilon}}, \qquad \mathbf{m}^B \equiv \frac{h^3}{12}\ \frac{d\mathcal{W}(\boldsymbol{\kappa})}{d\boldsymbol{\kappa}} \quad (4.44)$$

Differentiation yields the constitutive equations for the stress and couple resultants,

$$\mathbf{n}^B = h\ [l\ (\mathrm{tr}\boldsymbol{\varepsilon})\mathbf{I} + 2\mathrm{G}\boldsymbol{\varepsilon}], \qquad \mathbf{m}^B = \frac{h^3}{12}\ [l\ (\mathrm{tr}\boldsymbol{\kappa})\mathbf{I} + 2\mathrm{G}\boldsymbol{\kappa}] \quad (4.45)$$

The three-dimensional formulation can be reduced to two dimensions by setting $\varepsilon_{12} = 0$, $\varepsilon_{23} = 0$, and $n_{12}^B = 0$, $n_{23}^B = 0$. Then, the constitutive equation is written only for

the components $\{11, 22, 33, 13\}$. Imposing the plane stress condition $n^B_{22} = 0$ and eliminating ε_{22} we obtain the following constitutive equation,

$$\mathbf{n}^B = \overset{4}{\mathbf{C}} : \boldsymbol{\varepsilon}, \qquad \overset{4}{\mathbf{C}} = \frac{2lG}{l+2G}\,\mathbf{1}\otimes\mathbf{1} + 2G\,\overset{4}{\mathbf{I}} \tag{4.46}$$

where $\boldsymbol{\varepsilon} = \{\varepsilon_{11}, \varepsilon_{33}, \varepsilon_{13}\}$, $\mathbf{n}^B = \{n^B_{11}, n^B_{33}, n^B_{13}\}$. Alternatively, $2lG/(l+2G) = E\nu/(1-\nu^2)$ and $2G = E/(1+\nu)$, where E is the Young modulus and ν is the Poisson ratio. In terms of components we have

$$n^B_{11} = Ch\left[\varepsilon_{11} + \nu\varepsilon_{33}\right], \qquad n^B_{33} = Ch\left[\nu\varepsilon_{11} + \varepsilon_{33}\right], \qquad n^B_{13} = kCh\frac{1-\nu}{2}(2\varepsilon_{13}) \tag{4.47}$$

where $C = E/(1-\nu^2)$ and $k = \frac{5}{6}$ is the shear correction factor accounting for a nonlinear, in reality, distribution of the shear stresses. Similar relations are obtained for the couple resultants,

$$m^B_{11} = C\frac{h^3}{12}\left[\kappa_{11} + \nu\kappa_{33}\right], \qquad m^B_{33} = C\frac{h^3}{12}\left[\nu\kappa_{11} + \kappa_{33}\right], \qquad m^B_{13} = kC\frac{h^3}{12}\frac{1-\nu}{2}(2\kappa_{13}) \tag{4.48}$$

Note that κ_{33} of eq.(16) is equal to zero, what is implied by the kinematical hypothesis. It can be recovered on use of the auxiliary condition $m^B_{33} = 0$, which yields $\kappa_{33} = -\nu\kappa_{11}$, and $m^B_{11} = E\frac{h^3}{12}\kappa_{11}$. Note that m^B_{13} is not present in the virtual work equation (36).

4.2 Layer-wise models of multi-layer beams

In the present section the models of multi-layer beams are constructed. A general classification of the theories of laminated composites and the references are given in Section 1.2. Our approach falls into the class of the layer-wise theories, but, differently than in other works, a single layer is modeled by beam equations. This has the advantage, comparing to other approaches, that even extremely thin layers can be correctly accounted for in numerical calculations. The methodology of constructing such models has been proposed in [Wisniewski, Schrefler, 1993]. Two models for the multi-layer beams are constructed: the interface variable model and the hierarchical model. The multi-layer finite element comprising both models, has been developed and tested on several numerical examples.

4.2.1 Interface variables model for a single layer

In order to expose the methodology of constructing the multi-layer models from the beam models we simplify the basic equations. Assuming that the rotations are small we obtain $\mathbf{R} \approx \mathbf{I} + \beta\tilde{\boldsymbol{\theta}}$, where β is an angle of rotation, and $\tilde{\boldsymbol{\theta}}$ is a skew symmetric tensor. The inextensibility of the director yields $\lambda = 1$ (or $\mu = 0$). For these assumptions eq.(1) reduces to the standard Reissner hypothesis, and the expression for displacement (3) becomes

$$\mathbf{u}(\zeta) = \mathbf{u}_0 + \zeta\beta\tilde{\boldsymbol{\theta}}\mathbf{t}_3 = \mathbf{u}_0 + \zeta\beta\mathbf{t}_1 \tag{4.49}$$

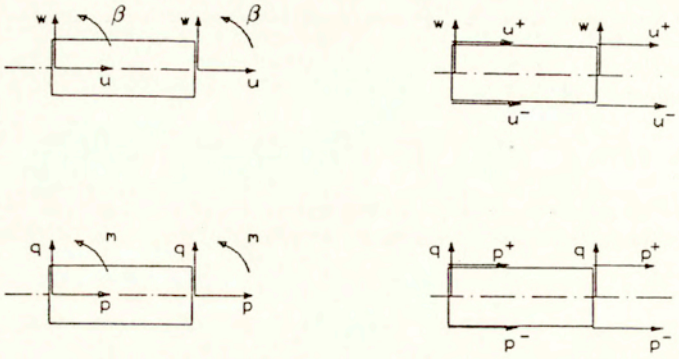

Fig.4.2 Transformation of variables for single lamina

where $\mathbf{u}_0$ and β denote the values at the middle axis of the cross-section. The accordingly simplified strain measures (15) and (16) yield

$$\varepsilon_{11} = u_{,S} - 1, \qquad 2\varepsilon_{13} = w_{,S}, \qquad \kappa_{11} = -\beta_{,S} \tag{4.50}$$

and are linear functions of the displacements and the rotation. The transverse normal strain $\varepsilon_{33} = 0$, as a result of the inextensibility in the thickness direction.

Assume that the displacements associated with the upper and the lower line bounding the beam, see Fig.4.2, are called the interface variables, and are denoted by $\mathbf{u}^+$ and $\mathbf{u}^-$. For the Reissner kinematics expressed by eq.(49) and $\zeta = \pm h/2$, the interface variables are

$$\mathbf{u}^+ = \mathbf{u}_0 + \frac{1}{2}h\beta\ \mathbf{t}_1, \qquad \mathbf{u}^- = \mathbf{u}_0 - \frac{1}{2}h\beta\ \mathbf{t}_1 \tag{4.51}$$

Next, assume that $\mathbf{u}^+$ and $\mathbf{u}^-$ are known and $\mathbf{u}_0$ and β are sought. On addition and subtraction of the above equations, and elementary algebraic manipulations we obtain the inverse relations,

$$\mathbf{u}_0 = \frac{1}{2}(\mathbf{u}^+ + \mathbf{u}^-), \qquad \mathbf{u}^+ - \mathbf{u}^- = -h\beta\mathbf{t}_1 \tag{4.52}$$

which, in components, read as

$$u_0 = \frac{1}{2}(u^+ + u^-), \qquad w_0 = w^+ = w^-, \qquad \beta = -\frac{1}{h}(u^+ - u^-) \tag{4.53}$$

Hence, $\mathbf{a} = \{u_0, w_0, \beta\}^T$ and $\mathbf{z} = \{w, u^+, u^-\}^T$ are two equivalent sets of unknowns, and the deformation of a single layer can be expressed in terms of the interface variables. Note that in the sequel we denote $w = w^+ = w^-$.

A similar formula can be derived for the external load from the definitions of the external forces and moments for the beam, eq.(40). Taking $\mathbf{a}_3 \approx \mathbf{t}_3$, what is justified by small rotations, and $\lambda \approx 1$, the definitions yield

$$\hat{\mathbf{p}} \equiv \hat{\mathbf{p}}^+ + \hat{\mathbf{p}}^-, \qquad \hat{q} \equiv \frac{h}{2}\mathbf{t}_3 \cdot (\hat{\mathbf{p}}^+ - \hat{\mathbf{p}}^-), \qquad \hat{\mathbf{m}} \equiv \frac{h}{2}\,\mathbf{t}_3 \times (\hat{\mathbf{p}}^+ - \hat{\mathbf{p}}^-) \tag{4.54}$$

where the subscript 3 of the load vectors $\hat{\mathbf{p}}_3^+$ and $\hat{\mathbf{p}}_3^-$ has been omitted for clarity.

Decomposing $\hat{\mathbf{p}}^+ = \hat{p}_1^+\mathbf{t}_1 + \hat{p}_3^+\mathbf{t}_3$, and $\hat{\mathbf{p}}^-$ in the same way, we obtain for the external moment

$$\hat{\mathbf{m}} = \frac{h}{2}(\hat{p}_1^+ - \hat{p}_1^-)(\mathbf{t}_3 \times \mathbf{t}_1) = \frac{h}{2}(\hat{p}_1^+ - \hat{p}_1^-)\mathbf{t}_2 \tag{4.55}$$

Then, instead of $\hat{\mathbf{m}}$ we can use its component $\hat{m}_2 = \frac{h}{2}(\hat{p}_1^+ - \hat{p}_1^-)$. Besides, in accordance with the inextensibility of the director we can assume that $\hat{q} = 0$, and the normal components of the tangent load at the top and the bottom of the beam are equal, i.e. $\hat{p}_3^+ = \hat{p}_3^- = \frac{1}{2}\hat{p}_3$. Thus, we have a set of equations,

$$\hat{p}_3 = \hat{p}_3, \qquad \hat{p}_1 = \hat{p}_1^+ + \hat{p}_1^-, \qquad \hat{m}_2 = \frac{h}{2}(\hat{p}_1^+ - \hat{p}_1^-) \tag{4.56}$$

which can be uniquely solved for the interface variables

$$\hat{p}_3 = \hat{p}_3, \qquad \hat{p}_1^+ = \frac{\hat{p}_1}{2} + \frac{\hat{m}_2}{h}, \qquad \hat{p}_1^- = \frac{\hat{p}_1}{2} - \frac{\hat{m}_2}{h} \tag{4.57}$$

Thus, $\hat{\mathbf{p}}_s = \{\hat{p}_3,\ \hat{p}_1^+,\ \hat{p}_1^-\}^T$, which is prescribed at the interfaces, and $\hat{\mathbf{p}} = \{\hat{p}_1, \hat{p}_3, \hat{m}_2\}$, which is associated with the middle line, are two equivalent sets of external loads.

To derive a two-noded finite element the linear approximation is used, $\mathbf{a} = \sum_{I=1}^{2} N_I \mathbf{a}_I$, where the shape functions $N_1(\xi) = \frac{1}{2}(1+\xi)$, $N_2(\xi) = \frac{1}{2}(1-\xi)$, and $\xi \in [-1, +1]$ for $\xi = 2S/L - 1$, and $S \in [0,\ L]$. The discretized virtual work equation yields

$$G(\mathbf{a}) = \delta\mathbf{a}_e^T\ \mathbf{K}\ \mathbf{a}_e - \delta\mathbf{a}_e^T\ \hat{\mathbf{p}} = 0 \tag{4.58}$$

where $\mathbf{a}_e = \{\mathbf{a}_1,\ \mathbf{a}_2\}^T$ is the vector of the elemental displacements and rotation, and $\hat{\mathbf{p}} = \{\hat{\mathbf{p}}_1, \hat{\mathbf{p}}_2\}^T$ is the vector of the elemental external forces and moment. For a single node I we have $\mathbf{a}_I = \{u_{0I}, w_{0I}, \beta_{0I}\}^T$, and $\hat{\mathbf{p}}_I = \{\hat{p}_{10I}, \hat{p}_{30I}, \hat{m}_{20I}\}^T$, where $\hat{p}_{10I}, \hat{p}_{30I}$ denote the external tangent and transverse load, and $\hat{m}_{20I}$ denotes the external moment. To prevent shear locking, the matrix $\mathbf{K}$ is uniformly under-integrated, what in this case does not result in spurious (zero energy) modes. In the sequel we shall present all the operations for a single node of the element, assuming that the extension to two nodes is standard.

The conversion of the middle-line variables and external loads to the interface variables and external loads is performed for the nodal values. Eq.(53) and (57), which are used for this conversion can be concisely written as follows

$$\mathbf{a} = \mathbf{A}\ \mathbf{z}, \qquad \hat{\mathbf{p}}_s = \mathbf{A}^T\ \hat{\mathbf{p}}, \qquad \mathbf{A} = \begin{bmatrix} 0 & +\frac{1}{2} & +\frac{1}{2} \\ 1 & 0 & 0 \\ 0 & -\frac{1}{h} & +\frac{1}{h} \end{bmatrix} \tag{4.59}$$

where $\det \mathbf{A} = -1/h$. On use of the above formulae, the component terms of the virtual work equation for a single layer given by eq.(58) can be transformed as follows

$$\delta \mathbf{a}^T\ \mathbf{K}\ \mathbf{a} = \delta \mathbf{z}^T\ \mathbf{A}^T \mathbf{K} \mathbf{A}\ \mathbf{z}, \qquad \delta \mathbf{a}^T\ \hat{\mathbf{p}} = \delta \mathbf{z}^T\ \mathbf{A}^T \hat{\mathbf{p}} = \delta \mathbf{z}^T \hat{\mathbf{p}}_s \tag{4.60}$$

Hence, the virtual work principle becomes

$$\delta \mathbf{z}^T \mathbf{K}_s - \delta \mathbf{z}^T \hat{\mathbf{p}}_s = 0 \tag{4.61}$$

where $\mathbf{K}_s = \mathbf{A}^T\ \mathbf{K}\ \mathbf{A}$, and the equilibrium equation in terms of the interface variables is

$$\mathbf{K}_s\ \mathbf{z} = \hat{\mathbf{p}}_s. \tag{4.62}$$

4.2.2 Aggregation of layers

The equations for layers are aggregated through the compatibility conditions written for the interface of each two adjacent layers. The condition that tangent displacements at the bottom of layer n and at the top of layer $n+1$ are equal can be written as $u_n^- = u_{n+1}^+$. It is apparent that it would be much more inconvenient to write this condition by means of the middle line variables. The same transverse displacement w is used for all layers, what complies with the hypothesis about the inextensibility of the layers in the thickness direction.

The corresponding assemblage of the basic vectors and matrices can be described by operations on the list of unknowns. For example, let us assume that the full set of unknowns for four separate (non-aggregated) layers is

$$\{w_1, u_1^+, u_1^- \ \mid\ w_2, u_2^+, u_2^- \ \mid\ w_3, u_3^+, u_3^- \ \mid\ w_4, u_4^+, u_4^-\} \tag{4.63}$$

We may assign to them the following numbers

$$\mathbf{l}_1 = \{1,2,3 \ \mid\ 4,5,6 \ \mid\ 7,8,9 \ \mid\ 10,11,12\} \tag{4.64}$$

To indicate operations on the list of unknowns due to the compatibility conditions the following convention is used: the unknown which is eliminated is marked by minus, and the number following the minus specifies the unknown which replaces it. For example, the condition that transverse displacements are the same for all layers, i.e. $w_1 = w_2 = w_3 = w_4$, changes $\mathbf{l}_1$ to

$$\mathbf{l}_2 = \{1,2,3 \ \mid\ -1,5,6 \ \mid\ -1,8,9 \ \mid\ -1,11,12\} \tag{4.65}$$

The condition that tangent displacements u are equal at the bottom of lamina n and at the top of lamina $n+1$ for every pair of adjacent layers, i.e. $u_2^+ = u_1^-$, $u_3^+ = u_2^-$ and $u_4^+ = u_3^-$ modifies the list to

$$\mathrm{l}_3 = \{1,2,3 \mid -1,-3,6 \mid -1,-6,9 \mid -1,-9,12\} \tag{4.66}$$

The final list is obtained by numbering the unknowns which are not eliminated, i.e. the positive elements of l_3,

$$\mathrm{l}_4 = \{1,2,3 \mid -1,-3,4 \mid -1,-4,5 \mid -1,-5,6\} \tag{4.67}$$

and it corresponds with the following independent variables of the aggregated multi-layer beam

$$\mathbf{z}_a = \{w_1, u_1^+, u_1^- \mid u_2^- \mid u_3^- \mid u_4^-\} \tag{4.68}$$

The virtual work equation for an aggregated beam can thus be written as

$$\delta \mathbf{z}_a^T \, \mathbf{K}_a \, \mathbf{z}_a - \delta \mathbf{z}_a^T \, \hat{\mathbf{p}}_a = 0 \tag{4.69}$$

where $\mathbf{K}_a$ and $\hat{\mathbf{p}}_a$, are the stiffness matrix and the load vector for the aggregated beam. To create these matrices the symbolic list l_4 is interpreted and the entries of $\mathbf{K}_s$ and $\hat{\mathbf{p}}_s$ are accordingly inserted into $\mathbf{K}_a$ and $\hat{\mathbf{p}}_a$. The equilibrium equation for the interface variables of the multi-layer cross-section is as follows

$$\mathbf{K}_a \, \mathbf{z}_a = \hat{\mathbf{p}}_a \tag{4.70}$$

As we see the above procedure leads to equations equivalent with the equations of the layer-wise theory.

4.2.3 Hierarchical model

In the model obtained in the previous section the deformation of the multi-layer beam is described by M components of $\mathbf{z}_a$ at every node, where $M = m + 2$ is dependent on the number of layers m. For beams consisting of many layers the reduction of the number of independent variables is a necessity. We perform this reduction expanding the tangent displacements u into a truncated Taylor or Chebyshev series

$$u(z) = \sum_{n=0}^{N-2} u_n \, T_n(z) \tag{4.71}$$

where $z \in [-H/2, +H/2]$, and H is the thickness of the whole composite cross-section, and T_n represents the Taylor or Chebyshev polynomials of $n-th$ order. A similar formula can be written for the tangent external load.

If eq.(71) is written for values of z indicating all interfaces of layers and a top and a bottom of the whole beam, then we obtain M equations, and the coefficients u_n can be used as new unknowns. In matrix notation the relation between the interface displacements and loads and the corresponding series coefficients can be written as

$$\mathbf{z}_a = \mathbf{T} \, \mathbf{z}_h, \qquad \hat{\mathbf{p}}_a = \mathbf{T} \, \hat{\mathbf{p}}_h \tag{4.72}$$

where
$\mathbf{z}_a$ and $\hat{\mathbf{p}}_a$ are the interface displacements and loads, $\dim \mathbf{z}_a = \dim \hat{\mathbf{p}}_a = M$,
$\mathbf{z}_h = \{w, \ u_0, \ u_1, \ u_2, ..., \ u_{N-2}\}^T$ is the vector of the series coefficients for displacements,
$\hat{\mathbf{p}}_h = \{\hat{p}_3, \ \hat{p}_{10}, \ \hat{p}_{11}, \ \hat{p}_{12}, ..., \ \hat{p}_{1(N-2)}\}^T$ is the vector of the series coefficients for loads,
$\mathbf{T} = \{\mathbf{t}_1, \mathbf{t}_2, ..., \mathbf{t}_M\}^T$ contains values of polynomials of z at the interfaces. For the tangent displacement u we use $\mathbf{t}_i = \{0, \ T_0, \ T_1, \ T_2, \ T_3, ..., \ T_{N-2}\}$, $i = 2, 3, ..., N-2$, while for the normal displacement w we use $\mathbf{t}_i = \{1, \ 0, \ 0, \ 0, \ 0, ..., \ 0\}$. Substituting eq.(72) into the virtual work principle (68) we obtain

$$\delta \mathbf{z}_h^T \ \mathbf{T}^T \mathbf{K}_a \mathbf{T} \ \mathbf{z}_h - \delta \mathbf{z}_h^T \ \mathbf{T}^T \mathbf{T} \ \hat{\mathbf{p}}_h = 0 \tag{4.73}$$

Finally, the equilibrium equation in terms of the expansion coefficients is as follows

$$\mathbf{K} \ \mathbf{z}_h = \hat{\mathbf{p}}_h^* \tag{4.74}$$

where $\mathbf{K} = \mathbf{T}^T \mathbf{K}_a \mathbf{T}$ and $\hat{\mathbf{p}}_h^* = \mathbf{T}^T \mathbf{T} \ \hat{\mathbf{p}}_h$. Besides, $\dim \mathbf{K} = M \times M$, $\dim \mathbf{T} = M \times N$, $\dim \mathbf{z}_h = N$ and $\dim \hat{\mathbf{p}}_h^* = N$.

Note that when $\mathbf{T}$ is inverted then the dimensions of $\mathbf{z}_a$ and $\mathbf{z}_h$ must be equal, i.e. $N = M$. However, eq.(74) requires only transposition of $\mathbf{T}$ hence also $N < M$ are admissible. This property can be used to reduce the number of independent variables.

It can be shown for $N \leq M$ that the generated models are hierarchical. For this purpose, we assume that only N first columns of $\mathbf{T}$ and N first rows of $\mathbf{T}^T$ are used to calculate $\mathbf{K}$. A model of a higher accuracy can be obtained by retaining higher order terms of the expansions of displacements and loads, and corresponding parts of the stiffness matrix. If we increase N by one to $N+1$, where $N+1 \leq M$, then we have to add a new column $\mathbf{c}$ to $\mathbf{T}$, i.e. $\mathbf{T}_{M \times (N+1)} = \{\mathbf{T}_{M \times N}, \ \mathbf{c}_{M \times 1}\}$. The matrix $\mathbf{K}_a$ is of the same size, $M \times M$. The new stiffness matrix is

$$\mathbf{K}_{(N+1)\times(N+1)} = \left\{ \begin{array}{c} \mathbf{T}^T \\ \mathbf{c}^T \end{array} \right\} \mathbf{K}_a \ \{\mathbf{T}, \ \mathbf{c}\} = \left[\begin{array}{cc} \mathbf{T}^T \mathbf{K}_a \mathbf{T} & \mathbf{T}^T \mathbf{K}_a \mathbf{c} \\ \\ \mathbf{c}^T \mathbf{K}_a \mathbf{T} & \mathbf{c}^T \mathbf{K}_a \mathbf{c} \end{array} \right] \tag{4.75}$$

The first sub-matrix coefficient in the obtained matrix is equal to $\mathbf{K}_{N \times N}$, the others are related to $\mathbf{c}$. Hence, if we include higher order terms of the expansion (69) then the matrix $\mathbf{K}_{N \times N}$ is not modified, but only supplemented with new rows and columns.

4.2.4 Numerical examples

In this section we examine the multi-layer (ML) beam element developed according to the presented formulas, and incorporated into the FEAP program, [Zienkiewicz, Taylor, 1989]. The element enables an analysis in terms of the interface variables (IFV), the Taylor series coefficients (HT), and the Chebyshev series coefficients (HCh). In subsequent numerical tests we analyze a beam, which is fixed at one end ($w = 0$ and $\beta = 0$ at $S = 0$), and loaded by a transverse force P at the other end, see Fig.4.3.

Test 1. Single-layer beam

Two tests are performed. The first is to confirm that the middle line solutions i.e. $\{w, u, \beta\}$, the HT beam solutions i.e. $\{w, u, u^{(1)}\}$, and the IFV solutions i.e. $\{w, u^+, u^-\}$

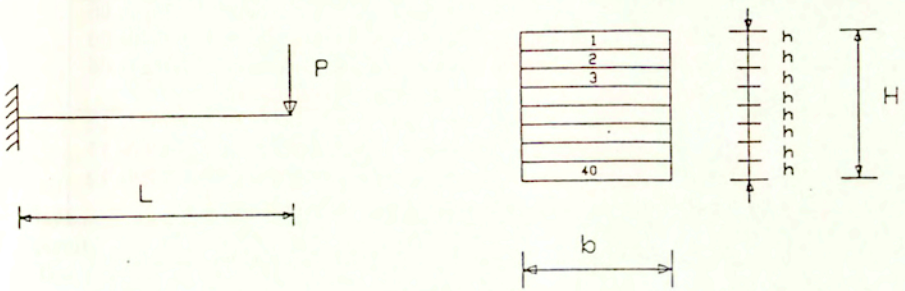

Fig.4.3 Beam with applied force, and multi-layer cross-section

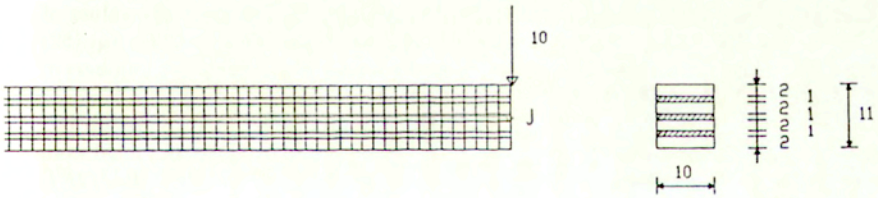

Fig.4.4 Mesh for 2D analysis, and composite cross-section

Table 4.1. Displacements at $S = L$ for various formulations.
Single layer, 100 two-noded elements.

l/H	*element type*	*displacements* 1	2	3	*ratio* D_{max}/D_{min}
10^0	MDV	4.000162e 00	1.110223e-14	6.000002e-02	7.7627e 06
	IFV	4.000160e 00	3.000000e-02	-3.000000e-02	3.3340e 06
	HT	4.000160e 00	0.000000e 00	6.000000e-02	7.7627e 06
	$IFV \rightarrow HT$		0.000000e 00	6.000000e-02	
10^3	MDV	4.003436e 09	1.110223e-14	6.004814e 07	7.7627e 12
	IFV	4.001100e 09	3.000794e 04	-3.000789e 04	7.4660e 17
	HT	3.997671e 09	0.000000e 00	5.996682e 07	7.7579e 12
	$IFV \rightarrow HT$		0.000005e 04	6.001583e 07	

Displacements $1, 2, 3$ indicate components in three different models:
MDV : middle line variables, $\mathbf{a} = \{w_0, u_0, \beta\}$,
IFV : interface variables, $\mathbf{z} = \{w, u^+, u^-\}$.
HT : hierarchical, Taylor series, $\mathbf{z}_h = \{w, u, u^{(1)}\}$.

are equivalent, even for very thin beams. The second is to determine the range of aspect ratios of the HT element, for which the solutions yielded by our element are close to the exact solution. Both tests are essential if the element is to be used for multi-layer cross-sections consisting of many, very thin layers.

The parameters used in calculations are: the transverse force $P = 1$, the beam length $L = 100$, the beam height $H = 1$, the beam width $b = 1$, Young's moduli $E = 10^6$, Poisson ratio $\nu = 0.3$.

The results obtained in the first test are presented in Table 4.1, and the values of $\{w_0, u_0, \beta\}$, $\{w, u^+, u^-\}$ and $\{w, u, u^{(1)}\}$, are equivalent. To calculate the values of $\{u, u^{(1)}\}$ for the IFV solution $\{u^+, u^-\}$, (marked in Table 4.1 as $IFV \rightarrow HT$) eqs.(52) were used. Besides, l denotes the length of element, D_{max}, D_{min} are pivot numbers of LDL^T decomposition.

In the second test the height H is an independent parameter. Results for various length to height ratios of the element given in Table 4.2 are scaled by values obtained from the solutions of the Bernoulli beam equations, i.e. $w_B = PL^3/3EI$ and $\beta_B = PL^2/2EI$. These results show that up to $l/H = 10^3$ the formulation guarantees a good accuracy, and proves that the under-integration used to prevent locking works very well.

Test 2. Multi-layer homogeneous beam

This test verifies the fact that the ML beam element, though based on a higher order approximation, for very thin beams yields results close to the Bernoulli solution. The beam is composed of many layers of the same material and of the same thickness. The thickness of the layers h changes when the number of layers is modified to give the same total beam height $H = 1$ or $H = 10^{-3}$. The other parameters are the same as in Test 1. The solution vector is $\mathbf{z}_h = \{w, u, u^{(1)}, u^{(2)}/2, u^{(3)}/3!, u^{(4)}/4!\}$, i.e. we use 6 degrees of freedom per node. The derivatives for the non-zero coefficients of the solution vector $\mathbf{z}_h$ are presented in Table 4.3. In this case the solution for 4 layers is close to that for 40

Table 4.2. Normalized displacements at $S = L$ for various aspect ratios. Single layer, $\mathbf{z}_h = \{w, u, u^{(1)}\}$, 100 two-noded elements.

l/H	w/w_B	$u_{,z}/\beta_B$	D_{max}/D_{min}
10^0	1.00004	1.00000	7.7627e 06
10^1	0.99997	1.00000	7.7622e 08
10^2	0.99997	0.99999	7.7622e 10
10^3	0.99941	0.99944	7.7579e 12
10^4	1.11952	1.11371	8.6915e 14
10^5	1.40199	0.19872	1.0749e 16

layers, and for both values of H almost the same results have been obtained. All the results are close to the Bernoulli solution. Thus for the range of l/H ratios checked in Test 1 and the subdivision into up to 40 layers a good accuracy is preserved.

Table 4.3. Displacements for different number of layers (n.o.l) at $S = L$. Layers of the same material. 100 two-noded elements

l/H	$n.o.l.$	w	$u^{(1)}$	$u^{(3)}$
10^0	4	4.000196e 00	5.999907e-02	3.119963e-05
	10	4.000209e 00	5.999919e-02	3.119963e-05
	20	4.000211e 00	5.999921e-02	3.119963e-05
	40	4.000212e 00	5.999922e-02	3.119963e-05
10^3	4	3.997809e 09	5.997091e 07	-0.9.1138e 04
	10	3.997438e 09	5.996638e 07	-1.127601e 04
	20	3.998296e 09	5.997726e 07	-1.035036e 04
	40	4.003050e 09	6.004530e 07	-0.907349e 04

$u^{(2)} = u^{(4)} = 0$

$\mathbf{z}_h = \{w,\ u,\ u^{(1)},\ u^{(2)}/2,\ u^{(3)}/3!,\ u^{(4)}/4!\}, \quad \dot{\mathbf{p}}_h = \{P/A, 0, 0, 0, 0, 0\}$

Test 3. Multi-layer composite beam

In this example we analyze a moderately thick beam composed of two types of layers, each made of a different material and having a different thickness. The layers of type 1 and 2 are aggregated in the following order: $1, 2, 1, 2, 1, 2, 1$. The used data is as follows: the Poisson ratios $\nu_1 = 0.294$, and $\nu_2 = 0.333$, the Young's moduli $E_1 = 2.1 \cdot 10^6$, and E_2 is manipulated to provide different E_1/E_2 ratios. The total beam height $H = 11.0$, with the layer thicknesses $h_1 = 2.0$ and $h_2 = 1.0$. The beam length $L = 90.0$, the beam width $b = 10.0$, the force $P = 10.0$.

To provide comparative results a 2D plane stress analysis of the beam, with a fine mesh of 7x45 9-noded elements shown in Fig.4.4, has been performed. The element aspect ratios are 1 or 0.5, and the model consists of 2730 dofs, and guarantees a very good accuracy of this analysis.

First, analyses were performed for the ratio $E_1/E_2 = 100$, which is unrealistic but can serve as a severe test for computational models. The thinner layers are subdivided into 2 sub-layers each, yielding the number of interface variables $M = 12$. The Taylor series and Chebyshev series have been tested with the number of unknowns $N = M = 12$. The transverse displacement w at $S = L$ obtained from the 2D analysis is equal to 1.620, while all the ML beam models (IFV, HT and HCh) yielded the value 1.637. The relative error of the ML beam solutions is 1.05%. Table 4.4 shows, for the HT beam model, that if the number of degrees of freedom per node N is increased then the displacement w converges to the value obtained for $N = 12$. The tangent displacements u at the cross-section $S = L$ are shown in Fig.4.5. The Taylor series gave very small errors near the point of expansion, and larger errors farther away, while the Chebyshev series lead to errors more uniformly distributed throughout the cross-section and a smaller maximum error. The Chebyshev solution and the solution in terms of the interface variables fit the 2D solution very well. Note that, more recently, also [Parish, 1995] assumed a Chebyshev polynomial as a shape function in the thickness direction for a continuum-based shell element.

Table 4.4. Displacement w at point $S = L$, $z = 0$ for various numbers of dofs per node. 7-layer beam, $E_1/E_2 = 100$, 100 two-noded elements, $M = 12$, $P = 10.0$

N	w	w / $w_{N=12}$
12	1.637221e-3	1.000
10	1.545883e-3	0.994
8	1.316523e-3	0.804
6	1.263449e-3	0.772
3	1.260037e-3	0.769

Next, analyses were performed for a reduced number of parameters of the ML beam, i.e. $N = 3$, what corresponds to a first-order shear deformation model. The obtained transverse displacements w at $S = L$ and $z = 0$ for various E_1/E_2 ratios are given in Table 4.5. We can notice that for higher E_1/E_2 ratios the displacement obtained by the 3-parameter model becomes too small. However, for the range of the ratios which are of practical interest, i.e for $E_1/E_2 \leq 20$, the error is still smaller than 5.3%. The distribution of tangent displacements u at the cross-section $S = L$ for a homogeneous cross-section ($E_1/E_2 = 1$) and a cross-section made of steel and epoxy ($E_1/E_2 = 7$) is shown in Fig.4.6. The curves obtained from the 2D and ML models are almost identical for both cross-sections.

Table 4.5. Displacements w at point $S = L$ and $z = 0$ of a 7-layer beam. 100 two-noded elements, $M = 12$, $N = 3$, $\mathbf{z}_h = \{w, u, u^{(1)}\}$, $P = 10.0$

E_1/E_2	ML	$2D$	$ML/2D$
1	1.053305e-3	1.053447e-3	0.999
7	1.227686e-3	1.247490e-3	0.984
20	1.250117e-3	1.320387e-3	0.947
50	1.257632e-3	1.442468e-3	0.872
100	1.260037e-3	1.620388e-3	0.778

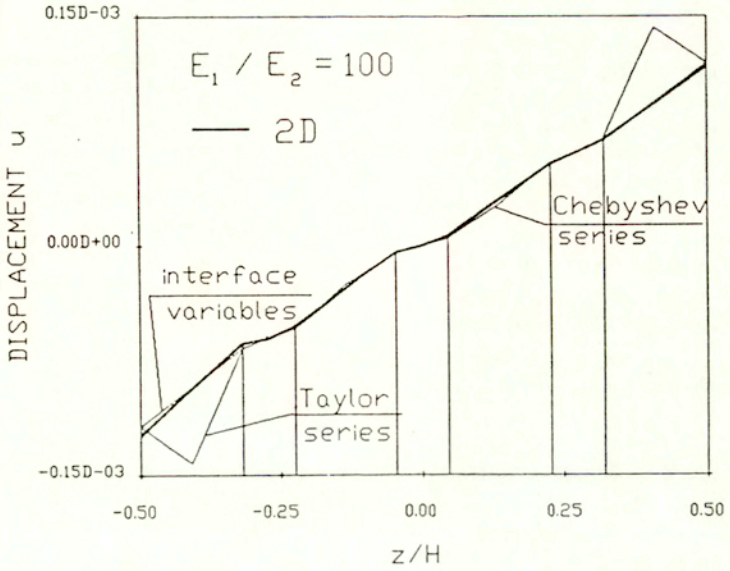

Fig.4.5 Displacements u at cross-section $S = L$ for $E_1/E_2 = 100$. 2D and various ML beam solutions. $M = 12$, $N = 12$

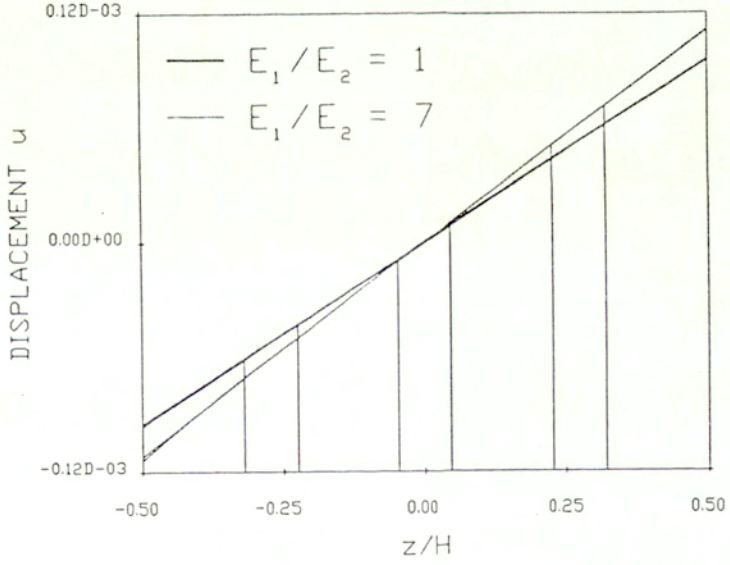

Fig.4.6 Displacements u at cross-section $S = L$ for $E_1/E_2 = 1$ and $E_1/E_2 = 7$. $M = 12$, $N = 3$. 2D and ML beam solutions coincide

4.3 Stress recovery for multi-layer models

The enhanced stress recovery (ESR) method for the multi-layer models has been proposed in [Wisniewski, Schrefler, 1993b]. A need for such a method stems from two facts: the stress and couple resultants are not useful for multi-layer beams, and a direct method of calculating stresses yields inaccurate shear stresses.

In the case of a beam with layers made of different materials the distribution of stresses is not as regular as that for a beam with a homogeneous cross-section. Hence, the stress and couple resultants used for beams (i.e. membrane force n^B_{11}, shear force n^B_{13}, and bending moment m^B_{11}) which are obtained by integrating stresses over the whole cross-section, are not useful measures. Therefore, instead of the stress and couple resultants, we compute the cross-sectional stresses,

$$\sigma_{11} = C_1 \, (\varepsilon_{11} + \nu \varepsilon_{33}), \qquad \sigma_{13} = C_2 \, \varepsilon_{13} \tag{4.76}$$

where $C_1 = E/(1-\nu^2)$ and $C_2 = \frac{1}{2}E/(1+\nu)$. Strains ε_{11}, ε_{13} and ε_{33} are defined as for two-dimensional elasticity.

In the sequel, first we show that accuracy of stresses calculated directly, is limited by properties of the approximation functions used by the IFV or H model. Next, we propose the enhanced stress calculation method, and finally, results of numerical computations are presented.

4.3.1 Direct stress calculation

The direct methods are those which exploit kinematical and constitutive equations, but, by definition, no other special techniques. Hence properties of approximation functions directly influence accuracy of shear stresses obtained by these methods.

A very important property of approximation functions used for u is continuity of derivative $u_{,\zeta}$ at interfaces of material layers. We show below that continuity of shear stresses depends on continuity of approximation functions for u. Let us write the equation of continuity of shear stresses at an interface, i.e. $\sigma^+_{13} = \sigma^-_{13}$, in terms of displacements

$$C^-_2 \, (w^-_{,S} + u^-_{,\zeta}) \; = \; C^+_2 \, (w^+_{,S} + u^+_{,\zeta}) \tag{4.77}$$

where plus and minus indicate two sides of an interface. For the multi-layer model aggregated of beams inextensible in the thickness direction we have $w^-_{,S} = w^+_{,S} = w_{,S}$, and eq.(77) can be transformed to the following form

$$u^-_{,\zeta} \; = \; w_{,S} \, (\alpha - 1) + \alpha \, u^+_{,\zeta} \tag{4.78}$$

where $\alpha = C^+_2/C^-_2$. Subtracting $u^+_{,\zeta}$ from both sides of the above equation we obtain an equation for the jump of derivatives

$$u^-_{,\zeta} - u^+_{,\zeta} \; = \; (\alpha - 1) \, \varepsilon^+_{13} \tag{4.79}$$

For layers made of the same material $\alpha = 1$ and $u^-_{,\zeta} - u_{,\zeta} = 0$, i.e. there should not be a jump of derivatives of the approximation functions for continuity of shear stresses. If

material properties are dissimilar, i.e. $\alpha \to 0$, then $u^-_{,\zeta} - u^+_{,\zeta} \to -\varepsilon^+_{13}$, i.e. the jump of derivatives must exist to preserve continuity of shear stresses at the interface.

Properties of approximation functions used by the IFV model and the H model impose limitations on the accuracy of shear stresses obtained by the direct methods. Let us recall that the IFV model exploits continuous layer-wise linear (C^0 continuous) functions for u, while the H model uses global C^N ($N \leq m+2$) continuous functions for u, where m denotes the number of layers. If we calculate stresses directly then properties of stresses are as follows.

For the IFV model the shear stresses are not continuous at interfaces because the derivative $u_{,\zeta}$ is constant within layers. The discontinuity of $u_{,\zeta}$ at interfaces does not improve shear stresses, and they are stepped.

Within the H model the derivative $u_{,\zeta}$ is a polynomial of $(N-1)$-th order, and shear stresses are discontinuous at interfaces. Hence, at interfaces we generate effects similar to boundary effects, which pollute the shear stress distribution.

Now, we would like to refer to the subsequent section, where examples of directly calculated stresses for the IFV and the H model are presented. Here we only mention that the accuracy of these stresses is not very good, especially for very dissimilar materials, and a better method needed to be designed.

4.3.2 Enhanced stress recovery

The enhanced stress recovery method has been proposed for the IFV and H models of the multi-layer beam in [Wisniewski, Schrefler, 1993]. In this method the multi-layer beam element is subdivided into quadrilateral 9-noded elements, one per each material layer. At least two computational sub-layers should be defined within each material layer. Below we present the basic steps of this method.

1. Parabolic approximation of u within layers. The solution of the equilibrium equation gives us the values of the interface variables $\mathbf{z}$, for the IFV model, or the series coefficients $\mathbf{z}_h$ for the H model. Having these values, known for each node of the multi-layer beam element, we calculate values of the tangent displacements at 9 nodes of the two-dimensional parabolic element. These nodes are located at interfaces of material layers, and at the middle axis of each material layer, as shown in Fig.4.7. The transverse displacements w are calculated at the same points taking into account that values of w are equal at each cross-section of the multi-layer beam element. Using values of displacements at these 9 nodes and parabolic shape functions we can obtain a linear distribution of $u_{,\zeta}$ within material layers.

2. Stresses at Gauss points. For each 9-noded element stresses are calculated at four Gauss points located at $\{\xi = \pm 1/\sqrt{3},\ \zeta = \pm 1/\sqrt{3}\}$. In Fig.4.7 Gauss points are marked by crosses and denoted by I, II, III, and IV. For a parabolic two-dimensional element stresses at these points are of good accuracy, see [Hinton, Campbell, 1974], [Zienkiewicz, Taylor, 1989].

3. Projection of stresses to corner nodes. The stresses at Gauss points should be extra-

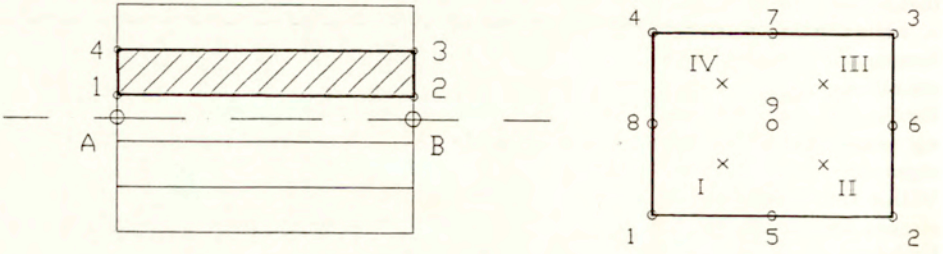

Fig.4.7 Subdivision of ML beam into quadrilaterals.
Crosses mark location of stress points

polated to nodes. An extrapolation formula can be obtained by minimization of

$$\chi = \int_\Omega (\boldsymbol{\sigma} - \boldsymbol{\sigma}^*)^2 \; d\Omega, \qquad \boldsymbol{\sigma}^* = \mathbf{N}\, \bar{\boldsymbol{\sigma}} \tag{4.80}$$

where $\boldsymbol{\sigma}$ denotes the unsmoothed stresses, $\boldsymbol{\sigma}^*$ - the smoothing function, $\mathbf{N}$ - the shape functions, and $\bar{\boldsymbol{\sigma}}$ - the nodal values. A condition of minimum of χ with respect to $\bar{\boldsymbol{\sigma}}$ yields

$$\int_\Omega \mathbf{N}\, (\boldsymbol{\sigma} - \boldsymbol{\sigma}^*) \; d\Omega \;=\; 0 \tag{4.81}$$

Denote by $\mathbf{J}$ a Jacobian matrix, i.e. a matrix of derivatives of the global coordinates with respect to the local coordinates of a finite element, see [Zienkiewicz, Taylor, 1989], p.162. For $\det \mathbf{J} = const$ (e.g. for quadrilaterals), linear shape functions $\mathbf{N}$, and a 2 x 2 Gaussian integration rule, we obtain

$$\begin{Bmatrix} \bar{\sigma}_1 \\ \bar{\sigma}_2 \\ \bar{\sigma}_3 \\ \bar{\sigma}_4 \end{Bmatrix} = \begin{bmatrix} a & c & b & c \\ c & a & c & b \\ b & c & a & c \\ c & b & c & a \end{bmatrix} \begin{Bmatrix} \sigma_I \\ \sigma_{II} \\ \sigma_{III} \\ \sigma_{IV} \end{Bmatrix} \tag{4.82}$$

where $a = 1 + \sqrt{3}/2$, $b = 1 - \sqrt{3}/2$ and $c = -1/2$. The subscripts $1, 2, 3, 4$ indicate corner nodes, while the subscripts I, II, III, IV refer to Gauss points. This formula allows to extrapolate the stress values to corner nodes.

4. Smoothing within material layers. The nodal stress values of adjacent elements are averaged to eliminate inter-element stress discontinuities within material layers. Smoothing is not performed across layers.

4.3.3 Numerical examples

In this section we examine the stress calculation procedures for the multi-layer beam element. The element has been incorporated into the FEAP program, [Zienkiewicz, Taylor, 1989].

The beam of geometrical and material properties specified in Test 3 of the preceding section is examined. Analyses are performed using the interface variables and the hierarchical, Chebyshev type multi-layer beam element. The 9-noded two-dimensional plane stress element is used for comparative calculations. The multi-layer beam stresses are calculated via direct procedures, (IFVD) and (HD), as well as the enhanced stress recovery (ESR) procedure. We do not distinguish the IFV and H results for the ESR procedure because for the presented examples they are identical.

First, a beam of a homogeneous cross-section $(E_1/E_2 = 1)$ is analyzed. For this case σ_{11} and σ_{13} should be continuous at layer interfaces. Let us recall that for such a beam the displacement w at $S = L$ is equal to 0.999 of the 2D solution (see Table 4.5), and displacements u obtained by these two models are indistinguishable in Fig.4.6.
The σ_{11} and σ_{13} stresses at $S/L = 0.5$ cross-section are presented in Fig.4.8, 4.9, 4.10 and 4.11. All procedures yield similar σ_{11} stresses, see Fig.4.8. The σ_{13} stresses obtained by the IFVD and the HD procedure are shown in Fig.4.9 and 4.10, while the results of the ESR procedure are shown in Fig.4.11. The IFVD stresses are stepped, the HD and the ESR stresses are very close to the 2D stresses.

Next, the same beam, but with layers of very dissimilar material properties $(E_1/E_2 = 100)$ is analyzed. For this case σ_{11} should have jumps and σ_{13} should be continuous at layer interfaces. Let us recall that for this beam and at $S = L$ cross-section the displacement w was about 1.01 of the 2D solution (see Table 4.4 and 4.5).
The 2D and all multi-layer procedures yield very similar σ_{11}, Fig.4.12. Stresses σ_{13} obtained by the IFVD procedure are shown in Fig.4.13, and, like in case of the homogeneous beam, are stepped. Their values are very close to the mean 2D stresses, and their maximum values at $z/H = 0.0$ are equal to 0.129 for 2D solution and 0.1288 for the IFVD solution. The HD stresses, shown in Fig.4.14, are evidently wrong. They are in correspondence with the distribution of $u_{,\zeta}$ presented in the same figure, and show influence of the high order terms of the series for u. The results obtained by the ESR procedure are shown in Fig.4.15, and are very close to the 2D stresses. This case clearly indicates that for large E_1/E_2 ratios the ESR procedure is superior to the direct stress calculation procedures.

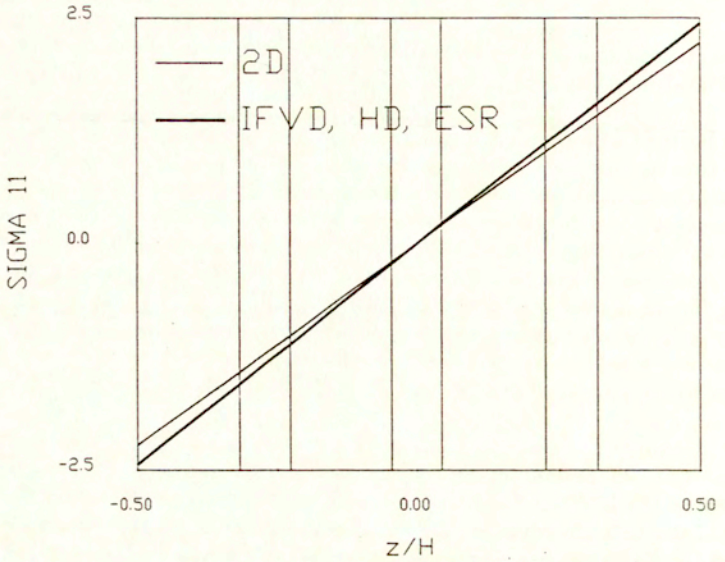

Fig.4.8 Stress σ_{11} by IFVD, HD, ESR and 2D procedures. $E_1/E_2 = 1$

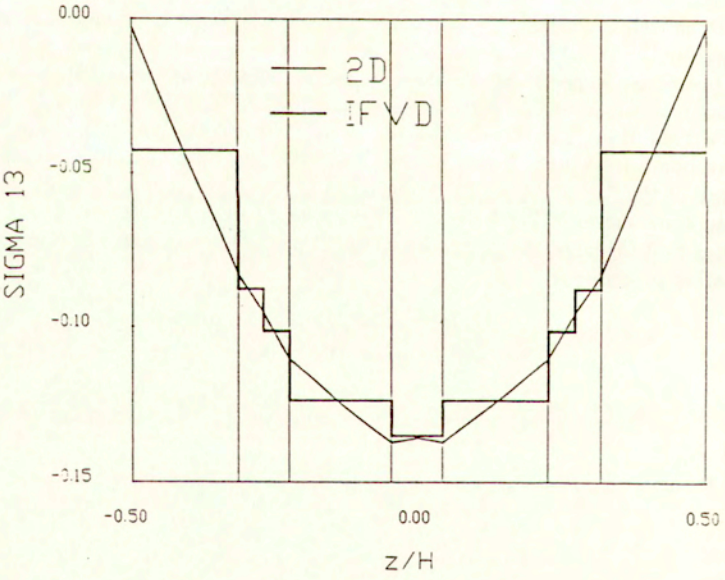

Fig.4.9 Stress σ_{13} by IFVD and 2D procedures. $E_1/E_2 = 1$

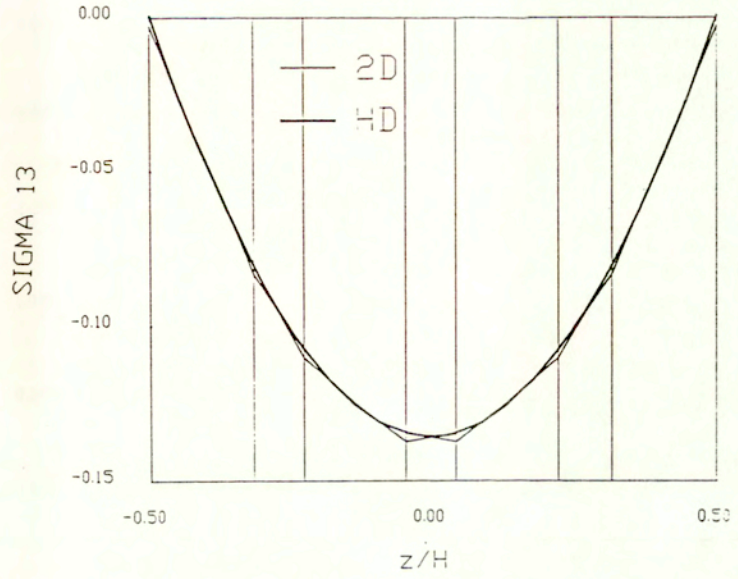

Fig.4.10 Stress σ_{13} by HD and 2D procedure. $E_1/E_2 = 1$

Fig.4.11 Stress σ_{13} by ESR and 2D procedures. $E_1/E_2 = 1$

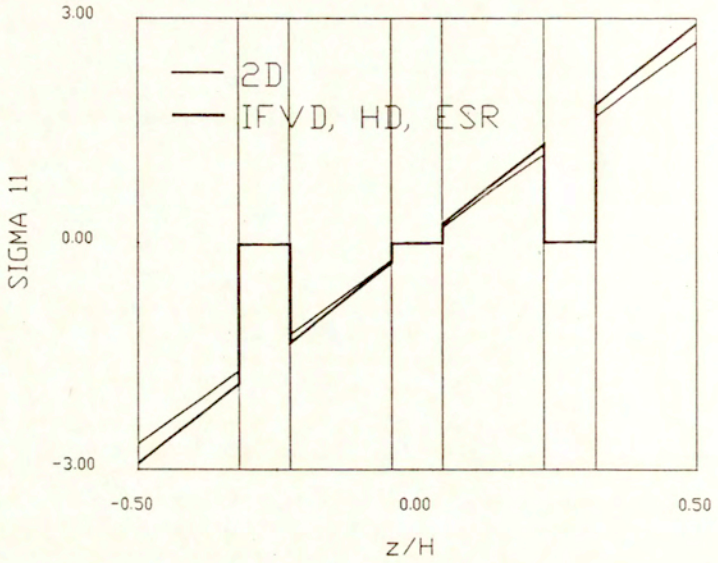

Fig.4.12 Stress σ_{11} by IFVD, HD, ESR and 2D procedures. $E_1/E_2 = 100$

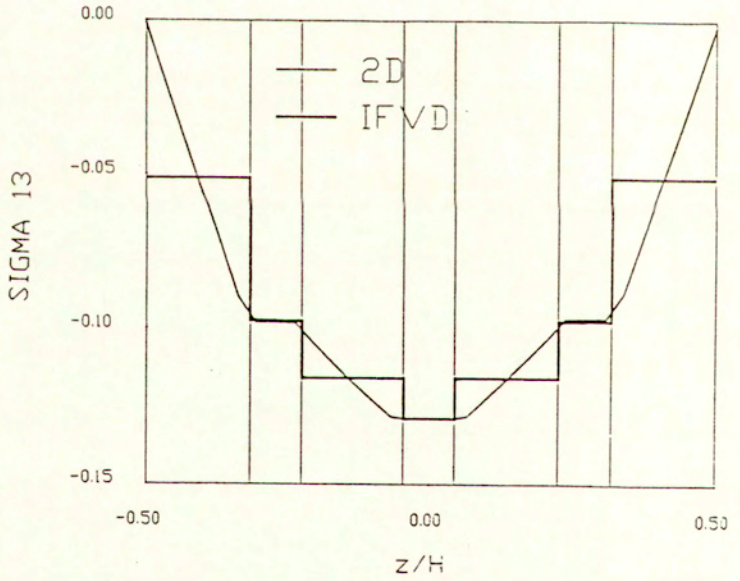

Fig.4.13 Stress σ_{13} by IFVD and 2D procedures. $E_1/E_2 = 100$

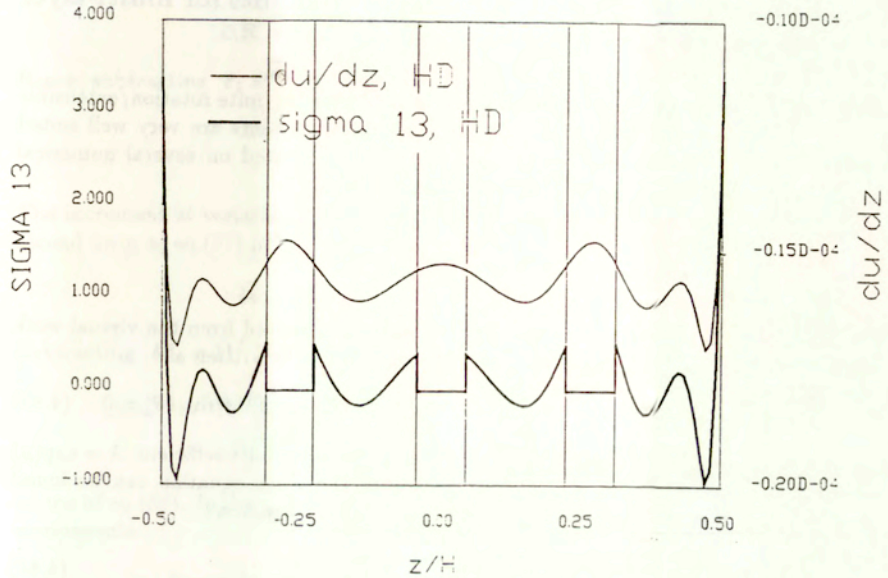

Fig.4.14 Stress τ_{13} by HD procedure, and derivative $u_{i,z}$. $E_1/E_2 = 100$

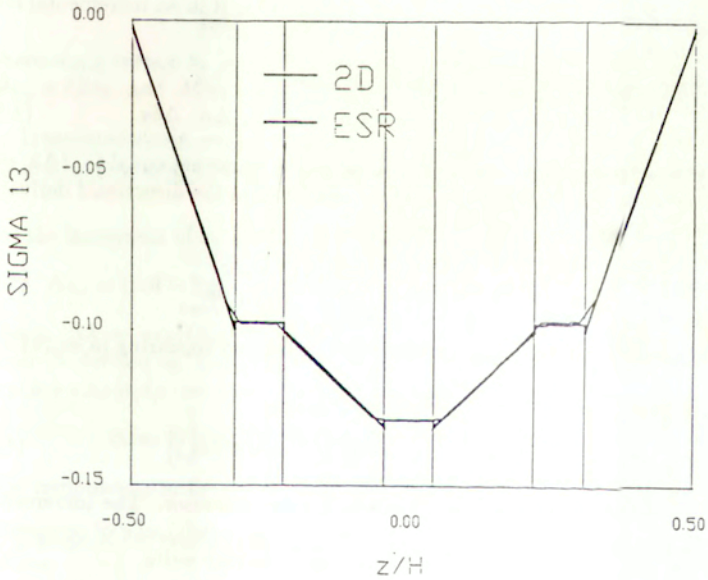

Fig.4.15 Stress σ_{13} by ESR and 2D procedure. $E_1/E_2 = 100$

4.4 Finite rotation/extensible director elements for multi-layer beams

In this section two finite element models are developed from the finite rotation/extensible director theory specified in Section 4.1. These nonlinear elements are very well suited for applications to multi-layer beams. Both elements are tested on several numerical examples, some exhibiting highly nonlinear characteristics.

4.4.1 Finite element formulation

The tangent operator for the Newton-Raphson method is derived from the virtual work equation $\delta\mathcal{W}_b - \delta\mathcal{A}_b = 0$, which from eq.(36) and (39) can be written as

$$G(\mathbf{a}) \equiv [\mathbf{n}_1^B \cdot \delta\boldsymbol{\varepsilon}_1 + \mathbf{n}_3^B \cdot \delta\boldsymbol{\varepsilon}_3] + \mathbf{m}_1^B \cdot [\delta\boldsymbol{\kappa}_1 \times \mathbf{t}_3] - [\hat{\mathbf{p}} \cdot \delta\mathbf{x}_0 + \hat{q}\ \delta\lambda + \hat{\mathbf{m}} \cdot \delta\boldsymbol{\theta}] = 0 \qquad (4.83)$$

where $\mathbf{a} = \{\mathbf{u}_0, \beta, \mu\}$. Recall that μ parameterizes the extension coefficient $\lambda = \exp(\mu)$ and composes additively, see eq.(12). A solution to the above equation can be found iteratively, e.g. using the Newton-Raphson method defined as follows

$$\left.\begin{array}{l} DG(\bar{\mathbf{a}}) \cdot \Delta\mathbf{a} = -G(\bar{\mathbf{a}}) \\ \mathbf{a} = \bar{\mathbf{a}} + \Delta\mathbf{a} \end{array}\right\} \qquad (4.84)$$

where $\bar{\mathbf{a}}$ denotes the last computed solution, $DG(\bar{\mathbf{a}}) \cdot \Delta\mathbf{a} = \frac{d}{dt}[G(\bar{\mathbf{a}} + t\Delta\mathbf{a})]_{t=0}$, i.e. is a derivative of G at $\bar{\mathbf{a}}$ in direction $\Delta\mathbf{a}$, and t is a scalar parameter.

Consider one of the products appearing in eq.(84) and write it in an incremental form as follows

$$\begin{aligned} G_i(\bar{\mathbf{a}} + t\Delta\mathbf{a}) &= (\bar{\mathbf{n}} + \Delta\mathbf{n}) \cdot (\delta\bar{\boldsymbol{\varepsilon}} + \Delta\delta\boldsymbol{\varepsilon}) \\ &= \bar{\mathbf{n}} \cdot \delta\bar{\boldsymbol{\varepsilon}} + \Delta\mathbf{n} \cdot \delta\bar{\boldsymbol{\varepsilon}} + \bar{\mathbf{n}} \cdot \Delta\delta\boldsymbol{\varepsilon} + \Delta\mathbf{n} \cdot \Delta\delta\boldsymbol{\varepsilon} \end{aligned} \qquad (4.85)$$

where the bar indicates the known value. Note that for the increment equal to $t\Delta\mathbf{a}$ only $\Delta\mathbf{n} \cdot \bar{\boldsymbol{\varepsilon}}$ and $\bar{\mathbf{n}} \cdot \Delta\delta\boldsymbol{\varepsilon}$ can be linear functions of t, and hence in the directional derivative of G_i two components are retained,

$$\left[\frac{dG_i(\bar{\mathbf{a}} + t\Delta\mathbf{a})}{dt}\right]_{t=0} = \left[\frac{d\Delta\mathbf{n}}{dt}\right]_{t=0} \cdot \delta\bar{\boldsymbol{\varepsilon}} + \left[\frac{d\Delta\delta\boldsymbol{\varepsilon}}{dt}\right]_{t=0} \cdot \bar{\mathbf{n}} \qquad (4.86)$$

Below we specify $\delta\bar{\boldsymbol{\varepsilon}}$, $\Delta\boldsymbol{\varepsilon}$ and $\Delta\delta\boldsymbol{\varepsilon}$ for all the strain vectors appearing in eq.(84).

a) Strain vector $\boldsymbol{\varepsilon}_1 = \mathbf{R}^T\mathbf{x}_{0,S} - \mathbf{t}_1$. Its variation is

$$\delta\boldsymbol{\varepsilon}_1 = \delta\mathbf{R}^T\mathbf{x}_{0,S} + \mathbf{R}^T\delta\mathbf{x}_{0,S} = \mathbf{R}^T\left[\delta\tilde{\boldsymbol{\theta}}^T\mathbf{x}_{0,S} + \delta\mathbf{x}_{0,S}\right] \qquad (4.87)$$

where $\delta\mathbf{R}^T = \mathbf{R}^T\delta\tilde{\boldsymbol{\theta}}^T$, and $\tilde{\boldsymbol{\theta}}$ denotes the skew-symmetric tensor. The increment of strain is defined as $\Delta\boldsymbol{\varepsilon}_1 \equiv \boldsymbol{\varepsilon}_1 - \bar{\boldsymbol{\varepsilon}}_1$, and for the multiplicative (left) rule of composition of rotations $\mathbf{R} = \Delta\mathbf{R}\bar{\mathbf{R}}$, and the additive rule for $\mathbf{x}_{0,S}$ we may write

$$\boldsymbol{\varepsilon}_1 = \mathbf{R}^T\mathbf{x}_{0,S} - \mathbf{t}_1 = (\bar{\mathbf{R}}^T\Delta\mathbf{R}^T)(\bar{\mathbf{x}}_{0,S} + \Delta\mathbf{x}_{0,S}) - \mathbf{t}_1 \qquad (4.88)$$

The increments can be linearized with respect to t as follows

$$\Delta\mathbf{R} = \mathbf{I} + t\Delta\tilde{\theta} + O(t^2), \qquad \Delta\mathrm{x}_{0,S} = t\Delta\mathbf{u}_{0,S} \tag{4.89}$$

Hence, subtracting $\bar{\boldsymbol{\varepsilon}}_1 = \bar{\mathbf{R}}^T\bar{\mathbf{x}}_{0,S} - \mathbf{t}_1$ from eq.(88) we obtain

$$\begin{aligned}\Delta\boldsymbol{\varepsilon}_1 &= \bar{\mathbf{R}}^T(\Delta\mathbf{R}^T - \mathbf{I})\bar{\mathrm{x}}_{0,S} + \bar{\mathbf{R}}^T\Delta\mathbf{R}^T\Delta\mathrm{x}_{0,S} \\ &= t\bar{\mathbf{R}}^T\left\{\Delta\tilde{\boldsymbol{\theta}}^T\bar{\mathbf{x}}_{0,S} + \Delta\mathbf{u}_{0,S}\right\} + O(t^2)\end{aligned} \tag{4.90}$$

The increment of variation of strain is defined as $\Delta\delta\boldsymbol{\varepsilon}_1 \equiv \delta\boldsymbol{\varepsilon}_1 - \delta\bar{\boldsymbol{\varepsilon}}_1$. Let us write the second form of eq.(87) in the incremental form,

$$\delta\boldsymbol{\varepsilon}_1 = (\bar{\mathbf{R}}^T\Delta\mathbf{R}^T)\left[\delta\tilde{\boldsymbol{\theta}}^T(\bar{\mathbf{x}}_{0,S} + \Delta\mathbf{x}_{0,S}) + \delta\mathbf{x}_{0,S}\right] \tag{4.91}$$

Subtracting $\delta\bar{\boldsymbol{\varepsilon}}_1 = \bar{\mathbf{R}}^T\left[\delta\tilde{\boldsymbol{\theta}}^T\bar{\mathbf{x}}_{0,S} + \delta\mathbf{x}_{0,S}\right]$ from the above equation we obtain

$$\begin{aligned}\Delta\delta\boldsymbol{\varepsilon}_1 &= \bar{\mathbf{R}}^T\left[(\Delta\mathbf{R}^T - \mathbf{I})\delta\tilde{\boldsymbol{\theta}}^T\bar{\mathbf{x}}_{0,S} + \Delta\mathbf{R}^T\delta\tilde{\boldsymbol{\theta}}^T\Delta\mathrm{x}_{0,S} + (\Delta\mathbf{R}^T - \mathbf{I})\delta\mathbf{x}_{0,S}\right] \\ &= t\,\bar{\mathbf{R}}^T\left[\Delta\tilde{\boldsymbol{\theta}}^T\delta\tilde{\boldsymbol{\theta}}^T\bar{\mathbf{x}}_{0,S} + \delta\tilde{\boldsymbol{\theta}}^T\Delta\mathbf{u}_{0,S} + \Delta\tilde{\boldsymbol{\theta}}^T\delta\mathrm{x}_{0,S}\right] + O(t^2)\end{aligned} \tag{4.92}$$

on use of eq.(89). In the basis $\{\mathbf{t}_i\}$ the above variations and increments have the following components

$$\begin{aligned}\delta\varepsilon_{11} &= \delta\beta\;\bar{x}_{03,S} + \delta x_{01,S}, \qquad & \delta\varepsilon_{13} &= -\delta\beta\;\bar{x}_{01,S} + \delta x_{03,S} \\ \Delta\varepsilon_{11} &= \Delta\beta\;\bar{x}_{03,S} + \Delta x_{01,S}, \qquad & \Delta\varepsilon_{13} &= -\Delta\beta\;\bar{x}_{01,S} + \Delta x_{03,S} \\ \Delta\delta\varepsilon_{11} &= -\Delta_{\beta}\delta\beta\bar{x}_{01,S} + \delta\beta\;\Delta x_{03,S} + \Delta\beta\;\delta x_{03,S}, \\ \Delta\delta\varepsilon_{13} &= -\Delta_{\beta}\delta\beta\bar{x}_{03,S} - \delta\beta\;\Delta x_{01,S} - \Delta\beta\;\delta x_{01,S}\end{aligned} \tag{4.93}$$

where $x_{01,S} = \mathbf{x}_{0,S}\cdot\mathbf{a}_1$ and $x_{03,S} = \mathbf{x}_{0,S}\cdot\mathbf{a}_3$. In the derivation of the above also equalities $\delta\tilde{\boldsymbol{\theta}}\mathbf{a}_1 = \delta\beta\mathbf{a}_3$ and $\delta\tilde{\boldsymbol{\theta}}\mathbf{a}_3 = -\delta\beta\mathbf{a}_1$ were used.

b) Transverse strain vector $\boldsymbol{\varepsilon}_3 = (\lambda - 1)\mathbf{t}_3$, where $\lambda = \exp(\mu)$. Its variation is

$$\delta\boldsymbol{\varepsilon}_3 = \delta\lambda\mathbf{t}_3 = \exp(\mu)\mathbf{t}_3\delta\mu \tag{4.94}$$

For the increment of strain defined as $\Delta\boldsymbol{\varepsilon}_3 \equiv \boldsymbol{\varepsilon}_3 - \bar{\boldsymbol{\varepsilon}}_3$ we obtain

$$\Delta\boldsymbol{\varepsilon}_3 = (\Delta\lambda - 1)\bar{\lambda}\mathbf{t}_3 = [\exp(t\Delta\mu) - 1]\exp(\bar{\mu})\mathbf{t}_3 = t\Delta\mu\exp(\bar{\mu})\mathbf{t}_3 + O(t^2) \tag{4.95}$$

where $\Delta\lambda = \exp(t\Delta\mu)$ and $\bar{\lambda} = \exp(\bar{\mu})$ are used. The increment of variation of strain is defined as $\Delta\delta\boldsymbol{\varepsilon}_3 \equiv \delta\boldsymbol{\varepsilon}_3 - \delta\bar{\boldsymbol{\varepsilon}}_3$. For the incremental form of variation $\delta\boldsymbol{\varepsilon}_3 = \exp(\bar{\mu} + t\Delta\mu)\mathbf{t}_3\delta\mu$ we obtain

$$\Delta\delta\boldsymbol{\varepsilon}_3 = [\exp(\bar{\mu} + t\Delta\mu) - \exp(\bar{\mu})]\,\mathbf{t}_3\delta\mu = t\Delta\mu\exp(\bar{\mu})\mathbf{t}_3\delta\mu + O(t^2) \tag{4.96}$$

The components in the basis $\{\mathbf{t}_i\}$ can be easily identified.

c) Change of curvature vector $\boldsymbol{\kappa}_1 = \lambda_{,S}\mathbf{t}_3 - \lambda\beta_{,S}\mathbf{t}_1 - \mathbf{t}_{3,S}$. A variation of this vector is as follows

$$\delta\boldsymbol{\kappa}_1 = (\delta\lambda_{,S})\mathbf{t}_3 + (\delta\lambda)\beta_{,S}\mathbf{t}_1 - \lambda(\delta\beta_{,S})\mathbf{t}_1 \tag{4.97}$$

The increment of strain is defined as $\Delta\boldsymbol{\kappa}_1 \equiv \boldsymbol{\kappa}_1 - \bar{\boldsymbol{\kappa}}_1$, and for the incremental form

$$\boldsymbol{\kappa}_1 = (\Delta\lambda\bar{\lambda})_{,S}\mathbf{t}_3 - (\Delta\lambda\bar{\lambda})(\bar{\beta} + t\Delta\beta)_{,S}\mathbf{t}_1 - \mathbf{t}_{3,S} \tag{4.98}$$

we obtain

$$\begin{aligned}\Delta\boldsymbol{\kappa}_1 &= [(\Delta\lambda - 1)\bar{\lambda}]_{,S}\mathbf{t}_3 - [(\Delta\lambda - 1)\bar{\lambda}\bar{\beta}_{,S} + \Delta\lambda\bar{\lambda}\Delta\beta_{,S}]\mathbf{t}_1 \qquad (4.99)\\ &= t[\Delta\mu_{,S}\exp(\bar{\mu}) + \Delta\mu\exp(\bar{\mu})_{,S}]\mathbf{t}_3 - t[\Delta\mu\exp(\bar{\mu})\bar{\beta}_{,S} + \exp(\bar{\mu})\Delta\beta_{,S}]\mathbf{t}_1 + O(t^2)\end{aligned}$$

The increment of variation of strain is defined as $\Delta\delta\boldsymbol{\kappa}_1 \equiv \delta\boldsymbol{\kappa}_1 - \delta\bar{\boldsymbol{\kappa}}_1$. For the incremental form of the variation

$$\delta\boldsymbol{\kappa}_1 = (\delta\lambda)_{,S}\mathbf{t}_3 - [\delta\lambda(\bar{\beta} + \Delta\beta)_{,S} + (\Delta\lambda\bar{\lambda})\delta\beta_{,S}]\mathbf{t}_1 \tag{4.100}$$

after several transformations, we obtain

$$\begin{aligned}\Delta\delta\boldsymbol{\kappa}_1 &= t\left[\delta\mu\exp(\bar{\mu})\mu_{,S}\Delta\mu + \delta\mu\exp(\bar{\mu})\Delta\mu_{,S} + \delta\mu_{,S}\exp(\bar{\mu})\Delta\mu\right]\mathbf{t}_3\\ &- t\left[\delta\mu\exp(\bar{\mu})\beta_{,S}\Delta\mu + \delta\mu\exp(\bar{\mu})\Delta\beta_{,S} + \delta\beta_{,S}\exp(\bar{\mu})\Delta\mu\right]\mathbf{t}_1 + O(t^2) \qquad (4.101)\end{aligned}$$

The components in the basis $\{\mathbf{t}_i\}$ can be easily identified.

The above expressions when used in eq.(86) provide formulae from which the tangent matrix $\mathbf{K}$ is derived. To develop a two-noded isoparametric finite element the approximation shape function are introduced as follows

$$\mathbf{a}(\xi) = \sum_{I=1}^{2} N_I(\xi)\mathbf{a}_I, \qquad \mathbf{x}(\xi) = \sum_{I=1}^{2} N_I(\xi)\mathbf{x}_I \tag{4.102}$$

where $\mathbf{a}_I$ and $\mathbf{x}_I$ denote values at node I, and the shape functions are $N_1(\xi) = \frac{1}{2}(1+\xi)$, $N_2(\xi) = \frac{1}{2}(1-\xi)$, and $\xi \in [-1,\ 1]$ for $\xi = 2x/l - 1$, and $x \in [0,\ l]$.

The displacement stiffness matrices, obtained from the first term of the directional derivative (85), can be calculated as $\mathbf{K}_0 + \mathbf{K}_L = \mathbf{B}^T\mathbf{D}\mathbf{B}$, where $\mathbf{D}$ is the constitutive matrix specified in accordance with Section 4.1.5. Consider the tangent operator of the strain-displacement relation, $\mathbf{B} \equiv \partial\boldsymbol{\varepsilon}/\partial\mathbf{a}$, where $\boldsymbol{\varepsilon}$ has the components $\varepsilon_{11}, \varepsilon_{13}, \varepsilon_{33}, \kappa_{11}, \kappa_{13}$. The derived earlier variations of strain components can be written as $\delta\boldsymbol{\varepsilon} = \mathbf{B}\delta\mathbf{a}$, so the form of $\mathbf{B}$ is

$$(\mathbf{B})_I = \begin{bmatrix} N_{I,\xi} & 0 & \bar{x}_{03,S}N_I & 0\\ 0 & N_{I,\xi} & -\bar{x}_{01,S}N_I & 0\\ 0 & 0 & 0 & \exp(\bar{\mu})N_I\\ 0 & 0 & -\exp(\bar{\mu})N_{I,\xi} & -\exp(\bar{\mu})\beta_{,S}N_I\\ 0 & 0 & 0 & \exp(\bar{\mu})N_{I,\xi} + \exp(\bar{\mu})_{,S}N_I \end{bmatrix} \tag{4.103}$$

where I denotes the node. Note that the columns are multiplied by $\delta\mathbf{a}$ for the node I.

The initial stress matrix $\mathbf{K}_\sigma$, which is obtained from the second term of the directional derivative (85), is defined as follows

$$\mathbf{K}_\sigma = \begin{bmatrix} (\mathbf{K}_\sigma)_{11} & (\mathbf{K}_\sigma)_{12}\\ (\mathbf{K}_\sigma)_{21} & (\mathbf{K}_\sigma)_{22} \end{bmatrix}, \qquad (\mathbf{K}_\sigma)_{IJ} = \begin{bmatrix} 0 & 0 & b_3 & 0\\ 0 & 0 & b_4 & 0\\ b_1 & b_2 & b_5 & b_8\\ 0 & 0 & b_7 & b_6 \end{bmatrix} \tag{4.104}$$

where

$$b_1 = -N_I\, n^B_{13}\, N_{J,\xi}, \qquad b_3 = -N_{I,\xi}\, n^B_{13}\, N_J, \qquad b_2 = N_I\, n^B_{11}\, N_{J,\xi}, \qquad b_4 = N_{I,\xi}\, n^B_{11}\, N_J$$

$$b_5 = N_I\, c_0\, N_J, \qquad b_6 = N_I\, c_1\, N_J, \qquad b_7 = N_I\, c_2\, N_{J,\xi} \qquad b_8 = N_{I,\xi}\, c_2\, N_J \tag{4.105}$$

and the coefficients are as follows

$$c_0 = -n^B_{11}\bar{x}_{01,S} - n^B_{13}\bar{x}_{03,S}, \qquad c_1 = n^B_{33}\exp(\bar{\mu}) - m^B_{11}\exp(\bar{\mu})\beta_{,S}, \qquad c_2 = -m^B_{11}\exp(\bar{\mu}) \tag{4.106}$$

The element is integrated at one Gauss point, located at the middle of the element.

4.4.2 Stabilization of tangent matrix

Let us consider a two-noded element obtained via direct finite element discretization and reduced (one-point) integration. The equations for the normal extension nodal variables μ_1 and μ_2, are identical, and, in consequence, the tangent matrix of the element is singular and cannot be inverted. To simplify the problem these rows and columns of the tangent matrix which are not related to the extension variables, are neglected, and the equations reduce to: $\mathbf{K}\Delta\boldsymbol{\mu} = \hat{\mathbf{q}}$, where

$$\mathbf{K} = k\begin{bmatrix} 1 & 1 \\ 1 & 1 \end{bmatrix}, \qquad \boldsymbol{\mu} = \begin{Bmatrix} \mu_1 \\ \mu_2 \end{Bmatrix}, \qquad \hat{\mathbf{q}}_{\parallel} = \begin{Bmatrix} q_1 \\ q_2 \end{Bmatrix} \tag{4.107}$$

where the subscript 1 and 2 indicate the nodal values.

The tangent matrix $\mathbf{K}$ has two eigenpairs: $\{2k, \mathbf{s}\}$ and $\{0, \mathbb{h}\}$, where $\mathbf{s} = \{1, 1\}$ and $\mathbf{h} = \{1, -1\}$. The following modes of deformation are associated with the eigenvectors: $\mathbf{s}$ represents the uniform extension mode, while $\mathbf{h}$, represents the hourglass mode, which is spurious, and must be stabilized.

Method 1. Consider the following stabilization matrix

$$\mathbf{K}_{stab} = \alpha\begin{bmatrix} 1 & 0 \\ 0 & 1 \end{bmatrix} \tag{4.108}$$

where α is a stabilization coefficient. Note that for $\alpha \neq 0$ we have $\det(\mathbf{K} + \mathbf{K}_{stab}) = (2k + \alpha)\alpha \neq 0$. Solving $(\mathbf{K} + \mathbf{K}_{stab})\Delta\boldsymbol{\mu} = \hat{\mathbf{q}}$ we have

$$\Delta\mu_1 = \frac{k(q_1 - q_2) + q_1\alpha}{(2k + \alpha)\alpha}, \qquad \Delta\mu_2 = \frac{k(q_2 - q_1) + q_2\alpha}{(2k + \alpha)\alpha} \tag{4.109}$$

To check these solutions for the defined earlier two modes of deformation we note that these modes correspond to the loads $q_1 = q_2$ and $q_1 = -q_2$, respectively.

For $q_1 = q_2$ we obtain

$$\Delta\mu_1 = \Delta\mu_2 = \frac{q_1}{2k + \alpha} \tag{4.110}$$

For reference, we must find a correct solution for this loading. Introduce new variables, $\mu_m = \frac{1}{2}(\mu_1 + \mu_2)$ and $q_m = \frac{1}{2}(q_1 + q_2)$, associated with the middle point of the element. Adding the columns and rows of eq.(107) we obtain a new equation: $2k\Delta\mu_m = q_m$, which

has the solution $\Delta\mu_m = q_m/(2k)$. Note that for $\alpha \to 0$ the solution eq.(109) converges to the value for the middle point.

For $q_1 = -q_2$ we obtain

$$\Delta\mu_1 = -\Delta\mu_2 = \frac{q_1}{\alpha} \tag{4.111}$$

This solution always provides $\Delta\mu_m = \frac{1}{2}(\Delta\mu_1 + \Delta\mu_2) = 0$, what is correct. On the other hand, when $\alpha \to 0$ then $\Delta\mu_1 = -\Delta\mu_2 \to \infty$, hence a non-zero value of α must be used. Besides, α must be non-zero to provide a constitutive link, as the solution does not depend on the stiffness k. We observe that this requirement is in contradiction with the one for the first case of loading (mode of deformation), where $\alpha \to 0$ was assumed.

Method 2. Consider the following stabilization matrix

$$\mathbf{K}_{stab} = \alpha \begin{bmatrix} 1 & -1 \\ -1 & 1 \end{bmatrix} \tag{4.112}$$

Then, $\det(\mathbf{K} + \mathbf{K}_{stab}) = 4k\alpha \neq 0$, though the stabilization matrix is also singular. Solving $(\mathbf{K} + \mathbf{K}_{stab})\Delta\boldsymbol{\mu} = \hat{\mathbf{q}}$ we have

$$\Delta\mu_1 = \frac{k(q_1 - q_2) + (q_1 + q_2)\alpha}{4k\alpha}, \qquad \Delta\mu_2 = \frac{k(q_2 - q_1) + (q_2 + q_2)\alpha}{4k\alpha} \tag{4.113}$$

For $q_1 = q_2$ and $q_1 = -q_2$ we obtain, respectively,

$$\Delta\mu_1 = \Delta\mu_2 = \frac{q_1}{2k}, \qquad \Delta\mu_1 = -\Delta\mu_2 = \frac{q_1}{2\alpha} \tag{4.114}$$

Again, α must be finite and provide a physically justified link between $\Delta\mu_1$ and q_1. However, now the situation is different than for Method 1, because the solution for the first mode does not depend on α, and there is no previous contradiction.

The stabilization matrix eq.(112) can be also introduced with the help of the measure $\kappa_{13} = \frac{1}{2}\lambda_{,S}$, see eq.(16), which is missing in the virtual work of the beam resultants, eq.(36). Let us supplement the virtual work (36) and $G(\mathbf{a})$ in eq.(83) by the term $2\alpha_1\, \kappa_{13}\, \delta\kappa_{13}$. Note that $\lambda_{,S} = e^{\mu}\mu_{,S} \approx \mu_{,S}$, for a small normal strain. Then, the first of eq.(83) yields $(\mathbf{K} + \mathbf{K}_{stab})\Delta\boldsymbol{\mu} = \hat{\mathbf{q}} + \hat{\mathbf{q}}_{stab}$, where

$$\mathbf{K}_{stab} = \frac{\alpha_1}{2l^2} \begin{bmatrix} 1 & -1 \\ -1 & 1 \end{bmatrix}, \qquad \hat{\mathbf{q}}_{stab} = -\frac{\alpha_1}{2l^2}(\mu_2 - \mu_1) \begin{Bmatrix} -1 \\ 1 \end{Bmatrix} \tag{4.115}$$

The factor $\alpha_1/(2l^2)$ is replaced by α, which is assumed similarly as for the shear locking corrections, see e.g. [Fried, 1973] or [Hughes, Taylor, Kanoknukulchai, 1977]. The stabilization factor is taken in the form $\alpha = c_1 \frac{5}{6} Gbhl$, where l is the length, h is the thickness, and b is the width of the element. The unknown constant c_1 is determined from the problem of bending of a square membrane, see Test 4 in Section 4.4.5.

Note that at the Gauss point, $\kappa_{13} = \frac{1}{2l}(\mu_2 - \mu_1) = \frac{1}{2l}\mathbf{h}\{\mu_1, \mu_2\}$, where explicitly the hourglass mode $\mathbf{h}$ is used. This allows to draw the conclusion that Method 2 belongs to the class of the gamma stabilization methods, described for other applications e.g. in [Belytschko, Ong, Liu, Kennedy, 1984]. Note that the gamma method is never used for the beam elements based on the standard Reissner hypothesis, as then the under-integration does not imply singularity of the tangent matrix.

4.4.3 Conversion to four-noded quadrilateral

Assume that the displacements associated with the upper and the lower line bounding the beam, see Fig.4.16, are called the interface variables, and denoted by $\mathbf{u}^+$ and $\mathbf{u}^-$. For the Reissner kinematics with the extensible director, the interface variables are determined as follows

$$\mathbf{u}^+ = \mathbf{u}_0 + \frac{1}{2}h[\,\lambda\mathbf{R} - \mathbf{I}\,]\,\mathbf{t}_3, \qquad \mathbf{u}^- = \mathbf{u}_0 - \frac{1}{2}h[\,\lambda\mathbf{R} - \mathbf{I}\,]\,\mathbf{t}_3 \tag{4.116}$$

where $\mathbf{R}$ is the rotation tensor, $\mathbf{u}_0$ is the displacement at the middle line, and λ is the transverse extension coefficient. Next, assume that $\mathbf{u}^+$ and $\mathbf{u}^-$ are known and $\mathbf{u}_0$, $\mathbf{R}$ and λ are sought. On addition and subtraction of equations in (115), and elementary algebraic manipulations we obtain the inverse relations,

$$\mathbf{u}_0 = \frac{1}{2}(\mathbf{u}^+ + \mathbf{u}^-), \qquad \lambda\mathbf{R}\mathbf{t}_3 = \frac{1}{h}(\mathbf{u}^+ - \mathbf{u}^-) + \mathbf{t}_3 \tag{4.117}$$

Note that from the second of the above equations $\lambda = \|\frac{1}{h}(\mathbf{u}^+ - \mathbf{u}^-) + \mathbf{t}_3\|$. The above equations furnish the transformation formulae between $\{\mathbf{u}^+, \mathbf{u}^-\}$ and $\{\mathbf{u}_0, \mathbf{R}, \lambda\}$.

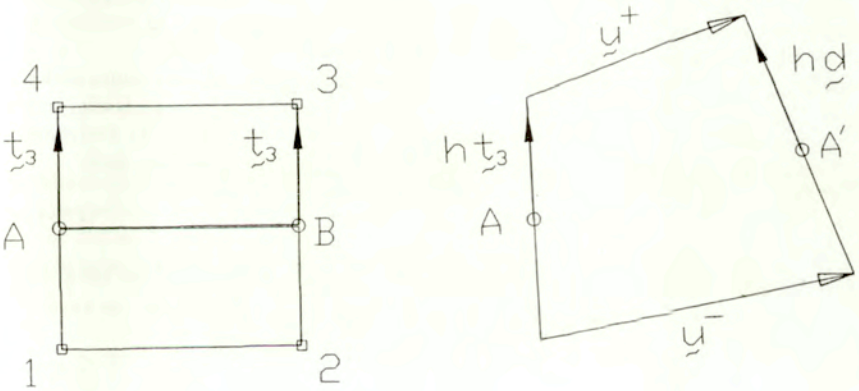

Fig.4.16 Notation for conversion to quadrilateral

For the deformation in the plane spanned by vectors $\mathbf{t}_1$ and $\mathbf{t}_3$, the representations are as follows: the middle line variables are $\mathbf{u}_0 = u\mathbf{t}_1 + w\mathbf{t}_3$, R is given by

$$\mathbf{R} = \cos\beta(\mathbf{t}_1 \otimes \mathbf{t}_1 + \mathbf{t}_3 \otimes \mathbf{t}_3) + \sin\beta(\mathbf{t}_3 \otimes \mathbf{t}_1 - \mathbf{t}_1 \otimes \mathbf{t}_3) + \mathbf{t}_2 \otimes \mathbf{t}_2 \tag{4.118}$$

the interface displacements are $\mathbf{u}^+ = u^+\mathbf{t}_1 + w^+\mathbf{t}_3$ and $\mathbf{u}^- = u^-\mathbf{t}_1 + w^-\mathbf{t}_3$. Then, $\mathbf{R}\mathbf{t}_3 = \cos\beta\mathbf{t}_3 - \sin\beta\mathbf{t}_1$, and in terms of components eq.(117) can be re-written as

$$u_0 = \frac{1}{2}(u^+ + u^-), \qquad w_0 = \frac{1}{2}(w^+ + w^-) \tag{4.119}$$

$$\lambda\sin\beta = -\frac{1}{h}(u^+ - u^-), \qquad \lambda\cos\beta = \frac{1}{h}(w^+ - w^-) + 1 \tag{4.120}$$

To establish a single formula for the rotation angle β we can use one of the two formulae resulting from eq.(120),

$$\beta = \arcsin\frac{-(u^+ - u^-)}{\lambda h}, \qquad \beta = \arccos\frac{(w^+ - w^- + h)}{\lambda h} \tag{4.121}$$

where the arguments of these functions belong to $[-1, +1]$. To find the extension coefficient λ we note that $\lambda^2 = (\lambda\sin\beta)^2 + (\lambda\cos\beta)^2$, and on use of eq.(120) we obtain

$$\lambda^2 = \frac{1}{h^2}\left\{\left[(w^+ - w^-) + h\right]^2 + (u^+ - u^-)^2\right\} \tag{4.122}$$

In accordance with the exponential parameterization described earlier, the new extension coefficient $\mu = \ln\lambda$ is introduced. Note that, for the planar deformation, four interface variables $\mathbf{z} = \{u^+, w^+, u^-, w^-\}$ are used to determine four middle line variables, $\mathbf{a} = \{u_0, w_0, \beta, \mu\}$, and that the standard Reissner hypothesis, which yields a theory with three parameters, $\{u_0, w_0, \beta\}$, does not suffice in case of finite rotations to establish a one-to-one transformation formula with the interface variables.

Two difficulties are related to the above transformation formulae. Firstly, values of the arcsin and arccos functions are in the range $[-\pi/2, +\pi/2]$ and $[0, \pi]$, respectively, and the rotations, which are out of this range cannot be obtained from eq.(121). To overcome this limitation, instead of this equation, the following incremental equation is used,

$$\beta^{n+1} = \beta^n + \frac{\partial\beta}{\partial\mathbf{z}}\Delta\mathbf{z} \tag{4.123}$$

where $\Delta\mathbf{z} = \mathbf{z}^{n+1} - \mathbf{z}^n$, and the superscripts $n+1$ and n indicate the iteration numbers. The expressions for $\partial\beta/\partial\mathbf{z}$ are as follows. For $\beta = \arcsin\frac{(u^+ - u^-)}{\lambda h}$ we have

$$\frac{\partial\beta}{\partial u^+} = -\frac{|w^+ - w^- + h|}{(\lambda h)^2}, \qquad \frac{\partial\beta}{\partial w^+} = s\frac{(u^+ - u^-)}{(\lambda h)^2} \tag{4.124}$$

where $s = sign(w^+ - w^- + h)$. Besides, $\partial\beta/\partial u^- = -\partial\beta/\partial u^+$ and $\partial\beta/\partial w^- = -\partial\beta/\partial w^+$. For $\beta = \arccos\frac{(w^+ - w^- + h)}{\lambda h}$ we have

$$\frac{\partial\beta}{\partial u^+} = s\frac{(w^+ - w^- + h)}{(\lambda h)^2}, \qquad \frac{\partial\beta}{\partial w^+} = -\frac{|u^+ - u^-|}{(\lambda h)^2} \tag{4.125}$$

where $s = sign(u^+ - u^-)$. Again $\partial\beta/\partial u^- = -\partial\beta/\partial u^+$ and $\partial\beta/\partial w^- = -\partial\beta/\partial w^+$.

Secondly, β and μ are nonlinear functions of $\mathbf{z}$, and must be linearized prior to use in the Newton-Raphson scheme. The increment of the rotation β is defined as follows

$$\Delta\beta \equiv \beta^{n+1} - \beta^n \approx \frac{\partial\beta}{\partial\mathbf{z}}\Delta\mathbf{z} \tag{4.126}$$

where the particular derivatives have been specified above. The increment of the extension coefficient $\mu = \ln\lambda$ is defined as follows

$$\Delta\mu \equiv \mu^{n+1} - \mu^n \approx \frac{\partial\mu}{\partial \mathrm{z}}\Delta \mathrm{z} \tag{4.127}$$

where

$$\frac{\partial\mu}{\partial u^+} = \frac{(u^+ - u^-)}{(\lambda h)^2}, \qquad \frac{\partial\mu}{\partial w^+} = \frac{(w^+ - w^- + h)}{(\lambda h)^2} \tag{4.128}$$

Besides, $\partial\mu/\partial u^- = -\partial\mu/\partial u^+$ and $\partial\mu/\partial w^- = -\partial\mu/\partial w^+$.

Finally, for all variables, the incremental conversion formula can be written as follows

$$\left\{\begin{array}{c} \Delta u_0 \\ \Delta w_0 \\ \Delta\beta \\ \Delta\mu \end{array}\right\} = \left[\begin{array}{cccc} \frac{1}{2} & 0 & \frac{1}{2} & 0 \\ 0 & \frac{1}{2} & 0 & \frac{1}{2} \\ \frac{\partial\beta}{\partial u^+} & \frac{\partial\beta}{\partial w^+} & \frac{\partial\beta}{\partial u^-} & \frac{\partial\beta}{\partial w^-} \\ \frac{\partial\mu}{\partial u^+} & \frac{\partial\mu}{\partial w^+} & \frac{\partial\mu}{\partial u^-} & \frac{\partial\mu}{\partial w^-} \end{array}\right] \left\{\begin{array}{c} \Delta u^+ \\ \Delta w^+ \\ \Delta u^- \\ \Delta w^- \end{array}\right\} \tag{4.129}$$

where the increments are defined as differences between the values for iteration $n+1$ and the values for iteration n. At $\mathbf{z} = 0$, the particular derivatives are

$$\frac{\partial\beta}{\partial u^+} = -\frac{1}{h}, \qquad \frac{\partial\beta}{\partial w^+} = 0, \qquad \frac{\partial\mu}{\partial u^+} = 0, \qquad \frac{\partial\mu}{\partial w^+} = -\frac{1}{h} \tag{4.130}$$

and the transformation matrix becomes

$$\left[\begin{array}{cccc} \frac{1}{2} & 0 & \frac{1}{2} & 0 \\ 0 & \frac{1}{2} & 0 & \frac{1}{2} \\ -\frac{1}{h} & 0 & +\frac{1}{h} & 0 \\ 0 & +\frac{1}{h} & 0 & -\frac{1}{h} \end{array}\right] \tag{4.131}$$

where its determinant is equal to $-1/h^2$. Let us additionally assume that the thickness changes can be neglected, i.e. $\lambda = 1$ (or $\mu = 0$), and that the normal displacements of the top and the bottom of the beam are approximately equal, i.e. $\Delta w^+ \approx \Delta w^- = \Delta w$. Then, eq.(129) reduces to

$$\left\{\begin{array}{c} \Delta u_0 \\ \Delta w_0 \\ \Delta\beta \end{array}\right\} = \left[\begin{array}{ccc} 0 & \frac{1}{2} & \frac{1}{2} \\ 1 & 0 & 0 \\ 0 & -\frac{1}{h} & +\frac{1}{h} \end{array}\right] \left\{\begin{array}{c} \Delta w \\ \Delta u^+ \\ \Delta u^- \end{array}\right\} \tag{4.132}$$

where the determinant of the transformation matrix is equal to $-1/h$. The above matrix was used for linear kinematics in Section 4.2.1.

Below, a scheme of converting of a discrete model of the beam with the extensible director to a four-noded element is explained. Linearization and the isoparametric linear approximation of the virtual work equation yields the first equation of the Newton-Raphson solution scheme eq.(84) in the following form

$$\delta\mathbf{a}^T\,\mathbf{K}^n\,\Delta\mathbf{a} \;=\; \delta\mathbf{a}^T\,\hat{\mathbf{p}} \;-\; \delta\mathbf{a}^T\,\mathbf{f}^n \tag{4.133}$$

where $\mathbf{K}^n$ denotes the tangent stiffness matrix, $\mathbf{f}^n$ is a vector of internal forces, $\hat{\mathbf{p}}$ is the vector of external loads applied at nodes. To prevent shear locking of the element

the tangent matrix $\mathbf{K}^n$ is uniformly under-integrated, and stabilized as described in Section 4.4.2. In this way, a two-noded isoparametric uniformly under-integrated element for the equations of the finite rotation beam with the extensible director is obtained.

This beam element is converted to a four-noded element expressed in terms of the interface variables $\mathbf{z}$ on use of the formula eq.(129). Let us denote the transformation (tangent) operator by $\mathbf{A} \equiv \partial \mathbf{a}/\partial \mathbf{z}$, and re-write eq.(129) as $\Delta \mathbf{a} = \mathbf{A}\, \Delta \mathbf{z}$. Using this operator also for $\delta \mathbf{a}$, the virtual work eq.(133) can be transformed as follows

$$\delta \mathbf{z}^T\, \mathbf{K}_s^n\, \Delta \mathbf{z} \;=\; \delta \mathbf{z}^T\, \hat{\mathbf{p}}_s \;-\; \delta \mathbf{z}^T\, \mathbf{f}_s^n \tag{4.134}$$

where $\mathbf{K}_s^n = \mathbf{A}^T\, \mathbf{K}^n\, \mathbf{A}$ is the tangent stiffness matrix, and $\mathbf{f}_s^n = \mathbf{A}^T\, \mathbf{f}^n$ is the internal force vector for the four-noded element. The external loads $\hat{\mathbf{p}}_s$ must be prescribed as for a four-noded plane stress element.

4.4.4 Virtual work of external moment for quadrilateral

Let us consider the virtual work of an external moment $\delta \mathcal{A}_b = \hat{\mathbf{m}} \cdot \delta \boldsymbol{\theta}$. For the planar deformation, when $\hat{\mathbf{m}} = \hat{m}\mathbf{t}_2$ and $\boldsymbol{\theta} = \beta \mathbf{t}_2$, we have

$$\delta \mathcal{A}_b = \hat{\mathbf{m}} \cdot \delta \boldsymbol{\theta} = \hat{m}\, \delta \beta \tag{4.135}$$

As shown in the earlier section, the middle-line variables can be expressed in terms of the variables associated with the upper an lower bounding lines, for an arbitrary cross-section. For the rotation angle β, the appropriate relation is given by eq.(121), and it symbolically can be written as $\beta = \beta(\mathbf{z})$, where $\mathbf{z}$ denotes the interface variables. Then, on use of the chain rule of differentiation, $\delta \beta = \frac{\partial \beta}{\partial \mathbf{z}} \delta \mathbf{z}$, where the derivatives of β are specified by eq.(124) and (125) for β depending on arcsin and arccos, respectively. Besides, $\partial \beta/\partial u^- = -\partial \beta/\partial u^+$ and $\partial \beta/\partial w^- = -\partial \beta/\partial w^+$, and, hence

$$\delta \mathcal{A}_b = \hat{m} \left[(\delta u^+ - \delta u^-) c + (\delta w^+ - \delta w^-) d \right] \tag{4.136}$$

where $c \equiv \partial \beta/\partial u^+$ and $d \equiv \partial \beta/\partial w^+$.

Recall that in Section 4.4.1 the derivative of G at $\bar{\mathbf{z}}$ in direction $\Delta \mathbf{z}$ has been considered to find the tangent matrix. Note that $\delta \mathcal{A}_b$ depends on c and d, which are functions of $\mathbf{z}$, and hence they also contribute to the directional derivative. Now, $G_m(\mathbf{z}) = \delta \mathcal{A}_b$ is used instead of $G(\mathbf{z})$, and the derivative with respect to $\mathbf{z}$ is as below

$$\frac{\partial G_m}{\partial \mathbf{z}} \Delta \mathbf{z} = \hat{m} \left[(\delta u^+ - \delta u^-) \frac{\partial c}{\partial \mathbf{z}} \Delta \mathbf{z} + (\delta w^+ - \delta w^-) \frac{\partial d}{\partial \mathbf{z}} \Delta \mathbf{z} \right] \tag{4.137}$$

For $\beta = \arcsin \frac{-(u^+ - u^-)}{\lambda h}$ we have

$$c = -\frac{\sqrt{(w^+ - w^- + h)^2}}{(\lambda h)^2}, \qquad d = s \frac{(u^+ - u^-)}{(\lambda h)^2} \tag{4.138}$$

where $s = sign(w^+ - w^- + h)$, for which we obtain the following derivatives

$$\frac{\partial c}{\partial u^+} = \frac{2(u^+ - u^-)|w^+ - w^- + h|}{(\lambda h)^4}, \qquad \frac{\partial c}{\partial w^+} = s \frac{(w^+ - w^- + h)^2 - (u^+ - u^-)^2}{(\lambda h)^4} \tag{4.139}$$

Besides, $\partial d/\partial u^+ = \partial c/\partial w^+$ and $\partial d/\partial w^+ = -\partial c/\partial u^+$. For $\beta = \arccos\frac{(w^+ - w^- + h)}{\lambda h}$ we have

$$c = s\frac{(w^+ - w^- + h)}{(\lambda h)^2}, \qquad d = -\frac{\sqrt{(u^+ - u^-)^2}}{(\lambda h)^2} \tag{4.140}$$

where $s = sign(u^+ - u^-)$, for which we obtain the following derivatives

$$\frac{\partial c}{\partial u^+} = -\frac{2(w^+ - w^- + h)|u^+ - u^-|}{(\lambda h)^4}, \qquad \frac{\partial c}{\partial w^+} = s\frac{(u^+ - u^-)^2 - (w^+ - w^- + h)^2}{(\lambda h)^4} \tag{4.141}$$

and again, $\partial d/\partial u^+ = \partial c/\partial w^+$ and $\partial d/\partial w^+ = -\partial c/\partial u^+$. On use of the above derivatives the tangent operator (load matrix) is as follows

$$\mathbf{K}_m = \frac{\partial G_m}{\partial \mathbf{z}} = \hat{m}\begin{bmatrix} c_{,u} & c_{,w} & -c_{,u} & -c_{,w} \\ d_{,u} & d_{,w} & -d_{,u} & -d_{,w} \\ -c_{,u} & -c_{,w} & c_{,u} & c_{,w} \\ -d_{,u} & -d_{,w} & d_{,u} & d_{,w} \end{bmatrix} = \hat{m}\begin{bmatrix} c_{,u} & c_{,w} & -c_{,u} & -c_{,w} \\ c_{,w} & -c_{,u} & -c_{,w} & c_{,u} \\ -c_{,u} & -c_{,w} & c_{,u} & c_{,w} \\ -c_{,w} & c_{,u} & c_{,w} & -c_{,u} \end{bmatrix} \tag{4.142}$$

where only the derivatives of c with respect to u^+ and w^+ are present. Note that the above load matrix is symmetric. When the external moment is replaced by a pair of co-rotational forces, what is a common approach to external moments, then an unsymmetric load matrix is obtained. Symmetry of the load matrix in the present formulation is an apparent effect of the kinematical hypotheses used to introduce the relation $\beta = \beta(\mathbf{z})$.

4.4.5 Numerical examples

In this section we examine the two-noded beam element with transverse stretch and the four-noded element, both accounting for finite rotations. The elements were developed and tested within the FEAP environment, see e.g. [Zienkiewicz, Taylor, 1989].

Test 1. Stabilization methods for stretching

The eigenvalue calculations reveal that the two-noded beam element possesses four zero eigenvalues, one spurious. Below, the stabilization methods developed in Section 4.4.2, are verified on an example involving only stretching. Assume the following data: the length $L = 10$, the cross-sectional area $A = 1$, the Young's modulus $E = 10^7$, the Poisson ratio $\nu = 0.25$, boundary condition: $u, w, \beta = 0$ at $S = 0$, and a stretching load: $P = 0.5$ at $S = L$. The exact solution is: $u = 5.0 \cdot 10^{-7}$, $\mu = -1.25 \cdot 10^{-8}$, and it is yielded by Method 2.

The results and the conditioning indicators for Method 1 used with various values of the stabilization coefficient $\alpha = 10^n$ are given in Table 4.6. Note that D_{max} and D_{min} are pivot numbers of the $\mathrm{LDL}^{\mathrm{T}}$ decomposition, and $Cond = D_{max}/D_{min}$. The correct values are obtained for $n \in (-4, +1)$; for smaller n this method yields oscillations of μ, while for larger ones the solution is stable but becomes inaccurate. We can see that, when the flexural mode is not excited by the external loads, Method 1 also provides a range of values of n, for which the conditioning is good and the solution is accurate.

Table 4.6. Stabilization Method 1: solution for various $\alpha = 10^n$

	Conditioning			Solution	
n	D_{max}	D_{min}	$Cond$	$u \cdot 10^7$	$\mu \cdot 10^8$
-5	0.2273E+08	0.2200E-3	0.1033E+12	5.00000	-1.24998
-4	0.2273E+08	0.2200E-2	0.1033E+11	5.00000	-1.25000
+1	0.2273E+08	0.2199E3	0.1034E+06	5.00000	-1.25000
+2	0.2273E+08	0.2192E4	0.1037E+05	4.99999	-1.24997

Test 2. Comparison of beam elements with extensible and inextensible director

This example demonstrates that the constitutive equations defined in Section 4.1.5 provide results, which are as accurate as for the inextensible director equations, and additionally correct values of the thickness parameter are obtained. The second purpose is to show that the element with the extensible director can be used within the same range of length/thickness ratios as the element without the transverse stretch.

Let us consider a beam of: $L = 100$, the width $b = 1$, $E = 10^6$, $\nu = 0.3$. The height of the beam h is an independent parameter. One end of the beam is clamped, i.e. $u_1, u_2, \beta = 0$ at $S = 0$, and the other is free. At the free end, $S = L$, the external loads are applied: the axial force P, the transverse force Q, and the moment M. The discrete model consists of 100 two-noded elements. The linear solutions at $S = L$ are reported in Table 4.7. In the tests the height of the beam is varied, $h = 10^n$, and we can see that up to $l/h = 1000$, where l is the element length, the results are accurate. These results also prove that the under-integration used to prevent locking and the stabilization related to the extension parameter μ work very well.

Note that in this test accuracy of the results is an indicator of the conditioning of the tangent matrix, depending on the thickness. Hence, we compare regularity of the results, without attributing them physical meaning.

Table 4.7. Comparison of extensible and inextensible elements for varying thickness

Element with transverse stretch							
		$P=1$		$Q=1$		$M=1$	
n	$Cond$	u_1	μ	u_2	β	u_2	β
0	0.21E07	1.0E-4	-3.00000E-7	4.00021E00	6.00000E-02	6.00000E-02	1.20000E-03
-1	0.21E09	1.0E-3	-3.00000E-6	3.99990E03	6.00000E01	6.00000E01	1.20000E00
-2	0.21E11	1.0E-2	-3.00000E-5	3.99990E06	6.00000E04	6.00000E04	1.20000E03
-3	0.21E13	1.0E-1	-3.00000E-4	3.99994E09	5.99998E07	5.99998E07	1.19999E06
-4	0.21E15	1.0E0	-3.00000E-3	4.05675E12	6.07222E10	6.07222E10	1.20914E09
-5	0.27E16	1.0E1	-2.99997E-2	2.55119E14	7.25949E12	7.25949E12	4.16655E11
-6	0.20E17	1.0E2	-3.00442E-1	1.84556E16	1.23241E15	1.23241E15	1.71403E14
Element without transverse stretch							
0	0.20E07	1.0E-4	-	4.00021E00	6.00000E-02	6.00000E-02	1.20000E-03
-1	0.20E09	1.0E-3	-	3.99990E03	6.00000E01	6.00000E01	1.20000E00
-2	0.20E11	1.0E-2	-	3.99993E06	6.00004E04	6.00004E04	1.20001E03
-3	0.20E13	1.0E-1	-	3.99992E09	6.00012E07	6.00012E07	1.20003E06
-4	0.20E15	1.0E0	-	4.05675E12	6.07222E10	6.07222E10	1.20914E09
-5	0.21E16	1.0E1	-	2.08635E14	6.34269E12	6.34269E12	3.89822E11
-6	0.19E17	1.0E2	-	2.11137E16	1.46705E15	1.46705E15	1.88261E14

Test 3. Highly nonlinear shallow arch under point load

The geometry of the arch, [Chroscielewski, Schmidt, 1986], is shown in Fig.4.17, and the data is as follow: $R = 150\ in$, $L = 100\ in$, $A = 1\ in^2$, $I = 1\ in^4$. The given cross-sectional area A and moment of inertia I correspond to the thickness $h = 3.4641\ in$ and the width $b = 0.2887\ in$. The slenderness parameters are as follows: $\lambda = \beta^2 R/h \approx 23$, where β is a characteristic angle of the arch, and $L/h \approx 29$. Both edges of the arch are hinged. The cross-section is homogeneous, and $E = 10^7\ lb/in^2$, $\nu = 0.25$. The external vertical force $P = -5 \cdot 10^{-5}$ is applied at the axis of symmetry.

A half of the arch is modeled by 20 two-noded beam elements. Two analyses are performed: with and without a transverse stretch. A response of this arch is very complicated, and the arc-length method is necessary to trace it. The normal displacement w_0, at the axis of symmetry, as a function of the load multiplier is shown in Fig.4.17. Note that the curves for both types of elements coincide. Additionally, the distribution of the stretch parameter μ along the arch is presented in this figure for the chosen points on the $w_0 - load\ multiplier$ curve. The value of μ read from the figure should be multiplied by 10^{-3}. This example demonstrates that the developed two-noded beam element with the transverse stretch performs very well for the highly non-linear example, and yields smooth distributions of the thickness parameter μ.

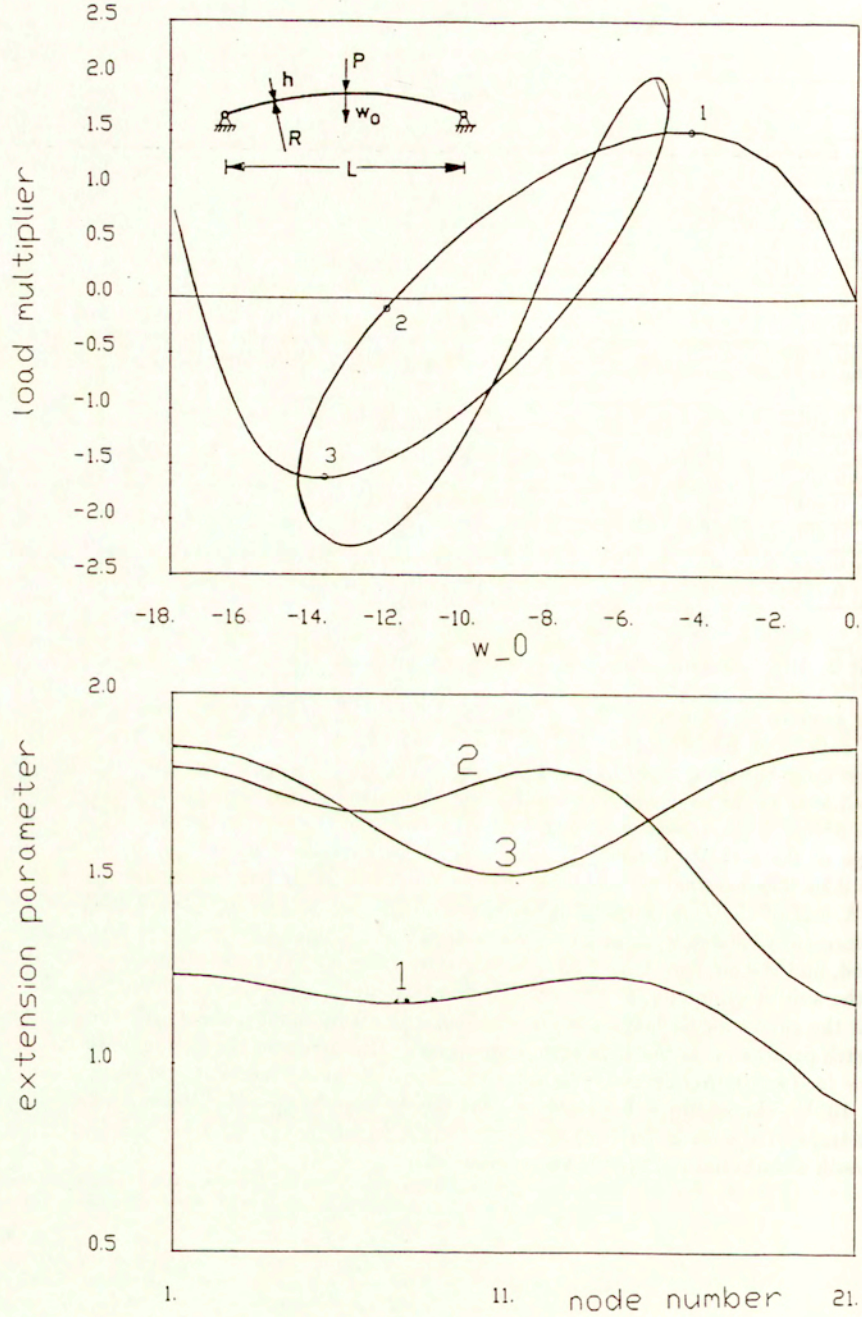

Fig. 4.17 Shallow arch problem

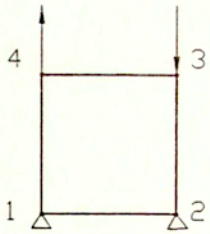

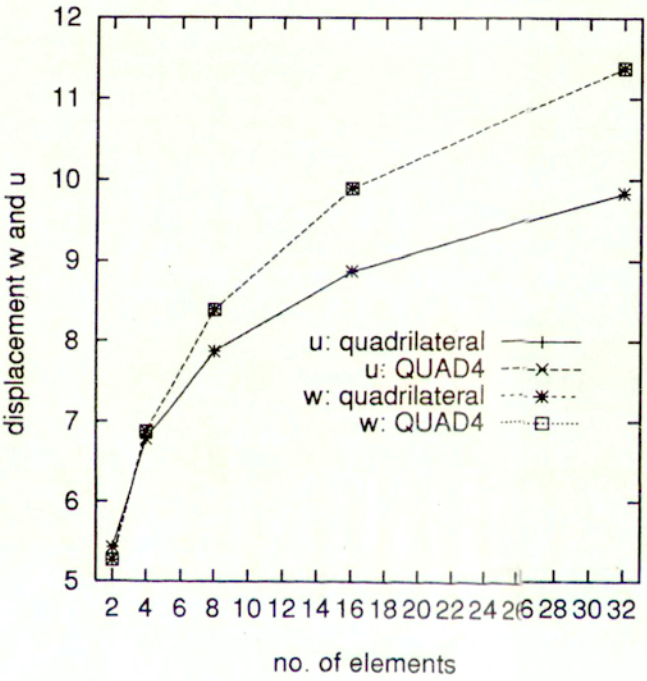

Fig.4.18 Bending of a square problem

Test 4. Bending of a square

The square is shown in Fig.4.18 and the data is: $L = h = b = 1$, $E = 1$ and $\nu = 1/3$. Direct calculations confirm that the element without stabilization possesses 4 zero eigenvalues; three corresponding to the rigid body modes, and one to the spurious bending mode. If the stabilization Method 2 is used then only 3 zero eigenvalues corresponding to the rigid body modes remain.

The test of bending of a single element is essential for deriving the value of the stabilization factor α for Method 2. Assume that displacements of node 1 and 2 are restrained, and forces $P = \pm 1$ are applied at nodes 3 and 4, see Fig.4.18.

The unknown stabilisation constant c_1 is determined by comparison with a solution for the element QUAD4 with 2x2 Gauss point integration. For the mesh of 2x2 elements the optimal value was $c_1 = 0.4$, and this value provided a perfect accuracy also for finer meshes, with up to 32 elements per side of the square. The results are shown in Fig.4.18, where the results yielded by our element and the QUAD4 element fully coincide.

Next, the element is tested to ensure that it yields symmetric response when it should. Several tests performed in both directions, such as stretching and simple shear, confirm that the symmetry of displacements is preserved. Also, a test with a diagonal force applied at node 3 and nodes 1,2 and 4 fully restrained yields that $u = w$ at node 3.

Test 5. Performance of four-noded element for various aspect ratios

The data is the same as used in Test 2 : $L = 100$, $b = 1$, $E = 10^6$, $\nu = 0.3$. The height of the beam h is an independent parameter. The end of the beam at $x = 0$ is clamped, i.e. and the applied boundary conditions are: $u, w = 0$ at node 1, and $u = 0$ at node 102. The other end at $x = L$ is free, and at it the external loads are applied: the axial force P, and the moment M.

A discrete model consists of 100 four-noded elements. The linear solutions at $x = L$ are reported in Table 4.8. The conditioning of the tangent matrix is given as $Cond = D_{max}/D_{min}$, where D_{max} and D_{min} are pivot numbers of the LDL^T decomposition.

In the tests the height of the beam is varied. The value of the transverse extension parameter is calculated from the formula: $\mu = \ln \frac{|w^+ - w^- + h|}{h}$, while the rotation angle from $\beta = \arctan\left(-\frac{u^+ - u^-}{w^+ - w^- + h}\right)$. For stretching we can see that up to $l/h = 1000$, where l is the element length, the results are accurate. For bending this range is diminished and results are acceptable for up to $l/h = 50$. Note that for the elements developed in [Wood, Zienkiewicz, 1977], the stiffness matrix becomes ill-conditioned at $l/h = 25$, but it is not explained which mode of deformation it affects.

Table 4.8. Linear tests of four-noded element for various aspect ratios

Load: $P = 1$					
h	$Cond$	$u^- = u^+$	w^-	w^+	μ
1.0	0.36E07	1.0E-4	-2.95663E-13	-3.00000E-7	-2.99999E-7
0.1	0.29E11	1.0E-3	1.82336E-9	-2.98177E-7	-3.00000E-6
0.01	0.16E15	1.0E-2	-4.80411E-6	-5.10411E-6	-3.00004E-5
0.001	0.64E15	1.0E-1	-2.16948E-5	-2.19948E-5	-3.00045E-4
0.0001	0.16E18	1.0E-0	1.18837E-6	8.88369E-7	-3.00451E-3
Load: $M/h^3 = 1$					
h	u^-	u^-	w^+	w^+	$\beta \cdot 10^{-3}$
1.0	6.00000E-4	6.00000E-2	-6.00000E-4	6.00000E-2	1.19999
0.1	6.00042E-5	6.00061E-2	-6.00042E-5	6.00061E-2	1.20008
0.05	3.00690E-5	6.01958E-2	-3.00690E-5	6.01958E-2	1.20275
0.04	2.39441E-5	5.97872E-2	-2.39441E-5	5.97872E-2	1.19720
0.03	1.77485E-5	5.87927E-2	-1.77485E-5	5.87927E-2	1.18323
0.02	1.20843E-5	6.05314E-2	-1.20843E-5	6.05314E-2	1.20842
0.01	1.66895E-7	-2.58015E-2	-1.66895E-7	-2.58015E-2	0.03337

Test 6. Rectangular membrane

The data for the rectangle is as follows: $L = 64$, $h = 32$, $b = 1$, $E = 1$ and $\nu = 1/3$. At the vertical boundary, $S = 0$, the displacement of nodes is constrained. The external vertical forces are uniformly distributed at the vertical boundary $S = L$, and their sum is equal to 1. This problem is solved using several meshes, with 2,4,8,16 and 32 four-node elements per side. The normal displacements by our element and the standard element QUAD4 (for 1 and 2x2 point Gauss integration) are shown in Fig.4.19. The presented curves are normalised by 37.70. We can see that the results for our quadrilateral are accurate and converge better than these of QUAD4.

Test 7. Cook's membrane

The geometry of the Cook's membrane is shown in Fig.4.20, and the data is: $b = 1$, $E = 1$ and $\nu = 1/3$, the force $P = 1$. This problem is solved using several meshes, with 2,4,8,16 and 32 four-noded elements per side. The normal displacements by our element and the standard element QUAD4 (for 1 and 2x2 point Gauss integration) are shown in Fig.4.20. The reference value used in normalisation of displacements is 23.81, see e.g. [Yuan, Huang, Pian, 1993]. This test indicated that when a mesh is skew then some loss of accuracy appears in the limit, despite the fact that for crude meshes the accuracy is better than of QUAD4. This can be linked to the fact that in the computer implementation the directors coincide with the sides of the element, and are not normal to its middle line.

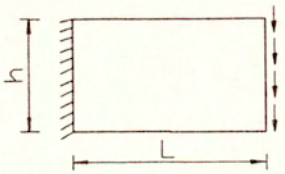

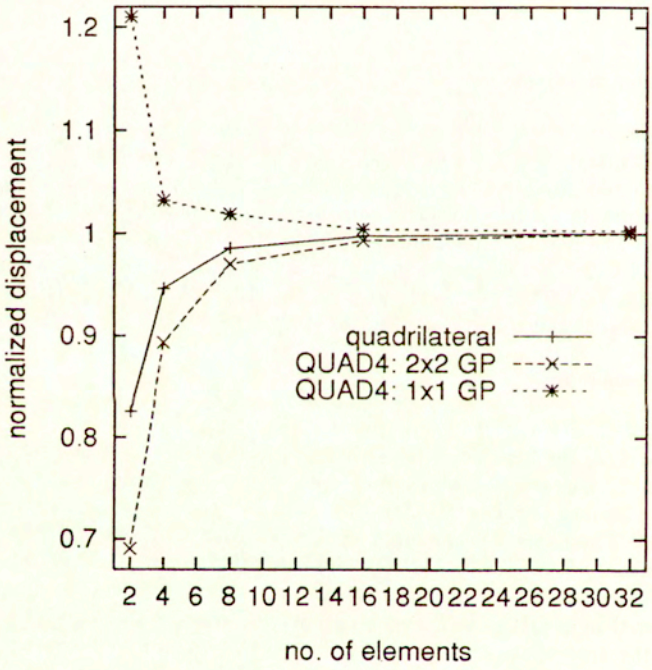

Fig.4.19 Rectangular membrane problem

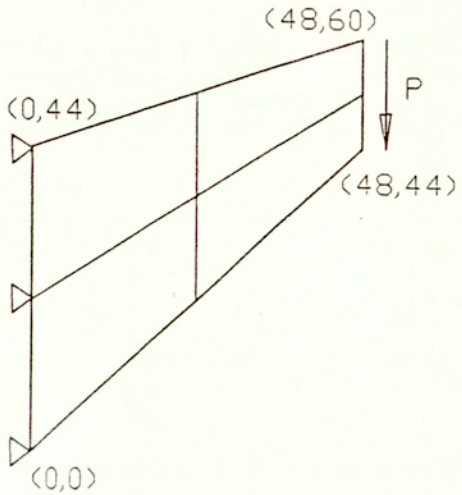

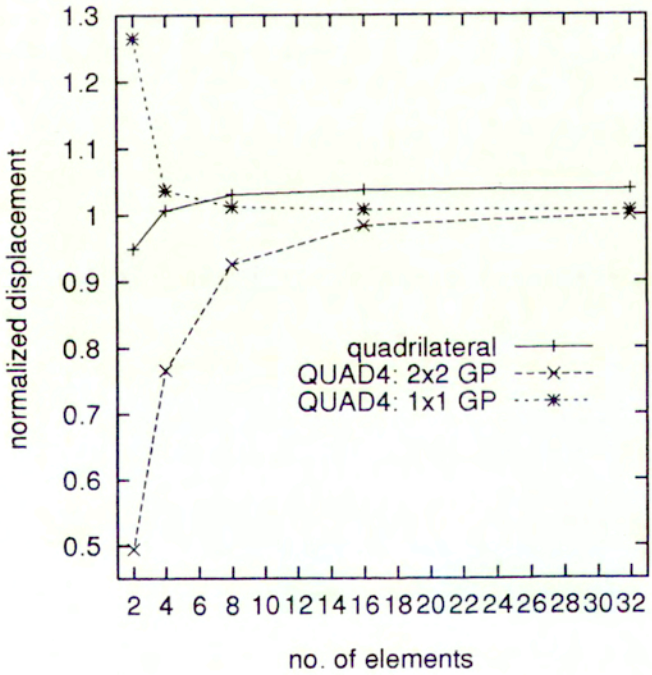

Fig.4.20 Cook's membrane problem problem

Test 8. Finite rotations of a beam of four-noded elements subjected to moment

This test shows that the formulas converting the two-noded element with a transverse stretch into a four-noded element work correctly in the range of finite rotations.

The data for the beam is as follows: $L = 10\ in$, $h = b = 0.1 in^2$, $E = 3 \cdot 10^4\ lb/in^2$, $\nu = 0.25$. The slenderness of the beam $\lambda = L/h = 100$. One edge of the beam is clamped, and the other is loaded by a moment $M = 10^{-3}$.

The beam is modeled using 10 elements: 9 four-noded elements, and one special element developed to apply the moment in the easiest way. In this special element the transformation matrix is modified, and the middle-line variables, $\mathbf{a} = \{u_0, w_0, \beta, \mu\}$ are retained for the end where the moment is applied. In this way we avoid replacing the moment by a pair of co-rotational forces, although the formulae of Section 4.4.4 can also be used for this purpose.

The moment multiplier is increased until the beam bends into a circle, see Fig.4.21,

Using the thin Kirchhoff beam equations we can estimate that a full circle is obtained for $M = EI\ \frac{2\pi}{L}$, which for the given data yields $M = 0.157 \cdot 10^{-3}$. The arc-length procedure is used for calculations. The curve for u, w, β of a tip of the beam as functions of the moment multiplier is also shown in Fig.4.21. In this figure the curves obtained for the two-noded element with transverse stretch, are also presented, and both sets of curves fully coincide.

The Euclidean and the energy norm of the residual are presented in Table 4.9 to illustrate the convergence rates. The results for the tip point rotated by an angle $\beta = 0, \sim \pi, \sim 2\pi$ are given. For $\beta = 0$ the Newton-Raphson method was used, while for the others the arc-length procedure. The obtained results demonstrate that the stabilization and the conversion have been properly implemented, and a quadratic convergence rate is maintained.

Table 4.9. The Euclidean and energy norm of the residual for Test 8.

	$\beta = 0$		$\beta = 1.7606$		$\beta = 3.1139$	
iteration	Euclidean	Energy	Euclidean	Energy	Euclidean	Energy
1	1.00E-03	3.74E-05	4.80E-02	8.64E-02	8.00E-02	2.40E-01
2	4.62E 00	6.57E-04	5.22E 00	8.44E-04	6.78E 00	1.42E-03
3	1.66E-03	5.36E-11	2.23E-03	6.43E-07	4.23E-03	7.34E-06
4	2.03E-07	1.43E-18	5.78E-05	7.50E-13	2.21E-04	1.39E-11
5	4.32E-12	4.94E-27	2.89E-05	1.87E-13	2.21E-04	1.39E-11
6	9.33E-13	2.59E-28	1.33E-11	3.35E-26	3.95E-11	1.03E-21

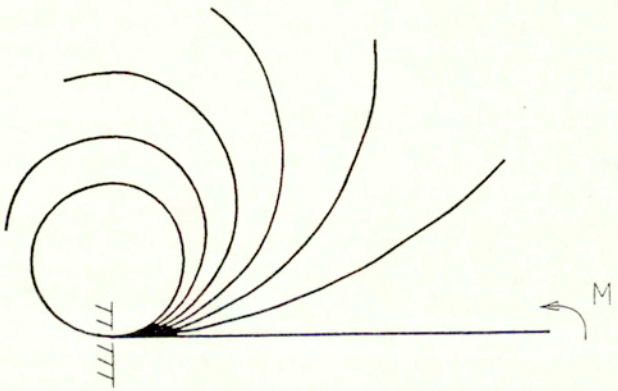

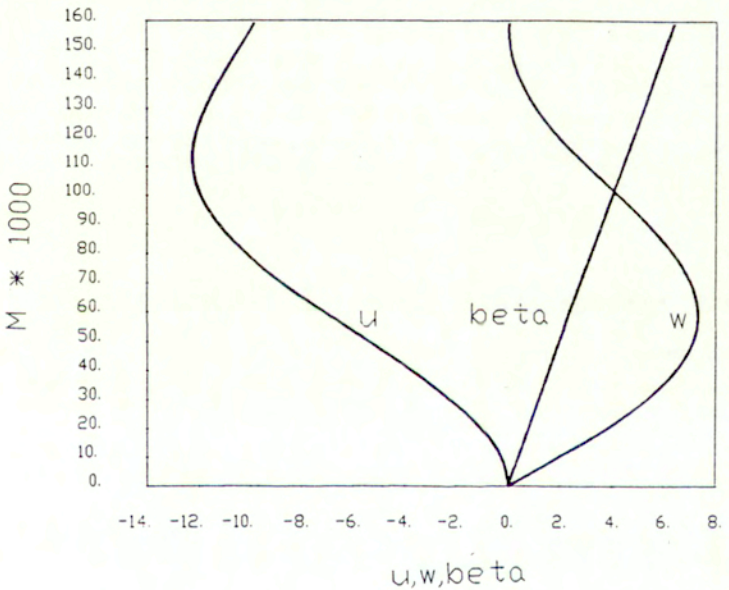

Fig.4.21 Finite rotations of a beam of four-noded elements subjected to moment

Test 9. Finite rotation of a thick beam of 4-noded elements under point load

The geometry of the beam is shown in Fig.4.22, and the data is: $L = 90\ cm$, $b = 10\ cm$, $h = 11\ cm$. The cross-section is made of one material, with $E = 2.1 \cdot 10^6\ kG/cm^2$ and $\nu = 0.294$. One edge of the beam is clamped, and the other is loaded by a transverse force, $P = 10^5$. A linear analysis of this beam by a multi-layer element and a plane stress element was presented in [Wisniewski, Schrefler, 1993a] Here, a nonlinear analysis with rotations up to almost 90 degrees is performed.

The beam is modeled using four-noded elements, and the following meshes: 1x10, 2x10, 3x10, 4x10, 5x10, 10x10 and 10x45 elements. This example can be analyzed with $\alpha = 0$, as only a trace of the hourglass mode is noticed for a single layer of elements. The normal displacement at the force vs. the load multiplier for different meshes is indicated by the letter (H) in Fig.4.21. A number following the letter H indicates the number of elements across the thickness. The obtained results are similar, what means that the deplanation of cross-sections due to large rotations is well captured even by a single layer of elements.

Then, a calculation which allows to compare results for different strain measures, namely the right stretch strain and the Green strain, and the same the constitutive equation is performed. The four-noded element CPS4I of ABAQUS, which is based on the Green strain, is used for this purpose. A fine 90x11 mesh yields the element aspect ratio equal to 1, and the model consists of 2184 dofs. The results obtained are indicated by the letter (E) in Fig.4.21. In this figure also the maximum principal value of the Green strain for the chosen element is shown and indicated as (E, strain). The biggest principal strain at Gauss points in the lower element at the clamped edge is reported, and note that in the final stage of deformation it reaches almost 50%. It is generally accepted that the same constitutive equation and different strain measures may be used only for small strains, not exceeding 2 %, and in this range the obtained results fully coincide.

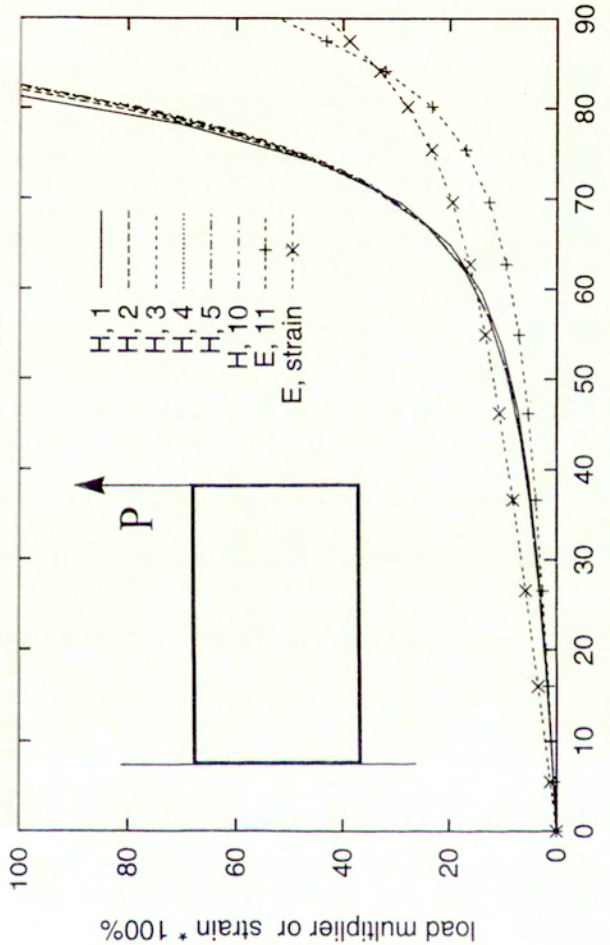

Fig.4.22 Finite rotation of a thick beam of 4-noded elements under point load

4.5 Conclusions

In this chapter the methodology of constructing the layer-wise models of multi-layer beams from the beam equations has been developed. The Reissner type beam equations, accounting for finite rotations and thickness changes, have been derived for this purpose. Several questions related to the numerical implementation of these models are addressed and solved. The results obtained are summarized below.

In Section 4.2 the models of multi-layer beams are developed and tested for a simplified kinematics, see also [Wisniewski, Schrefler, 1993a].

1. Two multi-layer models are proposed and developed in the present work: the interface variable (IF) model and the hierarchical (H) model. The IF model can be classified as the layer-wise model, as the layers are aggregated together by means of compatibility conditions for the layer interfaces. The H model introduces new variables for the aggregated multi-layer cross-section: the coefficients of the Taylor or Chebyshev series expansion of tangent displacements. The number of terms retained in the series is optional, and, as it is shown, the element is hierarchical in the thickness direction. This model requires additional multiplications of matrices, as shown by eq.(73), but not the inversion of $[\ K^p_{11}\ ]$ as in the method by [Owen, Li, 1987].

2. The accuracy of the beam element for a single layer is confirmed in several tests. The formula used to transform the equations to the interface variables is positively verified in Test 1. As the Reissner-type kinematics of the beam incorporates also the shear effects, hence the element is uniformly under-integrated to eliminate shear locking. Test 1 and 2 prove that this element can be used even for very thin layers as the under-integration preserves a 3-digit accuracy for the aspect ratios up to $l/H = 10^3$.

3. The good accuracy of the multi-layer beam element is assessed by comparison with two-dimensional solutions. The comparison of the solutions by the multi-layer beam element with the 2D element for a homogeneous moderately thick, multi-layer beam (Test 3) shows that they correspond very well. In a very severe test $(E_1/E_2 = 100)$ the interface variables, the Taylor series and the Chebyshev series yielded the value of the normal displacement w with 1.05% error, despite the inextensibility of the multi-layer beam in the thickness direction. The tangent displacements u obtained from the 2D analysis have been fitted very well by the interface variables and the Chebyshev series. It has also been verified that for $E_1/E_2 = 7$, i.e. for layers made of steel and epoxy, even a simple 3-parameter multi-layer beam element provides displacements of good accuracy.

These tests indicate that both the developed models are accurate, but they are also convenient, because a large part of the data can be generated automatically, and the input data is very compact.

In Section 4.3 the method of enhancing the accuracy of the stress for the multi-layer models, proposed in [Wisniewski, Schrefler, 1993b], is presented. The enhanced stress recovery (ESR) method combines the following features:

1. It provides a linear distribution of shear stresses within each material layer. At least two computational layers are used per one material layer, what renders that the shear stresses for the IFV model have different values in sub-layers.

2. It filters-out the spurious oscillations of derivatives related to higher order terms of the H model. This is achieved by sampling the displacements at layer interfaces and in the middle of material layers, and on use of low order (parabolic) shape functions to calculate derivatives.

3. It provides stresses of very good accuracy, because they are calculated at Gauss points and projected to nodes.

The numerical tests show that the ESR method yields stresses which are very accurate even for large E_1/E_2 ratios. They are not only much better than those yielded by the direct method, but very favorably compare with 2D stresses.

In Section 4.4, a two-noded beam element and a four-noded quadrilateral are derived from the finite rotation/extensible director equations of a beam, as proposed in [Wisniewski, 1996b]. It requires not only calculation of a tangent operator, but also a stabilization method for the beam with the extensible director, and the conversion formula for the mid-line variables and the IF variables.

1. The conversion formula is derived consistently with the generalized Reissner kinematics, and subsequently linearized to be used in the incremental equations. This furnishes the extension of the procedure used for linear kinematics to the case of finite rotations. Besides, it is shown that, when finite rotations are involved, the interface model cannot be derived from a three parameter theory based on the standard Reissner hypothesis. An interesting observation is made for external moments: the load matrix for the interface model is symmetric.

2. The tests (1,2 and 3) of the two-noded element indicate that the under-integration and the Method 2 of stabilization (belonging to the class of the gamma methods) work very well. Spurious zero eigenvalue is eliminated, and no oscillations are present. Comparing with the beam element without a transverse stretch, the conditioning of the present element is the same, and the results are accurate for the elemental length/thickness ratio up to 10^3. Hence, the thin beam limit properties, established for the element with linear kinematics, are maintained by the present formulation. The highly nonlinear example of the shallow arch proves that the presence of the extension parameter does not further complicate the solution, being very complicated in itself, and that a smooth distribution of the extension parameter is yielded.

3. Also the four-noded element is subjected to several tests (4,5,6,7,8 and 9). When this element is obtained from the stabilized two-noded one then it possesses only three singular body modes, as required. Besides, the developed stabilization method preserves symmetry of the response. The accuracy of the four-noded element is verified in the thin beam limit and for different mesh densities. In the thin beam limit, in case of stretching, the accuracy is the same as for the two-noded element, while in case of bending it is maintained for the elemental length/thickness ratio up to 50. For different mesh densities, the accuracy of the solution is verified on several examples, and compared with results yielded by the QUAD4 element. The results are very accurate for rectangular meshes, which are of interest in case of multi-layer cross-sections.

4. The conversion formula is verified on the example with rotations up to 360 degrees, and the accuracy, compared with the beam solution, is excellent. The linearization of the conversion formula and the implementation are correct as the Newton-Raphson scheme maintains a quadratic convergence rate. Another finite rotation example involves strains

reaching 50 %. Several meshes are used, and deflections of the middle-line tip point are alike. The results obtained for the Green strain are also provided to indicate the range in which the right stretch strain and the Green strain yield similar results. This element is especially well suited to multi-layer cross-sections of plane stress rectangular elements.

Summarizing, we can say that all presented in this chapter the advanced finite elements for multi-layer beams are accurate and efficient. They allow to analyze multi-layer beams with the accuracy which is adjusted to the problem at hand, and either global or precise local responses can be sought.

5 Final remarks

A detailed discussion of the derived equations and the developed finite element models is provided within the chapters and in Conclusions closing them. Below, only the novel results of the work, in the author's opinion, are listed.

1. The equations of a finite rotation shell, based on the right stretch strain and the Reissner hypothesis and incorporating rotations as an independent variable in a manner consistent with the polar decomposition equation. The obtained 6-parameter shell theory naturally includes the drilling rotation, which is of value in numerous finite element applications.

2. The constitutive equations for the incompressible Mooney-Rivlin material applicable to thin shells. They can be used in conjunction with the strain measures for the Reissner kinematics, and on use of the linear expansion of the recovered normal strain. Also the proof (in Appendix A) that the structure of the constitutive (4th rank) tensor is transferred to the forward-rotated measures.

3. The demonstration that on use of the Reissner hypothesis the rotation constraint yields two constraint equations for a shell, which, in general, are contradictory. This result is quite general, and can be related to the approximations used for the rotations and the deformation gradient. It applies also to other shell formulations (e.g. in terms of Green strain) using the rotation constraint.

4. The finite rotation equations of a beam with kinematics based on the generalized Reissner hypothesis, with an additional scalar parameter for transverse extension, i.e. accounting for membrane, shear, bending and transverse stretch effects.

5. The conversion formula between the interface and middle-line variables which is valid for finite rotations. This formula cannot be derived for the standard Reissner hypothesis. and is introduced consistently with the generalized Reissner kinematics. It is exactly linearized for further use in the Newton-Raphson equations.

6. The development of several finite elements from the derived earlier equations. Among them, two nonlinear four-node finite elements for finite rotations, such as: the membrane part of the shell element with the drilling rotation, and the quadrilateral specialized for multi-layer beams, derived from the finite rotation/extensible director beam element on use of the conversion formula. The elements are under-integrated and the stabilization methods are developed. Also, the finite rotation/extensible director beam element, the multi-layer beam elements in terms of interface and hierarchical variables, and the procedure enhancing the quality of calculated stresses are developed. The accuracy and efficiency of the developed elements is established by extensive testing.

7. The extension of the continuum Adjoint System Method of the design sensitivity analysis to the problems with rotational parameters is implemented. The validation tests include several highly nonlinear examples, which needed advanced techniques, such as the arc-length method and the update of rotations.

The developments of the work, although self-contained, form a good basis for constructing other variants of enhanced shell and beam equations, and developing the respective finite element models.

6 References

1. Altman, S.L.: *Rotations, Quaternions and Double Groups.* Clarendon Press, Oxford (1986)

2. Argyris J.: *An excursion into large rotations.* Comput. Methods Appl. Mech. Engng., Vol.32, 85-155 (1982)

3. Argyris J., Poterasu V.F.: *Large rotations revised application of Lie algebra.* Comput. Methods Appl. Mech. Engng., Vol.103, 11-42 (1993)

4. Arora J.S., Wu C.C., *Design sensitivity analysis and optimization of nonlinear structures.* In C.A. Mota Soares (ed.) Computer Aided Optimal Design: Structural and Mechanical Systems. NATO ASI Series, Vol.27, pp.589-603, Springer-Verlag (1987)

5. Atluri S.N.: *Alternate stress and conjugate strain measures, and mixed variational formulations involving rigid rotations, for computational analyses of finitely deformed solids, with application to plates and shells.* Computers & Structures, Vol.18, No.1, 93-116 (1984)

6. Atluri S.N., Cazzani A.: *Rotations in computational solid mechanics.* Archives of Computational Methods in Engineering, Vol.2, No.1, 49-138 (1995)

7. Baczynski Z.F.: *Mathematical models of elastomechanics of layered bodies* (in Polish) IFTR Reports 15 (1985)

8. Badur J., Pietraszkiewicz W.: *On geometrically non-linear theory of elastic shells derived from pseudo-Cosserat continuum with constrained micro-rotations,* Finite Rotations in Structural Mechanics. W. Pietraszkiewicz (ed.) 19-32, Springer-Verlag (1986)

9. Basar Y., Ding Y.: *Transverse normal strains in the nonlinear analysis of composite laminates.* Advances in Non-Linear Finite Element Methods, B.H.V. Topping and M. Papadrakakis (eds), 237-241 (1994)

10. Bates D.N.: *The mechanics of thin walled structures with special reference to large rotations.* Dept. of Civil Engineering. Imperial College of Science and Technology, Lond on (1987)

11. Bathe, K-J.: *Finite Element Procedures in Engineering Analysis.* Prentice-Hall (1982)

12. Bathe, K-J., Dvorkin E.N.: *A four-node plate bending element based on Mindlin/Reissner plate theory and mixed interpolation.* Int. J. Num. Meth. Engng, Vol.21, 367-383 (1985)

13. Belytschko T., Ong J.S., Liu W.K., Kennedy J.D.: *Hourglass control in linear and nonlinear problems.* Comput. Methods Appl. Mech. Engng., Vol.43, 251-276 (1984)

14. Blinowski A.: *Rotations of deformable bodies. I. Geometry and kinematics* (in Polish) IFTR Reports 7 (1994)

15. deBoer R.: *Vector- und Tensorrechnung für Ingenieure.* Springer-Verlag (1982)

16. deBoer R., Walther W.: *Fundamental equations and extremum principles in the theory of thin shells.* Finite Rotations in Structural Mechanics. W. Pietraszkiewicz (ed.) 121-130, Springer-Verlag (1986)

17. Bolotin V.V.: *Nonconservative Problems of the Theory of Elastic Stability.* Pergamon Press (1963)

18. Buechter N., Ramm E.: *Shell theory versus degeneration - a comparison in large rotation finite element analysis.* Int. J. Num. Meth. Engng, Vol.34, 39-59 (1992)

19. Bufler H.: *The Biot stresses in nonlinear elasticity and associated generalized variational principles.* Ing.-Arch., Vol.55, 450-462 (1985)

20. Cardona A., Geradin M.: *A beam finite element nonlinear theory with finite rotations.* Int. J. Num. Meth. Engng, Vol.26, 2403-2438 (1988)

21. Cazzani A., Atluri S.N.: *Four-noded mixed finite elements, using non-symmetric stresses, for linear analysis of membranes.* Comput. Mech., Vol.11, 229-251 (1993)

22. Choi K.K., Santos J.L.T., *Design sensitivity analysis of nonlinear structural systems.* Int. J. Num. Meth. Engng, Part I. Theory. Vol.24, 2039-2055, 1987

23. Chroscielewski J.: *The family of C^0 finite elements in the nonlinear six-parameter shell theory.* Zeszyty Naukowe Politechniki Gdanskiej 540. Budownictwo Ladowe Nr. LIII (1996)

24. Chroscielewski J., Makowski J., Stumpf H.: *Genuinely resultant shell finite elements accounting for geometric and material nonlinearity.* Int. J. Num. Meth. Engng, Vol.35, 63-94 (1992)

25. Chroscielewski L., Schmidt R.: *Comparison of numerical results for nonlinear finite element analysis of beams and shells based on 2-d elasticity theory and a novel finite rotation theories for thin shells.* Finite Rotations in Structural Mechanics. W. Pietraszkiewicz (ed.) 111-120, Springer-Verlag (1986)

26. Crisfield M.A.: *A consistent co-rotational formulation for non-linear, three-dimensional beam elements.* Comput. Methods Appl. Mech. Engng., Vol.81, No.2, 131-150 (1990)

27. Dennis J.E., Schnabel R.B.: *Numerical Methods for Unconstrained Optimization and Nonlinear Equations.* Prentice-Hall (1983)

28. Dienes J.K.: *On the analysis of rotation and stress rate in deforming bodies.* Acta Mechanica, Vol.32, 217-232 (1979)

29. Dluzewski P.H.: *Crystal orientation spaces and remarks on the modeling of polycrystal anisotropy.* J. Mech. Phys. Solids, Vol.5, No.5, 651-661 (1991)

30. Dvorkin E.N., Onate E., Oliver J.: *On a non-linear formulation for curved Timoshenko beam elements considering large displacement/rotation increments.* Int. J. Num. Meth. Engng, Vol.26, 1597-1613 (1988)

31. Epstein M., Glockner P.G.: *Nonlinear analysis of multi-layered shells.* Computers & Structures, Vol. 13, No. 5, 1081-1089 (1977)

32. Epstein M., Huttelmaier H.-P.: *A finite element formulation for multi-layered and thick plates.* Computers & Structures, Vol.16, No. 5, 645-650 (1983)

33. Eringen A.C., Kafadar Ch.B.: *Polar field theories.* Continuum Physics, A.C.Eringen (ed.), 1-73, Academic Press (1976)

34. Fraeijs de Veubeke B.: *A new variational principle for finite elastic displacements.* Int. J. Engng Sci., Vol.10, 745-763 (1972)

35. Fried I.: *Shear in C^0 and C^1 bending finite elements.* I. J. Solids and Struct., Vol.9, 449-460 (1973)

36. Goldstein H.: *Classical Mechanics. 2nd Edition.* Addison Wesley, Reading, Massachusetts (1980)

37. Gori R.E., Schrefler B.A.: *A partially bonded beam element for super-conducting magnet pancakes.* Int. J. Num. Meth. Engng, Vol. 27, 299-321 (1989)

38. Green A.E., Adkins J.E.: *Large Elastic Deformations. 2nd Edition.* Oxford Univ. Press (1970)

39. Green A.E., Naghdi P.M., Wenner M.L.: *Linear theory of Cosserat surface and elastic plates of variable thickness.* Proc. Camb. Phil. Soc., Vol.69, 227-254 (1971)

40. Gruttmann F., Taylor R.L.: *Theory and finite element formulation of rubber-like membrane shells using principal stretches.* Int. J. Num. Meth. Engng, Vol.35, 1111-1126 (1992)

41. Gruttmann F., Wagner W., Wriggers P.: *A nonlinear quadrilateral shell element with drilling degrees of freedom.* Archive of Applied Mechanics, Vol.62, 474-486 (1992)

42. Gruttmann F., Stein E., Wriggers P.: *Theory and numerics of thin elastic shells with finite rotations.* Ing. Archive, Vol.59, 54-67 (1989)

43. Haftka R.T., *Semi-analytical static nonlinear structural sensitivity analysis.* AIAA J., Vol 31, No.7., 1307-1312 (1993)

44. Hassenpflug W.C.: *Rotation angles.* Comput. Methods Appl. Mech. Engng., Vol.105, 111-124 (1993)

45. Haug E.J., Choi K.K., Komkov V.: *Design Sensitivity Analysis of Structural Systems.* Academic Press, New York (1986)

46. Hinton E., Campbell J.S.: *Local and Global Smoothing of Discontinuous Finite Element Functions Using a Least Squares Method.* Int. J. Num. Meth. Engng, Vol.8, 461-480 (1974)

47. Hughes, T.J.R.: *The Finite Element Method. Linear Static and Dynamic Finite Element Analysis.* Prentice-Hall (1987)

48. Hughes T.J.R., Brezzi F.: *On drilling degrees of freedom.* Comput. Methods Appl. Mech. Engng., Vol.72, 105-121 (1989)

49. Hughes T.J.R., Liu W.K.: *Nonlinear finite element analysis of shells. Part I. Three-dimensional shells.* Comput. Methods Appl. Mech. Engng., Vol.26, 331-362 (1981)

50. Hughes T.J.R., Liu W.K.: *Nonlinear finite element analysis of shells. Part II. Two-dimensional shells.* Comput. Methods Appl. Mech. Engng., Vol.27, 167-182 (1981)

51. Hughes T.J.R., Taylor R.L., Kanoknukulchai W.: *A simple and efficient finite element for plate bending.* Int. J. Num. Meth. Engng, Vol.11 1529-1543 (1977)

52. Ibrahimbegovic A.: *Stress resultant geometrically nonlinear shell theory with drilling rotations. Part 1. A consistent formulation.* Comput. Methods Appl. Mech. Engng., Vol.118, 265-284 (1994)

53. Ibrahimbegovic A., Frey F.: Stress resultant geometrically nonlinear shell theory with drilling rotations- Part II. computational aspects. Comput. Methods Appl. Mech. Engng., Vol.118, 285-308 (1994)

54. Ibrahimbegovic A., Frey F.: *Variational principles and membrane finite elements with drilling rotations for geometrically non-linear elasticity.* Int. J. Num. Meth. Engng, Vol.38, 1885-1900 (1995)

55. Iura M., Atluri S.N.: *On a consistent theory, and variational formulation of finitely stretched and rotated 3-D space-curved beams.* Computational Mechanics, Vol.4, No.1, 73-88 (1989)

56. Iura M., Atluri S.N.: *Formulation of a membrane finite element with drilling degrees of freedom.* Computational Mechanics, Vol.9, 417-428 (1992)

57. Jetteur, P., Frey F.R: *A four-node Marguerre element for non-linear shell analysis.* Engineering Computations, 276-282 (1986)

58. John F.: *Estimates for the derivatives of the stresses in a thin shell and interior shell equations.* Comm. Pure and Appl. Math., Vol.18, 235-267 (1965)

59. John F.: *Refined interior equations for thin elastic shells.* Comm. Pure and Appl. Math., Vol.24, 585-615 (1971)

60. Johnson G.C., Bammann D.J.: *A discussion of stress rates in finite deformation problems.* Int. J. Solids Structures, Vol.20, 725-737 (1984)

61. Kamat M.P., *Optimization of shallow arches against instability using sensitivity derivatives.* Finite Elements in Analysis and Design, Vol.3, 277-284 (1987)

62. Kamat M.P., Khot N.S., Venkayya V.B., *Optimization of shallow trusses against limit point instability.* AIAA J., Vol.22, No.3, 403-408 (1984)

63. Khatua T.P., Cheung Y.K.: *Bending and vibration of multi-layer sandwich beams and plates.* Int. J. Num. Meth. Engng, Vol. 6, 11-24 (1973)

64. Khot N.S., Kamat M.P., *Minimum weight design of truss structures with geometric nonlinear behavior.* AIAA J., Vol.23, No.1, 139-144 (1985)

65. Kleiber M.: *Incremental Finite Element Modeling in Non-Linear Mechanics.* Polish Scientific Publisher - Ellis Horwood (1989)

66. Kleiber M.: *Shape and non-shape structural design sensitivity analysis for problems with any material and kinematic non-linearity.* Comput. Methods Appl. Mech. Engng., Vol.81, 183-208 (1990)

67. M. Kleiber, T.D. Hien, *Parameter sensitivity of inelastic buckling and post-buckling response.* Comput. Methods Appl. Mech. Engng., accepted for publication (1997)

68. M. Kleiber, T.D. Hien, E. Postek: *Incremental finite element sensitivity analysis for nonlinear mechanics applications.* Int. J. Num. Meth. Engng, Vol.37, 3291-3308 (1994)

69. Krätzig W.B.: *'Best' transverse shearing and stretching shell theory for nonlinear finite element simulations.* Comput. Methods Appl. Mech. Engng., Vol.103, 135-260 (1993)

70. Koiter W.T.: *On the nonlinear theory of thin elastic shells.* Proc. Kon. Ned. Ak. Wet., Ser.B, Vol.69, No.1, 1-54 (1966)

71. Liu W.K., Ong J.S.-J., Uras R.A.: *Finite element stabilization matrices- a unification approach.* Comput. Methods Appl. Mech. Engng., Vol.53, 13-46 (1985)

72. Lee C.Y., Liu D., Lu X.: *Static and Vibration Analysis of Laminated Composite Beams with an Inter-laminar Shear Stress Continuity Theory.* Int. J. Num. Meth. Engng, Vol.33, 409-424 (1992)

73. Makowski J., Stumpf H.: *Finite strains and rotations in shells.* Finite Rotations in Structural Mechanics. W. Pietraszkiewicz (ed.) 175-194, Springer-Verlag (1986)

74. Makowski J., Stumpf H.: *Buckling equations for elastic shells with rotational degrees of freedom undergoing finite strain deformation.* Int. J. Solids Structures, Vol.26, No.3, 353-368 (1990)

75. Makowski J., Stumpf H.: *On the "symmetry" of tangent operators in nonlinear mechanics.* ZAMM, Vol.75, No.3, 189-198 (1995)

76. Mang H.A., Gallagher R.H.: *On the unsymmetric eigen-problem for the buckling of shells under pressure loading.* J. Appl. Mech., Trans. ASME, Vol. 50, 95-100 (1983)

77. Mroz Z., Haftka R.T., *Design sensitivity analysis of non-linear structures in regular and critical states.* In "Mathematical Methods in Computer Aided Optimal Design". Lecture Notes from Advanced TEMPUS Course, July 12-16, 1993 Faculty of Mathematics and Physics, The Charles University, Prague, 1-32 (1993)

78. Naghdi P.M.: *The Theory of Shells.* in: C.Truesdell (ed.) Handbuch der Physik, Vol.VIa/2 Mechanics of Solids II, Springer Berlin (1972)

79. Ogden R.: *Non-Linear Elastic Deformations.* Ellis Horwood, Chichester, UK (1984)

80. Owen D.R.J, Li Z.H.: *A refined analysis of laminated plates by finite element displacement method. Part I. Fundamentals and static analysis.* Computers & Structures, Vol. 26, 907-914 (1987)

81. Pagano N.J, Soni S.R.: *Global-local laminational mode.* Int. J. Solids Structures, Vol. 19, 207-228 (1983)

82. Parish H.: *A continuum-based shell theory for non-linear applications.* Int. J. Num. Meth. Engng, Vol.38, 1855-1883 (1995)

83. Park J.C, Choi K.K., *Design sensitivity analysis of critical load factor for nonlinear structural systems.* Computers & Structures, Vol.36, No.5, 823-838 (1990)

84. Pietraszkiewicz W.: *Introduction to the Non-Linear Theory of Shells.* Ruhr Universität Bochum, Mitt. Inst. für Mechanik, No.10 (1977)

85. Pietraszkiewicz W.: *Finite rotations and Lagrangean description in the non-linear theory of shells.* Polish Scientific Publisher, Warszawa - Poznan (1979)

86. Pietraszkiewicz W.: *Lagrangian description and incremental formulation in the nonlinear theory of thin shells.* Int. J. Nonlin. Mech., Vol.19, 115-140 (1984)

87. Pietraszkiewicz W.: *Geometrically nonlinear theories of thin elastic shells.* Adv. Mech., Vol.12, 51-130 (1989)

88. Pietraszkiewicz W., Badur J.: *Finite rotations in the description of continuum deformation.* Int. J. Engng Sci., Vol.21, No.9, 1097-1115 (1983)

89. Ramm E.: *Geometrisch nichtlineare Elastostatik und finite Elemente.* Bericht Nr.76-2, Institute für Baustatik, Universität Stuttgart, Germany (1976)

90. Ramm E.: *Strategies for Tracing the Nonlinear Response Near Limit Points.* Proc. Europe-U.S. Workshop, Bochum 1980, 63-89. Wunderlich, Stein, Bathe (eds). Springer-Verlag (1981)

91. Rankin C.C, Brogan F.A.: *An element-independent co-rotational procedure for treatment of large rotations.* Collapse Analysis of Structures, L.H.Sobel, K.Thomas, (eds) 85-100, ASME, New York (1984)

92. Reddy J.N.: *A generalization of two-dimensional theories of laminated composite plates.* Commun. Appl. Numer. Methods, Vol. 3, 113-180 (1987)

93. Reddy J.N.: *On refined computation models of composite laminates.* Int. J. Num. Meth. Engng, Vol. 27, 361-382 (1989)

94. Reddy J.N, Barbero E.J., Teply J.L.: *A plate bending element based on a laminate plate theory.* Int. J. Num. Meth. Engng, Vol. 28, 2275-2292 (1989)

95. Reissner E.: *On one-dimensional finite-strain beam theory: the plane problem.* J. Appl. Math. Physics (ZAMP), Vol.23, 795-804 (1972)

96. Reissner E.: *Formulation of variational theorems in geometrically nonlinear elasticity.* J. Eng. Mech. Vol.110 1377-1390 (1984)

97. Ringertz U.T., *Numerical methods for optimization of nonlinear shell structures.* Structural Optimization, Vol.4, 193-198 (1992)

98. Riks, E.: *The application of of Newton's method to the problem of elastic stability.* J.Appl.Mech. Vol.39, 1060-1066 (1972)

99. Rosenberg R.M.: *Analytical Dynamics of Discrete Systems.* Plenum Press (1977)

100. Santos J.L.T., Wisniewski K., Apostol V.: *Pre- and post-critical design sensitivity analysis for nonlinear structures undergoing finite rotations.* The First World Congress of Structural and Multidisciplinary Optimization, Goslar, Lower Saksony, Germany, May 28-June 2, 1995. Book of Extended Abstracts-Lectures, No.83, 102-103 (1995)

101. Santos J.L.T., Wisniewski K., Apostol V.: *Unified approach to pre- and post-critical design sensitivity analysis for nonlinear structures undergoing finite rotations.* in preparation (1997)

102. Sansour C.: *A theory and finite element formulation of shells at finite deformations involving thickness change: circumventing the use of a rotation tensor.* Archive of Applied Mechanics, Vol.65, 194-216 (1995)

103. Sansour C., Bufler H.: *An exact finite rotation shell theory, its mixed variational formulation and its finite element implementation.* Int. J. Num. Meth. Engng, Vol.34, 73-115 (1992)

104. Santos J.L.T., Choi K.K., *Design sensitivity analysis of nonlinear structural systems.* Int. J. Num. Meth. Engng, Part II: Numerical methods, Vol.26, 2097-2114 (1988)

105. Schieck B., Pietraszkiewicz W., Stumpf H.: *Theory and numerical analysis of shells undergoing large elastic strains.* Int. J. Solids Structures, Vol.29, No.6, 689-709 (1992)

106. Schweizerhof K.H., Ramm E.: *Displacement dependent pressure loads in nonlinear finite element analyses.* Computers & Structures, Vol. 18, No.6, 1099-1114 (1984)

107. Schweizerhof K.H., Wriggers P.: *Consistent linearization for path following methods in nonlinear FE analysis.* Comput. Methods Appl. Mech. Engng., Vol.59, 261-279 (1986)

108. Seki W., Atluri S.N, *Analysis of strain localization in strain-softening hyperelastic materials, using assumed stress hybrid elements.* Computational Mechanics, Vol.14, No.6,549-5685 (1994)

109. Simmonds J.G., Danielson D.A.: *Nonlinear shell theory with finite rotation vector.* Proc. Kon. Ned. Ak. Wet. Series B, Vol.73, 460-478 (1970)

110. Simmonds J.G., Danielson D.A.: *Nonlinear shell theory with finite rotation and stress function vectors.* J. Appl. Mech., Vol.39, 1085-1090 (1972)

111. Simmonds J.G.: *The nonlinear thermodynamical theory of shells: descent from 3-dimensions without thickness expansions.* Flexible Shells. Theory and Applications. E.L.Axelrad, F.A.Emmerling (eds), Springer Verlag, Berlin, 1-11 (1984)

112. Simo J.C.: *A finite strain beam formulation. The three-dimensional dynamic problem.* Comput. Methods Appl. Mech. Engng., Vol.49, 55-70 (1985)

113. Simo J.C., Fox D.D., Hughes T.J.R.: *Formulations of finite elasticity with independent rotations.* Comput. Methods Appl. Mech. Engng., Vol.95, 227-288 (1992)

114. Simo J.C., Rifai M.S., Fox D.D.: *On a stress resultant geometrically exact shell model. Part IV: Variable thickness shells with through-the-thickness stretching.* Comput. Methods Appl. Mech. Engng., Vol.81, 91-126 (1990)

115. Simo J.C., Taylor R.L.: *Quasi-incompressible finite elasticity in principal stretches. Continuum basis and numerical algorithms.* Comput. Methods Appl. Mech. Engng., Vol.85, 273-310 (1991)

116. Simo J.C, Vu-Quoc L.: *A three-dimensional finite strain rod model. The three-dimensional dynamic problem.* Comput. Methods Appl. Mech. Engng., Vol.58, 79-116 (1986)

117. Simo J.C., Vu-Quoc L.: *On the dynamics of finite strain rods undergoing large motions. The three-dimensional case.* ERL, College of Engineering, UCB, M86/11 (1986)

118. Simo J.C.: *The (symmetric) Hessian for geometrically nonlinear models in solid mechanics: Intrinsic definition and geometric interpretation.* Comput. Methods Appl. Mech. Engng., Vol.96, 189-200 (1992)

119. Stolarski H., Belytschko T., Lee S.-H.: *A review of shell finite elements and corotational theories.* Computational Mechanics Advances, Vol.2, 125-212 (1995)

120. Stuelpnagel J.: *On the parametrization of three-dimensional rotational group.* SIAM Review, Vol.6, No.4, 422-430 (1964)

121. Stumpf H., Makowski J.: *On large strain deformations of shells.* Acta Mechanica, Vol.65, 153-168 (1986)

122. Srinivas S.: *A refined analysis of composite laminates.* J. Sound Vibr., Vol. 30, 495-507 (1973)

123. Taylor R.L.: *Finite element analysis of linear shell problems.* im "The Mathematics of Finite Elements and Applications VI. MAFELAP 1987", Ed. J.R.Whiteman, Academic Press (1988)

124. Turska E., Wisniewski K., Schrefler B.A.: *Error propagation of staggered solution procedures for transient problems.* Comput. Methods Appl. Mech. Engng., Vol.114, 177-188 (1994)

125. Truesdell C., Noll W.: *The Non-Linear Field Theory.* Handbuch der Physik, Vol.III/3, Springer-Verlag (1965)

126. Wagner W.: *Nonlinear stability analysis of shells with the finite element method.* Nonlinear analysis of shells by finite elements, F.G.Rammerstorfer (ed.) CISM Courses and Lectures No.328, 91-130, Springer Verlag (1992)

127. Vlasov V.Z., Leontev U.N.: *Beams, Plates and Shells on Elastic Foundations.* G.I.F-M.L., Moskva (1960)

128. Wilson E.L., Taylor R.L., Doherty W.P., Ghaboussi J.: *Incompatible displacement models.* in. S.J. Fenves, N.Perrone, A.R. Robinson, W.C. Schnobrich (eds.) Numerical and Computer Methods in Finite Element Analysis. Academic Press, New York, 43-57 (1973)

129. Wisniewski K.: *Numerical analysis of the stability of cylindrical shells based on static criteria,* (in Polish) IFTR Reports 50 (1985).

130. Wisniewski K., Taylor R.L.: *Decomposition of the initial stability problem for a cylindrical shell under non-symmetric loads,* Engng Comput., Vol.7, No.2, 90-100 (1990)

131. Wisniewski K.: *A shell theory of independent rotations for relaxed Biot stress and right stretch strain.* submitted for publication in Comput. Mech.(1996)

132. Wisniewski K.: *Finite rotation-extensible director beam model and derivation of a quadrilateral finite element for multi-layer beams,* submitted for publication in Int. J. Num. Meth. Engng(1996)

133. Wisniewski K., Turska E., Simoni L. Schrefler B.A.: *Error analysis of staggered predictor-corrector scheme for consolidation of porous media.* The finite element method in the 1990's, E. Onate, J. Periaux, A. Samuelsson (eds), CIMNE, Springer, 192-201 (1991)

134. Wisniewski K., Turska E., Schrefler B.A.: *Performance of a Hermitian element for a beam with rotational constraints.* Comm. Num. Meth. in Eng., Vol. 9, 27-34 (1993)

135. Wisniewski K., Schrefler B.A.: *Hierarchical multi-layered element of assembled Timoshenko beams.* Computers & Structures, Vol.48, No.2, 255-261 (1993)

136. Wisniewski K., Schrefler B.A.: *On recovery of stresses for a multi-layered beam element.* Engng Comput., Vol.10, No.6, 563-569 (1993)

137. Wisniewski K., Turska E.: *A note on the hyperelastic constitutive equation for rotated Biot stress.* Archives of Mechanics, Vol.48, No.5, 947-953 (1996)

138. Wisniewski K., Turska E., Kleiber M.: *Comparison of two staggered schemes for optimization with a critical point constraint.* Computer Assisted Mechanics and Engineering Sciences, accepted for publication (1997)

139. Wisniewski K., Santos J.L.T.: *On design derivatives for optimization with a critical point constraint,* Structural Optimization, Vol.11, 120-127 (1996)

140. Wood R.D., Zienkiewicz O.C.: *Geometrically nonlinear finite element analysis of beams, frames, arches and azisymmetric shells.* Computers & Structures, Vol.7, 725-735 (1977)

141. Wozniak Cz.: *Nonlinear Theory of Shells* (in Polish) Polish Scientific Publisher, Warszawa (1966)

142. Wozniak Cz.: *Constrained continuous media I,II,III.* Bull. Acad. Polon. Sci., Ser.sci.techn., Vol.21, No.3, 109-116, No.4, 167-173, 175-182 (1973)

143. Wriggers P., Gruttmann F.: *Thin shells with finite rotations formulated in Biot stresses: theory and finite element formulation.* Int. J. Num. Meth. Engng, Vol.36, 2049-2071 (1993)

144. Wriggers P., Simo J.C.: *A general procedure for the direct computation of turning and bifurcation points.* Int. J. Num. Meth. Engng, Vol.30, 155-176 (1990)

145. Wu C.C., Arora J.S., *Design sensitivity analysis and optimization of nonlinear response using incremental procedure.* AIAA J., Vol.25, 1118-1125 (1987)

146. Yuan K., Huang Y.-S., Pian T.H.H. : *New strategy for assumed stress for 4-node hybrid stress membrane element.* Int. J. Num. Meth. Engng, Vol.36, 1747-1763 (1993)

147. Zhu Y.Y., Cescotto S.: *Unified and mixed formulation of the 4-node quadrilateral elements by assumed strain method: application to thermomechanical problems.* Int. J. Num. Meth. Engng, Vol.38, 685-716 (1995)

148. Zhu Y., Zacharia Th.: *A new one-point quadrature, quadrilateral shell element with drilling degrees of freedom.* Comput. Methods Appl. Mech. Engng., Vol.136, 165-203 (1996)

149. Zienkiewicz O.C, Taylor R.L.: *The Finite Element Method. Fourth Edition. Vol.1. Basic Formulation and Linear Problems.* McGraw-Hill (1989)

150. Zienkiewicz O.C, Taylor R.L.: *The Finite Element Method. Fourth Edition. Vol.2. Solid and Fluid Mechanics. Dynamics and Nonlinearity.* McGraw-Hill (1991)

A Hyperelastic constitutive equation for rotated Biot stress

The co-rotational formulations are applied to many problems of mechanics, ranging from finite strain plasticity to large rotation shells, mostly due to relative simplicity of manipulating the orthogonal rotation tensors.

In finite strain plasticity, see e.g. [Dienes, 1979] and [Johnson, Bammann, 1984], the so-called rotated description is based on a back-rotated Kirchhoff stress $\boldsymbol{\Sigma} = \mathbf{Q}^T\boldsymbol{\tau}\mathbf{Q}$ and a back-rotated spatial rate of deformation $\mathbf{D} = \mathbf{Q}^T\mathbf{d}\mathbf{Q}$, where $\mathbf{d} = \mathrm{sym}(\dot{\mathbf{F}}\mathbf{F}^{-1})$. The rotated measures are exploited to define a constitutive equation, which later is converted to $\overset{\circ}{\boldsymbol{\tau}}$ and $\mathbf{d}$, where $\overset{\circ}{\boldsymbol{\tau}}$ is the Green-McInnis-Naghdi objective stress rate.

It was noticed by several authors, e.g. see the introduction to [Crisfield, 1990], that nonlinearities resulting from large rotations of beams or shells can be eliminated if co-rotational local frames are introduced. Among recent works using the co-rotational frames we would like to mention contributions of [Rankin, Brogan, 1984], [Simo, 1985], [Simo, Vu-Quoc, 1986], and [Crisfield, 1990]. In [Rankin, Brogan, 1984] a general framework to handle large rotations has been constructed, in which already existing linear finite elements can be embedded. In [Simo, 1985] and [Simo, Vu-Quoc, 1986] a finite strain/rotation beam model for dynamics has been consistently derived from three-dimensional equations. In [Crisfield, 1990] an issue of symmetry of the tangent operator for the finite rotation beam has been undertaken. In all these papers separation of frame rotations simplified the equations.

In [Wisniewski, Turska, 1996] we extend the concept of the co-rotational frame used for beams and shells and introduce a forward-rotated description: the rotated stress and strain measures, and the co-rotational variation. We address in detail an issue of a hyperelastic constitutive equation and a constitutive operator for the rotated measures as derived from the constitutive relations for the Biot stress. The forward-rotated description, as a general concept, can be found convenient in problems involving independent rotation fields, not only in beam or shell theories but also in three-dimensional elasticity formulated as e.g. in [Simo, Fox, Hughes, 1992].

A.1 Rotated stress and strain

The Cauchy (true) stress, $\mathbf{T}$, can be expressed in terms of other stress measures as follows, see e.g.[Ogden, 1984],

$$\mathbf{T} = J^{-1}\boldsymbol{\tau} = J^{-1}\mathbf{P}\mathbf{F}^T = J^{-1}\mathbf{F}\mathbf{S}\mathbf{F}^T, \tag{A.1}$$

where $\boldsymbol{\tau}$ is the Kirchhoff stress, $\mathbf{P}$ is the 1st Piola-Kirchhoff stress, (its transpose is a nominal stress), $\mathbf{S}$ is the 2nd Piola-Kirchhoff stress. Besides, $\mathbf{F}$ denotes the gradient of deformation, and $J = \det\mathbf{F}$.

Let us introduce a symmetric Biot stress tensor, $\mathbf{T}_s^B \equiv \mathrm{sym}(\mathbf{Q}^T\mathbf{P})$. The rotation tensor $\mathbf{Q} \in SO(3)$ is obtained from the polar decomposition of the deformation gradient. The Biot stress $\mathbf{T}_s^B$ and the right stretch strain $\mathbf{H}$ are work conjugates because the

virtual work of stress can be expressed as follows

$$\mathbf{P} \cdot \delta\mathbf{F} = \mathbf{T}_s^B \cdot \delta\mathbf{H}, \tag{A.2}$$

where $\mathbf{H} = \mathbf{U} - \mathbf{I}$ is the right stretch strain, and $\mathbf{U} \equiv (\mathbf{F}^T\mathbf{F})^{\frac{1}{2}}$ is the right stretching tensor. This tensor appears also in the (right) polar decomposition of the deformation gradient, $\mathbf{F} = \mathbf{QU}$. On the basis of eq.(1) the Biot stress is related to other stress measures in the following way

$$\mathbf{T}_s^B \equiv \mathrm{sym}(\mathbf{Q}^T\mathbf{P}) = \mathrm{sym}(\mathbf{Q}^T\boldsymbol{\tau}\mathbf{F}^{-T}) = \mathrm{sym}(\mathbf{US}), \tag{A.3}$$

The Biot stress tensor $\mathbf{T}_s^B$ and the right stretch strain $\mathbf{H}$ can be used to introduce a set of rotated measures defined as follows

$$\mathbf{T}_s^\star \equiv \mathbf{Q}\ \mathbf{T}^B\ \mathbf{Q}^T, \qquad \mathbf{H}^\star \equiv \mathbf{Q}\ \mathbf{H}\ \mathbf{Q}^T \tag{A.4}$$

for which the virtual work of stress (2) yields

$$\mathbf{T}_s^B \cdot \delta\mathbf{H} = \mathbf{T}_s^\star \cdot \overset{\circ}{\delta}\mathbf{H}^\star, \tag{A.5}$$

where

$$\overset{\circ}{\delta}\mathbf{H}^\star \equiv \mathbf{Q}\ \delta\mathbf{H}\ \mathbf{Q}^T = \mathbf{Q}\ \delta(\mathbf{Q}^T\mathbf{H}^\star\mathbf{Q})\ \mathbf{Q}^T.$$

The above co-rotational variation corresponds with the Green-McInnis-Naghdi objective time derivative, and consists of the rotate-back, take a variation and rotate-forward operations. The definition (4) yields

$$\mathbf{H}^\star = \mathbf{V} - \mathbf{I}, \tag{A.6}$$

where $\mathbf{V} = \mathbf{QUQ}^T$ is a left stretching tensor defined as $\mathbf{V} \equiv (\mathbf{FF}^T)^{\frac{1}{2}}$. Hence, $\mathbf{H}^\star$ is the left stretch strain. The rotated Biot stress is related to other stress measures as follows

$$\mathbf{T}_s^\star = \mathrm{sym}(\mathbf{PQ}^T) = \mathrm{sym}(\boldsymbol{\tau}\mathbf{V}^{-1}) = \mathrm{sym}(\mathbf{FSV}^{-1}). \tag{A.7}$$

We can see that $\mathbf{T}_s^\star$ is different than other spatial stress measures, such as Cauchy stress $\mathbf{T}$ or Kirchhoff stress $\boldsymbol{\tau}$.

A.2 Constitutive equation for rotated measures

Let us assume the existence of a strain energy function $\mathcal{W}(\mathbf{U})$. On arguments discussed e.g. in [Ogden, 1984] a strain energy given in terms of $\mathbf{U}$ is objective, and provides a response function, which is invariant under an observer transformation. On the basis of the representation theorem for isotropic functions, we can write

$$\mathcal{W}(\mathbf{U}) = \tilde{\mathcal{W}}(I_1(\mathbf{U}), I_2(\mathbf{U}), I_3(\mathbf{U})) \tag{A.8}$$

where the principal invariants of $\mathbf{U}$ are defined as follows

$$I_1(\mathbf{U}) = \mathrm{tr}\mathbf{U}, \qquad \mathrm{I}_2(\mathbf{U}) = \frac{1}{2}\left[(\mathrm{tr}\mathbf{U})^2 - \mathrm{tr}\mathbf{U}^2\right], \qquad \mathrm{I}_3(\mathbf{U}) = \det\mathbf{U}. \tag{A.9}$$

A constitutive equation for the Biot stress tensor is defined as

$$\mathbf{T}_s^B \equiv \frac{\partial \mathcal{W}(\mathbf{U})}{\partial \mathbf{U}} = \frac{\partial \tilde{\mathcal{W}}(I_1(\mathbf{U}), I_2(\mathbf{U}), I_3(\mathbf{U}))}{\partial \mathbf{U}}. \tag{A.10}$$

From the chain rule of differentiation we obtain

$$\frac{\partial \tilde{\mathcal{W}}}{\partial \mathbf{U}} = \frac{\partial \tilde{\mathcal{W}}}{\partial I_1}\frac{\partial I_1}{\partial \mathbf{U}} + \frac{\partial \tilde{\mathcal{W}}}{\partial I_2}\frac{\partial I_2}{\partial \mathbf{U}} + \frac{\partial \tilde{\mathcal{W}}}{\partial I_3}\frac{\partial I_3}{\partial \mathbf{U}}. \tag{A.11}$$

Taking into account that

$$\frac{\partial I_1}{\partial \mathbf{U}} = \mathbf{I}, \qquad \frac{\partial I_2}{\partial \mathbf{U}} = I_1\,\mathbf{I} - \mathbf{U}, \qquad \frac{\partial I_3}{\partial \mathbf{U}} = I_3\,\mathbf{U}^{-1}, \tag{A.12}$$

the constitutive equation can be rewritten as a polynomial of $\mathbf{U}$

$$\mathbf{T}_s^B = \beta_0\mathbf{I} + \beta_1\mathbf{U} + \beta_2\mathbf{U}^{-1}, \tag{A.13}$$

where β_0, β_1 and β_2 are scalar coefficients depending on the invariants and derivatives of $\tilde{\mathcal{W}}$ with respect to the invariants. Note that using the Cayley-Hamilton theorem, the above equation can be converted to a second order polynomial of $\mathbf{U}$. A variation of stress with respect to the strain can be written as

$$\delta\mathbf{T}_s^B = \frac{\partial \mathbf{T}_s^B}{\partial \mathbf{U}} \;:\; \delta\mathbf{U} = \overset{4}{\mathbf{C}} :\; \delta\mathbf{U} \tag{A.14}$$

where the constitutive operator (elasticity tensor) can be defined as a 4-th rank tensor

$$\overset{4}{\mathbf{C}} \equiv \frac{\partial \mathbf{T}_s^B}{\partial \mathbf{U}} = \frac{\partial^2 \mathcal{W}(\mathbf{U})}{\partial \mathbf{U}\partial \mathbf{U}} = \frac{\partial^2 \tilde{\mathcal{W}}(I_1(\mathbf{U}), I_2(\mathbf{U}), I_3(\mathbf{U}))}{\partial \mathbf{U}\partial \mathbf{U}}. \tag{A.15}$$

Hence, from the formula for the derivative of the product of a scalar and a second rank tensor we have

$$\overset{4}{\mathbf{C}} = \frac{\partial \mathbf{T}_s^B}{\partial \mathbf{U}} = \mathbf{I} \otimes \frac{\partial \beta_0}{\partial \mathbf{U}} + \beta_0 \frac{\partial \mathbf{I}}{\partial \mathbf{U}} + \mathbf{U} \otimes \frac{\partial \beta_1}{\partial \mathbf{U}} + \beta_1 \frac{\partial \mathbf{U}}{\partial \mathbf{U}} + \mathbf{U}^{-1} \otimes \frac{\partial \beta_2}{\partial \mathbf{U}} + \beta_2 \frac{\partial \mathbf{U}^{-1}}{\partial \mathbf{U}} \tag{A.16}$$

where

$$\frac{\partial \beta_i}{\partial \mathbf{U}} = \frac{\partial \beta_i}{\partial I_k}\frac{\partial I_k}{\partial \mathbf{U}} \qquad \text{for} \quad i = 0, 1, 2 \qquad \text{and} \quad k = 1, 2, 3 \tag{A.17}$$

due to the chain rule of differentiation. We can say that in eq.(16) the 1st, 3rd and 5th components are expressed in terms of nine tensorial products, provided by all combinations of $\mathbf{I}$, $\mathbf{U}$ and $\mathbf{U}^{-1}$. Furthermore, for the 2nd, 4th and 6th components (and a symmetric $\mathbf{U}$), we have

$$\frac{\partial \mathbf{I}}{\partial \mathbf{U}} = \overset{4}{\mathbf{0}}, \qquad \frac{\partial \mathbf{U}}{\partial \mathbf{U}} = \frac{1}{2}(\overset{4}{\mathbf{I}}_a + \overset{4}{\mathbf{I}}_c), \tag{A.18}$$

$$\frac{\partial \mathbf{U}^{-1}}{\partial \mathbf{U}} = -\frac{1}{2}\left\{\mathbf{U}^{-1}(\mathbf{i}_i \otimes \mathbf{i}_j)\mathbf{U}^{-1}\right\} \otimes \{\mathbf{i}_i \otimes \mathbf{i}_j + \mathbf{i}_j \otimes \mathbf{i}_i\}, \tag{A.19}$$

where $\mathbf{i}_i$ are vectors of an orthonormal frame. The 4th rank invariants used here are $\overset{4}{\mathbf{I}}_a = \mathbf{i}_i \otimes \mathbf{i}_j \otimes \mathbf{i}_i \otimes \mathbf{i}_j$ and $\overset{4}{\mathbf{I}}_c = \mathbf{i}_i \otimes \mathbf{i}_j \otimes \mathbf{i}_j \otimes \mathbf{i}_i$, and operate on an arbitrary 2nd rank $\mathbf{A}$ as follows: $\overset{4}{\mathbf{I}}_a\,\mathbf{A} = \mathbf{A}$ and $\overset{4}{\mathbf{I}}_c\,\mathbf{A} = \mathbf{A}^T$, see [deBoer, 1982].

The derivation of $\partial \mathbf{U}^{-1}/\partial \mathbf{U}$, being more complicated, is described below. Consider $\mathbf{I} = \mathbf{U}\mathbf{U}^{-1}$ as a tensor-valued function of a tensor argument. As $\mathbf{U}$ is symmetric, it may be replaced by $\frac{1}{2}[\mathbf{U} + \mathbf{U}^T]$, and thus $\mathbf{U}^{-1}$ can also be considered as a function of $\frac{1}{2}[\mathbf{U} + \mathbf{U}^T]$. A directional derivative of $\mathbf{I}$ at $\mathbf{U}$ in direction $\mathbf{A}$ yields

$$\frac{\partial \mathbf{I}}{\partial \mathbf{U}} \; : \; \mathbf{A} \equiv \left[\frac{d}{d\epsilon} \mathbf{I}(\mathbf{U} + \epsilon \mathbf{A}) \right]_{\epsilon=0} = \mathbf{0}, \tag{A.20}$$

where $\mathbf{A}$ is an arbitrary 2nd rank tensor. After straightforward calculations from (20) we obtain

$$\frac{\partial \mathbf{U}^{-1}}{\partial \mathbf{U}} \; : \; \mathbf{A} = -\frac{1}{2} \mathbf{U}^{-1} (\mathbf{A} + \mathbf{A}^T) \mathbf{U}^{-1}. \tag{A.21}$$

To introduce a constitutive operator we have to rewrite the above equation as a contraction of a fourth rank tensor and a second rank tensor $\mathbf{A}$. Introducing the 4th rank invariants we have

$$(\mathbf{A} + \mathbf{A}^T) = (\overset{4}{\mathbf{I}}_a + \overset{4}{\mathbf{I}}_c) : \mathbf{A} = \mathbf{i}_i \otimes \mathbf{i}_j \; \{ [\mathbf{i}_i \otimes \mathbf{i}_j + \mathbf{i}_j \otimes \mathbf{i}_i] \cdot \mathbf{A} \}, \tag{A.22}$$

where the identity $(\mathbf{T} \otimes \mathbf{S}) : \mathbf{Q} = \mathbf{T}(\mathbf{S} \cdot \mathbf{Q})$ is used. Note that the product in the parentheses is a scalar. Substituting eq.(22) into eq.(21), and recovering the 4th rank tensor, we obtain

$$\frac{\partial \mathbf{U}^{-1}}{\partial \mathbf{U}} : \mathbf{A} = \left[-\frac{1}{2} \left\{ \mathbf{U}^{-1} (\mathbf{i}_i \otimes \mathbf{i}_j) \mathbf{U}^{-1} \right\} \otimes \{ \mathbf{i}_i \otimes \mathbf{i}_j + \mathbf{i}_j \otimes \mathbf{i}_i \} \right] : \mathbf{A}, \tag{A.23}$$

where the 4th rank tensor given by eq.(19) can be easily identified. □

Having derived the constitutive equation (13) and the elasticity tensor (14) for the Biot stress $\mathbf{T}_s^B$, we can find the respective equations for the rotated stress $\mathbf{T}_s^*$. For $\mathbf{T}_s^B$ given by eq.(13) we obtain

$$\mathbf{T}_s^* \equiv \mathbf{Q} \, \mathbf{T}_s^B \, \mathbf{Q}^T = \mathbf{Q} \left(\beta_0 \mathbf{I} + \beta_1 \mathbf{U} + \beta_2 \mathbf{U}^{-1} \right) \mathbf{Q}^T, \tag{A.24}$$

On the basis of identities

$$\mathbf{Q}\mathbf{I}\mathbf{Q}^T = \mathbf{I}, \qquad \mathbf{Q}\mathbf{U}\mathbf{Q}^T = \mathbf{V}, \qquad \mathbf{Q}\mathbf{U}^{-1}\mathbf{Q}^T = \mathbf{V}^{-1} \tag{A.25}$$

we have

$$\mathbf{T}_s^* = \beta_0 \mathbf{I} + \beta_1 \mathbf{V} + \beta_2 \mathbf{V}^{-1}, \tag{A.26}$$

which is a polynomial of the left stretching tensor $\mathbf{V}$.

Next, we find the elasticity tensor for the rotated stress $\mathbf{T}_s^*$,

$$\overset{\circ}{\delta} \mathbf{T}_s^* \equiv \mathbf{Q} \, \delta \mathbf{T}_s^B \, \mathbf{Q}^T = \mathbf{Q} \left[\overset{4}{\mathbf{C}} : \delta \mathbf{U} \right] \mathbf{Q}^T = \mathbf{Q} \left[\frac{\partial \mathbf{T}_s^B}{\partial \mathbf{U}} : \delta \mathbf{U} \right] \mathbf{Q}^T, \tag{A.27}$$

where the expression for $\partial \mathbf{T}_s^B / \partial \mathbf{U}$ is given by eq.(16). Consider the 1st, 3rd and 5th component of this equation contracted with $\delta \mathbf{U}$. As mentioned earlier, these components contain nine tensorial products, and the contraction can be written as $(\mathbf{A}_i \otimes \mathbf{A}_j) : \delta \mathbf{U}$,

where $\mathbf{A}_i, \mathbf{A}_j \in \{\mathbf{I}, \mathbf{U}, \mathbf{U}^{-1}\}$. Furthermore, $(\mathbf{A}_i \otimes \mathbf{A}_j) : \delta\mathbf{U} = \mathbf{A}_i\,(\mathbf{A}_j \cdot \delta\mathbf{U})$, where in the parentheses we have a scalar. Hence,

$$\mathbf{Q}\,[(\mathbf{A}_i \otimes \mathbf{A}_j) : \delta\mathbf{U}]\,\mathbf{Q}^T = \left[\mathbf{Q}\mathbf{A}_i\mathbf{Q}^T\right]\,(\mathbf{A}_j \cdot \delta\mathbf{U}) = \mathbf{B}_i\,(\mathbf{A}_j \cdot \delta\mathbf{U}) \tag{A.28}$$

where $\mathbf{Q}\mathbf{A}_i\mathbf{Q}^T = \mathbf{B}_i$ and $\mathbf{B}_i \in \{\mathbf{I}, \mathbf{V}, \mathbf{V}^{-1}\}$ in accordance with eq.(25). Besides, for the scalar product we have

$$\mathbf{A}_j \cdot \delta\mathbf{U} = \mathrm{tr}(\mathbf{A}_j\delta\mathbf{U}) = \mathrm{tr}\left(\mathbf{Q}^T(\mathbf{Q}\mathbf{A}_j\mathbf{Q}^T)(\mathbf{Q}\delta\mathbf{U}\mathbf{Q}^T)\mathbf{Q}\right) = \mathrm{tr}(\mathbf{B}_j\,\mathring{\delta}\mathbf{V}) = \mathbf{B}_j \cdot \mathring{\delta}\mathbf{V}, \tag{A.29}$$

where $\mathbf{Q}\mathbf{A}_j\mathbf{Q}^T = \mathbf{B}_j$. Hence

$$\mathbf{Q}\,[(\mathbf{A}_i \otimes \mathbf{A}_j) : \delta\mathbf{U}]\,\mathbf{Q}^T = (\mathbf{B}_i \otimes \mathbf{B}_j) : \mathring{\delta}\mathbf{V}. \tag{A.30}$$

For the 2nd component of eq.(16) we have $\partial\mathbf{I}/\partial\mathbf{U} = \overset{4}{\mathbf{0}}$ and the respective term does not need to be considered. For the 4th and 6th component we have

$$\frac{\partial\mathbf{U}}{\partial\mathbf{U}} : \delta\mathbf{U} = \frac{1}{2}(\overset{4}{\mathbf{I}}_a + \overset{4}{\mathbf{I}}_c) : \delta\mathbf{U} = \frac{1}{2}(\delta\mathbf{U} + \delta\mathbf{U}^T), \tag{A.31}$$

$$\frac{\partial\mathbf{U}^{-1}}{\partial\mathbf{U}} : \delta\mathbf{U} = -\frac{1}{2}\mathbf{U}^{-1}(\delta\mathbf{U} + \delta\mathbf{U}^T)\mathbf{U}^{-1}, \tag{A.32}$$

where eq.(21) was used to derive the second equation. Applying the rotation operations to both of these equations we obtain

$$\mathbf{Q}\left(\frac{\partial\mathbf{U}}{\partial\mathbf{U}} : \delta\mathbf{U}\right)\mathbf{Q}^T = \frac{1}{2}\mathbf{Q}(\delta\mathbf{U} + \delta\mathbf{U}^T)\mathbf{Q}^T = \frac{1}{2}(\mathring{\delta}\mathbf{V} + \mathring{\delta}\mathbf{V}^T), \tag{A.33}$$

$$\mathbf{Q}\left(\frac{\partial\mathbf{U}^{-1}}{\partial\mathbf{U}} : \delta\mathbf{U}\right)\mathbf{Q}^T = -\frac{1}{2}\mathbf{Q}\mathbf{U}^{-1}(\delta\mathbf{U} + \delta\mathbf{U}^T)\mathbf{U}^{-1}\mathbf{Q}^T = -\frac{1}{2}\mathbf{V}^{-1}(\mathring{\delta}\mathbf{V} + \mathring{\delta}\mathbf{V}^T)\mathbf{V}^{-1}. \tag{A.34}$$

Note that as a result of the rotate-forward operation in the above formulas, $\mathbf{U}$ is replaced by $\mathbf{V}$, $\mathbf{U}^{-1}$ by $\mathbf{V}^{-1}$, and $\delta\mathbf{U}$ by $\mathring{\delta}\mathbf{V}$. Hence, we may introduce an elasticity tensor $\overset{4}{\mathbf{C}}{}^*$ relating $\mathring{\delta}\mathbf{T}^*_J$ with $\mathring{\delta}\mathbf{V}$,

$$\mathring{\delta}\mathbf{T}^*_J = \mathbf{Q}\left[\overset{4}{\mathbf{C}} : \delta\mathbf{U}\right]\mathbf{Q}^T \equiv \overset{4}{\mathbf{C}}{}^* : \mathring{\delta}\mathbf{V} \tag{A.35}$$

of the same structure as $\overset{4}{\mathbf{C}}$.

For an infinitesimal deformation, when $\mathbf{F} \approx \mathbf{I}$, we have

$$\mathbf{U} = \mathbf{V} = \mathbf{I}, \qquad \frac{\partial\mathbf{U}^{-1}}{\partial\mathbf{U}} = -\frac{1}{2}(\overset{4}{\mathbf{I}}_a + \overset{4}{\mathbf{I}}_c), \qquad \frac{\partial\mathbf{V}^{-1}}{\partial\mathbf{V}} = -\frac{1}{2}(\overset{4}{\mathbf{I}}_a + \overset{4}{\mathbf{I}}_c) \tag{A.36}$$

and therefore the linearized elasticity tensors $\overset{4}{\mathbf{C}}$ and $\overset{4}{\mathbf{C}}{}^*$ are identical.

Concluding, we have shown that under the rotate-forward operation the structure of a general hyper-elastic constitutive equation and the respective constitutive operator for the Biot stress is carried over to the respective relations for the rotated Biot stress, with $\mathbf{U}$ replaced by $\mathbf{V}$, and $\delta\mathbf{U}$ by $\mathring{\delta}\mathbf{V}$, where the co-rotational variation is of the Green-McInnis-Naghdi type.

B Figure captions

Fig.2.1 Rotation of vector $\mathbf{v}$ around axis $\mathbf{e}$

Fig.2.2 Components vectors of $\Delta\mathbf{v} = (\mathbf{R} - \mathbf{I})\mathbf{v}$

Fig.2.3 Position of shell director, [Ramm, 1986]

Fig.2.4 Position of shell director, [Wriggers, Gruttmann, 1993]

Fig.2.5 Scheme of increments of rotations

Fig.3.1 Local bases on the middle surface of shell

Fig.3.2 Geometrical interpretation of strain measures ε_1 and ε_1^*

Fig.3.3 In-plane bending. Initial and deformed mesh.

Fig.3.4 In-plane bending. Drilling rotation and in-plane displacements

Fig.3.5 In-plane bending. Sensitivity of drilling rotation w.r.t. the thickness

Fig.3.6 Cylindrical roof under a point load. Geometry and load.

Fig.3.7a Cylindrical roof under a point load. Z-displacement at the middle of free edge.

Fig.3.7b Cylindrical roof under a point load.
Sensitivity to thickness of Z-displacement at the middle of free edge.

Fig.3.8a Cylindrical roof under a point load. Y-rotation at the middle of free edge.

Fig.3.8b Cylindrical roof under a point load.
Sensitivity to thickness of Y-rotation at the middle of free edge

Fig.3.9a Cylindrical roof under a point load. X-displacement under the force.

Fig.3.9b Cylindrical roof under a point load.
Sensitivity to thickness of X-displacement under the force.

Fig.3.10a Cylindrical roof under a point load.
Y-displacement at the middle of the shell quarter.

Fig.3.10b Cylindrical roof under a point load.
Sensitivity to thickness of Y-displacement at middle of shell quarter.

Fig.3.11a Cylindrical roof under a point load. Z-displacement at middle of shell quarter.

Fig.3.11b Cylindrical roof under a point load.
Sensitivity to thickness of Z-displacement at the middle of shell quarter.

Fig.3.12a Cylindrical roof under a point load. Y-rotation at the middle of shell quarter.

Contents